

# **The Role of Annexin 2 in RPE Phagocytosis of Photoreceptor Outer Segments**

**Ah-Lai Law**

**The thesis is submitted to the University College  
of London for the degree of Doctor of Philosophy**

**June 2009**

**Division of Cell Biology  
UCL Institute of Ophthalmology  
11-43 Bath Street  
London  
EC1V 9EL**

## Declaration

I, Ah-Lai Law, confirm that the work presented in this thesis is my own. Where information has been derived from other sources, I confirm that this has been indicated in the thesis.

Ah-Lai Law

**For Mum and Dad**

## Abstract

The Retinal Pigmented Epithelium (RPE) has many functions, one of which is the phagocytosis of shed photoreceptor outer segments (POS). This process is vital to the maintenance of both the RPE and photoreceptors. Outer segment shedding and internalisation are under circadian regulation, such that shedding is followed by a burst of phagocytosis at the onset of light. Annexin 2 is well placed to have a role in this process. Its direct involvement in actin dynamics and association to vesicle membranes during endocytosis may be significant in RPE outer segment phagocytosis, as this process requires extensive re-organisation of actin and re-distribution of membrane on the apical processes of the RPE. This thesis examines cell differentiation in two RPE cell lines and in primary porcine RPE cells, in order to evaluate the best system for conducting phagocytosis experiments.

*In vitro* experiments provided evidence that annexin 2 localises to the phagocytic cup during POS internalisation but dissociates once internalisation is complete. Following knock down of annexin 2, phagocytosis was shown to decrease. Furthermore annexin 2 was shown to be phosphorylated during phagocytosis. We also found that c-Src is phosphorylated alongside annexin 2 and therefore may phosphorylate annexin 2, which contains a c-Src phosphorylation site. To investigate the circadian aspects of POS phagocytosis by the RPE, apical and basal phagosomes were quantified in the RPE from annexin 2 knock out and wild type eyes, harvested before and after light onset. Phagosomes from eyes harvested one hour after light onset were also mapped relative to Bruch's membrane. The annexin 2 knock out animals lack the characteristic burst of phagocytosis one hour after light onset exhibited in wild type animals. Phagosomes were also retarded in the apical processes one hour after light onset, at the peak of phagocytosis, when they are normally internalised into the cell body for processing and degradation. Lysates from wild type eyes showed that annexin 2 is phosphorylated before light onset along with c-Src and FAK, key molecules in the RPE phagocytic machinery. Importantly, the absence of annexin 2 in knock out eyes delayed phosphorylation of c-Src and FAK. This delay in phosphorylation of two key RPE phagocytosis molecules may account for the delay in ingestion of outer segments into the cell body and the accumulation of phagosomes in the apical processes observed in the knock out animals.

In conclusion, work in this thesis has demonstrated that annexin 2 is required for efficient RPE internalisation of rod outer segments both *in vitro* and *in vivo*. Annexin 2 is required for the timely phosphorylation of FAK and c-Src, which may account for the delay in POS internalisation observed in the annexin 2 knock out mice.

## Acknowledgements

I would like to take this opportunity to thank the many people who have made this thesis possible, the Wellcome trust for funding my research and a dedication to all my furry friends.

I would like to thank my supervisor Prof. Steve Moss for giving me the opportunity to take on a PhD with him and for his encouragement, support, guidance and belief. Steve, thank you for giving me such a wonderful opportunity and a fantastic project to work on. I would also like to thank my second supervisor Dr Clare Futter, who has also given me the support, guidance and encouragement, which has made this PhD possible.

I wish to thank the many people at Ophthalmology and everyone in Cell Biology, who have all at some point or other given me support and guidance throughout my PhD. I am grateful to Matt Hayes, Becca, Marcin, Katy, James D, Veronika, Emily E, Rush, Silène, Anna, Jay, Emily Steed, James E, Bhairavi, Shweta, Shazeen, Vanda, Tim, Claire, Charmie, Aida, Matt Pearson, Peter Munroe and the BRU staff. This list also includes Adam, who I am grateful to for being Adam and Maria D, for her support and care. These people have really contributed to the fantastic time I have had throughout my time at Ophthalmology. I thank you all for the smiles you've generated and for the support and patience you have given to me. I would like to give my special thanks to Lux and Jenny in my lab, who have both shared many of my woes and have smoothed my ruffled feathers over the years as well as making my PhD such great fun. Jenny and Lux, thank you both for being patient, caring, supportive, encouraging me when I'm right and telling me off when I'm wrong. Thank you Jenny, for the fruit deliveries, supplies of Ainsley's cous cous and packet soup that have kept me alive during the final six months of my PhD. Thank you for putting up with me and my working lab bench and desk. I'm sure you will miss the excitement of my toppling books ; ). I would also like to thank the 'sweet' and 'innocent' youngster who is one of the most self-less, kind and talented people I know. Thank you for always being there for me throughout my PhD. I however, don't thank you for hanging Doggy and for not accepting my home made raisins.

My family at Ophthalmology wouldn't be complete without Amanda, Jenny (McKenzie) and Shalini. Thank you all for the Friday pub lunches and out-of- hour mischiefs! Thank you all for your love and keeping me sane (ish). I am forever indebted to Amanda and Jenny, for their scientific input. Amanda, thank you for the lessons in primer designing, PCRs, RNA extraction and statistics! You have been a wonderful, smiley teacher and have never failed to give me inspiration. Jenny, thank you for teaching me how to dissect and flat-mount, the magic way and for all the magic ingredients, magical advice and your magical spell. You have also become

one of my closest friends during my PhD, who I have learnt to come to when things are going great or bad. You are always dependable and have encouraged and supported me with absolutely everything. Thank you Jenny. You all have truly been fantastic and have set a very high standard for post docs. I really aspire to be as hard working, talented and good natured as you all are.

I would also not have come this far without the love and support from my close friends outside Ophthalmology. Throughout the years, Alex and Kate have continuously supported me. They have always made time for me, have always looked out for me and have been behind me throughout my PhD. Thank you for everything you have done for me, the time you have given to me, keeping me grounded and sane throughout the years. I would also like to thank Ruby and Vicki for their understanding and support during my PhD. Thank you both for not giving up on me. There is also Louisa who I have shared many Saturdays at NatWest with. Thank you for being such a great friend. You have always listened to me and been there for me through many happy and unhappy times. Can't wait for our next shopping trip to 'Primarni' xxx.

Finally, I would like to thank my parents who have put me on the right path from day one. Thank you for shaping me, believing in me and supporting me so that I can walk my path. Without your love, support and patience, this PhD would not have been possible. I would also like to thank my sisters Ga-Lai, Pui-Lai and Bo-Yee for all the arguments and mischief we've had over the years and for understanding me. Thank you all for who I am and for putting up with my grouchiness over the years. Last but not least is my special thanks to Blair, who truly has seen me at my ugliest and best for most of my PhD. Thank you for being a rock and shouldering the load. You haven't only walked with me but have at times carried me on my path. Thank you for keeping me on the right track and for all your love, support and understanding, which words can't describe. I truly am the happiest and luckiest.

# Contents

Abstract.....	4
Acknowledgements.....	5
Contents .....	7
List of Figures.....	11
List of Tables .....	14
List of Abbreviations .....	15
1. Introduction.....	20
1.1. The Retina.....	20
Figure 1.1 Morphological organisation of a normal mouse retina.....	20
1.2. The Retinal Pigment Epithelium.....	22
1.2.1. Polarity and Integrity of the RPE.....	24
1.3. The Visual Cycle.....	26
Figure 1.2 The visual cycle.....	27
1.4. Circadian regulation of photoreceptor shedding and phagocytosis by the RPE .....	28
1.5. Phagocytosis .....	29
1.5.1. FcγR-mediated phagocytosis .....	29
1.5.2. CR3-mediated phagocytosis .....	30
Figure 1.3 Activation of complement and complement-mediated phagocytosis .....	31
1.5.3. POS phagocytosis by the RPE .....	32
Figure 1.4 Schematic diagram of the current RPE phagocytosis model.....	34
1.4. Actin Dynamics in Phagocytosis .....	34
1.4.1. Actin polymerisation.....	36
1.4.2. Arp 2/3 activity and actin nucleation .....	36
1.4.3. Regulation of actin assembly and disassembly .....	36
1.4.4. Motor proteins in phagocytosis.....	38
Figure 1.6 The regulation of actin polymerisation.....	40
1.5. The Annexins.....	41

1.6.	Annexin 2.....	43
1.6.1.	Structure.....	43
Figure 1.9 Configurations of the membrane-bound annexin A2–S100A10 complex.....		44
1.6.2.	Interactions involving annexin 2.....	45
1.6.3.	Post-translational Modifications .....	46
1.6.4.	The project .....	47
2.	Materials and Methods.....	49
2.1.	Cells .....	49
2.2.	Equipment .....	49
2.2.1.	Microscopes .....	49
2.2.2.	Plate readers .....	49
2.2.3.	PCR Machines .....	49
2.3.	Animals .....	50
2.4.	Cell Culture.....	50
2.4.1.	Cell Lines .....	50
2.4.2.	Primary RPE cultures.....	50
2.4.3.	Phosphotyrosine Immunoprecipitation .....	51
2.4.4.	Cell Characterisation.....	51
2.5.	Annexin 2 siRNA treatment.....	51
2.6.	Photoreceptor Outer Segments.....	52
2.6.1.	Isolation.....	52
2.6.2.	Fluorescent Labelling.....	52
2.7.	Quantification of POS Binding and Internalisation .....	52
2.8.	Preparation for Microscopy .....	53
2.8.1.	Toluidine Blue .....	53
2.8.2.	Immunofluorescence .....	53
Table 2.1 All antibodies and reagents used for immunofluorescent microscopy .....		55
2.8.3.	Electron Microscopy .....	56

2.9.	Immunoprecipitation.....	56
2.9.1.	Tyrosine-phosphorylated proteins in ARPE-19 cells.....	56
2.9.2.	Tyrosine-phosphorylated proteins in annexin 2 knock out and wild type eyes ...	57
2.10.	Flat-mounting eye cups.....	57
2.10.1.	Mowiol Mountant .....	57
2.11.	SDS-PAGE and Western Blotting .....	58
Table 2.2	Antibodies used for Western blotting .....	59
2.12.	Quantification of POS Binding and Internalisation .....	60
2.13.	Reverse Transcription-Polymerase Chain Reaction (RT-PCR).....	60
2.13.1.	Reverse Transcription .....	60
2.13.2.	DNA Polymerase Chain Reaction (PCR) Amplification .....	61
Table 2.3	Primer Sequences for ARPE-19 cells .....	62
Table 2.4	Primer Sequences for RPE-J cells.....	63
Table 2.5	Primer Sequences for primary porcine RPE cells.....	64
3.	Model Systems for Retinal Phagocytosis.....	67
3.1.	The RPE.....	67
3.2.	Experimental Approaches to RPE Phagocytosis.....	67
3.3.	Characterisation of immortalised cell lines.....	69
3.3.1.	ARPE-19 .....	69
3.3.2.	RPE-J cells .....	75
3.4.	Characterisation of primary RPE culture .....	80
3.4.1.	Primary Porcine RPE Culture .....	80
3.5.	Characterisation of the RPE <i>in vivo</i> .....	86
3.5.1.	The Mouse Eye .....	86
3.5.2.	The Pig Eye.....	87
3.6.	Discussion.....	93
4.	Does Annexin 2 have a role in RPE phagocytosis of rod outer segments <i>in vitro</i> ?.....	103
4.1.	Transient co-localisation of annexin 2 with phagosomes .....	104

4.2.	Annexin 2 knockdown in ARPE-19 and RPE-J cells leads to a decreased efficiency in POS internalisation .....	107
4.3.	Annexin 2 and c-Src are phosphorylated upon POS phagocytosis in ARPE-19 cells 109	
4.4.	Discussion .....	112
5.	Does annexin 2 have a role in phagocytosis in the eye <i>in vivo</i> ? .....	118
5.1.	Phagocytosis of photoreceptor outer segments is delayed in the annexin 2 knock out mouse 120	
5.2.	FAK and c-Src activation are delayed in the annexin 2 knock out mouse.....	132
5.3.	Discussion .....	135
6.	Conclusions and Summary.....	141
6.1.	Future perspectives .....	145
7.	Appendix.....	148
	Table 7.1 Two Way Analysis of Variance.....	148
	Table 7.2 One Way Analysis of Variance.....	149

## List of Figures

Figure 1.1 Morphological organisation of a normal mouse retina.....	20
Figure 1.2 The visual cycle.....	27
Figure 1.3 Activation of complement and complement-mediated phagocytosis .....	31
Figure 1.4 Schematic diagram of the current RPE phagocytosis model.....	34
Figure 1.5 Signalling events associated with activation of Fcγ receptor(s) on phagocytic cells. ....	35
Figure 1.6 The regulation of actin polymerisation.....	40
Figure 1.7 Schematic drawing of an annexin that is peripherally attached to a membrane surface through bound Ca <sup>2+</sup> ions .....	42
Figure 1.8 Structure of human annexin A2 in the absence (A) and presence (B) of calcium ions .....	43
Figure 1.9 Configurations of the membrane-bound annexin A2–S100A10 complex.....	44
Figure 3.1 A ARPE-19 cells express annexin 2 and develop a cobblestone appearance over time. ....	70
Figure 3.2 Western blot analysis of protein expression in ARPE-19 cells grown in 10% serum .....	73
Figure 3.3 ARPE-19 cells grown in 10% serum express genes required for POS phagocytosis	74
Figure 3.4 ARPE-19 cells are pigmented and differentiate into a cobblestone pavement of cells .....	74
Figure 3.5 A RPE-J cells express annexin 2 and develop discrete cortical F-actin accumulation over time. ....	76
Figure 3.6 Western blot analysis of protein expression in RPE-J cells.....	78
Figure 3.7 RPE-J cells express molecules required for POS specific phagocytosis .....	79
Figure 3.8 A Primary porcine RPE cells express annexin 2, maintain their native morphology but lose pigment over time in culture.....	82

Figure 3.9 Western blot analysis of protein expression in cultured primary porcine RPE cells	84
Figure 3.10 Porcine RPE cells grown in culture express genes required for POS phagocytosis	85
Figure 3.11 Annexin 2 is expressed in control mouse RPE	87
Figure 3.12 Electron micrograph of mouse RPE and photoreceptors	88
Figure 3.13 Mouse eye flatmount showing ZO1 and rhodopsin staining	89
Figure 3.14 Mouse RPE cells express genes required for POS specific phagocytosis	90
Figure 3.15 Western blot analysis of protein expression in pig, wild type and annexin 2 knock out RPE and retina	91
Figure 3.16 Porcine RPE cells express molecules required for POS specific phagocytosis	92
Figure 4.1 Annexin 2 and F-actin distribution in human, rat and pig RPE cells	105
Figure 4.2 Annexin 2 co-localises with the partially internalised phagosome	106
Figure 4.3 Time course of POS phagocytosis by ARPE-19 and RPE-J cells	108
Figure 4.4 Annexin 2 and c-Src are phosphorylated upon POS phagocytosis in ARPE-19 cells.	110
Figure 4.5 c-Src is localised to the forming phagosome	111
Figure 4.6 RPE phagocytosis of photoreceptor outer segments.	116
Figure 5.1 Morphological organisation of annexin 2 knock out and wild type retinas	121
Figure 5.2 Annexin 2 knock out mice have a normal retinal ultrastructure.	121
Figure 5.3 Annexin 2 is present in wild type RPE	122
Figure 5.4 Annexin 2 is localised to the early phagosomes in wild type RPE	123
Figure 5.5 Circadian analysis of POS shedding and phagocytosis by the RPE	126
Figure 5.6 Absence of annexin 2 delays internalisation of POS into the RPE	127
Figure 5.7 Phagosomes are retarded in the apical processes in the annexin 2 knock out mouse	128

Figure 5.8 Visualisation of the RPE in retinal flatmounts .....	129
Figure 5.9 Native phagosomes can be identified and quantified using immunofluorescent staining for rhodopsin .....	130
Figure 5.10 Diurnal phagocytosis of photoreceptor outer segments (POS) is retarded in mice lacking annexin 2 .....	131
Figure 5.11 Tyrosine kinase signalling is defective in annexin 2 deficient retinas .....	133
Figure 5.12 Schematic diagram of the role of annexin 2 in RPE phagocytosis .....	139

## List of Tables

Table 2.1 All antibodies and reagents used for immunofluorescent microscopy .....	55
Table 2.2 Antibodies used for Western blotting .....	59
Table 2.3 Primer Sequences for ARPE-19 cells .....	62
Table 2.4 Primer Sequences for RPE-J cells.....	63
Table 2.5 Primer Sequences for primary porcine RPE cells .....	64
Table 2.6 Primer Sequences for mouse.....	65
Table 7.1 Two Way Analysis of Variance .....	148
Table 7.2 One Way Analysis of Variance.....	149

## List of Abbreviations

µg	Micro gram
µl	Micro litre
µM	Micro molar
11-cis RDH	11-cis retinol dehydrogenase
11-cis RDH	11- <i>cis</i> retinol dehydrogenase
A10	Annexin A10
A13	Annexin A13
A2	Annexin A2
A9	Annexin A9
ADP	Adenosine Diphosphate
ADP	Adenosine Triphosphate
AHNAK	AHNAK Nucleoprotein (desmoyokin)
AMD	Age Related Macular Degeneration
Anova	Analysis of variance
AP	Alternative Pathway
Arp 2/3	Actin-related protein 2/3 protein
ATP	Adenosine-5'-triphosphate
avβ5	Integrin alpha v beta 5
BP	Base pairs
BSA	Bovine serum albumin
C3	Complement component 3
C5	Complement component 5
C57BL/6	C57 black 6
Ca <sup>2+</sup>	Calcium
CAPZ	Capping protein muscle Z-line
CC	Choriocapillaris
CD36	Cluster of Differentiation 36
CD45	Cluster of Differentiation 45
CD81	Cluster of Differentiation 81
Cdc42	Cell division cycle 42
CP	Capping protein
CP	Classical pathway
CR	Complement receptor
CR3	Complement receptor 3
CRALBP	Cellular retinaldehyde binding protein
CRB1	Crumbs homolog 1
CRBP	Cellular retinol binding protein
c-Src	Cellular Src
Ctsd	Cathepsin D
Da	Daltons
DAG	Diacylglycerol

DAip1	<i>Dictyostelium</i> actin-interacting protein1
DIA1	Diaphanous-related formin 1
DMEM	Dulbecco's modified Eagle's medium
DNA	Deoxyribonucleic acid
dNTP	Deoxyribonucleotide (5'-) triphosphates
ECM	Extracellular Matrix
EDTA	Ethylenediaminetetraacetic acid
EM	Electron microscope
EMT	Epithelial-mesenchymal transition
EP	Early phagosomes
FAK	Focal adhesion kinase
FCS	Foetal calf serum
FcγR	Fc gamma receptor
FRET	Fluorescence resonance energy transfer microscopy
Gas6	Growth arrest specific gene 6
GFP	Green fluorescent protein
HESC	Human embryonic stem cells
IgG	Immunoglobulins
InsP3	Inositol 1,4,5-trisphosphate
IPL	Immunoprecipitation
IPL	Inner plexiform layer
IRBP	Interstitial retinal binding protein
ITAM	Immunoreceptor tyrosine-based activation motif
Itgav	Integrin alpha v
Itgb5	Integrin beta 5
JNK	c-jun N-terminal kinase
k	Kilo
LCA	Leber's congenital amaurosis
LIMK	Lim Kinase
LP	Late phagosomes
LP	Lectin pathway
LRAT	Lecithin retinol acyltransferase
M	Molar
MAC	Membrane-attack complex
MAPK	Mitogen-activated protein kinase
MDCK	Madin-Darby canine kidney
MerTK	Mer tyrosine kinase
MET	Mesenchymal Epithelial Transition
MFG-E8	Milk fat globule-EGF factor 8 protein
mg	Milli gram
mm	Milli metre
MYO7A	Myosin VIIA
Na/K-ATPase	Sodium/Potassium ATPase
NADPH	Nicotinamide adenine dinucleotide phosphate
NEM	N-ethylmaleimide

NF $\kappa$ B	Nuclear factor kappa B
NT	No template control
N-WASP	Wiskott-Aldrich Syndrome Protein
OCT	Optimal cutting temperature compound
PAK	p21-activated Kinase
PBS	Phosphate buffered saline
PCR	Polymerase chain reaction
PFA	Paraformaldehyde
PFY	Profilin
PKA	Protein kinase A
PKC	Protein Kinase C
PLC	Porcine lens capsule
PMN	Polymorphonuclear
PMNL	Polymorphonuclear leukocytes
POS	Photoreceptor outer segments
ProS1	Protein S
PtdIns 3,4,5P <sub>3</sub>	Phosphatidylinositol (3,4,5) trisphosphate
PtdIns4,5P <sub>2</sub>	Phosphatidylinositol (4,5) bisphosphate
PTEN	Phosphatase and tensin homolog
PVDF	Polyvinylidene Difluoride
Rac	Ras-related C3 botulinum toxin substrate
Rap1	Ras superfamily of small GTPases
RCS	Royal college of surgeons
RGD	Arginine-Glycine-Aspartic acid
Rho	Ras homolog gene family
Rho GTPases	Rho guanosine triphosphatases
RNA	Ribonucleic acid
ROK	Rho kinase
ROS	Rod outer segment
RPE	Retinal pigment epithelium
RPE-65	Retinal pigment epithelium-specific protein 65 kDa
RT	Reverse transcription
RT-PCR	Reverse Transcription-Polymerase Chain Reaction
SAPK	Stress-activated protein kinases
SCAR	Suppressor of cAMP receptor
SDS-PAGE	Sodium dodecyl sulfate polyacrylamide gel electrophoresis
SEM	Standard error of the mean
SH1	Src homology 1
SH2	Src homology 2
SH3	Src homology 3
siRNA	Small interfering RNA
$\beta$ 2	Beta 2
$\beta$ 5	Beta 5
SV40	Simian vacuolating virus 40

Syk	Spleen tyrosine kinase
TEM	Transmission electron microscope
TER	Transepithelial electrical resistance
TsA	Temperature-sensitive A mutant
Tyr-23	Tyrosine 23
USH1B	Usher syndrome type 1B
VASP	Vasodilator-Stimulated Phosphoprotein
Vav	Vav oncogene
VE-cad	Vascular endothelial cadherin
WASP	Wiskott-Aldrich Syndrome Protein
WAVE	WASP family Verprolin-homologous protein
ZO	Zona occludens

# **Chapter 1**

## **Introduction**

# 1. Introduction

## 1.1. The Retina

The retina is the innermost layer of the eye and is composed of multiple layers of specialised cells, each with distinct functions (Figure 1.1). These layers can be sub-divided into a pigmented layer, the retinal pigment epithelium (RPE) (1), and a sensory layer which consists of rod and cone photoreceptors (2), external limiting membrane (3), outer nuclear layer (4), outer plexiform layer (OPL) (5), inner nuclear layer (6), inner plexiform layer (IPL) (7) and ganglion cell layer (8). Proximal to the ganglion cell layer lies the inner limiting membrane (not shown).

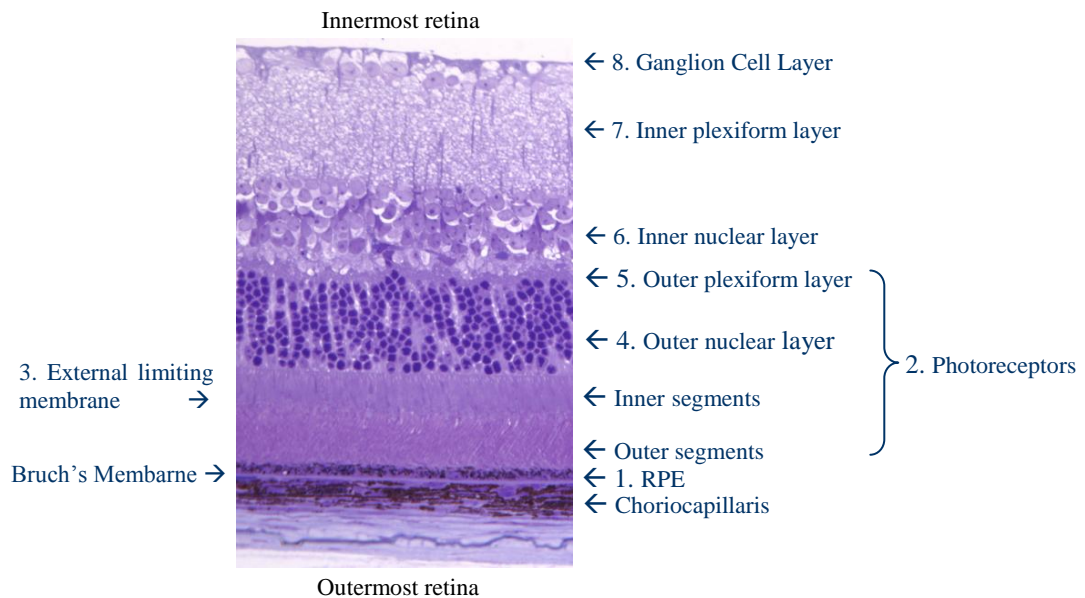


**Figure 1.1 Morphological organisation of a normal mouse retina**

Toluidine blue staining was used on transverse sections from wild type retina obtained from a 2 month old mouse to show the morphological arrangements of the RPE and neuroretina.

The choriocapillaris is the outermost vascular layer of the choroid, containing endothelial cells that are thin and heavily fenestrated. The choroid functions to deliver oxygen and nutrients to the external layers of the retina, which includes the RPE through to the inner nuclear layer. The basal lamina of the choriocapillaris forms most of the external part of Bruch's membrane. Bruch's membrane was named after Carl Bruch (1844) who first demonstrated the presence of an 'invisible membrane' later termed 'Bruch's'. This 'invisible membrane' consists of three layers: two collagenous layers, with a central elastic layer sandwiched between<sup>2</sup>. Bruch's

membrane lies directly beneath the RPE and its innermost layer is formed by the basal lamina of the RPE. It separates the RPE from the fenestrated endothelium of the choriocapillaris<sup>3, 4</sup>. Many mild pathological changes in Bruch's membrane can be observed in the elderly, and these changes are particularly important in age-related eye diseases such as Age-related Macular Degeneration (AMD). Coated, membrane-bound residual bodies and abnormal extracellular deposits known as drusen, accumulate between the RPE basal lamina and the inner collagenous layer of Bruch's membrane from as early as the patients' thirties, with deposits appearing on the basal lamina around 40 years of age<sup>5,6-8</sup>

The RPE is a pigmented monolayer forming part of the blood/retina barrier. The basolateral membrane faces Bruch's membrane and the apical surface interacts directly with the photoreceptor outer segments (POS). Microvilli extend from the apical surface and surround the outer segments, establishing a loose but complex structural interaction between the RPE and the light sensitive photoreceptor outer segments<sup>3</sup>. The sensory layer of the retina can be further divided into three layers of nerve cell bodies and two layers of synapses. The photoreceptors belong to the outer nuclear layer of cell bodies, followed by a thin outer plexiform layer where the photoreceptors synapse with the neural cells of the inner nuclear layer, so that the neural signals generated from the rods and cones are passed on for processing.

The inner nuclear layer contains the cell bodies of bipolar, horizontal, amacrine and Müller cells. The bipolar cells are the most abundant and serve to connect the photoreceptor and ganglion cell layers. There are more than ten subtypes of cone bipolar cells and one subtype of rod bipolar cells. The large number of bipolar subtypes means that they are able to mediate a range of signals from rod and cone photoreceptors. The cone bipolar cells directly connect cone photoreceptors to ganglion cells and bridge synaptic connections with amacrine cells that synapse with rod bipolar cells. This allows cross talk between the rod and cone photoreceptors to enable rod signalling during dark, and cone signalling at light onset. Each rod bipolar cell can synapse with one to four ganglion cells, and also synapse with amacrine cells to allow further cross talk between the rod and cone photoreceptors. The horizontal cells receive inputs from the photoreceptors and conduct information laterally, and also make connections with bipolar cells to mediate feedforward connections<sup>9</sup>. Synapses formed by bipolar cells with retinal ganglion cells are few, and the majority of the input from the bipolar cells is mediated by amacrine cells forming connections with bipolar and retinal ganglion cells<sup>10</sup>. Finally, Müller cells fill the retinal space with cytoplasmic processes that reach the external limiting membrane. The Müller cells provide glucose and glycogen and have the key role of removing glutamate from the extracellular space (glutamate cytotoxicity plays an important role in glaucoma).

Moreover, Müller cells have been suggested to be crucial for the survival of the other neurons and for maintaining the structural integrity of the retina<sup>11</sup>.

The IPL is the second synaptic layer, and the site of synapses between ganglion, bipolar and amacrine cells. Müller cell processes are also observed in the IPL along with rare astrocytes and the occasional displaced cell from the inner nuclear or the ganglion cell layers. The third layer of neural cells described in this chapter is the ganglion cell layer, where the cell bodies of the ganglion cells lie. Ganglion cells are the only output neurons in the retina and possess the unique ability to process and transmit information from the retina to the visual processing centres in the brain. The axons from the ganglion cells bundle into tracts that continue to form the nerve fibre layer. The bundled tracts run radially along the inner surface of the retina and finally meet at the optic nerve<sup>12</sup>. This project focuses on the RPE cell layer and the photoreceptors so these two layers will be covered in more depth here.

## **1.2. The Retinal Pigment Epithelium**

The RPE is a polarised cobblestone-like layer of post-mitotic pigmented cuboidal cells that are highly metabolic. The total number of pigmented epithelial cells in the human eye ranges from 4.2 to 6.1 million and each pigment cell measures 12-18  $\mu\text{m}$  in width and 10-14 $\mu\text{m}$  in height<sup>13</sup>. The mouse retina contains RPE cells that are smaller (from 3-5 $\mu\text{m}$  in height) but the ultrastructure of the RPE is very similar to that in humans. Both species have a well-developed basal surface which is characterised by complex infoldings about 1  $\mu\text{m}$  in length from the basal plasma membrane. Numerous mitochondria are distributed near the basal surface, the abundance of which reflects the highly metabolic nature of these cells. The mid-body of the RPE cell contains a large oval shaped nucleus about 5-12 $\mu\text{m}$  in length and chromatin is spread diffusely within. Two or more nuclei are commonly observed in each RPE cell<sup>14</sup>. Also present in the cytoplasm are melanosomes, the presence of which gives the RPE its name.

Melanosomes are abundant on the apical side of the RPE cytoplasm and are typically spindle or ovoid shaped, about 1 $\mu\text{m}$  in diameter and 1-2 $\mu\text{m}$  long<sup>15</sup>. Maturation of the melanosome occurs in three stages, forming firstly the premelanosome, then the melanosome, before progressing into a mature melanin granule that is heavily pigmented with brown or black eumelanin. The important role of melanisation in the RPE has been implicated in many functions of the neural retina and the RPE<sup>16, 17</sup>, including the normal development and maturation of the photoreceptors<sup>18</sup>. Thus, human albino retinæ which lack melanin granules have thin inner and outer nuclear layers. Whilst cone numbers are not affected, rod numbers are reduced by approximately 30%. Signalling pathways that activate melanisation may increase melanin at the

apical microvilli; an increase in melanisation in the apical RPE region contributes to an effective blocking and absorption of light reaching the photoreceptor outer segments. Melanisation attenuates retinal illuminance and thus reduces oxidative damage of the RPE and POS, which may be implicated in the down regulation of rod outer segment (ROS) phagocytosis by the RPE.<sup>16</sup> Furthermore, pathways that up-regulate melanin synthesis were suggested to adjust the consumption of oxygen by the photoreceptors, apolipoprotein E4 levels and photoisomerisation<sup>16</sup>. These events may affect the accumulation of drusen and the toxic bis-retinoid lipofuscin. Melanin within melanosomes in the RPE also absorbs light scatter and so is likely to be protective against oxidative events that lead to photo-chemical damage in the retina<sup>19</sup>.

Directly juxtaposed on the apical surface of the RPE are the photoreceptors, which comprise the highly light sensitive rods, and the cones which are less sensitive to light but have greater acuity and can differentiate colour. This research project focuses on phagocytosis of the rod outer segments and hence the rod photoreceptors will be discussed in greater detail here. The photoreceptors are highly specialised and differentiated neurons composed of a large synaptic terminal, a central body and a distal end formed of photosensitive membranous discs. These are the POS and they contain the visual pigment opsin. Photoreceptors contain a high content of photosensitive molecules that are susceptible to generation of photo-oxidative radicals. These toxins thus build up during the course of the day and accumulate at the tips of the photoreceptor outer segments. To maintain their function, the POS are shed on a circadian basis, followed by phagocytic uptake by the RPE cell for degradation. Rod photoreceptor length is maintained by continuous biogenesis of new membranous stacks at the base of the inner segment, which descends into the proximal end of the outer segment. These new disks gradually move towards the distal end and are shed shortly after light onset where they are phagocytosed by the RPE. RPE cells extend microvilli from the apical cell membrane that surrounds the POS. Following POS shedding, particles are phagocytosed into the RPE cell, where they fuse with lysosomes and the contents are degraded<sup>20, 21</sup>. This process of clearance of the shed photoreceptor outer segments is essential for the viability and function of the photoreceptors. Failure of phagocytosis causes shed POS to accumulate in the sub-retinal space, leading to photoreceptor degeneration and blindness, as observed in the Royal College of Surgeons (RCS) rat. Defective phagocytosis of shed POS may also contribute to AMD pathology in humans. Outer segment shedding and phagocytosis must also be tightly synchronised between the RPE and the photoreceptors. A failure in this coordination might lead not only to photoreceptor death as discussed above, but could also result in photoreceptors that are either too long or too short<sup>22</sup>.

### 1.2.1. Polarity and Integrity of the RPE

The RPE have many functions, which include the transport of ions, water and metabolic waste from the subretinal space to the choriocapillaris, where it also takes up nutrients such as glucose, retinol and fatty acids to the photoreceptors. Photoreceptors are also unable to reisomerize all-*trans*-retinal to 11-*cis*-retinal required for phototransduction. 11-*cis*-retinal is instead formed in the RPE and exchanged to the photoreceptors. Furthermore, the voltage-dependent ion conductance of the RPE apical membrane enables the RPE to stabilize ion composition in the subretinal space, which is essential for the maintenance of photoreceptor excitability. Photoreceptor excitability is also maintained by phagocytosis of spent POS by the RPE, which will be discussed in detail later on. The RPE are able to perform these functions because of their unique properties, which are governed by their unique polarity.

Like other epithelial cells, the RPE have an apical and a basolateral domain. They adhere to each other through complexes that form junctions between the cells, which include Gap junctions, desmosomes, adherens junctions and tight junctions. Gap junctions are distributed along the lateral membrane and form intercellular pores that allow exchange of small molecules between cells. Desmosomes and adherens junctions are adhesive junctions, which are linked to intermediate filaments and the actin cytoskeleton respectively. Tight junctions are normally located towards the apical surface of the epithelial cells and form a paracellular gate that regulates epithelial permeability. The tight junctions are linked to the actin cytoskeleton and the adherens junctions via cytoskeletal connectors: the ZO proteins which include ZO-1, ZO-2 and ZO-3. These proteins have domains that mediate binding to adherens junctions and tight junctions in addition to the actin cytoskeleton<sup>23-25</sup>.

More specifically, the Crumbs protein plays a hugely important role in RPE polarisation. The Crumbs protein, first identified in *Drosophila* as an apical protein required for polarity in ectodermal epithelia, contributes to the polarisation of epithelial cells and the assembly of the apical junctional complex and is perhaps one of the most significant cell morphology proteins in the RPE. Crumbs is localised throughout the apical membrane in simple epithelial cells but is strongly enriched just above the adherens junctions in the marginal zone; a small area of cell-cell contact<sup>26</sup> and is required for epithelial cell integrity<sup>27</sup>. Mutant crumbs (*crb*) in *Drosophila* fail to develop adherens junctions and in embryos lacking Crumbs, epithelial cells fail to develop adherens junctions<sup>26, 28</sup>. In fact, Crumbs is a major determinant of apical membrane polarity, since the overexpression of *crumbs* results in the conversion of the basolateral to apical membrane<sup>26, 29</sup>. Importantly, mutations in the human homologue CRB1 are associated with severe forms of retinal dystrophy, Leber's congenital amaurosis (LCA)<sup>30-32</sup> and Retinitis

Pigmentosa 12 (RP12)<sup>33</sup> which leads to blindness. These diseases emphasize the importance of establishing apical, circumferential junctional complexes in mediating cell-cell contact, epithelial integrity, cell shape and polarisation in the RPE.

### 1.3. The Visual Cycle

Photoreceptors require 11-*cis*-retinal for phototransduction, which is essentially the conversion of light into a transmittable signal in the retina. 11-*cis*-retinal is generated in the RPE, in a process known as the visual cycle. Light transduction starts with photon absorption by rhodopsin, which is a seven transmembrane G-protein coupled receptor, opsin and the chromophore 11-*cis*-retinal. When struck by a photon, 11-*cis*-retinal undergoes isomerisation into all-*trans*-retinal, which changes the conformation of the G-protein coupled receptor. Retinal no longer fits into the opsin binding site and so opsin undergoes a conformational change to metarhodopsin II, which is unstable and splits, yielding opsin and all-*trans* retinal. The opsin is then able to activate transducin which mediates the phototransduction cascade. To terminate the process, the active state of rhodopsin is changed to an inactive state by phosphorylation by rhodopsin kinase and binding to arrestin. Inactive rhodopsin releases the all-*trans*-retinal and is able to bind 11-*cis*-retinal again for phototransduction. All-*trans*-retinal is reduced into all-*trans*-retinol by a membrane-bound retinol dehydrogenase. All-*trans*-retinol is then carried by interstitial retinal binding protein (IRBP) to the RPE, where it is bound to cellular retinol binding protein (CRBP). Lecithin retinol acyltransferase (LRAT) initiates the esterification of all-*trans*-retinol by adding an acyl group to retinol, forming all-*trans*-retinyl ester<sup>3, 34, 35</sup>. The retinal pigment epithelium-specific protein 65 kDa (RPE65) functions as a chaperone and serves as the palmitoyl donor for LRAT. Mutations in this gene are associated with Leber's congenital amaurosis type 2 (LCA2) and retinitis pigmentosa<sup>3</sup>. Isomerisation of all-*trans*-retinyl ester into 11-*cis* retinol is mediated by an as yet unidentified isomerohydrolase. 11-*cis* retinol is finally oxidised to 11-*cis* retinal by 11-*cis* retinol dehydrogenase (11-*cis* RDH), which is supported by a cellular retinaldehyde binding protein (CRALBP), which accelerates the enzymatic process. 11-*cis*-retinal is then transported back into the rods, where it binds with rhodopsin ready for another cycle of photoactivation and transduction. The visual cycle illustrates the importance of the close interaction between the RPE and photoreceptors in visual function<sup>3, 34, 35</sup>. Figure 1.2 is a diagrammatic representation of the reactions involved in the visual cycle.

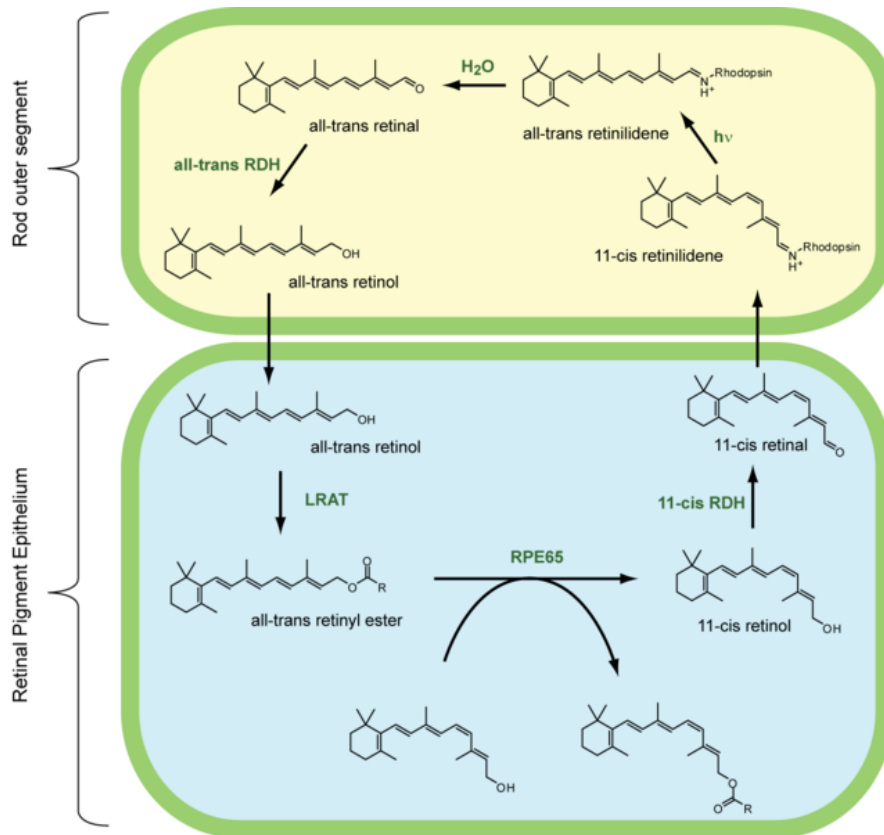


**Figure 1.2 The visual cycle**

Light transduction starts with photo absorption by the 11-*cis*-retinal containing rhodopsin, which results in isomerisation into all-*trans*-retinal. This mediates a change in conformation of the G-protein coupled receptor which results in the formation of active rhodopsin, metarhodopsin, which activates transducin in mediating phototransduction. Inactive rhodopsin releases the all-*trans*-retinal, which is reduced into all-*trans*-retinol. All-*trans*-retinol is then translocated to the RPE, where LRAT initiates the esterification of all-*trans*-retinol, forming all-*trans*-retinyl ester. Isomerisation of all-*trans*-retinyl ester into 11-*cis* retinol is mediated by an isomerohydrolase. 11-*cis* retinol is finally oxidised to 11-*cis* retinal by 11-*cis* RDH, where it binds with rhodopsin.

Figure taken from [http://en.wikipedia.org/wiki/Visual\\_phototransduction](http://en.wikipedia.org/wiki/Visual_phototransduction)

## 1.4. Circadian regulation of photoreceptor shedding and phagocytosis by the RPE

As mentioned earlier, phagocytosis of POS by the RPE is synchronised by circadian rhythms. Although there is only circumstantial evidence to suggest that phagocytosis is directly regulated by circadian rhythms, POS shedding is influenced by a circadian light-dark cycle, with a clear burst of shedding and clearance occurring about one hour after light onset for rod photoreceptors and one hour after dark onset for cones in mice<sup>36</sup>. Remarkably, the synchronised shedding of POS is maintained over a period of 3 days in the absence of light, suggesting that the process of POS shedding is not regulated by light alone but that the phenomenon nevertheless follows a light-entrained circadian rhythm<sup>37</sup>. Phagocytic activity has been suggested to be transiently down-regulated following the two circadian peaks but there is currently no clear understanding of the inactivation of the molecular components involved in RPE phagocytosis of shed POS.

The circadian regulation of photoreceptor shedding and phagocytosis is fascinating, and there have been extensive studies aimed at identifying the photoreceptor molecules responsible for this light-entrained process. Rods and cones were the first obvious cell types to be investigated for roles in circadian photoreception. Researchers studied blind animals and humans where blindness was a result of loss of either rods or cone photoreceptors. Studies in mice homologous for the autosomal recessive alleles, *rd/rd* and *rds/rds*, which results in the loss of almost all rod cells, developed a severe degeneration of rod and cone photoreceptors and almost a complete loss of visual function with the exception of a small population of cone immunoreactive cells<sup>38</sup> which could be detected even after two years<sup>39</sup>. Despite these anatomical losses, these animals still exhibit normal light-induced melatonin suppression and phase shifts. These studies support earlier work which had shown that *rd/rd* mice are still able to entrain to a light-dark cycle despite massive retina damage<sup>40</sup>. These data suggest that circadian photoreception is maintained by 1) a very small number of surviving rod or cone cells or 2) an unidentified retinal photoreceptor<sup>41, 42</sup>.

There are many candidate opsins for this role, which include the RPE-retinal G protein-coupled receptor, peropsin, encephalopsin and melanopsin, as well as non-opsin molecules such as cryptochromes and biliverdin<sup>41</sup>. Currently melanopsin remains the prime candidate for the circadian photoreceptor molecule in mammals. Melanopsin was originally identified in skin melanophore cells, which are able to sense and respond to light<sup>41, 43</sup>. Melanopsin is structurally similar to all known opsins, which allows it to operate with biochemical independence, without the need for interaction with chromophore generating molecules. Melanopsin is expressed at low levels in the ganglion cell layer, with only 0.2% - 0.8% of melanopsin expressing ganglion cells in the human retina<sup>44</sup>, but is expressed at high levels in primate amacrine cells. Notably,

expression is not observed in retinal photoreceptor cells, the opsin-containing cells of the outer retina that initiate vision<sup>45</sup>. Melanopsin expression in the retina was still maintained in blind humans with severe retinal disease<sup>44</sup>, which supports earlier studies displaying intact circadian responses to light in blind humans<sup>46, 47</sup>. These studies support a role for melanopsin as a candidate for the circadian photopigment.

## **1.5. Phagocytosis**

Phagocytosis is a highly conserved and complex process that functions to bind and internalise particles over 0.5  $\mu\text{m}$  in diameter. Binding is mediated by receptors and particle uptake is driven by actin polymerisation which proceeds in a zipper-like manner<sup>48</sup>. With the exception of yeasts, all eukaryotic organisms have evolved this mechanism of binding and engulfing and subsequently destroying particles to safeguard against pathogens, effete cells and debris that may be dangerous to healthy cells. Most studies on phagocytosis have been conducted using bacteria and macrophages, where phagocytosis is mediated by either recognition of the constant portion (Fc) of immunoglobulins (IgG) on the opsonised bacteria by the Fc receptors (Fc $\gamma$ R) or complement-opsonised particles by the complement receptor (CR3).

### **1.5.1. Fc $\gamma$ R-mediated phagocytosis**

In mammals, IgGs act as opsonins by binding to foreign particles and initiating their internalisation through recognition of the Fc domain by the Fc receptors<sup>49</sup>. Following ligation of the Fc $\gamma$ R with complexed IgG, tyrosine phosphorylation of residues within an immunoreceptor tyrosine-based activation motif (ITAM) domain is mediated by Src-family tyrosine kinases. This is essential for local actin polymerisation and phagocytosis. The tyrosine phosphorylated residues provide docking sites for Src homology 2 (SH2) domain containing proteins, which include the non-receptor tyrosine kinase Syk, which activates Vav and Rac<sup>50</sup>. The absence of Syk abolishes internalisation of IgG-opsonised particles and is critical for ITAM-dependent phagocytosis. Rac belongs to a family of proteins known as the Rho-family G proteins, also known as Rho guanosine triphosphatases (Rho GTPases). These molecules act as molecular switches that act downstream of a number of cell surface receptors to control localised actin polymerisation. Rho GTPases cycle between inactive GDP-bound and active GTP-bound conformations, and together, both Rac1 and Cdc42 have been shown to be indispensable for Fc $\gamma$ R-mediated phagocytosis. Blocking the activity of both abolished phagocytic cup formation<sup>51</sup> whilst dominant inhibition of Rac1 or Cdc42 did not affect F-actin accumulation at the phagocytic cup but eliminated internalisation of opsonised particles<sup>52</sup>. This indicates that Rac1 and Cdc42 have distinct and complementary functions. In fact, in a Rac1

mutant cell line, particles bound at the cell surface were enclosed within thin membranous protrusions that did not fuse. In contrast, inhibition of Cdc42 function resulted in pedestal-like structures with particles at their tips<sup>52</sup>. More recently, a FRET study has shown that Cdc42 activation and accumulation occurs early and was restricted to the tips of pseudopodia whereas Rac1 activation and localisation of Rac1 occurs throughout the phagocytic cup and during closure<sup>53</sup>. Rac1 and Cdc42 have been implicated in the recruitment of Arp2/3 to the phagosome, and the activity of the Arp2/3 complex is required for actin polymerisation at phagosomes and subsequent ingestion<sup>54</sup>. FcγR-mediated phagocytosis is therefore characterised by dynamic protrusions, ruffling and formation of a continuous F-actin cup. Ligation of the FcγR and activation of Cdc42 and Rac1 also produces an inflammatory response which contrasts to the more ‘silent’ complement receptor 3 (CR3)-mediated phagocytosis, which will be discussed below. Cdc42 and Rac are also implicated in the transcriptional activation of nuclear factor kappa B (NFκB) through the c-jun N-terminal kinase (JNK) and the p38 mitogen-activated protein kinase (MAPK) pathways<sup>55-57</sup>. Rac1 also regulates nicotinamide adenine dinucleotide phosphate (NADPH) oxidase enzyme complex which is responsible for the respiratory burst<sup>58, 59</sup>. Taken together, FcγR mediated phagocytosis which is dependent on Cdc42 and Rac is termed Type 1 phagocytosis<sup>54, 60</sup>.

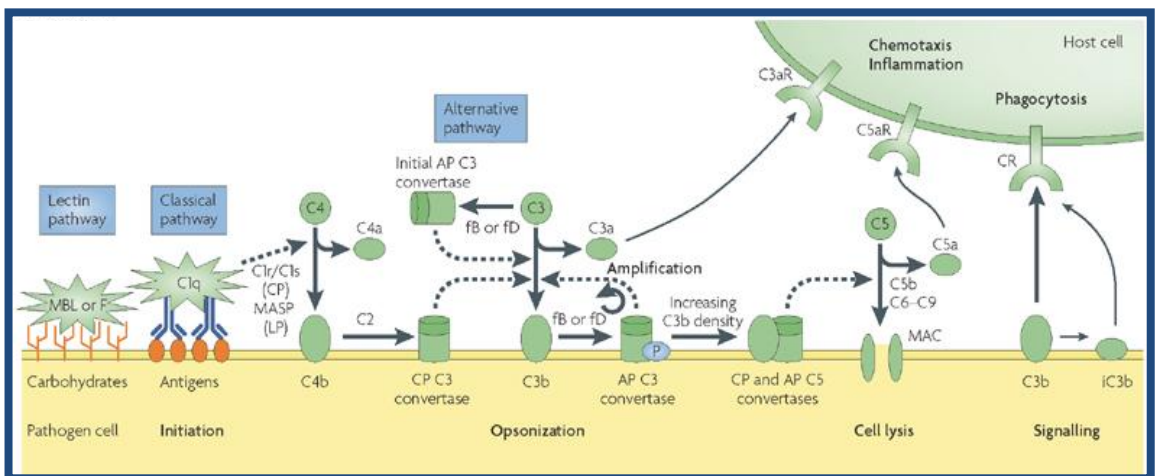
### **1.5.2. CR3-mediated phagocytosis**

‘Complement’ is a term introduced by Paul Ehrlich in the late 1890s<sup>61</sup>, based on his theory that the immune system consists of cells that have specific receptors that recognise antigens. Soluble forms of these receptors were called antibodies or ‘amboceptors’ by Ehrlich. Antibodies recognise and bind to specific antigens and to the heat-labile antimicrobial component found in serum, known as ‘complement’. Complement proteins participate in various ways to aid immune surveillance, which include binding onto antigen and opsonising them for uptake by macrophages. Complement can be activated via the classical, lectin and alternative pathways. All three result in the generation of C3b and C3bi via a series of enzymatic cascades. The C3b and C3bi fragments bind to microbes or infected cells for opsonisation to facilitate their engulfment by macrophages<sup>62</sup> (Figure 1.3).

CR3 binds to C3 and C3bi (inactivated C3b) on complement-opsonised particles, and in contrast to Type 1 phagocytosis, phagocytosis mediated by CR3 does not rely on tyrosine phosphorylation. Instead, CR3 is not constitutively active and internalisation of C3bi-opsonised particles requires receptor activation. CR3 (αMβ2) is a member of the beta 2 integrin family which is expressed exclusively on leukocytes. Integrin binding is regulated by small GTPases of the Ras subfamily by inside-out signalling<sup>51, 54</sup>. The small GTPase, Rap1, is reported to

mediate activation of CR3 in response to release of inflammatory mediators, resulting in subsequent binding and internalisation of particles opsonised with C3bi into macrophages. Moreover, Rap1 has been shown to act upstream of CR to regulate binding to C3bi opsonised particles<sup>54, 63</sup>. Once CR3 is activated by the small GTPase Rap1, actin remodelling is dependent on another Rho GTPase; RhoA. Rho function is mediated by two distinct regions of the  $\beta 2$  receptor in two steps. Rho is activated on the 16 amino acid  $\alpha$  helical region, whereby the recruitment of activated Rho is controlled by threonines 758-760 on the C-terminus of the  $\beta 2$  cytoplasmic tail<sup>64</sup>. In studies co-transfecting the two chains of the CR3 receptor with dominant negative Rho into COS cells, or treatment with C3 transferase, a Rho specific inhibitor, blocked the recruitment of the Arp 2/3 complex to the phagocytic cup and completely abolished CR3-dependent internalisation while having no effects on Fc $\gamma$ R-dependent internalisation<sup>54, 60</sup>. Rho-dependent CR3 mediated phagocytosis leads to a foci of transient accumulation of F-actin and cytoskeletal molecules underneath the bound particle<sup>65</sup> and results in passive uptake of the complement-opsonised particle which characteristically ‘sinks’ into the cell with very few (if any) pseudopodia. This is termed Type 2 phagocytosis<sup>60</sup>.

**Figure 1.3 Activation of complement and complement-mediated phagocytosis**



The complement system is activated by antibody complexes (classical pathway (CP), terminal mannose lectin pathway (LP) or by spontaneous and induced C3 hydrolysis (alternative pathway (AP)). C3 convertases then cleave C3 to its active fragments C3a and C3b. Covalent binding of C3b (opsonisation) amplifies the cascade and mediates phagocytosis and adaptive immune responses by binding to complement receptors (CRs). Accumulation of deposited C3b also leads to the assembly of C5 convertases that activate C5 to C5a and C5b. C5b initiates the formation of the lytic membrane-attack complex (MAC) which cause cell lysis. C3a and C5a induce pro-inflammatory and chemotactic responses by binding to their receptors (C3aR and C5aR) Nature Reviews Microbiology 6, 132-142<sup>(66)</sup>

### 1.5.3. POS phagocytosis by the RPE

Phagocytosis by the RPE requires POS shedding followed by three key steps, recognition and binding, ingestion and digestion. Although the mechanistic details of RPE phagocytosis are not well understood, there are currently five key molecules with proven roles in this process. These are CD36, MerTK,  $\alpha\beta5$  integrin receptor, the  $\alpha\beta5$  ligand, milk fat globule-EGF8 (MFG-E8), and focal adhesion kinase (FAK). Figure 1.4 shows a schematic diagram illustrating the roles of these molecules in RPE phagocytosis. Binding of POS requires the activation of  $\alpha\beta5$ , a unique member of the integrin family that is expressed on the apical surface of RPE cells. Binding involves recognition of the RGD motif by ligands that are presumed to exist on the POS surface or in the subretinal space. When RGD peptides or antibodies against  $\alpha\beta5$  were added to RPE cells in culture, POS binding was reduced by 85%<sup>(67)</sup>. This observation is replicated in the  $\beta5$  integrin knock out mouse, where a second role was discovered for  $\alpha\beta5$ . Firstly, it contributes to retinal adhesion and thus maintains a tight interaction between the RPE and photoreceptors, essential for visual function<sup>68</sup>. Secondly,  $\alpha\beta5$  synchronises diurnal POS phagocytosis by the RPE. Upon POS engagement,  $\alpha\beta5$  activates other proteins in the RPE to mediate cytoplasmic internalisation signals<sup>67,68</sup>, critical for the synchronisation of phagocytosis following POS shedding. In the absence of  $\beta5$ , rhythmic activation of FAK and MerTK is lost, resulting in the disappearance of the burst of ingestion which follows POS shedding<sup>69</sup>.

Recently, it has been reported that engagement of the  $\alpha\beta5$  integrin by its ligand, MFG-E8 is indispensable for the circadian synchronisation of phagocytosis<sup>70</sup>. MFG-E8 deficient RPE cells appeared normal in culture and  $\alpha\beta5$  receptor expression was not affected. Whilst the absence of MFG-E8 resulted in a negligible decrease in retinal adhesion, binding and internalisation of isolated POS was significantly impaired. In wild type and MerTK deficient RPE supplemented with MFG-E8, POS binding was significantly increased whilst there was no effect on  $\alpha\beta5$  deficient RPE. Together, these recent results identify MFG-E8 as the ligand for  $\alpha\beta5$  and show that it is absolutely critical for synchronised circadian POS phagocytosis<sup>70</sup>.

Upon POS engagement,  $\alpha\beta5$  integrin activates FAK. Multiple tyrosine residues are phosphorylated on FAK which are responsible for the direct binding to  $\alpha\beta5$  and downstream phosphorylation of MerTK<sup>71</sup>. POS binding to  $\alpha\beta5$  receptors increases FAK interaction with  $\alpha\beta5$  at the apical surface of the RPE which is essential for FAK activation. Subsequent engulfment of POS coincides with dissociation of activated FAK from  $\alpha\beta5$ . Inhibition of FAK signaling had no effect on  $\alpha\beta5$ -dependent binding but internalisation was blocked. Inhibition of FAK signaling also diminished MerTK phosphorylation which suggests that MerTK is either

directly or indirectly targeted by FAK, thus providing a critical link between particle binding and internalisation<sup>71</sup>.

Mer is a receptor tyrosine kinase (MerTK) that is required for the internalisation of POS. It is activated by phosphorylation and initiates a cascade of downstream events that lead to the uptake of the shed POS into the RPE. Much has been learned about the function of this protein from the RCS rat, which has a mutation in the coding sequence for MerTK leading to the production of a non-functional truncated protein. RPE cells from the RCS rat that lack MerTK are able to bind shed POS but are unable to internalise them. In the rat this leads to an accumulation of shed POS in the sub-retinal space and rapid progressive photoreceptor degeneration<sup>72</sup>. This phenotype is completely corrected when wild type MerTK is transferred back into RCS rat RPE cells, demonstrating that MerTK is an essential component of the phagocytic machinery<sup>73</sup>. Phagocytosis is triggered by intracellular signals from MerTK which are likely to involve second messenger molecules. In fact, there is a rise in intracellular inositol 1,4,5-trisphosphate (InsP<sub>3</sub>) following binding of POS to cells with intact MerTK. This effect is not observed in cells with disrupted MerTK. The liberation of InsP<sub>3</sub> and diacylglycerol (DAG) into the cytosol results from hydrolysis of phosphatidyl-inositol 4,5 bisphosphate (PtdIns4,5P<sub>2</sub>) following receptor-ligand binding. InsP<sub>3</sub> releases calcium from the endoplasmic reticulum stores, which together with DAG activates protein kinase C<sup>74</sup>. Whilst a rise in InsP<sub>3</sub> is clearly important in the activation of phagocytosis, increased calcium and protein kinase C activity have been previously reported to switch off POS phagocytosis<sup>75</sup>.

Several studies have previously documented that the scavenger receptor CD36 participates in human macrophage and dendritic cell phagocytosis<sup>76-78</sup> and it has also had a long-standing role in the phagocytosis of POS by the RPE<sup>79, 80</sup>. More recently its precise role has been elucidated, whereby it specifically regulates the rate of POS internalisation by the RPE. Finnemann *et al* (2001)<sup>81</sup> found that CD36 antibodies affected the rate of POS internalisation by the RPE without affecting binding. Their study demonstrated that CD36 ligation by POS was sufficient to activate POS internalisation, which suggests that CD36 acts as a signalling molecule independently of  $\alpha\beta 5$  following POS binding<sup>81</sup>. Intiguently, in the recent literature, tetraspanin CD81 has been shown to promote POS binding by interaction with integrin  $\alpha\beta 5$  despite having no known function as a binding receptor. Further studies on CD81, which is the only tetraspanin to be highly expressed in the RPE will provide further insight into the mechanisms mediated by this transmembrane protein<sup>82</sup>.

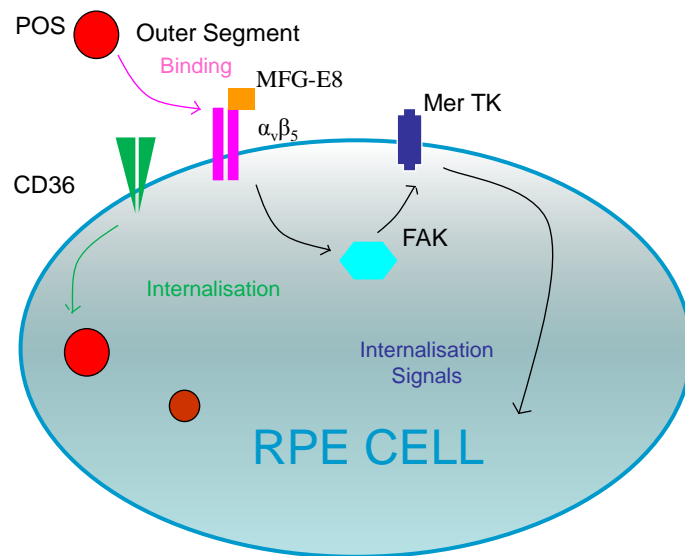


**Figure 1.4 Schematic diagram of the current RPE phagocytosis model**

In the current model, POS binds to  $\alpha v \beta 5$  which activates focal adhesion kinase (FAK), which in turn phosphorylates MerTK which mediates signal transduction, resulting in POS internalisation<sup>67, 71</sup>.  $\alpha v \beta 5$  is localised specifically to the apical microvilli of the RPE and contributes to retinal adhesion and thus maintains the RPE and photoreceptor interaction, essential for visual function<sup>68</sup>. Furthermore,  $\alpha v \beta 5$  synchronises diurnal POS phagocytosis by the RPE which is dependent on engagement with MFG-E8.

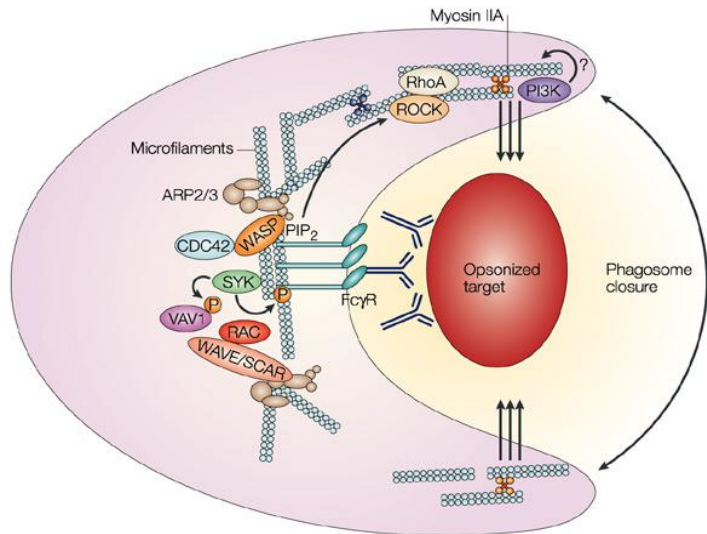
#### 1.4. Actin Dynamics in Phagocytosis

The biological actions of the Rho family GTPases are mediated by their GTP-dependent recruitment and interaction with downstream effectors, which in turn are able to bind and activate the actin nucleating Arp 2/3 complex that regulates the actin cytoskeleton during phagocytosis. As discussed above, recruitment and activation of the Arp 2/3 complex is indispensable for both Type 1 and Type 2 phagocytosis. The WASP (Wiskott-Aldrich Syndrome Protein) and Scar/WAVE (Suppressor of cAMP receptor/WASP family Verprolin-homologous) proteins are two key effectors identified downstream of Cdc42 and Rac. WASP and its close relative N-WASP, which belong to the WASP family of five molecules that indirectly link the plasma membrane receptors to actin polymerisation, are essential for cell activities such as phagocytosis<sup>83</sup>. WASP and N-WASP directly bind to Cdc42 and Src family kinases and are responsible for mediating the cytoskeletal effects induced by active Cdc42.

WASP exists in an auto-inhibitory conformation which is activated by binding to active, GTP-bound Cdc42 and PtdIns4,5P<sub>2</sub>, which then can subsequently interact with and activate the Arp 2/3 complex<sup>84, 85</sup>. It is therefore likely that the localisation and activation of Cdc42, which is coincidental to the transient enrichment of PtdIns4,5P<sub>2</sub> at the forming phagosome, is involved in the activation of WASP. Figure 1.5 shows the interaction of these cytoskeletal proteins during type 1 phagocytosis.

**Figure 1.5 Signalling events associated with activation of Fcγ receptor(s) on phagocytic cells.**

Following ligation of the FcγR with complexed IgG, tyrosine phosphorylation of residues within an immunoreceptor tyrosine-based activation motif (ITAM) domain is mediated by Src-family tyrosine kinases. The tyrosine phosphorylated residues provide docking sites for Src homology 2 (SH2) domain containing proteins, which include the non-receptor tyrosine kinase Syk, which activates Vav and Rac<sup>50</sup>. The Rho-GTPases, Rac1 and Cdc42 have been implicated in recruitment of Arp2/3 to the phagosomes and the activity of the Arp2/3 complex is required for actin filament polymerisation at FcγR mediated phagosomes and subsequent ingestion<sup>54</sup>. WASP and WASP family verprolin-homologous protein (WAVE/SCAR) are activated by directly binding to Cdc42, Src kinases and PtdIns4,5P<sub>2</sub>, which then can subsequently interact with and activate the Arp 2/3 complex<sup>84, 85</sup> to mediate actin filament polymerisation..



Nature Reviews Immunology 4, 110-122<sup>(86)</sup>

### **1.4.1. Actin polymerisation**

Actin is a highly conserved globular protein of approximately 42 kDa and is expressed in all eukaryotic cells. Actin monomers, also known as globular actin (G-actin), bind one molecule of ATP which is hydrolysed to ADP on polymerisation. Polymerisation of actin monomers is essential to form filamentous actin (F-actin), a component of the cell cytoskeleton with roles in mediating cell transport, motility, cell division, cytokinesis, and establishment and maintenance of cell junctions and shape. Actin filaments grow and shrink by addition or loss of monomeric actin from either end of the filament. The two ends are referred to as 'barbed' or 'pointed' and actin monomers are predominantly added to the barbed ends, whilst monomers are lost at the pointed ends. In this way, proteins that bind filament ends are able to control actin polymerisation. Capping proteins bind to the filaments so that actin monomers cannot be added or removed, whilst others bind onto filaments to mediate branching and nucleation<sup>87-89</sup>. Capping proteins are counteracted by formins such as DIA1 and the scaffolding protein vasodilator-stimulated phosphoprotein (VASP), both of which induce actin polymerisation at barbed ends through incorporation of actin monomers bound to the actin-binding protein, profilin<sup>90</sup>.

### **1.4.2. Arp 2/3 activity and actin nucleation**

The Arp 2/3 complex was originally described as a complex of seven molecules, of which two unconventional actins were known as actin-related proteins or Arps. The Arp 2/3 complex is an actin nucleator and its recruitment and activation is responsible for *de novo* actin nucleation and branching of pre-existing actin filaments. Arp 2/3 stimulates actin filament growth from the barbed ends by acting as a structural mimic of actin dimers and trimers, to prevent monomer dissociation and thus enables polymerisation. Nucleation promotion factors such as WASP/SCAR/WAVE trigger conformational changes in the Arp 2/3 complex to bring Arp 2 and Arp 3 together for actin dimer mimicry. They also recruit actin monomers, provide a template for nucleation, and catalyse polymerisation of new (daughter) filaments from an existing (mother) filament via filament branching<sup>88</sup>. Once nucleated, actin filaments extend freely at the barbed ends until actin monomers (G actin) are depleted or the ends are capped by actin capping proteins. Whilst free barbed ends are created for actin nucleation and polymerisation, cessation of polymerisation, mediated by capping proteins may be necessary to control polymerisation at different times and at different locations.

### **1.4.3. Regulation of actin assembly and disassembly**

Actin assembly and disassembly is important during phagocytosis, where actin dynamics are regulated by actin depolymerisation, severing, capping and uncapping. During phagocytosis,

actin filaments are disassembled both during and after particle internalisation, as has been observed in the disappearance of F-actin from phagosomes in *Dictyostelium* and mammalian phagocytes after internalisation<sup>51</sup>. Actin disassembly may occur by debranching, severing or depolymerisation, and may be mediated by various molecules, including cofilin.

The activity of cofilin is regulated by phosphorylation, such that phosphorylation on the N-terminus of cofilin results in inactivity, whilst dephosphorylation induces activity<sup>91</sup>. Cofilin is necessary for phagocytosis, which requires a turnover in cofilin-dependent depolymerising activity. In *Dictyostelium*, GFP-cofilin accumulates into actin bundles at the phagocytic cup<sup>92</sup>, and in mammalian cells cofilin is dephosphorylated and recruited to the phagocytic cup during the phagocytosis of serum-opsonised zymosan. Dephosphorylation of cofilin is also accompanied by a transient increase in F-actin<sup>93</sup>. Cofilin is directly phosphorylated by LIM kinase (LIMK) to control actin filament turnover. Phosphorylation of a serine residue in its N-terminus by LIMK blocks the actin binding and depolymerisation activity of cofilin. Cells expressing a dominant negative mutant of LIMK1 have been shown to suppress the total amount of F-actin in macrophage-like U937 cells<sup>94</sup>, which is consistent with the transient increase in F-actin observed when cofilin is dephosphorylated<sup>93</sup>. These results suggest that LIMK1 regulates the functions of phagocytes through phosphorylation of cofilin and enhances the formation of filamentous actin. Different isoforms of LIMK are phosphorylated by p21-activated kinase 1 (PAK1), an effector of Rac1, Cdc42 and ROK (RhoA effector), which has been shown to accumulate at the phagosome<sup>95-98</sup>. LIMK is stimulated by direct phosphorylation on Thr 508 in the activation loop of its kinase domain, and direct phosphorylation of cofilin by LIMK blocks cofilin activity<sup>95</sup>. This suggests that the Rho GTPases could control actin polymerisation downstream of both FcγR- and CR3-mediated phagocytosis. Cofilin is presumably regulated by the 64 kDa protein DAip1 from *Dictyostelium*, which is homologous to the actin-interacting protein 1, Aip1p, from *Saccharomyces cerevisiae*. DAip1 depleted cells are impaired in phagocytosis<sup>92, 99</sup>.

Gelsolin is a 82 kDa actin binding molecule, regulated by calcium and PtdIns4,5P<sub>2</sub>, that acts on actin filaments by either severing or capping them and is another key regulator of actin assembly and disassembly<sup>100</sup>. Gelsolin has been found to localise to the phagocytic cup during internalisation of particles in both polymorphonuclear (PMN) leukocytes and in macrophages<sup>101</sup>. In neutrophils devoid of gelsolin, attachment and ingestion of particles by FcγR-mediated phagocytosis were both reduced, although actin was still able to polymerise around the phagocytic cup. In contrast, CR3-mediated phagocytosis in gelsolin-deficient neutrophils was

only merely delayed. Gelsolin was therefore hypothesised to be specifically involved in cytoskeletal changes associated with pseudopod formation during the early stages of FcγR-mediated phagocytosis. Once internalisation is complete, actin filament formation around the ingested phagosome is not affected by gelsolin. Gelsolin activity is specific for FcγR-mediated phagocytosis, where actin dynamics are more active, and where it forms part of the molecular machinery that distinguishes Type 1 and Type 2 phagocytosis<sup>102</sup>.

#### 1.4.4. Motor proteins in phagocytosis

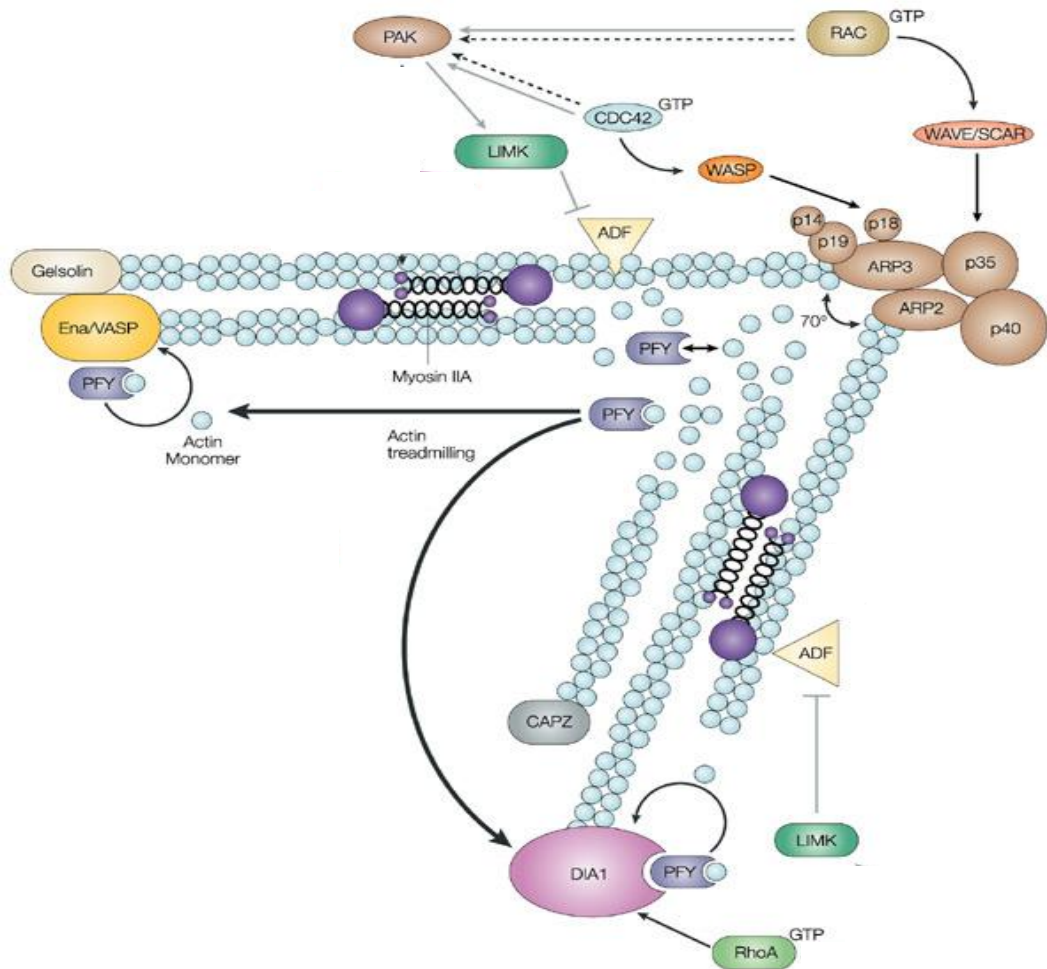
Most research on phagocytosis so far has concentrated on actin remodelling as the key mediator of particle internalisation but there is growing evidence that motor proteins of the myosin family also have an important role in FcγR-mediated phagocytosis. Different isoforms have been reported by several groups to be recruited to the phagosome during internalisation. These include myosin I to phagosomes engulfing zymosan particles, myosin II recruitment in FcγR-mediated phagocytosis by polymorphonuclear leukocytes (PMNL)<sup>103</sup> and mouse macrophages<sup>104</sup>, during which myosin IC, myosin Va and myosin IXb were also observed to localise to the phagosome<sup>104</sup>. At least one of these isoforms may be involved in generating a contractile force, which has been proposed to exist after stimulation of the pseudopod extension during engulfment, to mediate constriction of the pseudopod for phagosome closure. Some of these myosins are also implicated in signal transduction and membrane trafficking and so the myosins may have an additional role in regulating membrane availability<sup>49, 104</sup>. In addition, in *Dictyostelium*, myosin IB, myosin IK, myosin II and myosin VII have been reported to be involved in phagocytosis<sup>49, 105-107</sup>. Of these myosins, myosin II and VII have also been shown to have roles in RPE phagocytosis<sup>108, 109</sup>.

The importance of myosin II in the retina is highlighted in a recent publication reporting that it is directly linked to MerTk, which as described earlier, is a tyrosine kinase indispensable for particle internalisation. Strick *et al*, (2009) showed that whilst the absence of MerTK does not affect the recruitment of actin to the phagocytic cup, the loss of MerTK function was shown to severely disrupt the localisation of myosin II and inhibition of myosin II was shown to inhibit phagocytosis in RPE cells. They propose that myosin II may function in RPE POS phagocytosis in regulating the extension or closure of pseudopodia that form the phagocytic cup<sup>109</sup>. Mutations in the myosin VIIa gene (*MYO7A*) cause blindness and deafness, collectively known as Usher syndrome type 1B (USH1B). The retinas of *Myo7a* mutant mice, also known as Shaker 1 mice, are deaf and have abnormal electroretinograms. In the eye, these animals display an absence of melanosomes from the apical processes<sup>110</sup> and a slower rate of disk

membrane renewal<sup>111</sup>. Furthermore, the absence of myosin VIIa resulted in the retardation of phagosomes in the apical processes of the RPE, resulting in slower degradation of the phagosomes<sup>108</sup>. Phagocytosis of POS was not blocked and so its inhibition may cause a more subtle and progressive blindness that occurs at a slower pace in comparison to the MerTK null phenotype, which results in blockage of ingestion and photoreceptor degeneration<sup>112</sup>. Retarded degradation of the phagosome contents could also have adverse effects on the RPE and photoreceptor viability over time. The observed accumulation of apical phagosomes in the Shaker 1 retina may arise from slower transport through the connecting cilium of the photoreceptors, which was shown previously to retard disk membrane renewal in these animals<sup>111</sup>. Gibbs *et al*, (2003)<sup>108</sup> suggested in this study that if the ingestion of disk membranes is regulated by the presence of phagosomes in the apical region, ingestion could be inhibited because of phagosome retention in the apical region, as the addition of new disks to the base of the photoreceptors and phagocytosis of POS, in part to maintain the length of the photoreceptors, come hand-in-hand. Alternatively, the observed defect in POS phagocytosis may cause the retarded photoreceptor disk renewal originally observed in the Shaker 1 mouse. Myosin VIIa is suggested to participate in the normal apical to basal transport of phagosomes into the RPE for lysosomal degradation by delivering the phagosome to a microtubule motor system, using short actin filaments. Myosin VIIa is therefore involved in the post-engulfment trafficking of phagosomes in the retinal pigment epithelium. In support of this idea, phagosome transport was inhibited in the presence of the microtubule depolymerising agent, colchicine<sup>113</sup>.

Although roles in retinal phagocytosis have not yet been formally described or elucidated, for many of the actin-regulatory proteins discussed here, the likelihood is that most of the fundamental mechanisms controlling phagocytosis in other cell types will also apply in RPE cells. Figure 1.6 is a schematic diagram illustrating how these regulators of actin dynamics act in the regulation of actin polymerisation. Another key regulator of actin dynamics, absent from this figure, is annexin 2, one of a large protein family which through its activities as an actin capping and G-actin binding protein, might be hypothesised to have a role in retinal phagocytosis. Since this question forms the major focus of this thesis, the role of annexin 2 as an actin regulator follows a general introduction of the annexin family.

**Figure 1.6 The regulation of actin polymerisation**



The schematic illustrates the mechanisms that are involved in the regulation of actin polymerisation (black arrows), actin polymer stability (grey arrows) and contraction (dashed arrows). WASP and WASP family verprolin-homologous protein (WAVE/SCAR) are activated by directly binding onto Rac and Cdc42, which then can subsequently interact with and activate the Arp 2/3 complex<sup>84, 85</sup> to mediate pointed- end nucleation. Barbed-end growth is limited by capping proteins such as CAPZ (capping protein muscle Z-line) and gelsolin. Capping proteins are counteracted by formins such as DIA1 (activated by RhoA), and the scaffolding protein vasodilator-stimulated phosphoprotein (VASP). Both of them induce actin polymerisation at the barbed end through incorporation of actin monomers bound to profilin (PFY). Rac and Cdc42 activate p21-associated kinase (PAK), which results in the phosphorylation of LIM kinase (LIMK), and in turn blocks the actin binding and depolymerisation activity of cofilin by phosphorylating its N-terminus.

Adapted from Nature Reviews Immunology 4, 110-122<sup>(86)</sup>

## 1.5. The Annexins

Annexins can be defined as  $\text{Ca}^{2+}$  and phospholipid-binding proteins that are able to bind to negatively-charged phospholipids in a calcium-dependent manner. All annexins contain a conserved C-terminal protein core which typically consists of four repeats of about 70 amino acid residues. Each repeat is made up of five  $\alpha$  helices and the four repeats form together a highly packed  $\alpha$ -helical curved disk with two faces<sup>114</sup>. The convex side contains type II and type III  $\text{Ca}^{2+}$  binding sites and binds phospholipid membranes. The concave side is orientated away from the membrane and interacts with the N-terminal domain (Figure 1.7). The core mediates  $\text{Ca}^{2+}$ -regulated membrane binding which is usually reversible. In the presence of phospholipids, the affinity of type II  $\text{Ca}^{2+}$  binding sites for  $\text{Ca}^{2+}$  increases. Carbonyl and carboxyl groups of the amino acid backbone and phosphoryl structures of phospholipid membranes are co-ordinated to mediate  $\text{Ca}^{2+}$ -binding<sup>115</sup>.

The annexin N-terminal domain is variable in length, consisting of about 10-150 amino acid residues, and is thought to modulate the  $\text{Ca}^{2+}$ -and membrane binding activities of the core domain<sup>115</sup>. In a  $\text{Ca}^{2+}$  free environment, the N-terminus of annexin 1 is normally hidden in the conserved carboxyl core of the protein, but is released in the presence of  $\text{Ca}^{2+}$ . In this way, and perhaps for other annexins,  $\text{Ca}^{2+}$  is able to mediate a conformational change, resulting in the presentation of the N-terminus as well as regulating phospholipid binding. Once exposed, various cytosolic protein ligands can bind to the N-terminal domains of the annexins. Many of these ligands belong to the EF-hand superfamily of  $\text{Ca}^{2+}$ -binding proteins, enabling annexin monomers to interact with each other to form dimers and tetramers. These structures therefore contain at least two annexin membrane binding domains that are bridged by the bound ligand and so are able to form connections or links between two membrane surfaces<sup>115</sup>. An example of such an annexin-ligand interaction will be given in the next section. These features also explain the name 'annexin', derived from the Greek meaning 'bring/hold together'<sup>116</sup>. In addition to interacting with other proteins, the N-terminal domain is also subject to post-translational modifications, including myristoylation and phosphorylation<sup>115</sup>. For example, non-myristoylated annexin A13b only binds to acidic phospholipids at high  $\text{Ca}^{2+}$  concentrations. Myristoylation of annexin A13b allows  $\text{Ca}^{2+}$ -independent binding to phosphatidylcholine, raft-like liposomes and acidic phospholipids<sup>117</sup>. Phosphorylation of the N-terminal domains of annexins 1 and 2 has been shown to increase proteolytic sensitivity and alter the  $\text{Ca}^{2+}$  affinities of their core domains<sup>115</sup>. The N-terminal domain is unique to each annexin and is largely responsible for the diverse functions of the annexins, despite their overall structural and biochemical similarities.

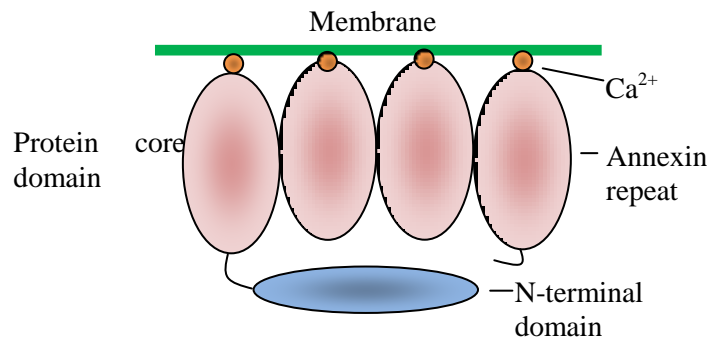


**Figure 1.7 Schematic drawing of an annexin that is peripherally attached to a membrane surface through bound  $\text{Ca}^{2+}$  ions**

A typical annexin utilises  $\text{Ca}^{2+}$  (orange) to bind to the inner leaflet of the plasma membrane (green), such that the N-terminus (blue) is oriented away from the membrane and lies in close proximity to the C-terminus. Note that although all four repeats are depicted as binding  $\text{Ca}^{2+}$ , there is no individual annexin known to contain type II  $\text{Ca}^{2+}$ -binding sites in all repeats. Adapted from Nature Reviews Molecular Cell Biology 6, 449-461<sup>(115)</sup>

Annexins are expressed in all eukaryotic cells and are generally localised to the cell cytosol, existing in a soluble form or in association with a variety of structural proteins<sup>114</sup>. Some annexins have also been shown to localise to the nucleus and to be expressed on the cell surface where they exert their functions, for example the regulation of blood clotting by annexin 2<sup>118, 119</sup>. The expression and tissue distribution of the 12 members of the annexin family also varies from widespread for annexins 1, 2, 4, 5, 6, 7, 11 to selective for annexin 3 in neutrophils, and annexin 8 which is expressed specifically in the placenta and skin<sup>120</sup>. The expression of some annexins may also be classed as ‘restrictive’ in that they are only expressed under specific conditions. Both annexins 9 and 10 are non-conventional members. Annexin 9 contains mutations in residues considered crucial for  $\text{Ca}^{2+}$  co-ordination and is only able to bind to phosphatidylserine-containing liposomes when  $\text{Ca}^{2+}$  levels exceed 2 mM<sup>121</sup>. Annexin 10 contains a codon deletion in the conserved repeat 3 and ablation of type II  $\text{Ca}^{2+}$  binding sites in repeats 1, 3 and 4 of its carboxyl terminal core. Annexin 10 expression is rare and expression at the mRNA level is tissue restricted and developmentally regulated<sup>120</sup>. Annexin 13 is the oldest member of the annexin family and is considered the progenitor of the 11 other members of the family. Its expression is highly tissue specific, being restricted to intestinal and kidney epithelial cells<sup>122</sup>. The conserved carboxyl core is important for mediating the  $\text{Ca}^{2+}$ -regulated membrane binding activities of annexins. Changes to this highly conserved domain as described for annexins 9 and 10 are believed to adapt the annexin to the particular needs of the host species and host tissue.

## 1.6. Annexin 2

### 1.6.1. Structure

Annexin 2 is a 36 kDa protein, expressed in most eukaryotic cell types though predominantly epithelial and endothelial cells. It consists of a 33 kDa conserved carboxyl terminal region made up of four repeats of the conserved 70 amino acid domain and a 3 kDa N-terminal domain consisting of 30 amino acids. The annexin 2 core domain contains binding sites for  $\text{Ca}^{2+}$ , phospholipids and F-actin<sup>123</sup>. The N-terminal domain contains the binding site for its S100 ligand, S100A10, also known as p11, and has phosphorylation sites on tyrosine 23, serine 11 and serine 25. In fact, annexin 2 was discovered in 1980 by Erikson *et al* as one of the major substrates phosphorylated by c-Src<sup>124</sup>. They observed that a 34 kDa protein (later cloned as annexin 2) was a direct substrate for c-Src and that phosphorylation of this protein led to effects on cellular transformation<sup>125</sup>. Phosphorylation of annexin 2 has also been shown to affect the binding of p11 and calcium. In its unphosphorylated state, the three phosphorylation sites are hidden in the core domain, and in the absence of  $\text{Ca}^{2+}$  the N-terminal domain is hidden within the protein core. In the presence of  $\text{Ca}^{2+}$ , a conformational change is induced and the N-terminal domain of annexin 2 is released for interaction and modification (Figure 1.8).

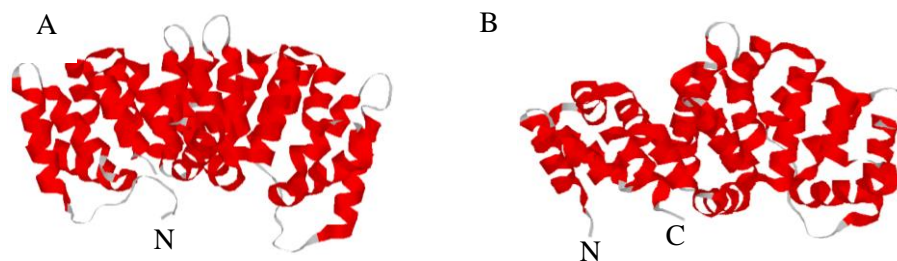


**Figure 1.8 Structure of human annexin A2 in the absence (A) and presence (B) of calcium ions**

Images from Protein data bank (PDB)

Annexin 2 binds to its specific ligand, S100A10 (p11), which is a small protein belonging to the EF hand super-family. S100 proteins are characterised by two EF hands, each of which is folded to form a helix-loop-helix  $\text{Ca}^{2+}$  binding domain. This feature of the S100 protein allows it to interact with and regulate target proteins in a  $\text{Ca}^{2+}$  dependent manner. However, S100A10 is the only member of the S100 family that contain mutations and deletions in this region, rendering the  $\text{Ca}^{2+}$  sites non-functional. The deletions hold the protein in an equivalent  $\text{Ca}^{2+}$  loaded structure and thus render it constitutively active with a high affinity for annexin 2<sup>(126)</sup>.

Annexin 2 binds to S100A10 via its N-terminal domain with high affinity and specificity. Binding leads to formation of a heterotetrameric complex consisting of two S100A10 dimers and two annexin 2 monomers. Annexin 2 usually exists in this form in most cell types<sup>123</sup>. In its tetrameric form, annexin 2 is able to link two separate phospholipid bilayers, bridged by the S100A10 dimer. In this way, annexin 2 is able to connect phospholipid membranes and form aggregates of membrane vesicles under the influence of micromolar levels of  $\text{Ca}^{2+}$  (Figure 1.9 (B)). However, when only one continuous membrane surface is available, the annexin 2-S100A10 complex binds with both annexin subunits to the membrane, probably in the configuration indicated in Figure 1.9 (A). In this configuration, S100A10 is able to interact with additional molecules in the cell cytosol. Under physiological conditions, S100A10 exists normally in its dimeric form, which is thought to be critical for its ability to mediate the described heterodimerisation with annexin 2. This localisation to the membrane cytoskeleton allows annexin 2 to interact with cell surface receptors and ion channels where it has been suggested to regulate cell-cell contacts and form membrane vesicle aggregates<sup>116, 127</sup>.

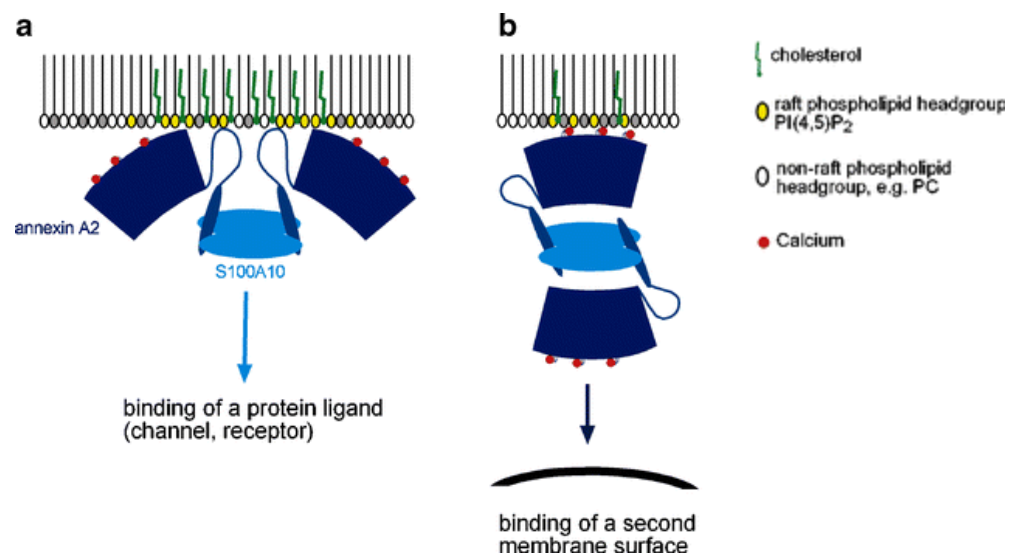


**Figure 1.9 Configurations of the membrane-bound annexin A2-S100A10 complex**

A) Both annexin A2 sub-units bound to the same membrane surface. An alternative configuration with the two annexin A2 sub-units bound to opposite membranes is seen in cryo-electron microscopy of lipid vesicles linked via the annexin A2-S100A10 complex (B). Membrane binding of annexin A2 occurs preferentially at sites rich in cholesterol and phosphatidylinositol (4,5) bisphosphate (PtdIns4,5P<sub>2</sub>).

Pflügers Archive - European Journal of Physiology 4, 575-582<sup>(127)</sup>

### 1.6.2. Interactions involving annexin 2

In addition to its interaction with S100A10, annexin 2 interacts with a number of cytoskeletal proteins. Annexin 2 binds *in vitro* to F-actin via its carboxyl protein core and has Ca<sup>2+</sup>-dependent actin bundling properties which are enhanced when annexin 2 is in its heterotetrameric complex<sup>128, 129</sup>. More recently annexin 2 has been shown to have a direct role in actin remodelling. Annexin 2 binds and sequesters G-actin and co-localises to the barbed ends of actin filaments. *In vitro* assays have demonstrated that annexin 2 can inhibit polymerisation at the barbed ends of F-actin filaments, whilst having little effect at the pointed ends. Incubation of growing F-actin filaments with annexin 2 also resulted in shorter actin filaments. From these studies it was proposed that annexin 2 can regulate actin filament turnover most likely through G-actin sequestration and its barbed-end capping activities<sup>130</sup>.

Annexin 2 has also been found to interact directly with PtdIns4,5P<sub>2</sub>, which provides another mode of membrane binding. Annexin 2 and its ligand S100A10 are found to localise to sites where PtdIns4,5P<sub>2</sub> is enriched and also where F-actin accumulates. Annexin 2 binds specifically to PtdIns4,5P<sub>2</sub>, a property not shared by all members of the annexin family, and its affinity for PtdIns4,5P<sub>2</sub> is comparable to that of other PtdIns4,5P<sub>2</sub> binding proteins<sup>131, 132</sup>. The specific properties of annexin 2 in actin regulation and binding to PtdIns4,5P<sub>2</sub> explain annexin 2 association with vesicle membranes during endocytosis<sup>133-137</sup> and pinocytosis<sup>138</sup>, and its localisation to phagosomes in J774 macrophages<sup>139</sup>. Its direct involvement with both actin and membrane dynamics suggests that annexin 2 mediates the bridging of membranes with the actin cytoskeleton. In support of this idea, a direct link has been shown between annexin 2, vesicle membranes and polymerising actin<sup>138</sup>, and recently it has been demonstrated that annexin 2 is able to nucleate actin polymerisation *in vitro* on beads coated with PtdIns4,5P<sub>2</sub><sup>140</sup>. Furthermore, F-actin nucleation and polymerisation on early endosomes was strictly dependent on annexin 2<sup>136</sup>.

Annexin 2 has also been shown to interact with the 3'-untranslated region of its own mRNA and so may thus have a role in the regulation of its own protein synthesis. It also binds to the localisation signal of *c-myc* mRNA<sup>141</sup> which leads to translation on cytoskeleton-bound polysomes. Annexin 2 has also been demonstrated to act as a nuclear shuttle protein and so may function in the transport and targeting of specific mRNAs<sup>142</sup>. The mRNA binding site of annexin 2 was located to domain IV, and shown to be Ca<sup>2+</sup>-dependent and specific<sup>143</sup>.

Annexin 2 is also localised to the extracellular surface of endothelial cells and certain tumour cells, where it acts as a surface anchor for a number of different molecules. One that has been

extensively studied involves its interaction with tissue plasminogen activator (tPA) which will be discussed in more detail later (1.6.3).

### 1.6.3. Post-translational Modifications

Annexin 2 activity is modulated by a variety of post-translational modifications, of which the best studied is phosphorylation. Annexin 2 is phosphorylated on its N-terminal domain by a number of tyrosine/serine/threonine kinases. Phosphorylation on tyrosine 23 by the c-Src kinase alters  $\text{Ca}^{2+}$  and membrane binding. Tyrosine phosphorylation of annexin 2 decreases its affinity for binding to phospholipids and  $\text{Ca}^{2+}$ , which has been shown to affect annexin 2-S100-A10 tetrameric activity in mediating aggregation of chromaffin granules. In support of the idea of negative regulation of  $\text{Ca}^{2+}$  and membrane binding by phosphorylation, there is an increase in phosphorylation on Tyr-23 by c-Src when annexin 2 is membrane bound<sup>116</sup>. Recently, phosphorylation of annexin 2 by activated c-Src was shown to lead to the co-localisation of annexin 2 with active c-Src and FAK at the cell membrane. When phosphorylated, annexin 2 mediates the targeting of c-Src to the cell membranes, where it is activated. Activation of c-Src then leads to subsequent phosphorylation of annexin 2 which is required for stimulation of actin dynamics<sup>144</sup>. In addition to this, de Graauw *et al* (2008) have shown that annexin 2 phosphorylation is important in actin remodelling and is suggested to regulate the activation of cofilin<sup>145</sup>.

Annexin 2 is ubiquitinated *in vivo* but other studies *in vitro* failed to demonstrate annexin 2 ubiquitination or degradation, presumably due to lack of accessory proteins that are normally present in cells. In addition to mediating protein degradation, ubiquitination also regulates protein localisation, activity and binding partners, and is suggested to have importance in the role of annexin 2 in actin regulation<sup>146</sup>.

The N-terminal domain of annexin 2 is also modified during oxidative stress, resulting in *S*-glutathiolation of the Cys-8 residue, which is located in the S100A10 binding site. Whilst this modification does not affect S100A10 binding, a general cysteine modification with *N*-ethylmaleimide (NEM) of the annexin 2-S100-A10 complex which is also likely to modify the same Cys-8 residue, strongly reduces the ability of the complex to mediate lipid vesicle aggregation<sup>116</sup>. The importance of post-translational modifications is further highlighted with regard to the interaction of surface-bound annexin 2 with plasminogen and tissue plasminogen activator (tPA), which is inactivated by the atherogenic lipoprotein A and homocysteine respectively. Annexin 2 binds to tPA via its N-terminal domain, in which the Cys-8 residue may be replaced by homocysteine, rendering a decrease in tPA binding. Annexin 2 therefore

has an anti-thrombotic role in the vascular environment with major implications in cardiovascular disease<sup>116</sup>.

#### **1.6.4. The project**

Interest in the possible involvement of annexin 2 in RPE phagocytosis was sparked a few years ago when the functional differentiation of ARPE-19 cells was studied. ARPE-19 is an immortalised human RPE cell line that partially retains the phagocytic function of RPE cells. The functional differentiation of these cells was associated with both an up-regulation of phagocytosis and an up-regulation of annexin 2 at both mRNA and protein levels<sup>147</sup>. This observation is consistent with proteomic analyses of the RPE and RPE apical processes, which have identified many actin modulators including several members of the annexin family of Ca<sup>2+</sup> and phospholipid-binding proteins, that may mediate phagocytic cup formation and engulfment during POS phagocytosis<sup>148, 149</sup>.

This project thus extends earlier studies in the lab suggesting that annexin 2 has a role in the phagocytic function of RPE cells. Initial experiments revealed that annexin 2 colocalised with actin during the early stages of outer segment internalisation. This co-localisation was also apparent in the partially internalised outer segment, but annexin 2 dissociates away from the phagosome once internalisation is complete. Research commenced using two cell lines: ARPE-19, and RPE-J. In the first part of the project, cells were treated with annexin 2 siRNA in both cell lines to see if depleting annexin 2 affects phagocytosis of POS. The localisation of annexin 2 during phagocytosis of purified and labelled POS was also examined by confocal microscopy. This was followed by biochemical studies to elucidate the molecular mechanisms involved, and experiments on the annexin 2 knock out mouse to understand how and where annexin 2 fits into the current model of RPE phagocytosis.

# **Chapter 2**

## **Materials and Methods**

## **2. Materials and Methods**

### **2.1. Cells**

ARPE-19 is a spontaneously immortalised cell line, developed from primary RPE cultures isolated from a 19 year old male. RPE-J is a cell line derived from RPE isolated from the Long Evans rat. These cells were immortalised by infection with a temperature-sensitive A mutant (tsA) SV40 virus. TsA of SV40 viruses encodes the large T antigen which is transforming at the permissive temperature of 33°C and inactive at the non-permissive temperature (39-40°C). ARPE-19 cells were kindly donated by Dr Anthony Vugler (UCL Institute of Ophthalmology), and RPE-J cells from Silvia Finemann (Cornell University, USA). Porcine RPE and rod outer segments were harvested from porcine eyes (Cheale Meats Ltd, Brentwood UK).

### **2.2. Equipment**

#### **2.2.1. Microscopes**

A Leica TCS-SP2 confocal microscope was used for imaging cells plated on glass cover slips or glass bottom dishes. Cells plated onto plastic dishes were imaged using a Zeiss LSM510UV upright microscope. All flat-mounted eyes were imaged on a Leica DM IRB Image Capture Fluorescence microscope. Eyes processed for transmission electron microscopy (TEM) were viewed on a Joel 1010 transmission electron microscope and images were processed with Kodak electron microscope film 4489 or acquired digitally with a Gatan OriusSC100B CCD camera.

#### **2.2.2. Plate readers**

Phagocytosis assays with fluorescently labelled rod outer segments were read with a Safire plate reader (SAFIRE; Firmware: V.2.00 03/02 Safire; XFLUOR4 Version: V 4.20)

#### **2.2.3. PCR Machines**

Polymerase Chain Reactions (PCRs) were carried out on a Mastercycler egradient S or a Mastercycler gradient PCR machine (Eppendorf).

## **2.3. Animals**

Annexin 2 knock out mice and C57BL/6 wild type mice were kindly donated by Dr Katherine Hajar (Cornell University, USA). Previous characterisation of the annexin 2 knock out mice showed that these mice are viable and fertile<sup>119</sup>. The animals were housed under 12 h light and 12 h dark cycles and were maintained and bred on a regular diet of food and water *ad libitum* at the Biological Resources Unit at the UCL Institute of Ophthalmology, approved by the UK Home Office. Six week C57BL/6 control mice were also purchased from Harlan Laboratories for control experiments.

For experiments, the mouse cages were transferred onto the top shelves of the cage racks, three weeks prior to experiments. This was so that the all the mice received approximately the same levels of light intensity, equivalent to ~300 lux. Mice were killed by cervical dislocation and eyeballs were immediately enucleated and processed either for microscopy or preparation of cell lysates.

## **2.4. Cell Culture**

### **2.4.1. Cell Lines**

All tissue culture reagents were purchased from Invitrogen unless otherwise stated. For phagocytosis assays and imaging, RPE-J cells were cultured on 90 mm Petri dishes (Nunc) in high glucose/Glutamax Dulbecco's modified Eagle's medium (DMEM), containing 4% CELLect™ Gold foetal calf serum (FCS) (MP Biomedicals). Cells were seeded at 50% confluency for 7-8 days before experiments. ARPE-19 cells were cultured on 75 cm<sup>2</sup> culture flasks (Nunc) in high glucose DMEM, containing 10% foetal calf serum and used after 1 week at 100% confluency. All cultures were maintained at 37°C in a humidified atmosphere containing 5% CO<sub>2</sub>.

### **2.4.2. Primary RPE cultures**

Primary porcine RPE were isolated from whole eyes. Eyes were trimmed, and immersed in 7% povidine iodine (betadine) for 5 min followed by 10 min in 10x Penicillin and Streptomycin (Invitrogen) and transferred into PBS. Each eye was cut along the ora-serrata to separate the anterior and posterior segments, with the vitreous and lens carefully removed from the posterior segment. The posterior segment of each eye was filled with PBS and the neuroretina was carefully peeled away and removed. The remaining posterior segment was then incubated with 10x Trypsin for 30 min. After incubation, each eye was pulsed 6-8 times with the trypsin by

pipetting up and down to detach the RPE away from its surrounding tissues, after which the supernatant containing the RPE cells was transferred into a clean Falcon tube containing media to inactivate the trypsin. Each eye was further rinsed with 10x Trypsin and detached cells were collected in the Falcon tube and then pelleted at 600 RPM for 4 min at RT. RPE cells from one porcine eye were used to plate one well of a 6 well plate or one 35mm dish, in DMEM containing 10% FCS and antibiotics.

#### **2.4.3. Phosphotyrosine Immunoprecipitation**

To study tyrosine phosphorylation of annexin 2 and c-Src, human ARPE-19 cells were seeded onto 90mm Petri dishes and cultured in DMEM containing 4500 mg/L Glucose, L-Glutamine, Pyruvate (Invitrogen) and supplemented with Penicillin and Streptomycin (Invitrogen) for two weeks before experimentation. Cells were serum-starved for 24 h prior to experiments.

#### **2.4.4. Cell Characterisation**

For cell characterisation, ARPE-19 cells were seeded to 100% confluency with DMEM containing 10% FCS with antibiotics onto 6 well plates for RNA extraction and preparation of whole cell lysates. Cells were also seeded onto 35mm Petri dishes with 14mm microwells (MatTek) for immunofluorescence imaging. Cells were maintained for 1, 2, 4 and 8 weeks in DMEM containing 10% FCS with antibiotics, and provided with fresh medium twice per week. For characterisation at 6 months in culture, ARPE-19 cells were cultured on a 75cm<sup>2</sup> culture flask (Nunc) and fed twice per week in DMEM containing 1% FCS. RPE-J cells were cultured on 6 well plates for RNA extraction and preparation of whole cell lysates. For imaging, cells were seeded onto 35mm plastic Petri dishes. RPE-J cells were maintained for 1, 2, 4 and 8 weeks in DMEM containing 4% CELLelect Gold serum (MP Biomedicals) and antibiotics. Medium was changed twice per week with 75% of existing media aspirated followed by fresh media added gently dropwise to the remaining media.

### **2.5. Annexin 2 siRNA treatment**

ARPE-19 and RPE-J cells were cultured until 40-60% confluent and then incubated for two days in medium containing Oligofectamine™ with the annexin 2 human/rat specific siRNA construct 5'-AACCUUGGUUCAGUGCAUUGAG-3' and rat-specific siRNA target construct 5'-GUGCAUAGGGUCUGAA-3' (Dharmacon) respectively. Medium was removed and cells were exposed to a second round of siRNA treatment for a further three days prior to experimentation. The half life of the annexin 2 protein is 15 hours and the mRNA is 2 hours

and so the annexin 2 siRNA treatment as described resulted in incomplete knock down of annexin 2.

## **2.6. Photoreceptor Outer Segments**

### **2.6.1. Isolation**

Photoreceptor outer segments (POS) were isolated from fresh porcine eyes using a method adapted from Molday *et al*, (1987)<sup>150</sup>. Briefly, eyes from freshly slaughtered animals (Cheale Meats Ltd., Brentwood UK) were cut open to separate the anterior portion of the eye from the posterior. If not already removed during the separation, the lens and vitreous were carefully removed from the posterior eye cup, revealing the neuroretina. The neuroretina was peeled off and transferred into a homogenising buffer consisting of 20% w/v sucrose, 20 mM Tris acetate (p.H 7.2), 2 mM MgCl<sub>2</sub>, 10 mM glucose and 5 mM taurine. The mixture was shaken for 1 min to create a homogeneous suspension and filtered twice through cheesecloth. The suspension was then layered onto a sucrose step gradient made from 0.8 ml 25, 30, 40, 50 and 60 % sucrose in a solution containing 20 mM Tris acetate (pH 7.2), 10 mM glucose and 5 mM taurine. This was followed by centrifugation at 25,000 rpm for 45 min at 4°C in a Sorvall S80AT3-0051 rotor using a Sorvall RCM150 GX ultracentrifuge. A single pink band was collected in the upper third of the gradient, diluted with five volumes of homogenising buffer and centrifuged at 5000 rpm for 10 min. Most of the homogenising buffer was decanted, leaving a small volume in which the pellet was gently resuspended. Five volumes of 10 mM sodium phosphate solution was then added to the remaining suspension to wash the POS, followed by another spin at 5000 rpm for 10 min. The sodium phosphate solution was decanted, again leaving a trace volume to resuspend the pellet.

### **2.6.2. Fluorescent Labelling**

The purified POS were labelled in 0.1 M sodium bicarbonate (pH 9.0) with 5% volume of Alexa Fluor 488 or 555 carboxylic acid, succinimidyl ester (Molecular Probes), typically for  $8 \times 10^7$  POS per ml rotating in the dark at room temperature for 1 h. After labelling, the POS were washed twice with media without serum and resuspended at  $1 \times 10^7$  POS/ml ready for experiments.

## **2.7. Quantification of POS Binding and Internalisation**

ARPE-19 and RPE-J cells were seeded onto 48 well plates. Cells were treated with annexin 2 siRNA or Oligofectamine™ alone. Cells were seeded with labelled POS at  $1 \times 10^7$  per ml for

various times, after which they were washed twice with ice cold PBS and fixed with 4% PFA. In some cases, ice cold 0.2% Trypan Blue was added to cells for 10 min after washing to quench fluorescence derived from externally bound particles. This method allows bound POS to be distinguished from internalised POS<sup>67</sup>. Trypan blue was washed off with equal volumes of ice cold PBS before fixing. POS binding and internalisation were quantified using a Safire plate reader (SAFIRE; Firmware: V.2.00 03/02 Safire; XFLUOR4 Version: V 4.20).

## **2.8. Preparation for Microscopy**

### **2.8.1. Toluidine Blue**

Freshly enucleated eyes were fixed with 3% glutaraldehyde and 1% paraformaldehyde in 0.08 M sodium cacodylate-HCl buffer (pH7.4) and rinsed 3 times in PBS and immersed in 1% aqueous osmium tetroxide solution for 2 h at room temperature. The eyes were then rinsed in distilled water (3 times) and dehydrated by single 15 min incubations in 50, 70 and 90% ethanol followed by three 15 min incubations in 100% ethanol, two 20 min changes of propylene oxide and left overnight in a 1:1 mixture of propylene oxide:araldite for infiltration. This was changed for full resin and left on a rotator for 6 h before embedding and overnight polymerisation at 60°C.

Semithin sections (0.75 µm) were cut using a Leica ultracut S microtome and diamond knife, stained with a mixture of 1% borax and 1% toluidine blue in 50% ethanol at 60°C, dried and mounted in DPX. All stains and resins were supplied by Agar Scientific Ltd, Stansted Essex. Images of Toluidine Blue stained transverse retinal sections were taken using an Olympus BX50 microscope and a Nikon DXM 1200 Digital Camera.

### **2.8.2. Immunofluorescence**

#### **2.8.2.1. Fixed Cells**

For immunofluorescence imaging, cells were seeded onto 13 mm coverslips (VWR International) in 12 well plates (Nunc) or onto 35 mm Petri dishes with 14 mm microwells (MatTek), with the exception of RPE-J cells which were seeded onto 35 mm plastic Petri dishes. For all protein staining, cells were washed twice with ice cold PBS and fixed with 4% PFA for 20 min. After fixation, cells were washed twice with PBS and permeabilised with 0.2% Triton for 15 min. Cells were then blocked with 1% BSA for at least 1 h, and washed three times with PBS and incubated with primary antibody overnight. This was followed by five washes in PBS and incubation with Alexa 488, 568 or 647 conjugated secondary antibodies (Molecular Probes)

for 1 h at room temperature. In some experiments, F-actin was stained with Alexa Fluor® 488, Rhodamine and 660 Phalloidin (Molecular Probes), which was added with the secondary antibody. This was followed by five more washes with PBS before adding VECTASHIELD® mounting medium (Vector Laboratories) on top of the cells. For cells grown on coverslips, cells were mounted with VECTASHIELD® and sealed onto glass slides with nail varnish. For cells grown on plastic Petri dishes, cells were covered with VECTASHIELD® and covered with glass coverslips. PBS was used for all washes and all incubations were in PBS containing 0.2% Triton. Table 2.1 lists all the primary and secondary antibodies used for immunofluorescence imaging.

For immunofluorescence imaging of POS phagocytosis, cells were seeded onto 35mm Petri dishes with 14mm microwells (MatTek). Medium was aspirated and POS were fed to the RPE cells at a concentration of  $1 \times 10^7$ /ml. Cells were washed twice with warm PBS, followed by fixation and primary antibody incubation as described above. Annexin 2 conjugated cells were then incubated with Alexa Fluor® 488 conjugated anti-mouse IgG (Molecular Probes) and Alexa Fluor® 660 Phalloidin (Molecular Probes). Immunofluorescence imaging of flat-mounted eyes is described in 2.10.

All imaging was performed using a Leica SP2 AOBS confocal microscope, a Zeiss LSM510UV upright confocal microscope and a Leica DMIRB IRE 2 inverted fluorescence microscope and recompiled in either Metamorph, Photoshop, Zeiss LSM Image Browser software or Image J software. Z sections were assembled from stacked images using Zeiss LSM Image Browser software.

### **2.8.2.2. Tissue cryosections**

Enucleated eyes were pierced through the cornea and fixed in 4% PFA for 6 h, followed by infusion in 30% sucrose overnight. The cornea and lens were removed and the eye was embedded in OCT embedding medium (Raymond A Lamb Ltd). After freezing, 10 µm thick transverse sections were cut and allowed to adhere to SuperFrost slides (VWR). The adhered retinal sections were washed with PBS and fixed with 4% PFA for 2 min and rinsed further with PBS. The sections were permeabilised in 0.5% Triton and blocked in 0.01% BSA (Aurion) overnight and incubated with an affinity-purified rabbit anti-annexin 2 polyclonal antibody, kindly provided by Dr Jesus Ayala-Sanmartin (Paris), for 1 h at room temperature, followed by rinsing in PBS and incubation with Alexa Fluor® 488 conjugated anti-mouse IgG (Molecular Probes) in 0.5% Triton at room temperature for 1 h. Sections were washed in PBS and mounted with VECTASHIELD® mounting medium (Vector Laboratories) and covered with glass cover slips for imaging.

**Table 2.1 All antibodies and reagents used for immunofluorescent microscopy**

Antibody/ Reagent	Species raised in	Reactivity	Dilution	Source
Annexin 2 (HH7)	Mouse	Human, Pig, Rat	1:60	Volker Gerke (University of Muenster, Germany)
Rhodopsin (1D4)	Mouse	Cow, Human, Mouse	1:1000	Abcam
Src (36D10)	Rabbit	Human, Mouse, Rat, Hamster, Monkey, Cow	1:100	Cell Signaling Technology
ZO-1	Rabbit	Human	1:400	Karl Matter (UCL Institute of Ophthalmology)
Annexin 2	Rabbit	Mouse	1:200	Jesus Ayala-Sanmartin (Paris)
Alexa Fluor® 488 goat anti-mouse IgG (H+L) *2 mg/mL*	Goat	Mouse	1:500	Invitrogen Molecular Probes
Alexa Fluor® 568 donkey anti-rabbit IgG (H+L) *2 mg/mL*	Donkey	Rabbit	1:500	Invitrogen Molecular Probes
Alexa Fluor® 488 goat anti-rabbit IgG (H+L) *2 mg/mL*	Goat	Rabbit	1:500	Invitrogen Molecular Probes
Rhodamine Phalloidin		F-actin	1:60	Invitrogen Molecular Probes
Alexa Fluor® 660 phalloidin		F-actin	1:60	Invitrogen Molecular Probes

### **2.8.3. Electron Microscopy**

#### **2.8.3.1. Conventional EM**

Wild type and annexin 2 knock out mice were sacrificed at various times before and after light onset. Eyes were immediately removed into fixative containing 1% paraformaldehyde and 3% glutaraldehyde in 0.07 M cacodylate buffer. Eyes were then post-fixed in 1% osmium tetroxide, embedded in Epon and cut into 70-80 nm sections followed by staining with lead citrate. In quantitative experiments, phagosomes were identified as approximately round structures, with at least one of the following criteria: a) the presence of membranous stacks, b) a mean diameter of at least 75% of the diameter of the POS, c) for apical phagosomes, surface membranes enclosed and segregated from the apical membranes of the RPE. The entire RPE length of each eye was used for phagosome counting with the location of each phagosome mapped by measuring its distance from Bruch's membrane.

#### **2.8.3.2. Cryo-immuno EM**

For cryo-immuno EM, mouse eyes were fixed in 4% paraformaldehyde, 0.1% glutaraldehyde and then dissected and embedded in gelatine, infiltrated in sucrose, mounted on pins and frozen in liquid nitrogen as described previously<sup>151</sup>. Thawed cryosections were labelled with affinity-purified rabbit anti-annexin 2 polyclonal antibody (kindly provided by Dr Jesus Ayala-Sanmartin, Paris), followed by 10 nm protein A gold as described previously<sup>152</sup>.

## **2.9. Immunoprecipitation**

### **2.9.1. Tyrosine-phosphorylated proteins in ARPE-19 cells**

Immunoprecipitation of tyrosine phosphorylated proteins was performed using a protocol established from Deora *et al*, (2004)<sup>153</sup>. ARPE-19 cells were washed twice with ice cold PBS followed by incubation on ice with 500 µl of lysis buffer (20 mM Tris (pH 7.5), 150 mM NaCl, 1 mM EDTA, 1 mM EGTA, 2% Triton X-100, 2.5 mM sodium pyrophosphate, 1 mM β-glycerolphosphate, 1 mM Na<sub>3</sub>VO<sub>4</sub>) supplemented with 10 µg/ml Leupeptin and 1 mM PMSF before use. Cells were incubated for 10 min before harvesting and transferred into Eppendorf tubes on ice. Samples were microcentrifuged for 15 min at 13,000g at 4°C to pellet insoluble material. Supernatants were aspirated and incubated with 25 µl of immobilised anti-phosphotyrosine monoclonal IgG (P-Tyr; Cell Signaling Technology) at 4°C overnight, prior to SDS-PAGE and western blotting.

### **2.9.2. Tyrosine-phosphorylated proteins in annexin 2 knock out and wild type eyes**

Immunoprecipitation of tyrosine-phosphorylated proteins from eye cups was performed as follows: eye cups were trimmed and cut along the ora-serrata to separate the anterior and posterior segments of the eye. The vitreous and lens were removed from the posterior segment and the neuroretina was carefully peeled away and removed. The remaining posterior segment of the eye cup was incubated in 500  $\mu$ l of lysis buffer (as above) for 10 min and centrifuged for 1 minute at 13,000 x g to pellet insoluble material. Supernatants were aspirated and incubated with 25  $\mu$ l of immobilised anti-phosphotyrosine monoclonal IgG at 4°C overnight.

### **2.10. Flat-mounting eye cups**

Eyes were harvested at various points before and after light onset. Each eye was trimmed and the surface of the cornea was pierced before immersing in 2% PFA in 2x PBS for 2 min before incising along the ora-serrata, separating the eye into anterior and posterior segments. The lens and vitreous were removed from the posterior segment of the eye, and the neuroretina was carefully peeled away exposing the RPE. Incisions were made towards the optic nerve head from the peripheral edge to open the eye cup into a 'flower'. This was followed by further fixation in 4% PFA in 2x PBS for 4 min before immersing in 2x PBS and blocking for at least 2 h in 3% Triton, 0.5% Tween, 1% BSA, 0.1% sodium azide. The 'flowers' were then incubated with primary antibody made up in blocking solution overnight at room temperature. After primary antibody incubation, eyes were washed three times in blocking solution followed by 1 h incubation with fluorescent conjugated secondary antibody at room temperature and washing three times in blocking solution afterwards before mounting onto glass slides in Mowiol (see below) covered with glass cover slips.

For quantitative experiments, 1D4-positive phagosomes and RPE cells for each area of view were counted using Zeiss LSM Image Browser software. The whole flat-mounted eye shown in Figure 5.8 A was compiled in Photoshop by merging the different segments taken from the flat-mounted eye.

#### **2.10.1. Mowiol Mountant**

Mowiol mountant was made by adding 2.6 g of Mowiol 4-88 (Calbiochem) to 6 g glycerol and mixing on a roller for 30 min at room temperature. 12 ml of 0.25 M Tris-HCL (pH 8.5) was added to the mixture and incubated at 50°C for 10 min, with occasional agitation. The mountant was frozen in aliquots ready for use.

## **2.11. SDS-PAGE and Western Blotting**

Cultured cells were washed twice with ice cold PBS before lysing with 2 x reducing sample buffer. Whole cell lysates of RPE and neuroretina were made from freshly enucleated annexin 2 knock out and wild type mouse and pig eyes by cutting along the ora-serrata to separate the anterior portion of the eye to the posterior. The neuroretina from each eye was collected into a clean Eppendorf tube and whole cell lysates were made by adding 2 x reducing sample buffer. Whole cell lysates from RPE were collected by pipetting 2 x reducing sample up and down inside the eye cup. Immunoprecipitated beads were resuspended in 25  $\mu$ l 2 x reducing sample buffer. All samples were heat denatured at 95°C for 5 min. Protein samples were separated by 10% SDS-PAGE and transferred onto Hybond-P PVDF membranes (Amersham Biosciences) at 400 mA for 45 min. Membranes were blocked in 10% powdered milk for at least 2 h and incubated with primary antibody in 10% milk overnight at 4°C. This was followed with three washes in PBS containing 0.05% Tween-20 and incubation in horseradish peroxidase-conjugated secondary antibody in 10% milk (Dako Cytomation) for 45 min at room temperature and detected using ECL Western Blotting Detection reagent (Amersham Biosciences). Antibodies used for Western blotting are shown in Table 2.2.

**Table 2.2 Antibodies used for Western blotting**

Antibody/Reagent	Species raised in	Reactivity	Dilution	Source
Annexin 2	Mouse	Human, Dog, Rat, Mouse, Chick, Pig	1:1000	BD Biosciences
Src (36D10)	Rabbit	Human, Mouse, Rat, Hamster, Monkey, Cow, Pig	1:1000	Cell Signaling
FAK (C-20)	Rabbit	Mouse, Rat, Human, Chicken, <i>Xenopus laevis</i> , Zebrafish, Pig	1:1000	Santa Cruz Biotechnology, Inc.
MerTK	Rabbit	Human, Mouse	1:500	Abcam
Integrin $\alpha$ V (P2W7)	Mouse	Human	1:200	Santa Cruz Biotechnology, Inc.
Integrin $\alpha$ V (H-75)	Rabbit	Mouse, Rat, Human, <i>Xenopus laevis</i> , Pig	1:200	Santa Cruz Biotechnology, Inc.
Integrin $\beta$ 5 (E-18)	Goat	Human	1:200	Santa Cruz Biotechnology, Inc.
Integrin beta 5	Rabbit	Human, Mouse, Rat	1:500	Abcam
RPE65	Mouse	Human, Mouse, Rat, Cow, Monkey, Chicken, <i>Xenopus laevis</i> , Pig	1:5000	Chemicon International
Alpha Tubulin	Mouse	Human, Mouse, Rat, Chicken, Pig	1:1000	Zymed
Polyclonal Goat Anti Rabbit Immunoglobulins/HRP	Goat	Rabbit	1:2000	Dako Cytomation, Denmark
Polyclonal Goat Anti Mouse Immunoglobulins/HRP	Goat	Mouse	1:2000	Dako Cytomation, Denmark
Polyclonal Rabbit Anti-Goat Immunoglobulins/HRP	Rabbit	Goat	1:2000	Dako Cytomation, Denmark

## **2.12. Quantification of POS Binding and Internalisation**

RPE-J and ARPE-19 cells were seeded onto 48 well plates and fed with labeled POS at  $1 \times 10^7$  per ml (w/v) for 15, 30, 90 and 150 min followed by washing twice with ice cold PBS and fixing with 4% PFA. In some cases, ice cold 0.2% Trypan Blue was added to cells for 10 min after washing to quench fluorescence derived from externally bound particles. Trypan blue was washed off with equal volumes of ice cold PBS before fixing. POS binding and internalisation were quantified using a Safire plate reader (SAFIRE; Firmware: V.2.00 03/02 Safire; XFLUOR4 Version: V 4.20).

## **2.13. Reverse Transcription-Polymerase Chain Reaction (RT-PCR)**

### **2.13.1. Reverse Transcription**

#### **2.13.1.1. ARPE-19 cells**

Cells were grown in 10% serum and washed twice in ice cold PBS before RNA was extracted using Trizol™ (Invitrogen) according to manufacturer's protocol. Contaminating DNA was removed using QuantiTect® Reverse Transcription gDNA Wipeout Buffer (Qiagen) for 5 min at 42°C. First strand cDNA synthesis was performed from 1 µg of total RNA, mixed with 1 µl of Quantiscript Reverse Transcriptase, 4 µl 5x Quantiscript RT Buffer and 1 µl RT Primer Mix (Qiagen), in a total volume of 20 µl and incubated at 42°C for 15 min. Quantiscript Reverse Transcriptase was inactivated at 95°C for 3 min. Genomic DNA control reactions for each RNA sample excluded the reverse transcriptase (-).

#### **2.13.1.2. RPE-J, primary porcine RPE cells and annexin 2 knock out, wild type and pig retina**

RPE-J cells and primary porcine RPE cells were grown in 4% CELLeCt™ Gold foetal calf serum and standard 10% serum respectively and were washed twice in ice cold PBS before RNA was extracted using Trizol™ (Invitrogen) according to the manufacturer's protocol. RPE and neuroretina from one pig eye were separated and each placed into 1 ml of Trizol™ (Invitrogen) and extracted according to the manufacturer's protocol. RNA from annexin 2 knock out and wild type mouse RPE and neuroretina was extracted using 12 eyes from each strain. The eyes were cut along the ora serrata to separate the anterior of the eye from the

posterior. The neuroretina from the posterior portion of each eye was removed for all 12 eyes and collected into a tube containing 1 ml of Trizol™. RNA from the remaining RPE from each of the eyes was extracted using 50 µl of Trizol™ and collected into a clean Eppendorf tube, made up to 1 ml with Trizol™ and extracted according to the protocol supplied by Invitrogen.

Contaminating DNA was removed using RQ1 RNase-free DNase (Promega). First strand cDNA synthesis was performed from 3 µg of total RNA using Superscript Reverse Transcriptase III (Invitrogen). Briefly, 1 µl oligo (dT)<sub>12-18</sub> (0.5 µg/µl) and 1 µl 10 mM dNTP mix (10 mM each of dATP, dCTP, dGTP, dTTP) was added to the genomic DNA-free RNA and incubated at 65°C for 5 min, followed by 1 min at 4°C. Afterwards, 4 µl of First Strand Synthesis buffer, 1 µl 0.1 M DTT, 1 µl RNaseOUT Recombinant Ribonuclease Inhibitor (40 U/µl) and 1 µl Superscript Reverse Transcriptase III (50 U/µl) were added to the reaction mixture and incubated at 50°C for 1 h. The Reverse Transcription (RT) reaction was inactivated by heating at 70°C for 10 min. 1 µl of *E.coli* RNase H (2 U/µl) was added to each reaction mixture for 20 min at 37 °C at the end to degrade the RNA strand of the DNA:RNA hybrid, freeing the DNA strand for the PCR reaction. Genomic DNA control reactions for each RNA sample excluded the reverse transcriptase (-).

### **2.13.2. DNA Polymerase Chain Reaction (PCR) Amplification**

PCR was performed on the reverse transcription and control reactions generated using Go Taq Polymerase (Promega) with 0.4 µM of primer used for ARPE-19 cells, mouse and pig retinae and 0.2 µM of primer for RPE-J and primary porcine RPE (Eurofins MWG Operon). A no template control (NT), which contains all the synthesis reagents but without the DNA template was also prepared. PCR was performed on the reverse transcription (RT) products in a Mastercycler egradient S or a Mastercycler gradient PCR machine (Eppendorf) using the following PCR programme: initial DNA denaturing at 95°C for 2 min, amplified by 35 cycles (40 cycles for mouse and pig retinae) of denaturation at 95°C for 30 s, annealing at the temperatures stated in Table 2.3, Table 2.4, Table 2.5 and Table 2.6. Typically these were primer melting temperatures (minus 3°C) for 30 s and elongation at 72°C for 30 s. The PCR reaction was completed with a final elongation step at 72°C for 2 min. All products were resolved on 1.5% agarose gels with a 100 bp DNA ladder (Bioline). Details of gene-specific primers used to amplify cDNA from ARPE-19, RPE-J, primary porcine RPE cells and mouse and pig retinae are indicated in Table 2.3, Table 2.4, Table 2.5 and Table 2.6.

**Table 2.3 Primer Sequences for ARPE-19 cells**

Gene	Accession number	Forward Primer 5' → 3'	Reverse Primer 5' → 3'	T <sub>ann</sub>	Product Size
AnxA2	NM_001002857	CGTGCCCCACC TCCAGAAAG	GCGTCCCCTTGC CCTTCAT	58	188
Itgav	NM_002210	CCTGTGCCTGTG TGGGTGAT	GGTGGCCGGAC CCGTTTA	58	110
Itgb5	NM_002213	CGAGCGTGGGC ACTGTCTCT	GCAGGCACTCG ACGCAATCT	58	128
FAK	AY323812	ATGTGACGGGC CTGGTGAAAGG	TGGGTGCTGGC TGGTAGGAG	58	160
MerTK	NM_006343	GTGAGGCAGCG TGCATGAAAG	GGGCTTTGGGA TGCCTTGAG	58	95
Gas 6	NM_000820	GCGGAATCTGG TCATCAAGG	TCAGCCAGTTC CAGCTCCTC	56	199
MFG-E8	NM_005928	CTTGGCTTCTCA GCCCCTTT	GTGAGGACTGG GGGTTAGGG	56	209
RPE65	NM_000329	GCCCAGGAGCA GGACAAAAG	GCGCATCTGCA AGTTAAAACCA	52	246
Ctsd	NM_001909	AGCTGGGAGGC AAAGGCTAC	CCCTGTTGTTGT CACGGTCA	56	188
ProS1	NM_000313	CGGAAAATGGA TTGCTGGAA	ACCAGAAACCA AGGCAAGCA	52	340

Primers were designed to amplify human sequences for annexin 2 (AnxA2), alphaV integrin (Itgav), β5 integrin (Itgb5), Focal Adhesion Kinase (FAK), Mer Tyrosine Kinase (MerTK), Growth arrest specific gene 6 (Gas6), Milk fat globule-EGF factor 8 protein (Mfge8), Retinal pigment epithelium-specific protein 65kDa (RPE65), Cathepsin D (Ctsd) and Protein S (ProS1).

**Table 2.4 Primer Sequences for RPE-J cells**

Gene	Accession Number	Forward Primer 5' → 3'	Reverse Primer 5' → 3'	T <sub>ann</sub>	Product Size
AnxA2	NM_019905.1	GACCGGCTGTA TGACTCCAT	AACATTAGGT TGGGGCACAG	54.3	265
Itgav	NM_001106549.1	TGTTACTGGCC GTGTTGGTA	GGTGCCCTCA GCAATACAGT	54.3	244
Itgb5	NM_147139.2	ATAAGAAGGCA GGCTGAGCA	CCACATTGCTG TTCATCACC	54.3	161
FAK	NM_013081.1	GAAGCTGCTGA ACTCCGACT	CAAGGTTACTT CCTCGCTGC	56.4	279
MerTK	NM_022943.1	ATCCTGACTCC ATCATTGCC	CAGGAGATGC CATTTTTGGT	52.3	214
Gas 6	NM_057100.2	TGACTCTGGAG GTAAACGGG	CCTGCTTCACC GTGTCTTTT	54.3	154
MFG-E8	NM_012811.2	CCTTCTCTCAGG CATTCTGG	GAATGGAACA TGGAGGGATG	54.3	193
ProS1	NM_031086.2	ACCGAAACAAA AGCTCATGG	TGAAGGTGTT GGCTCAAGTG	52.3	225

Primers were designed to amplify rat sequences for annexin 2 (AnxA2), alphaV integrin (Itgav), β5 integrin (Itgb5), Focal Adhesion Kinase (FAK), Mer Tyrosine Kinase (MerTK), Growth arrest specific gene 6 (Gas6), Milk fat globule-EGF factor 8 protein (Mfge8) and Protein S (ProS1).

**Table 2.5 Primer Sequences for primary porcine RPE cells**

Gene	Accession Number	Forward Primer 5' → 3'	Reverse Primer 5' → 3'	T <sub>ann</sub>	Product Size
AnxA2	NM_004039.2	ACGCTGGAGTG AAGAGGAAA	ACAGGGGCTTG TTCTGAATG	54.3	207
Itgav	NM_002210	CCTGTGCCTGTG TGGGTGAT	GGTGGCCGGAC CCGTTTA	58	110
Itgb5	NM_002213	CGAGCGTGGGC ACTGTCTCT	GCAGGCACTCG ACGCAATCT	58	128
FAK	EU668155.1	AAAGCAACAGT GAGCCAACC	TTAATCCATAG CAGGCCACG	54.3	127
MerTK	NM_006343	GTGAGGCAGCG TGCATGAAAG	GGGCTTTGGGA TGCCTTGAG	58	95
MFG-E8	NM_008594.2	ATCTGTACCAA CCACCCCAA	AACCTGTCAAC CACCCAGAG	54.3	272
RPE65	NM_000329	GCCCAGGAGCA GGACAAAAG	GCGCATCTGCA AGTTAAAACCA	52	246
ProS1	L31379.1	GTTGGCCTTGGT TTCTGGTA	GGCTTTATCCA AGATGGCAA	52.3	259

Primers were designed to amplify pig sequences for annexin 2 (AnxA2), alphaV integrin (Itgav), β5 integrin (Itgb5), Focal Adhesion Kinase (FAK), Mer Tyrosine Kinase (MerTK), Milk fat globule-EGF factor 8 protein (Mfge8), Retinal pigment epithelium-specific protein 65kDa (RPE65) and Protein S (ProS1).

**Table 2.6 Primer Sequences for mouse**

Gene	Accession Number	Forward Primer 5' → 3'	Reverse Primer 5' → 3'	T <sub>ann</sub>	Product Size
Itgav	NM_008402.2	ACGTTGGGCCT ATTGTTCAAG	GATTCCTTTCTC CCTGTCCC	54.3	240
Itgb5	NM_010580.1	GGAGGGGGACT AAGGATGAA	GCCTTCAGAGG TTCATGGAG	56.4	246
FAK	NM_007982.2	ATGTCTGAGGA GGGAGGGTT	ACAGGGAGGGC AGAAGTTTT	54.3	169
MerTK	NM_008587.1	TCTGGGAAATG GCACCTATC	TGCAAACCTGA CTTGACAGC	54.3	259
Gas 6	NM_019521.2	ATGAAGCAGGG TTTGACAC	TCTTCACATCCG TTCTGCTG	54.3	249
MFG-E8	NM_008594.2	ATCTGTACCAA CCACCCCAA	AACCTGTCAAC CACCCAGAG	54.3	272
RPE65	NM_029987.2	TTCTGAGTGTG GTGGTGAGC	TTTGGGAATTG AACACACGA	50.2	217
ProS1	NM_011173.2	CACTTGAGCCA ACACCTTCA	TTGTGTGCTCTC AGCAGCTT	54.3	170

Primers were designed to amplify mouse sequences for alphaV integrin (Itgav), β5 integrin (Itgb5), Focal Adhesion Kinase (FAK), Mer Tyrosinase Kinase (MerTK), Growth arrest specific gene 6 (Gas6), Milk fat globule-EGF factor 8 protein (Mfge8), Retinal pigment epithelium-specific protein 65kDa (RPE65) and Protein S (ProS1).

## **Chapter 3**

# **Model Systems for Retinal Phagocytosis**

### 3. Model Systems for Retinal Phagocytosis

#### 3.1. The RPE

The RPE is a cobblestone monolayer of cells attached to Bruch's membrane. The basal region of the RPE consists of numerous infoldings of plasma membrane that may extend as far as 1µm from Bruch's membrane. The apical surface is formed into microvilli that extend between the outer segments of the photoreceptors that directly abut the RPE. With few adhesion molecules between the interphotoreceptor matrix and junctional complexes between the apical processes, the photoreceptors and RPE are only associated weakly together and thus the sensory neuroretina is prone to detachment.

The connection of the RPE and sensory retina is important in establishing the health of the retina and is closely linked to the functions of the RPE cell. The functions of the RPE which serve to maintain the health of the retina include the daily uptake of shed photoreceptor outer segments, which is the main focus of this thesis. Other important functions of the RPE are renewal of bleached visual pigments, formation and maintenance of Bruch's membrane and the interphotoreceptor matrix, and transepithelial transport of nutrients and waste products between the photoreceptors and choriocapillaris. Defects in any of these processes contribute to visual impairment. The unique properties of the RPE are made possible by its polarity, and the importance of RPE polarity is highlighted by the fact that several of the 144 genes identified for inherited retinal degenerative diseases (<http://www.sph.uth.tmc.edu/Retnet/>) encode proteins that affect polarity and trafficking<sup>154</sup>. RPE polarity is thus essential for RPE function and it is important to take this into account when culturing RPE cells for experiments.

#### 3.2. Experimental Approaches to RPE Phagocytosis

The rat has been the traditional animal model to study RPE phagocytosis. From as far back as 1938, research has been conducted on the anatomy and structure of the RPE and photoreceptors from wild type rat strains and the Royal College of Surgeons (RCS) rat. The RCS rat has a naturally occurring mutation giving rise to a non-functional truncated form of MerTK, rendering a defect in phagocytosis of shed photoreceptor outer segments by the RPE which leads to blindness in these animals<sup>73, 112, 155</sup>. Since the advent of knock out and transgenic technologies, new animal models using rats and mice have been generated to produce targeted gene mutations known to express in the RPE. This technology has made it possible to perform *in vivo* experiments to study individual genes or a particular gene defect. This is important as *in vivo* RPE cells normally only internalise POS whilst RPE cells in culture can bind and phagocytose

non-specific particles such as bacteria, yeast, red blood cells and latex beads in addition to POS<sup>21, 156-158</sup>. *In vivo* studies on RPE phagocytosis are generally performed by isolating eyes which are fixed and cut into cross-sections for electron microscopy or light microscopy. Phagocytosis may be quantified by counting phagosomes along the RPE, and because RPE phagocytosis *in vivo* is circadian as well as continuous, multiple samples must be collected over a time range. This process is technically arduous as well as time-consuming and also presents problems such as species and strain variability which renders reproduction of results difficult. Keeping animals for these experiments is also expensive and material may be limited by breeding problems. So although *in vivo* experiments represent the true biological process, *in vitro* RPE cell models may be more appealing with regards to cost, maintenance and unlimited availability of material.

There are two major types of *in vitro* RPE cell models used to study RPE phagocytosis. First, RPE cells can be isolated from donor or animal eyes and grown as a primary cell culture. Unpassaged primary cells retain many of the characteristics of RPE cells *in situ*; they grow as a cobblestone monolayer of hexagonal cells and retain many of their original proteins along with pigment granules and apical microvilli<sup>159</sup>. However, over time, cell polarity, protein expression and pigment granules are lost through culture. Despite this, primary cells are much more efficient at recognising and internalising isolated POS in comparison to immortalised RPE cells. Primary RPE cultures do have disadvantages in that they can be difficult to isolate and propagate and are thus limited in availability of material. Furthermore, heterogeneity arises between different animals, which may produce problems in reproducibility of experimental results. In contrast, immortalised RPE cells are clonal and have the advantage of reproducibility and availability for large scale experiments. There are currently several RPE cell lines derived from human (ARPE-19, D407)<sup>159-161</sup> and rat (RPE-J)<sup>159, 162</sup> cells that have been characterised by researchers and widely used. Whilst these cells are normally unlimited and cultures are cheap and easy to maintain, the lack of *in vivo* cues and immortalisation mean that some of their original non-immortalised characteristics have been lost. This may contribute to their slow binding and engulfment of POS in comparison to primary cultures. Even so, researchers in this field have published extensively using ARPE-19 and RPE-J cells, both of which have been shown to possess many of the molecules that make up the RPE phagocytic machinery.

This chapter reports on phenotype, gene expression at the mRNA and protein level of specific gene products in the widely used human cell line ARPE-19, the rat cell line RPE-J, and primary cultures of porcine RPE. This analysis examines both the expression of the key molecules that regulate RPE phagocytosis of POS and also the gene expression and localisation of annexin 2 in

these systems. Studying the gene expression of these molecules gives a more extensive insight than examining protein expression alone, and for some proteins that cannot be hybridised with antibody, allows interpretation at the mRNA level. These studies will ultimately determine the experimental approach to be used in subsequent studies.

### **3.3. Characterisation of immortalised cell lines**

Both ARPE-19 and RPE-J cells have been used for the study of POS phagocytosis<sup>67, 73</sup> which makes these cells ideal choices for initial investigations into the role of annexin 2 in phagocytosis. Because of the variability and heterogeneity of immortalised cell lines, the characterisation of the two cell lines aims to confirm the expression of annexin 2 in these cells, and the gene expression at the mRNA and/or protein level of key molecules involved in RPE phagocytosis of POS.

#### **3.3.1. ARPE-19**

ARPE-19 is a spontaneously occurring cell line, developed from original primary RPE cultures isolated from a 19 year old male. These cells have a normal karyotype and are diploid, whilst most spontaneously derived RPE cell lines are aneuploid. They form a polarised monolayer when grown on porous filter supports and are able to differentiate and form pigment granules, basal infoldings and apical microvilli<sup>163</sup>. These cells are used widely and are represented in more than 300 citations on Pubmed, illustrating their popularity with researchers studying RPE phagocytosis<sup>67, 164-166</sup>.

Cells were grown in DMEM containing 10% FCS with antibiotics and were fed twice a week for a period of 8 weeks. Indeed, as reported by Dunn *et al*, (1996)<sup>161</sup>, cells did differentiate into a hexagonal shape observed from 4 weeks in culture. However, these cells did not always have 6 sides and so are better described as polygonal. Spindle-like, elongated cells rearrange their cortical actin and differentiate into a ‘cobblestone’ like pavement of cells. This can be observed over time in Figure 3.1 A and Figure 3.1 B. Enrichment of annexin 2 and F-actin was observed at the cell junctions, which occurred concurrently with cell differentiation into polygonal shapes at around 4 weeks in culture. Multiple confocal sections were taken of cells harvested at the different time points to provide cross sectional views. Cells grown on plastic or glass in 10% serum did not contact inhibit and grew on top of each other post confluence (Figure 3.1 C- 2 weeks). Cross-sectional images (z-stacks) also showed that apical processes are present on differentiated cells and occasionally on non-differentiated cells.

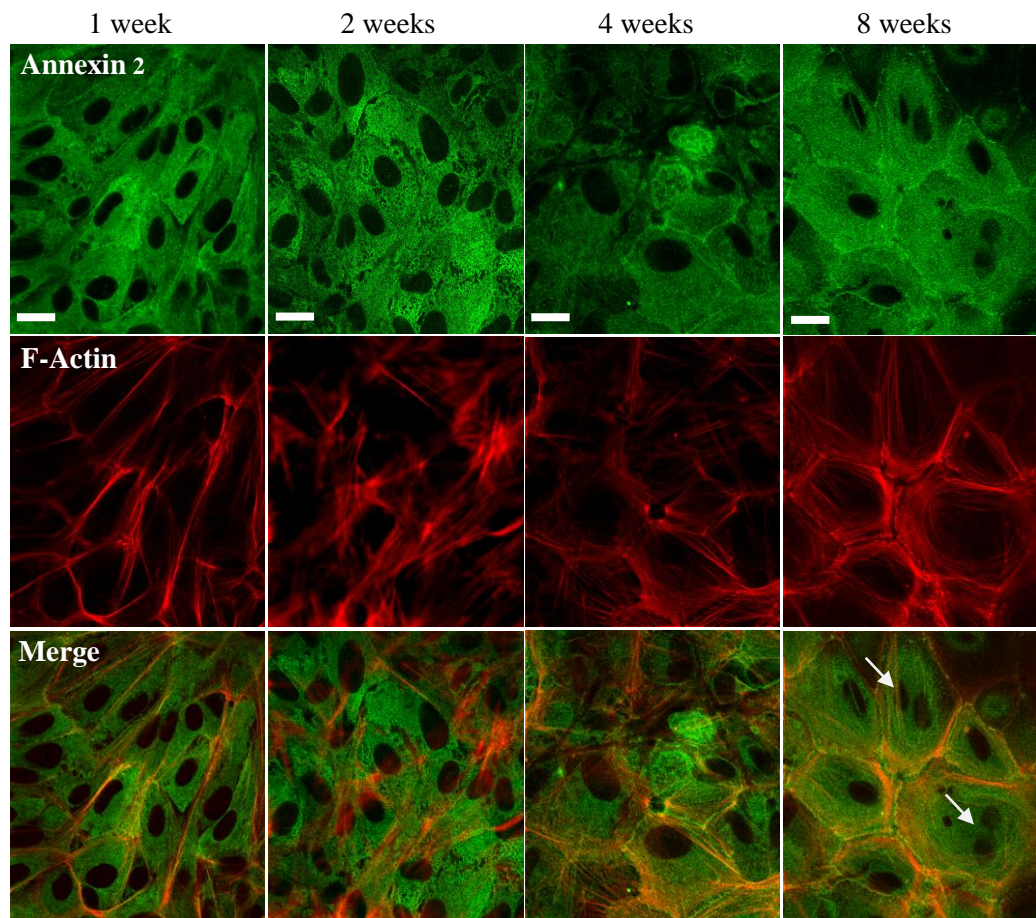


**Figure 3.1 A ARPE-19 cells express annexin 2 and develop a cobblestone appearance over time.**

ARPE-19 cells were grown in 10 % serum for 8 weeks after confluency was reached. Cells were fixed, permeabilised and immunostained for annexin 2 and F-actin at 1, 2, 4 and 8 weeks. Spindle like, elongated cells rearrange their cortical actin and differentiate into a ‘cobblestone’ like pavement of cells over time. From 4 weeks, cells display a polygonal shape, characteristic of RPE cells *in situ*. At 8 weeks, bi-nucleate cells are observed (white arrows), which is another characteristic feature of native RPE cells. Images were captured on a Zeiss LSM510UV upright confocal microscope and processed using Zeiss LSM Image Browser software. Scale bar = 20µm.

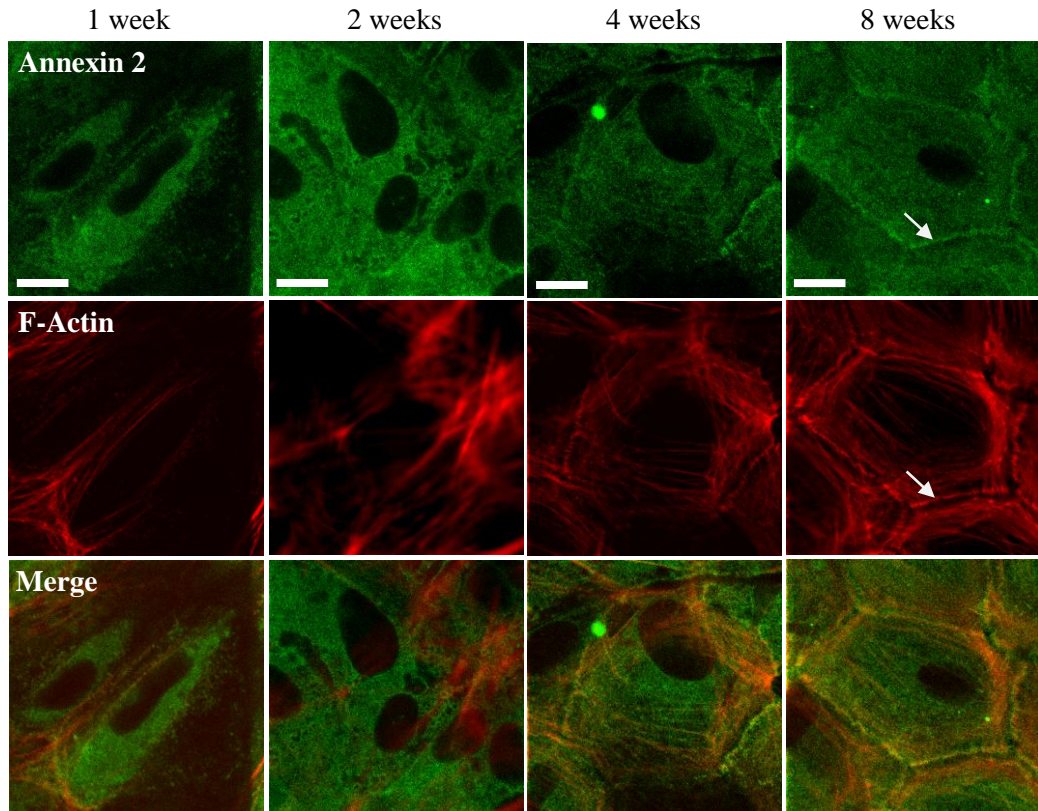
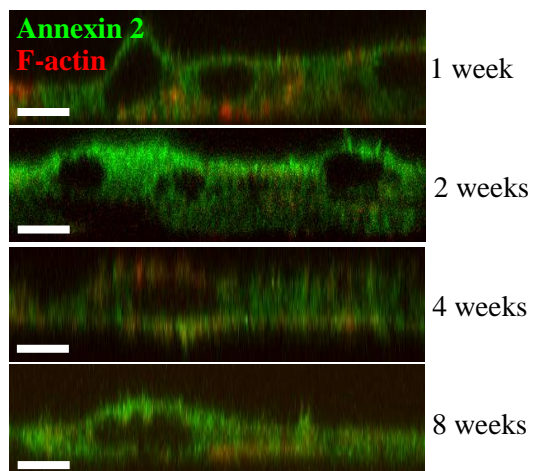


**Figure 3.1 B Higher magnification images from Figure 3.1A**

ARPE-19 cells were grown in 10 % serum for 8 weeks after confluency was reached. Cells were fixed, permeabilised and immunostained for annexin 2 and F-actin at 1, 2, 4 and 8 weeks. From 4 weeks, enrichment of annexin 2 and F-actin can be seen at the cell junctions (white arrows), which is concurrent with cell differentiation into polygonal shapes. Images were captured on a Zeiss LSM510UV upright confocal microscope and processed using Zeiss LSM Image Browser software. Scale bar = 10 $\mu$ m.

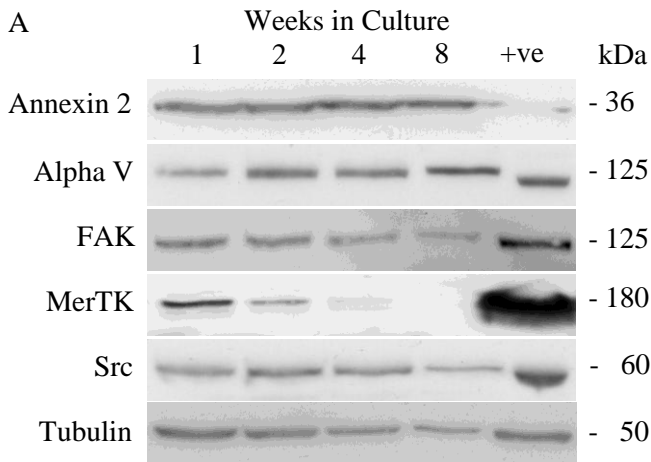
**Figure 3.1 C Confocal Z-stacks of ARPE-19 cultured over time**

ARPE-19 cells were seeded onto Matek™ dishes and fixed at 1, 2, 4 and 8 weeks of culture. Cells were fixed and immunostained for annexin 2 (green) and F-actin (red). Confocal sections were taken through the area of cells sampled to form z-stacks using a Zeiss LSM510UV upright confocal microscope and assembled using Zeiss LSM Image Browser software. The images shows that ARPE-19 cells do not contact inhibit and cells can overlay each over post confluency. Scale bar = 10 $\mu$ m.



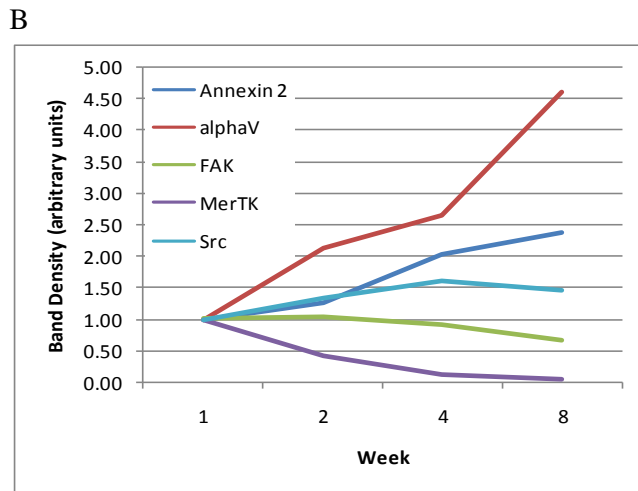
Expression of proteins of interest in these cells was investigated by western blotting (Figure 3.2) and/or PCR (Figure 3.3) of reversed transcribed mRNA (cDNA). Annexin 2 is found on both the apical processes and cell cytoplasm in ARPE-19 cells and expression of annexin 2 at both mRNA and protein levels did not appear to change with time in culture. These cells also express genes that contribute to the RPE phagocytic machinery: alphaV, beta5, FAK, MerTK, its ligand Gas6 and MFG-E8, the ligand for beta5. In addition, c-Src, which phosphorylates tyrosine 23 in the N-terminus of annexin 2, is also expressed at both mRNA and protein levels at 1, 2, 4, and 8 weeks of culture. Protein S (ProsS1), a vitamin K-dependent serum protein, which is structurally similar to Gas 6 and has been reported to activate MerTK<sup>167</sup> is also expressed at the mRNA level in ARPE-19 cells cultured for 8 weeks. We also examined cathepsin D expression, as this is a major proteolytic enzyme responsible for the lysosomal degradation of POS<sup>168</sup>. Cathepsin D mRNA was expressed in all ARPE-19 samples.

Intriguingly, RPE65, a 65 kDa protein expressed specifically in RPE cells, responsible for the conversion of all-trans retinol to 11-cis retinal during phototransduction, was expressed at 4 and 8 weeks of culture (Figure 3.3). This coincides temporally with differentiation of the cells, evident at 4 weeks in culture, when they start to acquire a polygonal shape, comparable to their native morphology (Figure 3.1A and B). This is consistent with previous reports that suggest RPE65 is synthesized in differentiated RPE *in vivo* and is expressed by ARPE-19 cells<sup>161, 169</sup>. Western blotting for MerTK, which is indispensable for RPE internalisation of POS, revealed that expression of the protein was lost through culture, although PCR showed expression of MerTK mRNA at all time points (Figure 3.3). Intriguingly, integrin alpha V protein expression showed a considerable increase from week 1 to week 8. Annexin 2 protein expression also increased from week 1 to week 8, although less pronounced. ARPE-19 cells start to pigment at about 3 months in culture with pigment granules visible by 4 months. Cells are closely packed, with well defined junctions, and most exhibit a polygonal morphology (Figure 3.4).



**Figure 3.2 Western blot analysis of protein expression in ARPE-19 cells grown in 10% serum**

ARPE-19 cells were grown in 10% FCS for 1, 2, 4 and 8 weeks and lysed in reduced sample buffer for whole cell lysates. 1/33 of the RPE extract was loaded into each lane. (A) Proteins were resolved by 10% SDS-PAGE, transferred onto PVDF membranes and incubated with antibodies for annexin 2, av, FAK, Src, and MerTK. Tubulin was blotted in all samples as loading control. ARPE-19 cultured for 4 months, previously shown to express the probed proteins was used as a positive control (+ve). (B) Protein expression profiles of annexin 2, alpha V, FAK, MerTK and Src at the measured time points were created by measuring pixel densities from the blots (A).



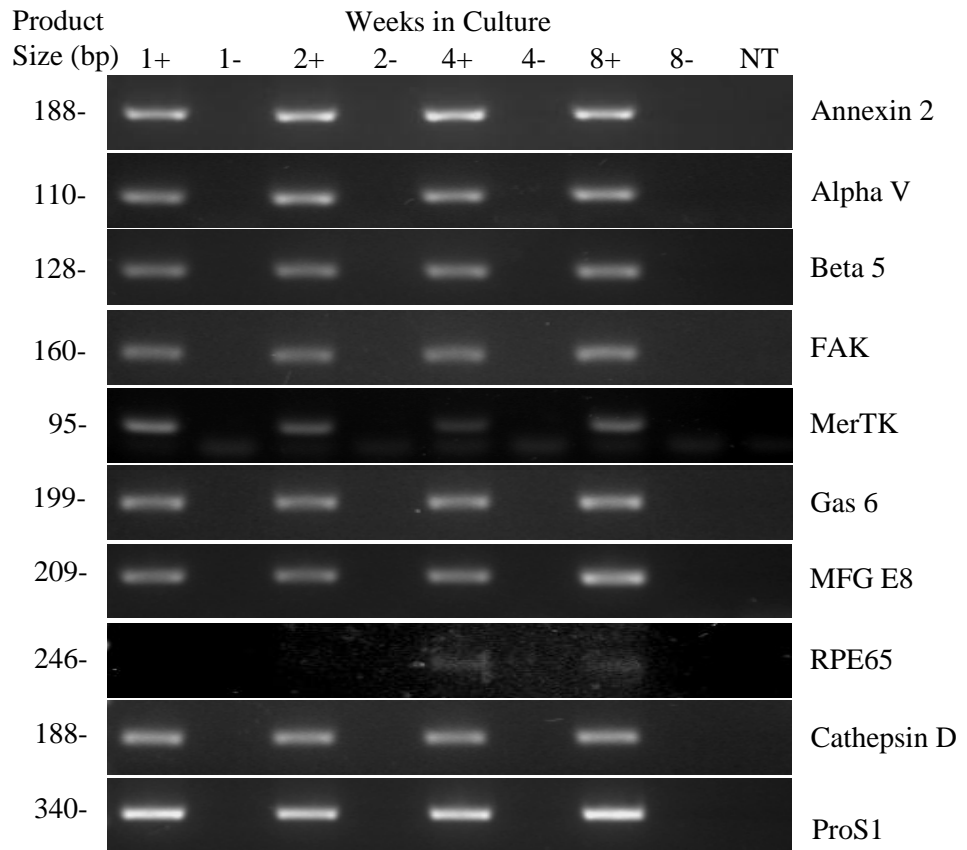


**Figure 3.3 ARPE-19 cells grown in 10% serum express genes required for POS phagocytosis**

Cells were grown in 10% serum and harvested in Trizol™. 1µg of RNA was used per cDNA synthesis reaction. 1µl of cDNA was used per cDNA synthesis reaction and amplicons were resolved by agarose gel electrophoresis (1.5% gel). See Materials and Methods section for PCR primer sequences, amplicon size and melting temperatures. +/- indicates exclusion (-) or addition (+) of reverse transcriptase and NT is no RNA template control for amplification of genomic DNA. Note that the purpose of this experiment was simply to determine qualitatively whether or not the mRNA for each gene was expressed, and not to quantify expression in each case.

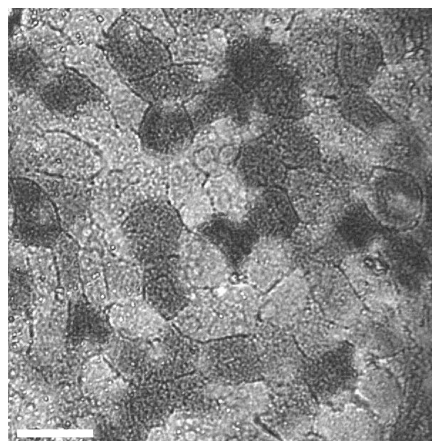


**Figure 3.4 ARPE-19 cells are pigmented and differentiate into a cobblestone pavement of cells**

ARPE-19 cells were grown on plastic and fed twice weekly in 1% serum for 4 months. Cells pigment to varying degrees and whilst most cells are polygonal, some remain irregular or round. These cells are highly packed with well defined junctions. The phase image was taken with a Leica DMIL microscope and Leica D200 camera. Scale bar = 20 µm

### 3.3.2. RPE-J cells

RPE-J cells are rat retinal pigment epithelial cells that have been immortalised by infection with a temperature-sensitive A mutant (tsA) SV40 virus. TsA of SV40 encodes the large T antigen which is transforming at the permissive temperature of 33°C and inactive at the non-permissive temperature (39-40°C). At the non-permissive temperature, RPE-J cells differentiate into a polarised phenotype typical to native RPE cells, whilst culturing at 33°C allows the cells to proliferate<sup>162</sup>. RPE-J cells were grown in DMEM containing 4% CELLelect Gold serum (MP Biomedicals) and maintained in culture before harvesting at 1, 2, 4 and 8 weeks. In initial experiments, the cells grew at 39-40°C but detached from the culture plate when transferred to 33°C. Having discussed these issues with Silvia Finnemann (personal communication), who has published extensively using these cells, temperature switching was not used and cells were instead cultivated at 37°C. For cells harvested after 1 week of culture, cultures were fed twice per week by carefully aspirating 75% of the media before replacing with fresh media containing 4% serum dropwise into the existing media. This prevented disruption of the integrity of the epithelial sheet which was easily damaged.

Unlike ARPE-19 cells, RPE-J exhibits a polygonal phenotype, similar to native RPE from day 1 of culture. These cells were not morphologically differentiated at the non-permissive temperature and were grown at 37°C until harvesting at the different time points. At one week, polygonal cells with 4-8 sides formed a mosaic monolayer that was not tightly packed (Figure 3.5 A and Figure 3.5 B). Confocal sections of these cells at one week in culture showed cortical F-actin that is non-linear to the cell periphery, and Z-stacks revealed that the cells were not tightly packed together. At two weeks, the F-actin arrangement shown in most of the cells was more organised to the cell periphery and cells started to grow on top of each other (Figure 3.5 C). It is clear from the images that RPE-J cells not only proliferate at 37°C but also do not contact inhibit. By 4 weeks in culture, cortical F-actin was arranged at the cell periphery and was completely co-linear with the cell junctions (Figure 3.5 A and Figure 3.5 B). Curiously, cortical F-actin accumulated at discrete points, which could also be observed at 8 weeks in culture. At 8 weeks, all the cells showed cortical F-actin, with clear definition of the cell boundaries. Despite the similarities with ARPE-19 cells in the rearrangement of cortical F-actin to develop a tightly packed polygonal shape (comparable to that of native RPE), RPE-J cells did not appear to develop pigment, as did ARPE-19 cells at 4 months.

Annexin 2 staining was evident at all the time points tested, with distribution in the cell cytoplasm and at the apical cell surface. Protein expression of annexin 2, integrin chains alpha

V and beta 5, FAK and Src was examined by western blotting (Figure 3.6). Since there is no good MerTK antibody available that reacts with rat tissue it was not possible to show protein expression of MerTK in these cells. Expression of key genes implicated in POS internalisation (alpha V, beta 5, FAK, c-Src, MerTK, Gas6 and MFG-E8) was determined by PCR (Figure 3.7) which confirmed the presence of MerTK at the mRNA level.

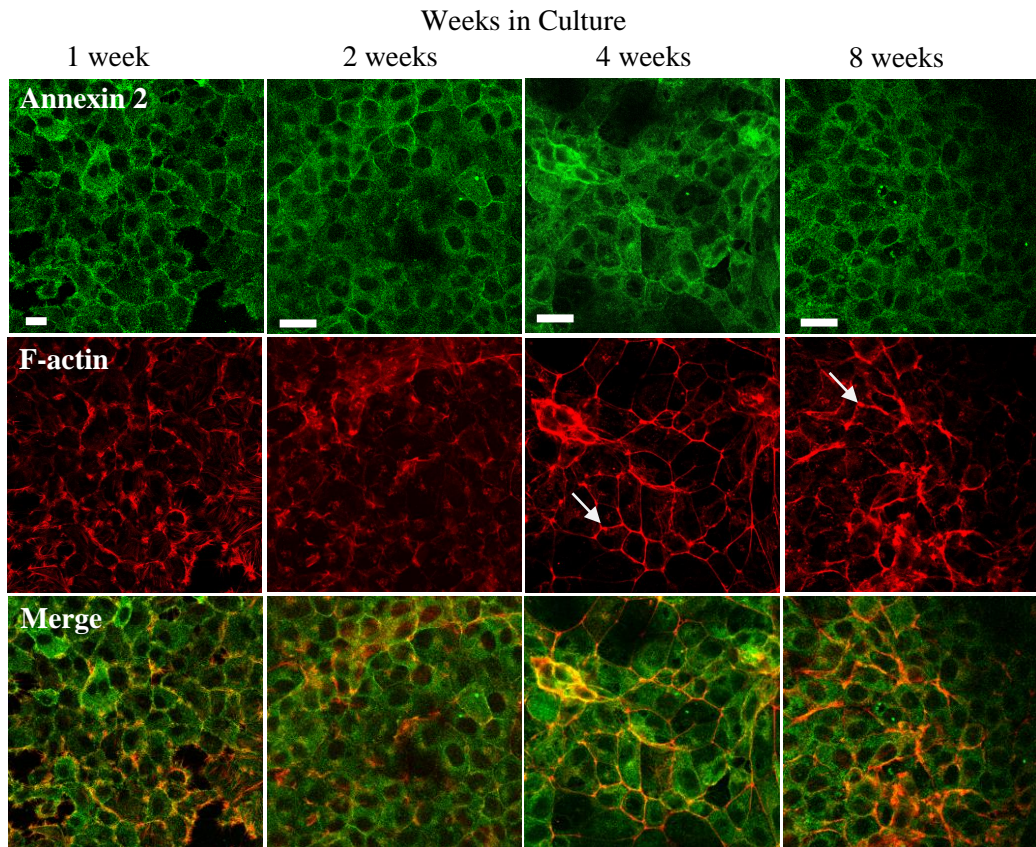


**Figure 3.5 A RPE-J cells express annexin 2 and develop discrete cortical F-actin accumulation over time.**

RPE-J cells were grown in media containing 4 % CELLeCt™ gold serum for 8 weeks after confluency was reached. Cells were fixed, permeabilised and immunostained for annexin 2 and F-actin at 1, 2, 4 and 8 weeks. Cells became more packed and developed junctions over time which is evident from 4 weeks in culture. Intriguingly, RPE-J cells also developed discrete cortical F-actin over time (indicated with white arrows). Images were captured on a Zeiss LSM510UV upright confocal microscope and processed using Zeiss LSM Image Browser software. Scale bar = 20µm.

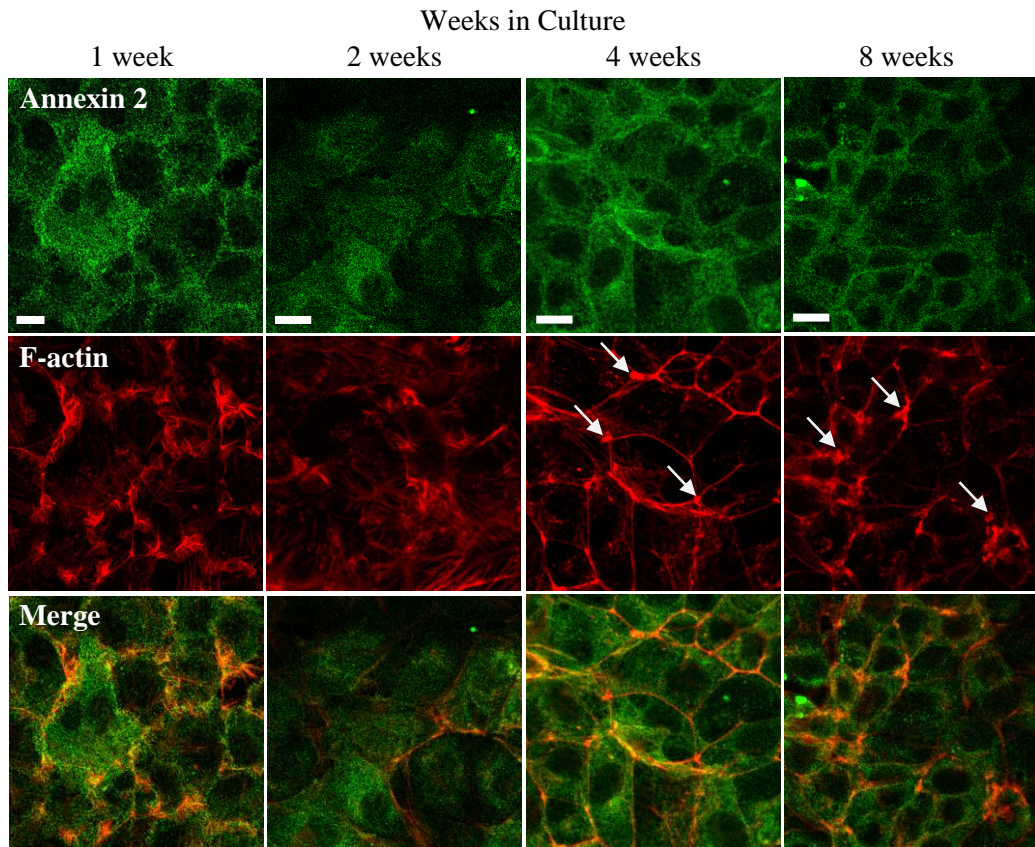


**Figure 3.5 B Higher magnification images from Figure 3.5A**

RPE-J cells were grown in media containing 4 % CELLelect™ gold serum for 8 weeks after confluency was reached. Cells were fixed, permeabilised and immunostained for annexin 2 and F-actin at 1, 2, 4 and 8 weeks. Cells became more packed and develop junctions over time which is obvious from 4 weeks in culture. Discrete cortical F-actin, visible from 4 weeks (indicated with the white arrows) can be seen more clearly in these higher magnification images. Images were captured on a Zeiss LSM510UV upright confocal microscope and processed using Zeiss LSM Image Browser software. Scale bar = 10µm.

**Figure 3.5 C RPE-J cells do not form morphological apical tight junctions after 1 week in culture**

RPE-J cells were seeded onto glass bottom Matek™ dishes or on plastic dishes for culturing over 1 week. Cells were fixed at 1, 2, 4 and 8 weeks of culture and immunostained for annexin 2 (green) and F-actin (red). Confocal image stacks were collected to form cross-sectional slices using a Zeiss LSM510UV upright confocal microscope and assembled using Zeiss LSM Image Browser software. The images show that RPE-J cells are closely packed together after 1 week in culture. By 2 weeks the cells appear to overlay each other, showing that these cells do not contact inhibit. Scale bar = 20µm.

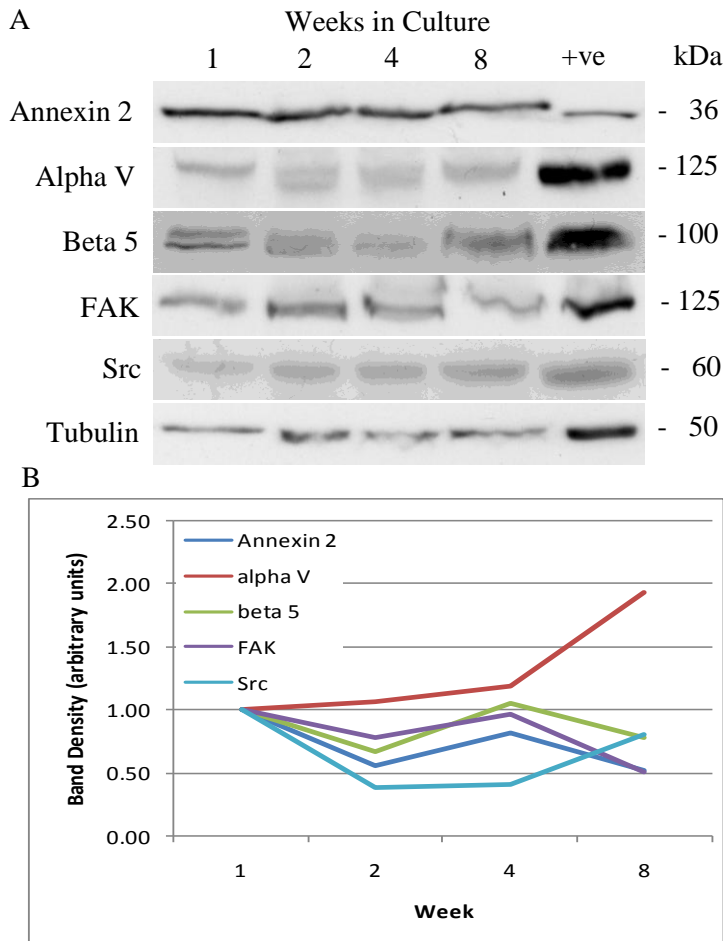
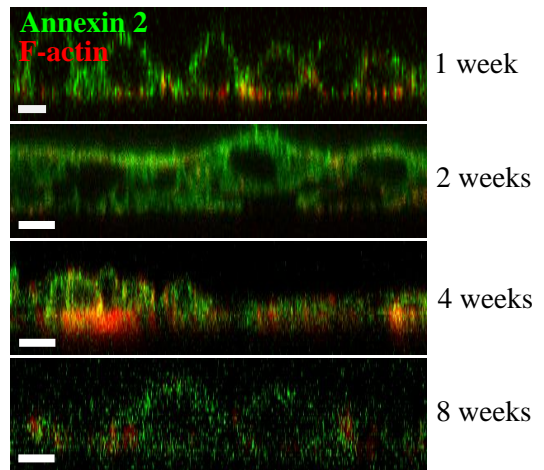


**Figure 3.6 Western blot analysis of protein expression in RPE-J cells**

RPE-J cells were grown in media containing 4% CELLECT™ gold serum for 1, 2, 4 and 8 weeks and lysed in reduced sample buffer for whole cell lysates. 1/33 of the RPE extract was loaded into each lane. (A) Proteins were resolved by 10% SDS PAGE, transferred onto PVDF membranes and incubated with antibodies for annexin 2,  $\alpha$ v,  $\beta$ 5, FAK and Src. Tubulin was blotted in all samples as loading control. ARPE-19 cultured for 4 months, previously shown to express the probed proteins was used as a positive control (+ve). (B) Protein expression profiles of annexin 2,  $\alpha$ v,  $\beta$ 5, FAK and Src at the measured time points were created by measuring

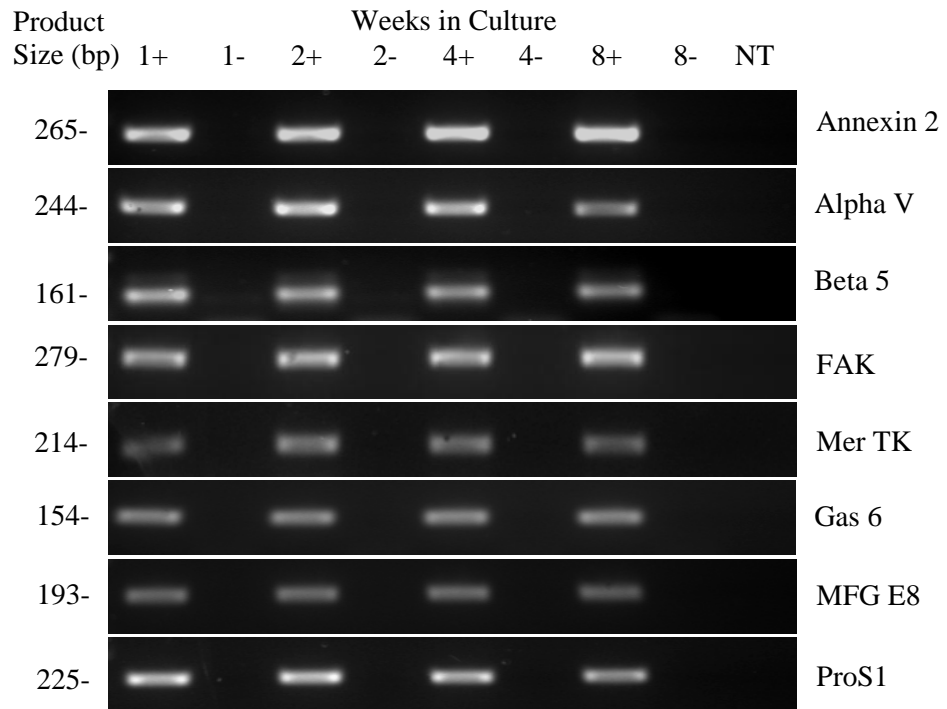


**Figure 3.7 RPE-J cells express mRNAs required for POS specific phagocytosis**

Cells were grown in 4% CELLelect™ gold serum and harvested in Trizol™. 3µg of RNA was used per cDNA synthesis reaction. 0.5µl of cDNA was used per PCR and amplicons were resolved by agarose gel electrophoresis (1.5% gel). See Materials and Methods section for PCR primer sequences, amplicon size and melting temperatures. +/- indicates exclusion (-) or addition (+) of reverse transcriptase and NT is no RNA template control for amplification of genomic DNA.

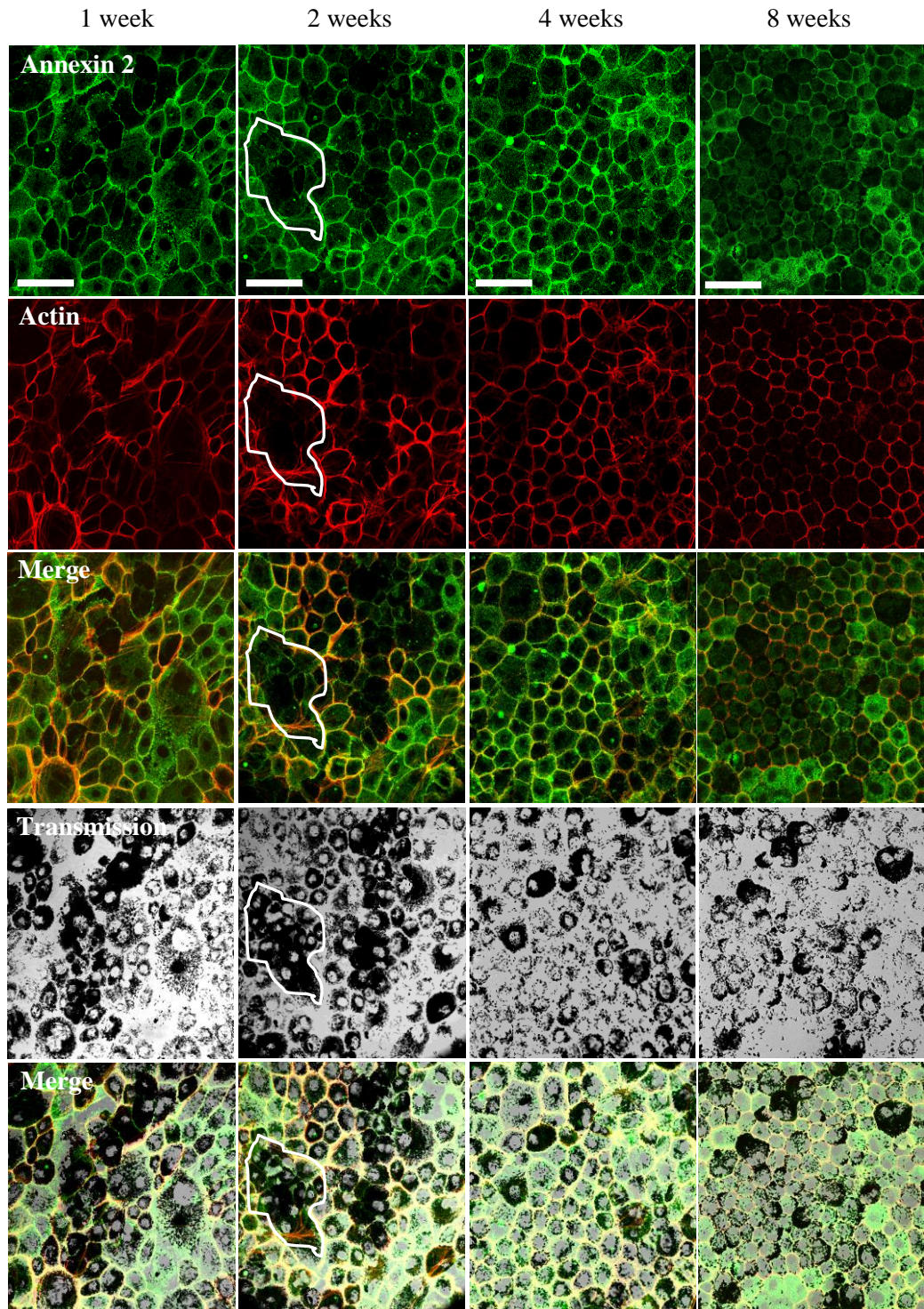
### 3.4. Characterisation of primary RPE culture

#### 3.4.1. Primary Porcine RPE Culture

As discussed earlier, primary cell cultures have many advantages over immortalised cell lines in that they retain many features and properties of the RPE *in vivo* and importantly, for the focus of this thesis, primary cells are much more efficient at recognising and internalising POS in comparison to immortalised RPE cells. Due to the low yield and technical difficulty of isolation and propagation of RPE cells from mouse retina, RPE cells were instead harvested from pig eyes. Using a protocol devised by Dr Anna Tsapara (UCL Institute of Ophthalmology), RPE cells were isolated from freshly enucleated pig eyes. The anterior segment of the eye cup containing the lens was separated away from the posterior segment. Any remaining vitreous was carefully removed from the posterior eye cup and PBS was added to dissociate the neuroretina from the RPE. When detachment was evident, the neuroretina was cut away from the optic nerve and removed from the eye. The exposed RPE was incubated with 0.5% Trypsin, 5.3mM EDTA for 30 min and pipetted up and down 6-8 times to extract the RPE. Cells were washed in DMEM with 10% serum and antibiotics, and seeded onto dishes. Cells extracted from one eye were used per 35mm dish.

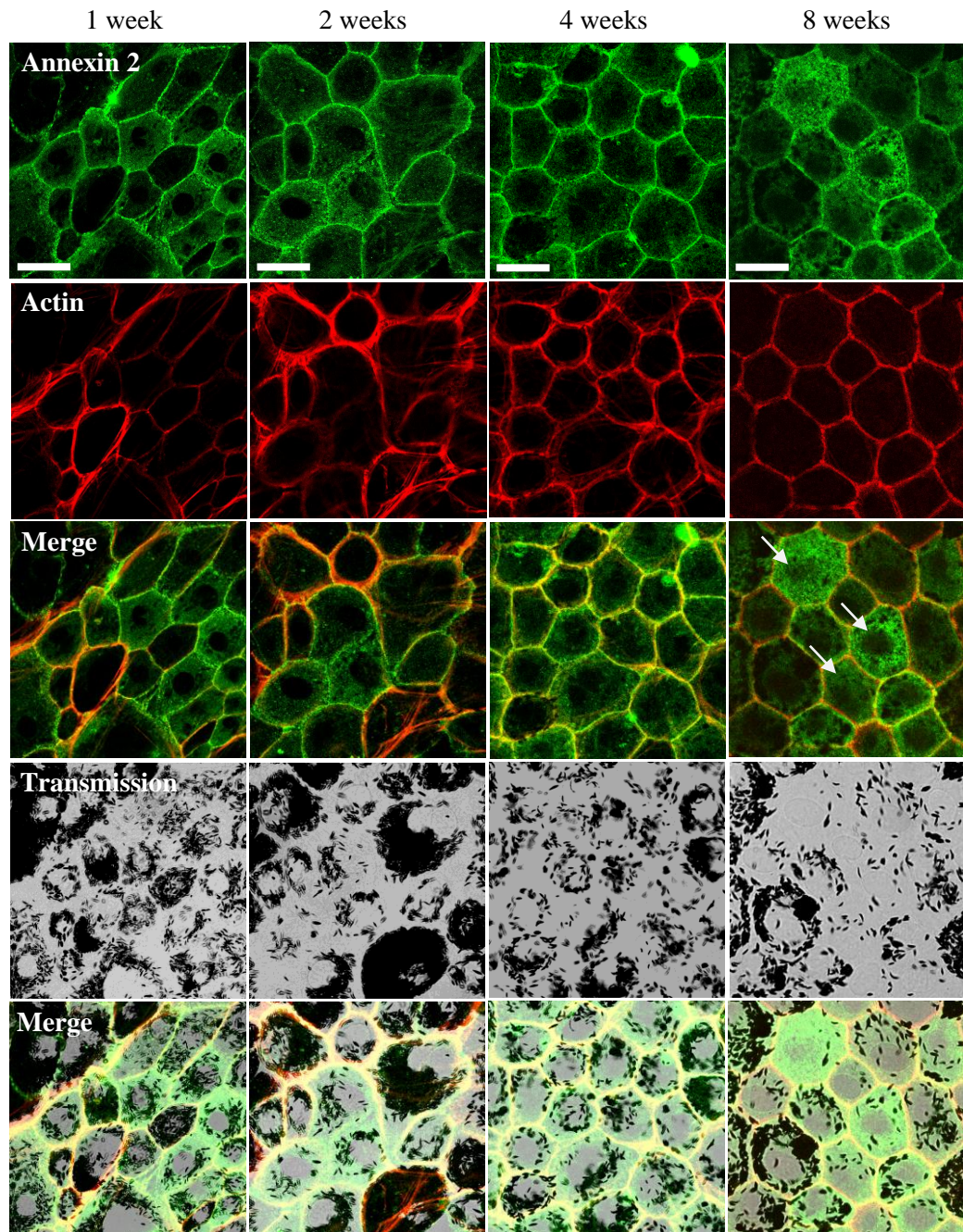
Outgrowth of RPE cells from the original isolates was visible overnight. Outgrowing cells were less pigmented in comparison to the parent cells, with decreasing pigmentation of the daughter cells with increasing distance from the original isolate. The primary porcine RPE were kept in culture, fed twice weekly and harvested at 1, 2, 4 and 8 weeks for immunofluorescence imaging, western blotting of whole cell lysates and rtPCR of RNA extracts. Pigmentation was partly lost over time in culture as observed in Figure 3.8 A and B but the cells remained polygonal and cuboidal in shape throughout the 8 weeks as shown in Figure 3.8 A, B and C. Consistent with Burke *et al* (1996)<sup>170</sup>, the cultured cells varied in size and uniformity and were also multinucleated, which is a typical feature of RPE cells *in vivo*. The cells also displayed apical processes that were clearly visible at weeks 1, 2 and 4, and although still present on some cells, apical processes were much shorter and less apparent at week 8 in culture (Figure 3.8 C). Immunofluorescence staining for annexin 2 showed that it is localised to the cytoplasm and to the cell membrane at all the time points. Intriguingly, annexin 2 also appeared to be more cytoplasmic in cells with least pigment (Figure 3.8 B). Annexin 2 may re-distribute and localise to the cell cytosol, away from the cell junctions when cells de-differentiate, (Figure 3.8 A and Figure 3.8 C respectively), although this observation could be the result of fluorescence quenching by the pigment granules. Junctional staining of both annexin 2 and F-actin also appeared more striking in comparison to ARPE-19 and RPE-J cells.

Figure 3.9 and Figure 3.10 confirms patterns of protein and gene expression of annexin 2 in primary porcine RPE cells at 1, 2, 4 and 8 weeks in culture. These cells also showed positive gene expression for integrin chains  $\alpha v$  and  $\beta 5$ , FAK, MerTK and MFG-E8. Furthermore, cells also showed expression of RPE65 at the mRNA level for all time points, although curiously, RPE65 at the protein level appeared to decrease from 1-2 weeks. These observations however were obtained from results using one eye and hence would need to be supported with more samples. Nevertheless, a decrease in protein expression of RPE65 is consistent with the report by Hamel *et al* (1993)<sup>169</sup>. Figure 3.9 also suggests that FAK expression decreases over time in culture. Intriguingly, protein expression of beta 5 appeared to increase from week 2, with maximal expression at 8 weeks. Again, these observations need to be supported from more eye samples before firm conclusions can be made.



**Figure 3.8 A Primary porcine RPE cells express annexin 2, maintain their native morphology but lose pigment over time in culture**

Primary cultures of porcine RPE were isolated and established in media containing 10% serum for 8 weeks. The RPE isolated from one pig's eye was used to seed one Matek™ dish. Cells were fixed, permeabilised and immunostained for annexin 2 and actin at 1, 2, 4 and 8 weeks. Areas of heavy pigmentation often result in areas of non-staining, perhaps due to fluorescence quenching by the pigment granules. An example is circled in white. Images were captured on a Leica TCS-SP2 AOBs DM IRE 2 confocal microscope and processed using Image J software. Scale bar = 50µm.



**Figure 3.8 B Higher magnification images from Figure 3.8A. Primary porcine RPE cells express annexin 2, keep their native morphology but lose pigment over time in culture**

Primary cultures of porcine RPE were isolated and established in media containing 10% serum for 8 weeks. The RPE isolated from one eye was used to seed one Matek™ dish. Cells were fixed, permeabilised and immunostained for annexin 2 and F-actin at 1, 2, 4 and 8 weeks. Note that the RPE cells are not uniform in shape and size and pigment granules are lost over time in culture. Annexin 2 also appears to be more cytoplasmic in cells with least pigment (cells shown with white arrows). This could be the result of less masking from the few pigment granules in these cells or annexin 2 may re-distribute and localise to the cell cytosol, away from the cell junctions when cells lose their pigment as a result of de-differentiation. Images were captured on a Leica TCS-SP2 AOBS DM IRE 2 confocal microscope and processed using Image J software. Scale bar = 20µm.

**Figure 3.8 C Primary porcine RPE cells are approximately cuboidal and retain their apical processes.**

Porcine RPE were isolated from pig's eyes and seeded onto glass bottom Matek™ dishes and maintained for 8 weeks. Cells were fixed at 1, 2, 4 and 8 weeks of culture and immunostained for annexin 2 (green) and F-actin (red). Confocal image stacks were collected to generate z-sections using a Leica TCS-SP2 AOBS DM IRE 2 confocal microscope and assembled using Zeiss LSM Image Browser software. These images show that both annexin 2 and F-actin is re-distributed with time in culture. F-actin appears to form tight junctions at 8 weeks and annexin 2 localisation appears to be more apical with time in culture. Apical and basal distribution of annexin 2 is equal at 1 week, in contrast to the mostly apical localisation at 8 weeks. Scale bar = 20µm.

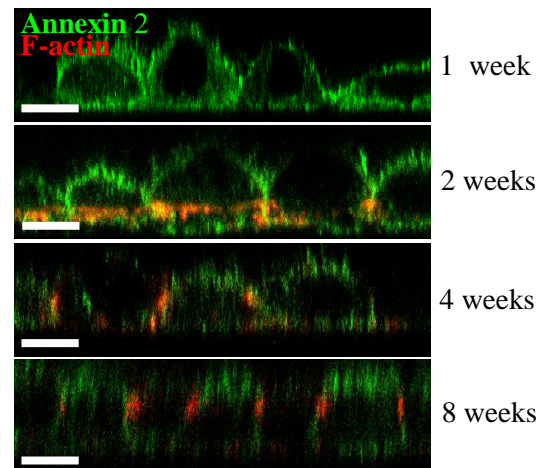
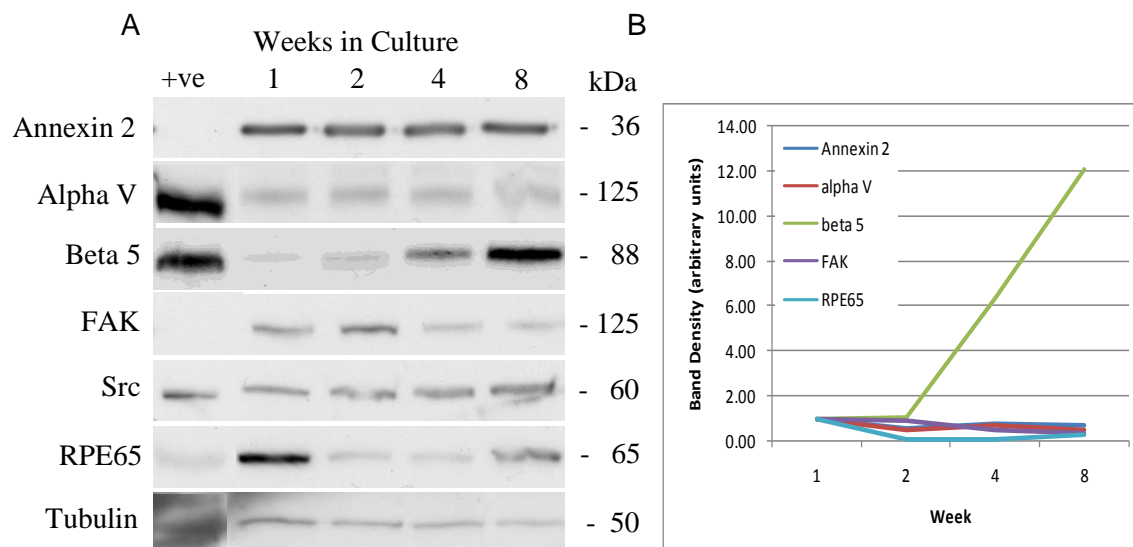


**Figure 3.9 Western blot analysis of protein expression in cultured primary porcine RPE cells**



RPE cells were isolated from pig's eyes and maintained in media containing 10% serum and lysed at 1, 2, 4 and 8 weeks in reduced sample buffer for whole cell lysates. 1/33 of the RPE Lysates were loaded into each lane. (A) Proteins were resolved by 10% SDS PAGE, transferred onto PVDF membranes and incubated with antibodies for annexin 2,  $\alpha_v$ ,  $\beta_5$ , FAK, Src and RPE65. Tubulin shows approximately equal loading for the samples. Differentiated Human Embryonic Stem Cells (HESC) previously shown to express the probed proteins was used as a positive control (+ve). (B) Protein expression profiles of annexin 2,  $\alpha_v$ ,  $\beta_5$ , FAK, Src and RPE65 at the measured time points were created by measuring pixel densities from the blots (A).

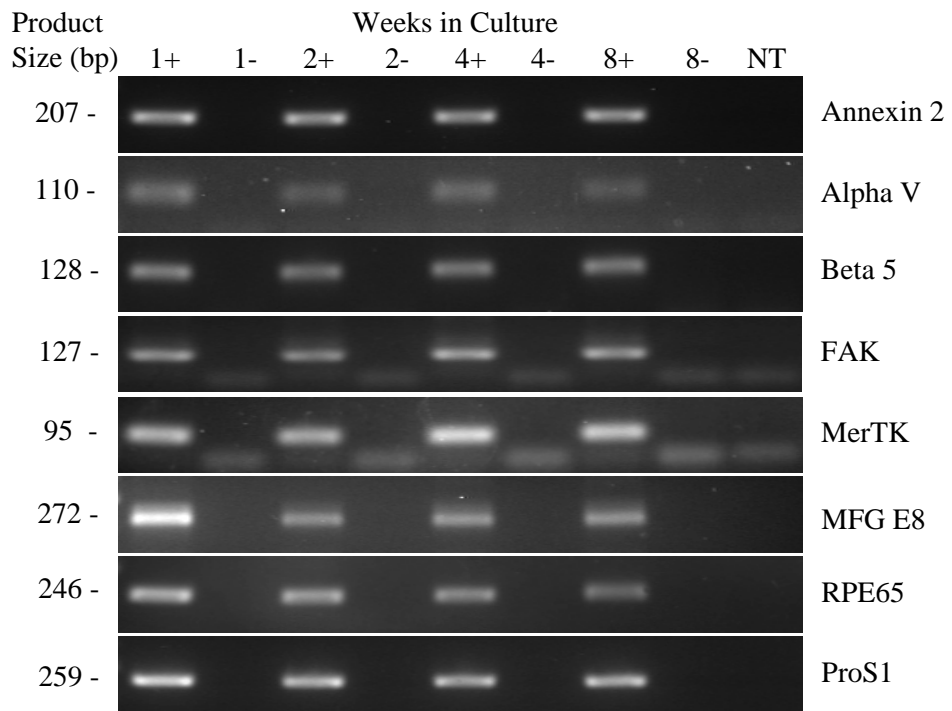


**Figure 3.10 Porcine RPE cells grown in culture express genes required for POS phagocytosis**

Porcine RPE cells were isolated and maintained for 8 weeks in media containing 10% serum and harvested in Trizol™. 3µg of RNA was used per cDNA synthesis reaction. 0.5µl of cDNA was used per PCR and amplicons were resolved by agarose gel electrophoresis (1.5% gel). See Materials and Methods section for PCR primer sequences, amplicon size and melting temperatures. +/- indicates exclusion (-) or addition (+) of reverse transcriptase and NT is no RNA template control for amplification of genomic DNA.

### 3.5. Characterisation of the RPE *in vivo*

#### 3.5.1. The Mouse Eye

To validate the observations made using immortalised and primary cells, it is necessary to compare these with gene expression in the RPE *in vivo*. To address this question, OCT embedded mouse eyes cut into 10µm semi-thin sections showed positive expression of annexin 2 in the RPE (Figure 3.11). 10µm semi-thin sections were used to allow staining to be visible which would otherwise be masked by the heavy pigmentation. The typical anatomical structure of the RPE and its adjacent photoreceptors are represented in the EM micrograph (Figure 3.12). The RPE lies directly in contact with Bruch's membrane which separates the retina from the choriocapillaris. The apical processes in the RPE are visible and extend upwards and interact with the photoreceptors. The spherical electron-dense objects labelled as 'B' are phagosomes. The RPE also contains numerous melanosomes which are scattered throughout the RPE (Figure 3.12). To study the native morphology of the RPE, mouse eyes were fixed and flat mounted, followed by staining for the tight junction marker ZO-1 to distinguish individual RPE cells. Resident phagosomes were also labelled with a rhodopsin antibody. RPE cells appeared polygonal in shape, typically with 5-6 sides (Figure 3.13).

Since a major objective of this thesis was to study POS phagocytosis in mice deficient of annexin 2<sup>(119)</sup>, comparison was also made between normal and annexin 2 knock out RPE with regard to expression of integrins  $\alpha$ v and  $\beta$ 5, FAK, MerTK, Gas6, MFG-E8, Protein S and RPE65 (Figure 3.14). The detection of most of these genes in the neuroretina fraction is consistent with the widely reported observation that small patches of RPE typically adhere to the retina upon detachment. RT-PCR analysis revealed all genes investigated to be expressed in both normal and annexin 2 knock out RPE, though with less contamination of neuroretina by RPE in the annexin 2 knock out samples. This may suggest that the RPE-neuroretina association is less tight in annexin 2 deficient retinae. The protein expression of annexin 2, integrins  $\alpha$ v and  $\beta$ 5, FAK, c-Src and RPE-65 in RPE whole cell lysates for both annexin 2 knock out and wild type mice is shown in Figure 3.15. As expected, annexin 2 is not expressed in samples from the knock out mice but is positively expressed in the wild type. Consistent with the PCR data, both knock out and wild type samples express integrin  $\alpha$ V, FAK, c-Src and RPE65 proteins. Integrin  $\beta$ 5 expression was not evident by western blotting but its gene expression is confirmed in Figure 3.14. Although not shown in the western blot, integrin  $\beta$ 5 protein is expressed in the RPE, indeed much work has been published using mouse RPE to study the function of integrin  $\beta$ 5 in RPE phagocytosis<sup>68, 69</sup>.

### 3.5.2. The Pig Eye

Gene and protein expression profiles were also studied in RPE and neuroretina extracted from fresh pig eyes. Expression of annexin 2,  $\alpha$ V, FAK, c-Src and RPE65 in the RPE was further confirmed at the protein level by the positive bands on Western blots shown in the pig RPE and neuroretina samples (Figure 3.15). Furthermore, Annexin 2, integrins  $\alpha$ V and beta 5, MerTK, MFG-E8 and RPE65 were also expressed in porcine RPE at the mRNA level (Figure 3.16). Detection of mRNA and protein expression in pig neuroretina samples is difficult to evaluate unless the gene is known to be RPE specific since the RPE is reported to attach to the neuroretina upon separation. Examination of contamination of the neuroretina by the associated RPE in the pig eye is also more difficult given that some eyes are albino and so the RPE lack pigment.

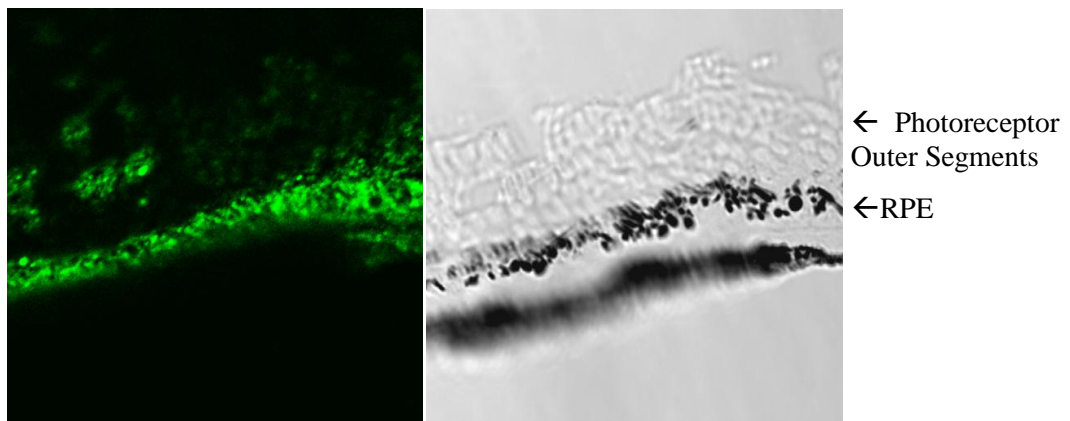


**Figure 3.11 Annexin 2 is expressed in control mouse RPE**

Eyes were harvested from C57BL/6 mice for fixing and OCT embedding. After freezing, 10  $\mu$ m thin transverse sections were cut and immunostained with antibody to annexin 2. The pigmented area, showing positive expression of annexin 2 (green) is the RPE and part of the photoreceptor outer segments remain intact and interact directly on the apical region of the RPE. The patches of green staining on the neuroretina are non-specific since the staining is present in the annexin 2 knock out RPE, shown in Figure 5.3. Images were captured on a Leica TCS-SP2 AOBS DM IRE 2 confocal microscope and processed using Image J software. Scale bar = 50  $\mu$ m.

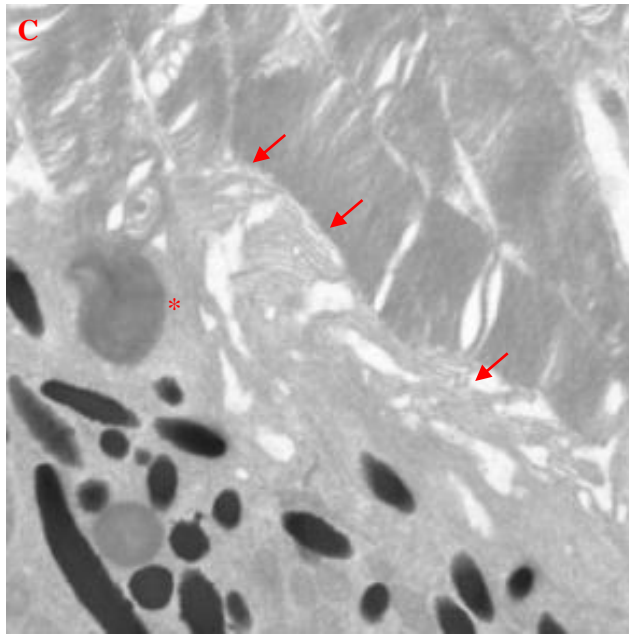
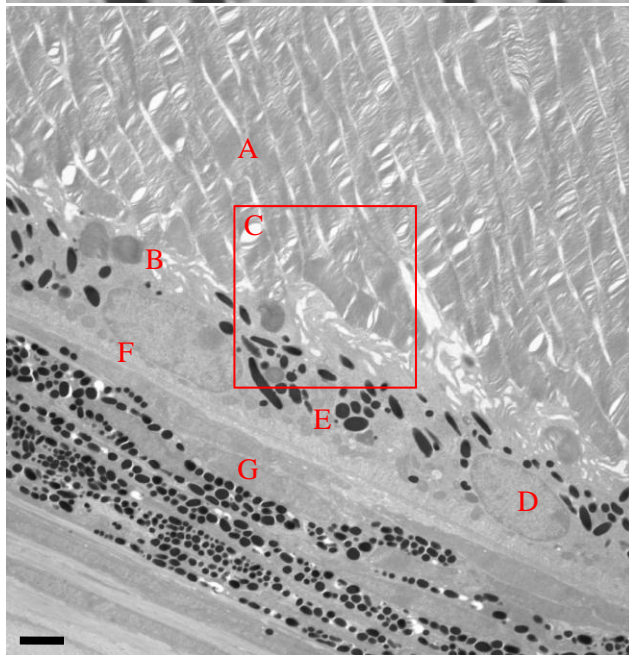


**Figure 3.12 Electron micrograph of mouse RPE and photoreceptors**

Freshly enucleated eyes from C57BL/6 mice were fixed in 1% paraformaldehyde and 3% glutaraldehyde in 0.07 M cacodylate buffer followed by imbedding in Epon. 70-80 nm sections were cut and stained with lead citrate (Dr Clare Futter). Red arrows point to the apical processes of the RPE and the red asterisk indicate a phagosome. Images were taken with Joel 1010 electron microscope and processed with Kodak electron microscope film 4489. Scale bar = 2  $\mu$ m.



A Photoreceptor Outer Segment

B Phagosomes

C RPE Apical Processes (red arrows)

D RPE Cell Nucleus

E Melanosomes

F Bruch's Membrane

G Choriocapillaris

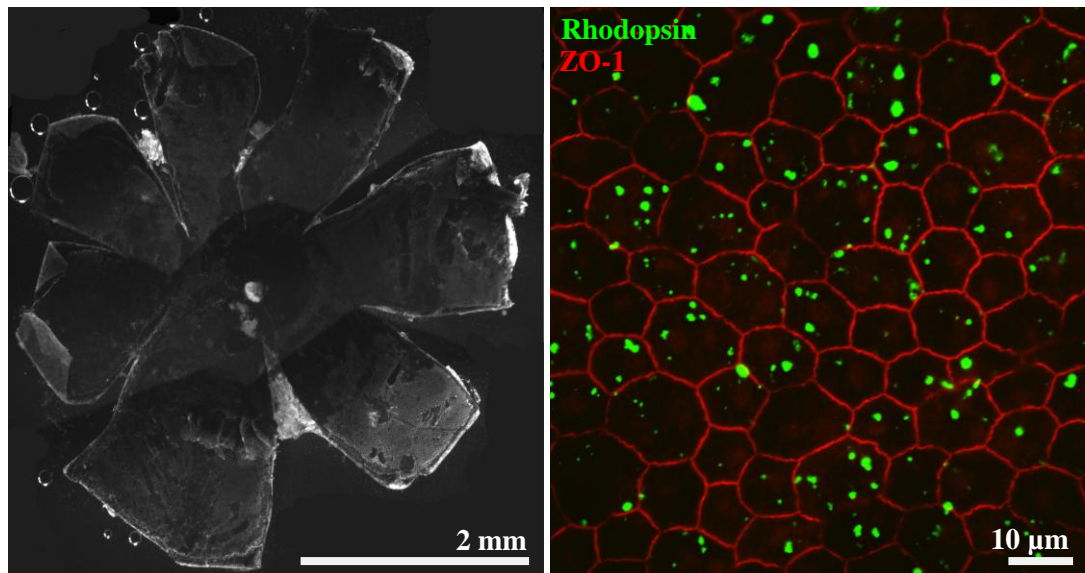


**Figure 3.13 Mouse eye flatmount showing ZO1 and rhodopsin staining**

The enucleated eye was trimmed and fixed before incising along the ora-serrata, separating the eye into anterior and posterior segments. The lens and vitreous were removed and the neuroretina was carefully peeled away exposing the RPE. Incisions were made from the peripheral edge of the eye cup towards the optic nerve head to open the eye cup into a ‘flower’. This was followed by fixing further with PFA before immersing into blocking solution containing 3% Triton, 0.5% Tween, 1% BSA, 0.1% sodium azide. The ‘flower’ was then incubated with ZO1 and 1D4 rhodopsin antibodies overnight at room temperature, ready for labelling with conjugated secondary antibody the next day. The eye was mounted onto glass slides in Mowiol and covered with glass cover slips. The left panel shows a whole flatmounted mouse eye, compiled by merging the different segments taken from the flatmount in Photoshop. The right panel shows a higher magnification of the flatmount from the left panel. Individual RPE cells are distinguished by the ZO-1 immunostain (red), and phagosomes are identified with rhodopsin antibody (green). The flatmount images were taken with a Leica DM IRB microscope and a Hamamatsu C4742-95 digital camera.

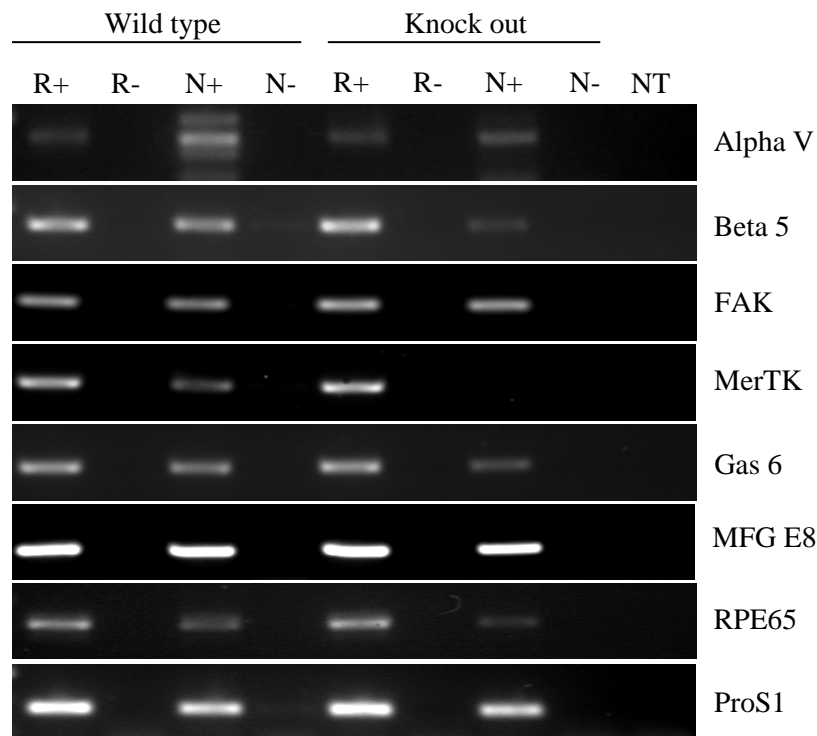


**Figure 3.14 Mouse RPE cells express genes required for POS specific phagocytosis**

RNA from annexin 2 knock out and control mouse RPE cells and neuroretina was isolated from mouse eyes in Trizol™. 3µg of RNA was used per cDNA synthesis reaction. 1µl of cDNA was used per PCR and amplicons were resolved by agarose gel electrophoresis (1.5% gel). See Materials and Methods section for PCR primer sequences, amplicon size and melting temperatures. R is RPE and N is neuroretina. +/- indicates exclusion (-) or addition (+) of reverse transcriptase and NT is no RNA template control for amplification of genomic DNA. Expression of RPE specific genes (RPE65 and MerTK) appears to show positive expression for both RPE and neuroretina. This is due to contamination resulting from the tight association between the RPE and neuroretina and indicates that some RPE cells/apical processes may have attached to the neuroretina during separation. Intriguingly, positive expression of RPE65 and MerTK appears less apparent in neuroretina from the annexin 2 -/- mice. This may suggest that the RPE-neuroretina association is less tight in annexin 2 deficient retinae.

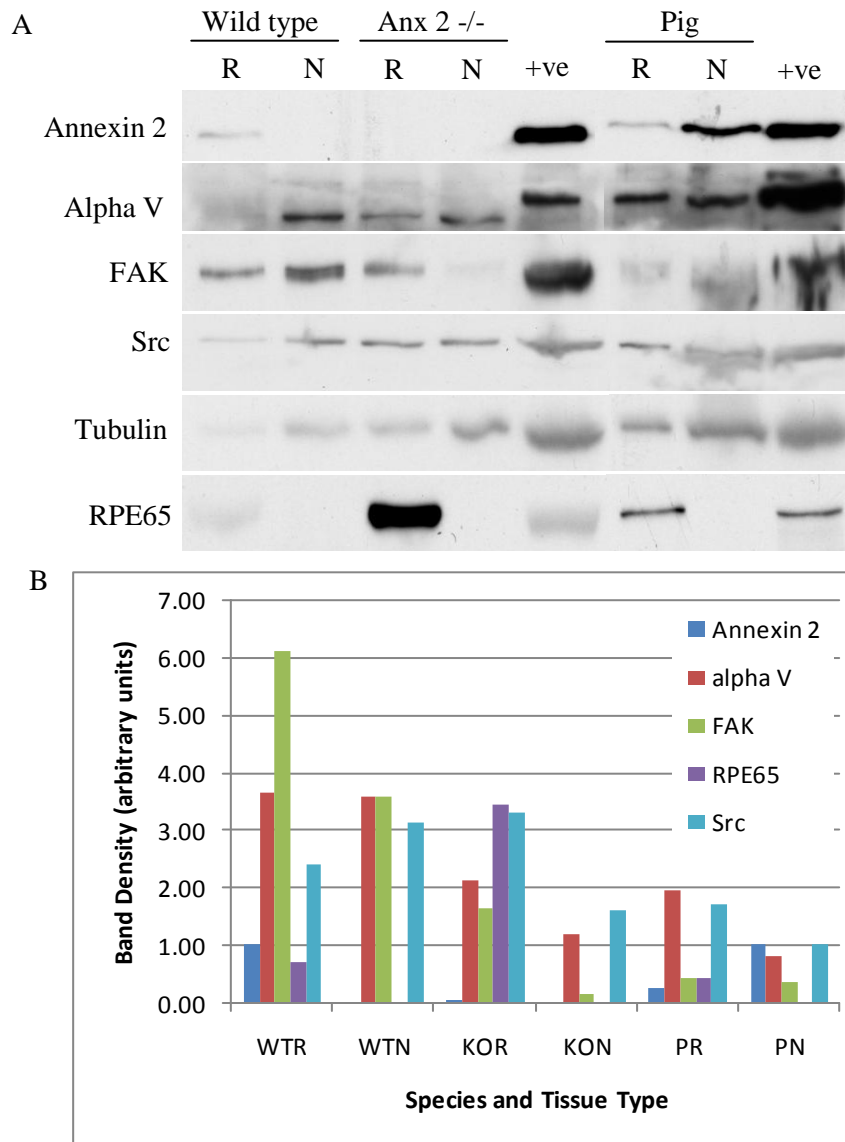
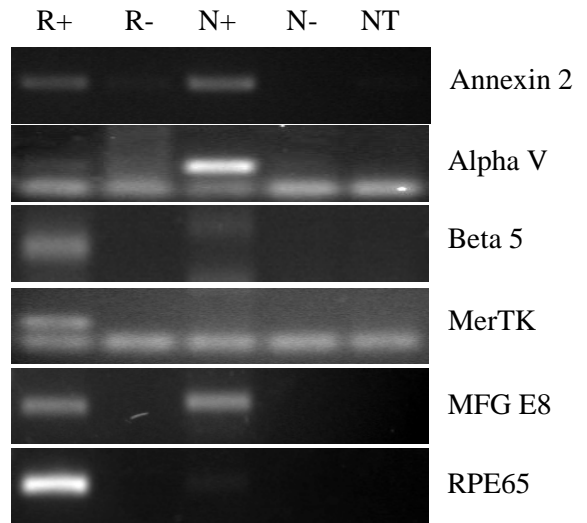


**Figure 3.15 Western blot analysis of protein expression in pig, wild type and annexin 2 knock out RPE and retina**

Neuroretina was separated from RPE in annexin 2 knock out eyes, wild type eyes and pig eyes. Neuroretina and the remaining eye cups were lysed in reducing sample buffer to make whole cell lysates. 1/8 of RPE/neuroretina extracts from wild type and annexin 2 knock out mice and 1/50 of RPE/neuroretina extract harvested from porcine eyes were loaded into each gel lane. (A) Proteins were resolved by 10% SDS PAGE gel, transferred onto PVDF membranes and incubated with antibodies for annexin 2, alpha V, FAK, RPE65 and Src. Tubulin blots were performed as a loading control. +ve is positive control, R is RPE and N is neuroretina. (B) Protein expression profiles of annexin 2, alpha V, FAK, RPE65 and Src for the different samples were created by measuring pixel densities from the blots (A).

**Figure 3.16 Porcine RPE cells express mRNAs required for POS specific phagocytosis**

RNA from porcine RPE cells and neuroretina was in Trizol™. 3µg of RNA was used per cDNA synthesis reaction. 1µl of cDNA was used per cDNA synthesis reaction and amplicons were resolved by agarose electrophoresis (1.5% gel). See Materials and Methods section for PCR primer sequences, amplicon size and melting temperatures. R is RPE and N is neuroretina. +/- indicates exclusion (-) or addition (+) of reverse transcriptase and NT is no RNA template control for amplification of genomic DNA.



Note that the positive expression of annexin 2 and integrin alpha V in the neuroretina samples (containing reverse transcriptase) which also appears to be expressed at higher levels than the RPE are likely to be contamination from RPE cells during separation.

### 3.6. Discussion

There are a number of immortalised RPE cell lines that have been extensively used in retinal phagocytosis studies, and RPE isolates from freshly harvested eyes have also been successfully propagated to form primary RPE cultures for this purpose. However, it is widely noted that *in vitro* RPE cell systems lack uniformity and cells are heterogeneous, even when generated from a single clone. Despite the generally consistent morphology of RPE cells *in situ*, RPE cells in eyes are in fact heterogeneous in cell shape<sup>170</sup>, a characteristic that may underlie the more prominent morphological differences observed in culture. Heterogeneity may also be conferred by the artificial environment of culture systems which lack many of the cues and cell interactions of the retina *in vivo*. Furthermore, immortalised cells may be genetically unstable and their phenotype and gene expression may alter when grown with different media components and on different substrates. These variables have been reported to affect polarity, and ultimately the expression of various genes that are important for RPE function<sup>147, 161, 171-173</sup>. As shown in this chapter, differentiation of RPE cell lines is time dependent and relies at least in part on interactions between the junctional proteins at the cell membrane with F-actin and other cytoskeletal components. In contrast to RPE cell lines, which mature and differentiate with time in culture, primary cultures established from RPE isolates from eyes de-differentiate and lose polarity and expression of RPE specific markers over time.

In the context of this project, it was important to study the gene and protein expression of annexin 2 and the key molecules that make up the RPE phagocytic machinery. Annexin 2 and F-actin were immunostained in these cells to determine their localisation and relationship to cell morphology. Expression of annexin 2 and the key molecules important for POS internalisation will not only determine the cell types to be used but also aid interpretation of results. The two cell lines, ARPE-19 and RPE-J were cultured on substrate-free tissue culture plastic or glass and maintained in simple media consisting of DMEM with 10% or 4% serum (respectively). Contrary to methods used previously, RPE-J cells were grown at 37°C throughout their 8 weeks in culture. Primary porcine RPE cultures were also propagated in DMEM containing 10% serum. The cells were harvested at 1, 2, 4 and 8 weeks for whole cell lysates for western blotting and RNA extracts. Samples were also stained for F-actin and annexin 2 at these time points.

RT-PCR for genes of interest in the samples collected was used in addition to western blotting to overcome difficulties of species recognition and specificity with some antibodies, and limited genome information for the pig. Both ARPE-19 and RPE-J cells expressed annexin 2, integrin chains  $\alpha V$  and  $\beta 5$ , FAK, MerTK, c-Src, Gas6 and MFG-E8 at mRNA and protein levels.

Intriguingly, RPE65 expression in ARPE-19 cells at the mRNA level only occurs from 4 weeks of culture (Figure 3.3), which coincided with enrichment of annexin 2 and F-actin at the cell junctions, and cell differentiation into polygonal shapes, also observed at 4 weeks in culture (Figure 3.1 A and B). Both mRNA and protein expression of RPE65 were negative in RPE-J cells grown up to 8 weeks (not shown) which is consistent with a previous report showing the absence of RPE65 along with other RPE proteins such as CRALBP and 11-*cis*-retinol dehydrogenase.<sup>174</sup> Morphologically, RPE-J cells showed a more native RPE phenotype in comparison to ARPE-19 cells early in culture (Figure 3.5 A and B). RPE-J cells are approximately cuboidal and display a polygonal shape from week 1 of culture, observed from the single confocal sections and stacked images of these cells. The cuboidal phenotype evident at week 1 was however lost through culture as the cells tended to become flatter and grew on top of each other. At week 1, these cells did not pack together tightly and cortical actin was not localised to the cell perimeter. Cortical actin rearranged in culture and by two weeks was aligned to the cell periphery in most cells. The cells also developed discrete F-actin focal points that became more pronounced with time in culture (Figure 3.5 C).

In contrast, ARPE-19 cells were elongated in shape and did not acquire the classic polygonal shape displayed by RPE cells *in situ* until 4 weeks in culture. The actin stress fibres observed during week 1 and week 2 in culture rearranged to form cortical actin bands from 4 weeks in culture (Figure 3.1 A and B). Despite developing a polygonal shape with time, ARPE-19 cells remained flat, and like RPE-J cells, showed no contact inhibition and also grew on top of each other (Figure 3.1 C). Intriguingly, these cells showed a decrease in MerTK protein expression from week 1 in culture with virtually no expression at week 8 (Figure 3.2) despite positive mRNA expression for this gene (Figure 3.3). Furthermore, concomitant to RPE65 expression, differentiation into polygonal cells did not occur until week 4 in culture.

Characterisation of these two cell lines revealed that both express annexin 2 in addition to key RPE phagocytosis molecules, and are thus suitable as model systems to study the role of annexin 2 in RPE phagocytosis. However, when using these cells, these characteristics must be taken into account to ensure accurate interpretation of results. Despite only acquiring a polygonal shape and RPE65 expression at week 4 in culture, because they lose MerTK protein expression in culture, ARPE-19 cells should be grown and used within 2 weeks to ensure that MerTK protein expression is still present at the time of experiment. In the context of phagocytosis experiments, MerTK is absolutely crucial for POS internalisation and so its expression in culture is more important than that of RPE65. RPE-J cells did not grow well on glass after 1 week in culture and were fragile, and because expression of crucial phagocytosis

molecules does not appear to be affected by time in culture, it may be best to use these cells at 1 week of culture. Using ARPE-19 at 2 weeks and RPE-J at 1 week in culture also limits their ability to grow on top of each other, which may adversely affect experiments.

RPE isolates from freshly harvested pig eyes were also propagated and characterised. These cells are easy to isolate and culture, with relatively few problems with regard to contamination. Isolation is however time-consuming and although a reasonable yield is obtained, it is by no means comparable to immortalised cells. Cells are also used unpassaged and so material is costly as well as time-consuming in preparation. In culture, primary porcine RPE retain a well-defined polygonal shape, typically of 5-6 sides, with cortical actin arranged as clear bands around the cell circumference. Cells are often multinucleated and are pigmented. Daughter cells were less pigmented than the original isolate and cells became notably less pigmented in culture over time (Figure 3.8 A and B). Annexin 2 staining in these cells was visible although grainy, most likely due to the pigment granules in these cells. In addition, primary cells in culture still retained their apical processes, which were evident up to 4 weeks. At 8 weeks in culture, the apical processes were much less well defined. This can be observed clearly in week 1 of Figure 3.8 C and less clearly for week 4 and 8 due to the lower resolution of these images. These cells however remained cuboidal throughout the course of the experiment and did not grow on top of each other. Expression of annexin 2,  $\alpha$ V and  $\beta$ 5 integrins, FAK, c-Src and RPE65 in the primary cells was observed at 1, 2, 4 and 8 weeks in culture. Molecules not shown by western blotting such as MerTK, MFG-E8 and Protein S were expressed at the mRNA level. Primary porcine RPE cells, despite the drawbacks mentioned earlier, grew as a single monolayer in culture and retained many of the features of the native RPE cell. Moreover, they did not lose expression of important proteins that take part in RPE POS internalisation, and are thus suitable as a cell model system to study phagocytosis. The slow disappearance of apical processes and pigment granule dilution over time in culture however, does indicate that some de-differentiation occurs and suggests that these cells should be used before one month in culture.

*In vitro* characterisation studies on ARPE-19, RPE-J and primary porcine RPE cells have shown that RPE cell lines and primary RPE behave differently with time in culture. Whilst ARPE-19 and RPE-J cells become more differentiated in culture, primary RPE cells appear to de-differentiate, before apparently re-differentiating again. The epithelial-mesenchymal transition (EMT) is a fundamental process that governs morphogenesis of epithelial monolayers in multicellular organisms. This phenomenon is based on transition of an epithelial cell to a mesenchymal cell or a mesenchymal cell into an epithelial cell (MET). In the context of this

chapter, EMT is a term that governs the differentiation of undifferentiated cell lines into differentiated polarised epithelial cells and vice-versa for the primary porcine RPE cells, where they are removed from their native environment and slowly de-differentiate, lose polarity and become less epithelial-like. There are several known factors and signalling pathways that have been shown to govern EMT, which include various growth factors that activate tyrosine kinase surface-receptor associated pathways<sup>175</sup>. Epithelial cells are polarised such that the cells have an apical and a basolateral domain. They adhere to each other through complexes that form junctions between the cells, which include Gap junctions, desmosomes, adherens junctions and tight junctions. Tight junctions are normally located towards the apical surface of the epithelial cells and form a paracellular gate that regulates epithelial permeability. Adherens junctions and desmosomes are adhesive junctions and are linked to the actin cytoskeleton and intermediate filaments respectively. Gap junctions are distributed along the lateral membrane and form intercellular pores that allow exchange of small molecules between cells. The functions of Gap junctions in mature RPE cells are not known, but they have a critical role in retinal development<sup>176-178</sup>. Of these complexes, the adherens junctions and the tight junctions are known to associate with the actin cytoskeleton; with the latter having a particular importance in EMT by being functionally linked to different types of signalling pathways that modulate cell behaviour. Tight junctions are involved in bidirectional signal transduction. Signals from the cell interior regulate their assembly and function, and signals are also transmitted from the tight junctions to the cell interior to modulate gene expression, proliferation and cell differentiation<sup>24</sup>.

To assume the polygonal shape exhibited by ARPE-19 cells over time, cell-cell adhesion is therefore tightly coordinated with cytoskeletal changes. Cell-cell contact requires dynamic interactions between cadherin receptors which distribute freely at the cell surface before forming adhesive bands between cells. Bond formation is followed by the activation of Rac and Arp2/3-dependent actin nucleation. Activation of Rac also induces lamellipodial extensions, which are driven by the actin dynamics mediated by Arp2/3 and other cytoskeletal proteins to push the membranes of adjacent cells over each other, a feature observed in both ARPE-19 and RPE-J cells which overlap each other with time in culture. Once cell-cell contacts are stabilised, cadherin contacts are rearranged in polarised epithelial cells so that they become associated with circumferential actin bundles that separate into two populations: junctional actin and peripheral thin bundles. Junctional actin stabilises adhesion of cadherin receptors, whilst peripheral actin is contracted to increase the height of the lateral domain to form a cuboidal cell, a defining characteristic of many epithelial cells. The two populations then become indistinguishable to form a cortical actin band, typically displayed by mature, fully polarised

cells<sup>179</sup>, and observed in these studies by the F-actin staining in both ARPE-19 and RPE-J cells and the development of polygonal shaped ARPE-19 cells at 8 weeks in culture.

In polarised cells, the separation of apical and basolateral domains is generally considered to be defined by tight junctions. Tight junctions encircle cells at the apical end of the lateral membrane where they function as a fence that prevents the apical-basolateral mixing of membrane proteins and also as a gate to regulate the paracellular diffusion of ions and solutes in between cells. Tight junction assembly has been shown to be mediated in part by the calcium dependent-epithelial adhesion protein E-cadherin. E-cadherin mediated cell-cell adhesion triggers the initial signal for the assembly of a primordial junction that contains both adherens junction and tight junction components which then matures to form distinct adherens junctions and tight junctions<sup>24</sup>. E-cadherin expression is required for the maintenance of stable junctions and *in vitro*, there is direct correlation between the lack of E-cadherin production and loss of the epithelial phenotype<sup>180</sup>. The different signalling molecules that mediate tight junction assembly include protein kinase A (PKA), monomeric and heterotrimeric G proteins and various protein kinase C (PKC) isotypes. Functional tight junctions assemble when epithelial cells reach high densities, which results in increased expression of tight junction proteins such as ZO-1. High density cells with fully assembled tight junctions function to suppress signalling pathways that stimulate proliferation and inhibit differentiation. Signalling may involve interactions with the Crumbs protein which was identified in *Drosophila* as an apical protein required for polarity in ectodermal epithelia. Mutant crumbs (crb) in *Drosophila* fail to develop adherens junctions, and mutations in the human homologue CRB1 are associated with severe forms of retinal dystrophy and Leber's congenital amaurosis (LCA)<sup>30-32</sup>. Inhibition of the Raf pathway, which is activated by the small GTPase Ras, results in the assembly of functional tight junctions and adherens junctions. Furthermore, over-expression of the tight junction protein occludin is sufficient to reverse cell transformation, and so high density cells with functional tight junctions are no longer proliferative and have high expression levels of differentiation markers<sup>24</sup>. In the context of the RPE cells lines used, once confluency is reached, functional tight junctions are assembled<sup>147</sup>, which decreases proliferation and increases differentiation over time in culture. In primary RPE cells, tight junction proteins and other junctional complexes between the epithelial cells become disrupted during isolation and so permit cells to de-differentiate in culture. The tight junctions are linked to the actin cytoskeleton and the adherens junctions via cytoskeletal connectors: the ZO proteins which include ZO-1, ZO-2 and ZO-3. These proteins have domains that mediate binding to adherens junctions and tight junctions in addition to the actin cytoskeleton. The formation and localisation of ZO-1 is associated with E-cadherin mediated assembly of adherens junctions, and ZO-1 has been proposed to connect to

transmembrane proteins and recruit cytoplasmic proteins such as kinases and transcription factors to the tight junctions.

Although both ARPE-19 and RPE-J cells showed F-actin realignment to form discrete cortical actin bands, and ARPE-19 cells acquired a polygonal morphology over time in culture, which are all features of fully polarised cells, immunostaining for the apical localisation of ZO-1 and Na/K-ATPase (which is uniquely polarised on the apical surface of the RPE)<sup>154</sup> and measurement of transepithelial electrical resistance (TER) to study the maturation of the tight junctions throughout the 8 weeks in culture would be required to provide direct evidence of polarisation in these cells, which have been grown without filters or biological substrates. Immunolocalisation of apical markers such as the Na/K-ATPase and TER studies have previously been performed on ARPE-19 grown on uncoated Transwell polyester filter and on porcine lens capsule (PLC) over a period of 6 weeks. Turowski *et al* (1994)<sup>147</sup> found that ARPE-19 grown on PLC had a significant increase in TER in comparison to cells grown on filters. Importantly, polarisation and TER are associated with the presence of intercellular junctional proteins and specifically functional tight junctions<sup>147</sup>.

Intriguingly, in addition to the changes in cell morphology that occurred over a few weeks, when observed at 4 months ARPE-19 cells also showed pigmentation (Figure 3.4). Immature ARPE-19 cells were also found to express some of the key molecules known to have roles in POS phagocytosis, at least at the mRNA level (Figure 3.3). However, this was not the case for RPE65, a RPE-specific protein involved in the conversion of all-*trans* retinol to 11-*cis* retinal during phototransduction. However, in parallel with the morphological changes over time in culture, ARPE-19 cells exhibited positive gene expression for RPE65 from 4 weeks. This may be a consequence of acquiring polarisation, or it may be that the expression of RPE65 occurs in response to extracellular factors secreted by the cells. Similarly, junctional staining of annexin 2 co-localised with that of F-actin from week 4. Given that annexin 2 has a role in the regulation of actin and can bind PtdIns4,5P<sub>2</sub> on membranes, it is therefore possible that annexin 2 may be involved in EMT. This idea is supported by a recent publication providing evidence that membrane-bound annexin 2 binds to vascular endothelial cadherin (VE-cad). Annexin 2 stabilises inter-endothelial adherens junctions and thus mediates the switch from an immature to a mature state<sup>181</sup>. In Madin-Darby canine kidney (MDCK) epithelial cells, tetrameric annexin 2, composed of two annexin 2 and 2 S100A10 molecules, was also shown to be involved in the formation of E-cadherin-based adherens junctions, which was inhibited when cells were treated with annexin 2 siRNA. The annexin 2-S100A10 complex may be involved in the recycling of E-cadherin in this process and may also function in formation of the actin cytoskeleton at the

adherens junctions<sup>182</sup>. Recently, it has been shown that tetrameric annexin 2 interactions with AHNAK regulate cortical actin organisation and cell membrane cytoarchitecture. AHNAK localises to the plasma membranes during cell-cell contact formation and associates with the S100A10 subunit of tetrameric annexin to form a multicomplex, containing annexin 2-S100A10 and actin. Using siRNA to knock down annexin 2 and its S100A10 ligand inhibited targeting of AHNAK to the plasma membranes, and cortical actin reorganisation was lost when AHNAK was knocked down in cells<sup>183</sup>. Tetrameric annexin 2 is also localised to the apical and lateral plasma membranes and has been shown to associate with the tight junction proteins ZO-1, occludin and claudin-1 at cell-cell contacts in MDCK cells. The authors propose that tetrameric annexin 2 has a role in tight junction assembly through linking adjacent lateral membranes together, thus forming a bridge between adjacent cells and providing a platform with which tight junction proteins associate and regulate permeability<sup>184</sup>.

These studies provide evidence that annexin 2 plays an important role in the rearrangement of actin during junctional protein formation, either by direct interaction with F-actin<sup>128</sup>, barbed end capping activity<sup>130</sup>, or the recruitment of actin cytoskeleton modulating factors. An interesting example includes the Rho-GTPase Cdc42, which has been shown to interact with the tetrameric annexin 2 complex in polarising epithelial cells. The protein phosphatase PTEN (phosphatase and tensin homolog deleted on chromosome ten), which removes phosphate from the three position of phosphatidylinositol (3,4,5) trisphosphate (PtdIns3,4,5P<sub>3</sub>), converting it into phosphatidylinositol (4,5) bisphosphate (PtdIns4,5P<sub>2</sub>), is targeted to the apical membrane in polarising cells to segregate PtdIns4,5P<sub>2</sub> to the apical membrane and PtdIns 3,4,5P<sub>3</sub> to the basolateral surface. Tetrameric annexin 2 binds to this apical PtdIns4,5P<sub>2</sub>, which is required for recruitment of Cdc42 to the apical plasma membrane. Here, Cdc42 initiates the formation of an actin belt (as observed in ARPE-19 and RPE-J cells at 8 weeks in culture and in primary porcine RPE cells, Figure 3.1, Figure 3.5 and Figure 3.8 respectively), followed by full morphological polarisation<sup>130, 185, 186</sup>.

Whilst MET (Mesenchymal Epithelial Transition) was observed in the cell lines, particularly in ARPE-19 cells, the opposite appeared to occur in primary porcine RPE. Pigmentation was lost through time in culture, and apical processes also appeared to shorten thus the cells gradually lost their RPE phenotype. Annexin 2 also appeared to be more cytoplasmic in cells with least pigment (3.8B). Although this could be due to fluorescence quenching, annexin 2 may redistribute from the plasma membrane to the cell cytosol when cells de-differentiate, again supporting the idea that annexin 2 may play a role in epithelial differentiation. Despite loss of pigment and apical processes, the expression of key genes required for POS phagocytosis was

maintained in cultured porcine RPE cells, at least for the time periods tested here. In z-sections, F-actin appeared to be present at tight junctions at 8 weeks, whereas annexin 2 localisation appeared to be more apical with time in culture. Apical presentation of annexin 2 and the appearance of F-actin at the apical junctions would suggest that the cells at least remained polarised with time in culture. However, primary porcine RPE cells probably de-differentiate with time in culture, which would be an expected effect of removing the RPE from its native environment. Thus, taken out of their *in vivo* environment and without adhesion to Bruch's membrane and the photoreceptors that interact with their apical processes, RPE cells may lose polarity and appear less RPE-like. Since cell lines are able to differentiate into cells that more closely represent their native origins, it is possible that when removed from their native environment, primary RPE cells may undergo initial de-differentiation which may be followed by re-differentiation as the cells lay down their own extracellular matrix. Studying the localisation and expression of E-cadherin, ZO-1 as well as the RPE cell polarity marker Na/K-ATPase during cell differentiation, would provide tangible evidence for differentiation and development of polarity in the RPE cells over time. This would also allow a more detailed evaluation of the involvement of these proteins in the various stages of EMT together with comparison of the localisation of annexin 2 throughout this period.

In comparison to RPE cells grown *in vitro*, the RPE *in situ*, represented by the wild type mouse eye (Figure 3.12) is dominated by numerous pigment granules, is physically attached to Bruch's membrane, and interacts directly with the photoreceptors. The RPE cell possesses long apical processes that extend upwards, interacting with POS and sequesters shed outer segments into the cell body for degradation. Phagosomes were observed in the EM micrographs as approximately round electron-dense objects, containing layers of membranes. These may be counted along the RPE in order to quantify the efficacy of phagocytosis<sup>21, 69</sup>. Annexin 2 was also shown to be present in the RPE *in vivo*, confirming the work in ARPE-19 cells<sup>147</sup> and making it possible to use the mouse eye for *in vivo* experiments for this project (Figure 3.11). The morphology of the RPE *in situ* was broadly similar to the confluent cultures of primary porcine RPE in cell shape and uniformity. Both primary RPE cultures and RPE cells *in situ* have a regular polygonal shape of typically 5-6 sides. RPE cells *in situ* however appear completely black as they are still attached to their surrounding tissues (Figure 3.13). The flat-mount also showed positive staining for native phagosomes, providing a powerful novel technique for quantifying phagosomes *in vivo*, with advantages over previous methods that involved the more laborious counting of phagosomes along the length of RPE on electron micrographs. The interaction between the photoreceptors and the RPE are tight, which often results in patches of RPE associated to the neuroretina upon detachment or after the process of

separation and so positive expression of genes and protein in the RPE and neuroretina may be cross contamination of material and so care must be taken when analysing gene and protein expression in the RPE and neuroretina *in situ*.

In conclusion, these characterisation studies provide essential preliminary data confirming that both human and rat immortalised cell lines (ARPE-19 and RPE-J respectively) are suitable for studying the role of annexin 2 in phagocytosis, providing that the cells are used at the correct time in culture. Work in this chapter has also established that for primary cell cultures, the pig eye is particularly suitable as porcine RPE are relatively simple to maintain and retain expression of important phagocytosis proteins.

## **Chapter 4**

**Does Annexin 2 have a role in RPE  
Phagocytosis of photoreceptor  
outer segments *in vitro*?**

#### **4. Does Annexin 2 have a role in RPE phagocytosis of rod outer segments *in vitro*?**

The retinal pigment epithelium (RPE) is a monolayer of highly specialised polarised epithelial cells that perform a range of functions essential for homeostasis and visual function in the eye. One of these functions is the daily phagocytosis of shed photoreceptor outer segments (POS) that lie adjacent to the RPE. This process is part of a vital relationship between the RPE and photoreceptors that maintains the life and function of both cell types. The apical processes of the RPE extend into the interphotoreceptor matrix where they interdigitate with the POS, forming an intimate relationship between the RPE and photoreceptors. Shed POS are engulfed and drawn into the RPE cell for processing and degradation. This process involves the active reorganisation of the cell membrane and cytoskeletal structure, and is dependent on actin dynamics within the apical processes of the RPE.

Annexin 2 is already implicated in endocytosis. It has been shown to associate with early endosomes<sup>134, 135</sup> and actin-propelled pinosomes<sup>138</sup>. Annexin 2 was also found on phagosomes in the J774 mouse macrophage cell line<sup>139</sup>. In this latter study, phagosomes were formed by the internalisation of 1 µm latex beads by the macrophages and purified by cell fractionation, followed by sucrose step flotation for isolation of phagosomes. By electron microscopy, annexin 2 was observed to be the most abundant annexin to associate with early endosomes and on the phagosome membrane. Whilst these studies that associate annexin 2 with endocytosis include a wide range of cell types and cell lines, the role of annexin 2 in RPE cell outer segment phagocytosis has not yet been investigated. POS phagocytosis by the RPE is not only essential for the maintenance of the health of the retina, it also provides a useful model for studying phagocytosis *in vivo*.

Four annexins have been identified in proteomic analyses of the RPE, including annexins 2, 4, 5 and 6, with annexins 2 and 5 also found enriched in the apical microvilli of RPE cells<sup>148, 149</sup>. The apical microvilli of the RPE play a key role in mediating outer segment phagocytosis, visual pigment recycling and nutrient and waste exchange between the photoreceptors and the RPE, suggesting that annexins 2 and 5 may have a role in these activities. In fact, annexin 2 is well placed to have a role in this process. Its direct involvement in actin dynamics may be significant in RPE outer segment phagocytosis, which requires extensive re-organisation of actin and re-distribution of membrane on the apical processes. Possible involvement of the annexins in the RPE first came to light in a report by Turowski *et al* (2004)<sup>147</sup>. This study revealed up-regulation of annexin 2 and annexin 4 in functionally differentiated ARPE-19 cells, along with increased phagocytic competence. The coincidence of both up-regulation of

annexins 2 and 4 with increased phagocytic competency would be consistent with possible roles for these two proteins in RPE phagocytosis. The work described in this chapter extends from this earlier work and aims to address whether annexin 2 is involved in RPE phagocytosis of POS *in vitro*.

#### **4.1. Transient co-localisation of annexin 2 with phagosomes**

In order to find out whether annexin 2 is involved in POS phagocytosis by the RPE *in vitro*, ARPE-19, RPE-J and primary porcine RPE cells were grown on glass-bottom Matek™ dishes for 1 week and seeded with purified, labelled POS before immunostaining the cells for annexin 2 and F-actin. As in other cell types annexin 2 was expressed throughout the cell cytoplasm and at the cell junctions (Figure 4.1). Annexin 2 staining in the porcine RPE cells appeared grainy, probably due to the pigment granules present in primary RPE cells. When challenged with POS, annexin 2 was seen to re-distribute to the phagocytic cup during POS phagocytosis in ARPE-19 cells (Figure 4.2 A). Annexin 2 is observed to co-localise with F-actin and remains on the partially internalised phagosome before dissociating once internalisation is complete. Annexin 2 was not observed on fully ingested phagosomes. Figure 4.2 B shows a confocal slice through primary porcine RPE cells in the process of POS phagocytosis. Annexin 2 is recruited to the POS and co-localises with F-actin, where it appears as a ‘belt’ around the POS. Annexin 2 is also observed on the phagosome during POS phagocytosis in RPE-J and primary porcine RPE. Taken together, these observations in a variety of RPE cells support the idea that annexin 2 is involved in the early stages of POS engulfment.

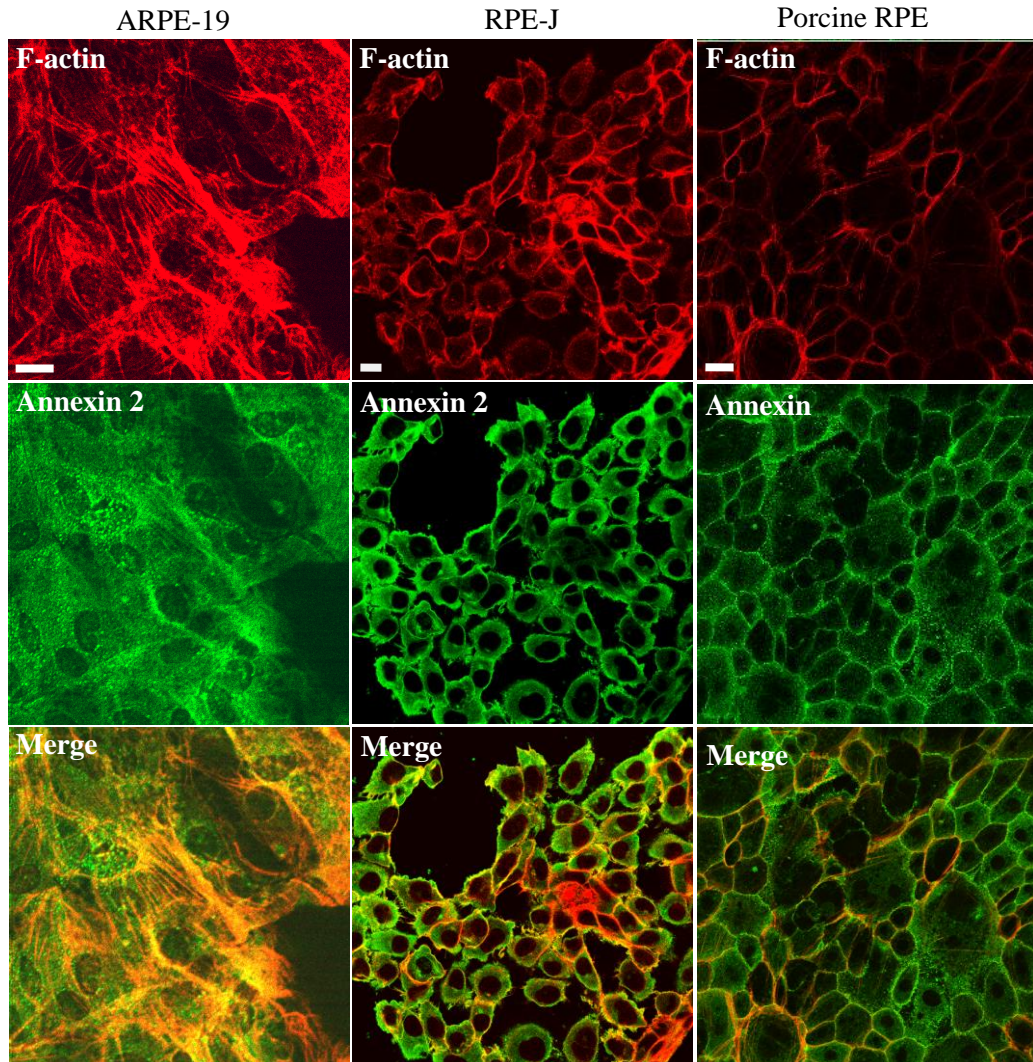


**Figure 4.1 Annexin 2 and F-actin distribution in human, rat and pig RPE cells**

Human ARPE-19, rat RPE-J and primary porcine RPE were grown in 10% serum, 4% CELLect™ gold serum and 10% serum respectively. Cells were fixed, permeabilised and immunostained for annexin 2 and F-actin and imaged using a Leica TCS-SP2 AOBS DM IRE 2 confocal microscope and processed using Metamorph or Image J software. The images show that annexin 2 is distributed throughout the cell cytoplasm and on the plasma membrane. Annexin 2 is also shown to co-localise to F-actin in these images. Scale bar = 20 µm.

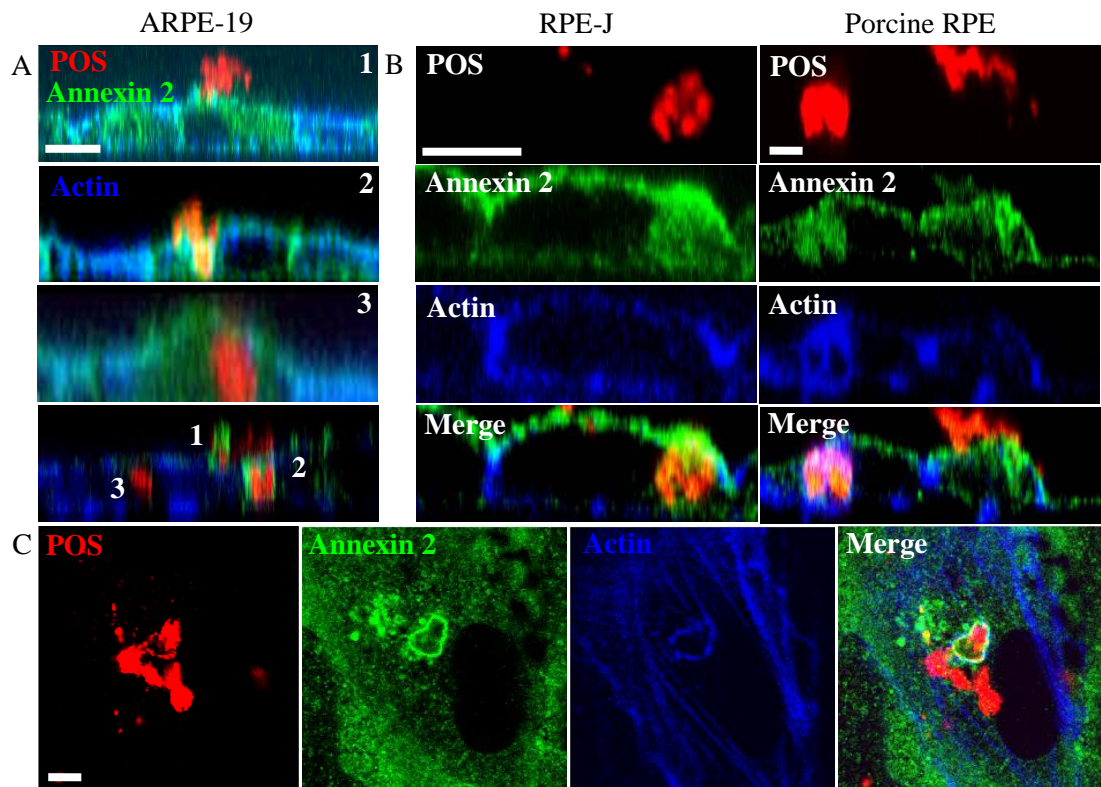


**Figure 4.2 Annexin 2 co-localises with the partially internalised phagosome**

ARPE-19, RPE-J and primary porcine RPE were plated onto glass bottom Matek™ dishes and seeded with purified and labelled POS. Cells were then immunostained for annexin 2 (green) and F-actin (blue). Confocal image stacks were collected to generate z-sections using a Leica TCS-SP2 AOBS DM IRE 2 confocal microscope and assembled using Zeiss LSM Image Browser software. (A) confocal z-section illustrating that annexin 2 is recruited to the phagocytic cup during early POS engulfment (1) and remains on the partially internalised phagosome (2). Once the POS is completely internalised, annexin 2 dissociates away from the phagosome (3). (B) confocal z-section showing that annexin 2 also co-localises to the partially internalised phagosome in RPE-J and porcine RPE. (C) shows a confocal x,y slice through primary porcine RPE cells during POS phagocytosis. Annexin 2 co-localises with F-actin and associates with the phagosome. Note that the outer segment is irregular in shape and so annexin 2 does not appear to associate with the entire outer segment here. Scale bars = 5 μm. The ARPE-19 z-sections were provided courtesy of M. Hayes, UCL Institute of Ophthalmology. London. UK.

## 4.2. Annexin 2 knockdown in ARPE-19 and RPE-J cells leads to a decreased efficiency in POS internalisation

To directly test the involvement of annexin 2 in POS phagocytosis, we used a standard *in vitro* fluorescent POS phagocytosis assay modified from Finnemann *et al* (1997)<sup>67</sup>. Human (ARPE-19) and rat (RPE-J) cells were grown on 48 well plates. Cells were treated with annexin 2 siRNA and control cells were treated with Oligofectamine™. Knock-down efficiency was determined by immunofluorescence (Figure 4.3 A and B) and western blotting for annexin 2 in both ARPE-19 and RPE-J cells. The western blots suggest that treatment with annexin 2 siRNA achieved about 60% knock-down in ARPE-19 cells and about 95% in RPE-J cells (Figure 4.3 C and D respectively). Fluorescently labelled POS were fed to cells for 0, 15, 30, 90 and 150 min, followed by fixing and Trypan blue quenching. Internalised labelled POS were quantified by measuring fluorescence emission on a Safire plate reader (SAFIRE; Firmware: V.2.00 03/02 Safire; XFLUOR4 Version: V 4.20). The human ARPE-19 cell line shows a steady rise in uptake of POS at 15 and 30 min before slowing down from 30 to 90 min. From 90 min, the rate of internalisation of POS increases. Knocking down annexin 2 gave a similar pattern to the untreated cells but with reduced POS uptake efficiency at all time points (Figure 4.3 E). Two way ANOVA confirmed that siRNA treated and Oligofectamine™ treated groups in ARPE-19 cells were significant ( $P = 0.023$ ), and variation across the time points were also significant  $P = < 0.001$ . Post hoc Bonferroni multicomparison tests identified significant differences between the means for RNAi and Oligofectamine™ for 15 vs 150, 30 vs 150, 90 vs 150 and 15 vs 90. In comparison to the human cells, the rat cell line (RPE-J) showed greater uptake efficiency. Untreated cells exhibited a rapid uptake of POS, with the rate peaking at 15 min before declining from 30 min. Knocking down annexin 2 in these cells decreased uptake by at least 50% at 15 min and 70% at 30 min, although internalisation caught up with the untreated cells from 90 min (Figure 4.3 F). Two way ANOVA confirmed that siRNA treated and Oligofectamine™ treated RPE-J cells were not significant ( $P = 0.89$ ) but variation across the time points were significant ( $P = < 0.001$ ). Post hoc Bonferroni multicomparison tests identified significant differences between the means for RNAi and Oligofectamine™ for 15 vs 15, 30 vs 150, 15 vs 90 and 30 vs 90 min. In both cell types, the picture that emerges is that in the absence of annexin 2, POS phagocytosis is delayed rather than completely inhibited.

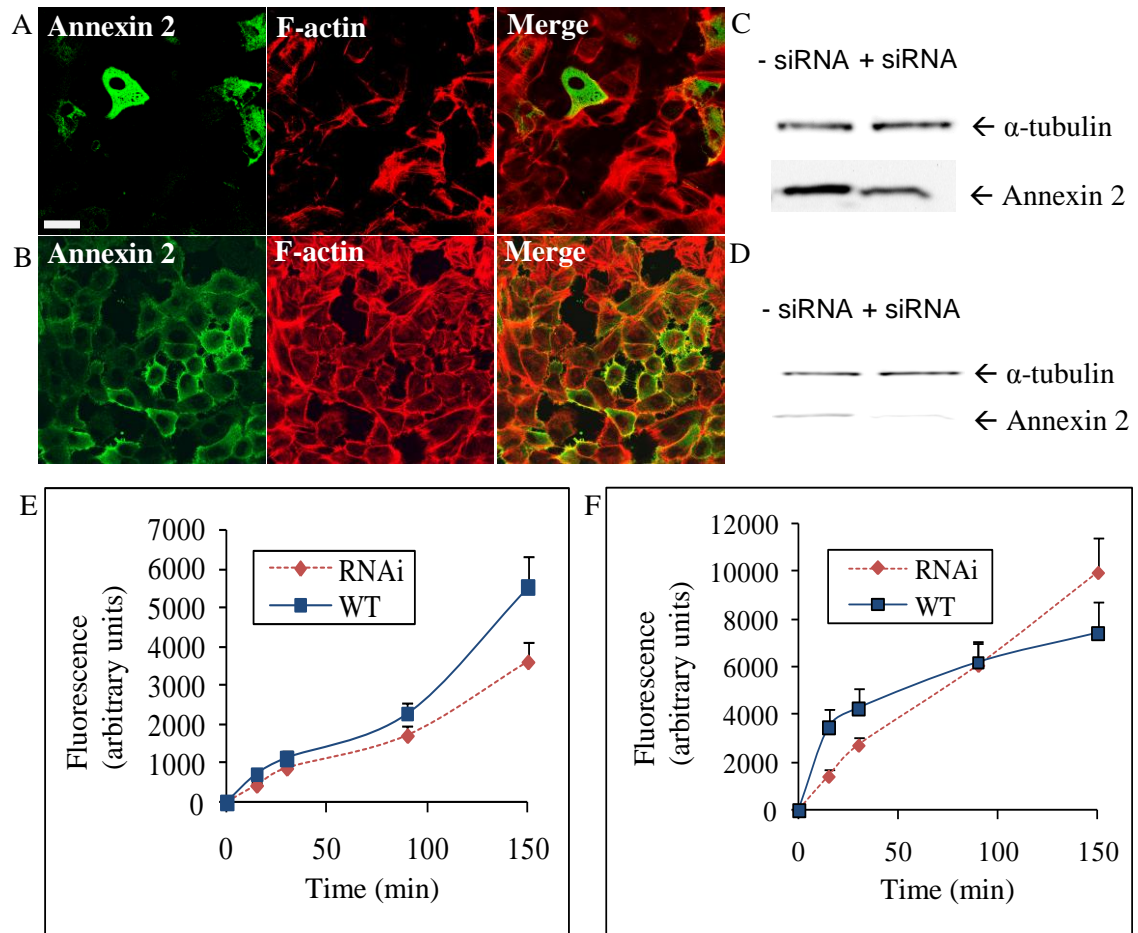


**Figure 4.3 Time course of POS phagocytosis by ARPE-19 and RPE-J cells**

ARPE-19 and RPE-J cells were grown on 48 well plates. Cells were treated with annexin 2 siRNA or Oligofectamine™ alone. Cells were seeded with labelled POS at  $1 \times 10^7$  per ml for various time points, after which they were washed, incubated with Trypan blue and fixed with 4% PFA. The extent of annexin 2 depletion by siRNA treatment can be observed by immunofluorescence staining for both ARPE-19 cells (A) and RPE-J cells (B), with annexin 2 in green and F-actin in red (scale bar = 20 μm). The levels of annexin 2 expression after siRNA treatment were examined by western blotting in ARPE-19 cells (C) and RPE-J cells (D). (E) and (F) show phagocytosis of POS in ARPE-19 cells and RPE-J cells (respectively) with and without treatment with annexin 2 siRNA. POS phagocytosis was measured as internalised fluorescence from fluorescently labelled POS after trypan blue quenching of extracellular fluorescence (surface bound POS). Two way ANOVA for (E): siRNA treated and Oligofectamine™ treated groups were significant ( $P = 0.023$ ), and variation across the time points were also significant  $P = < 0.001$ . Post hoc Bonferroni multicomparison tests identified significant differences between the means for RNAi and Oligofectamine™ for 15 vs 150, 30 vs 150, 90 vs 150 and 15 vs 90. Two way ANOVA for (F): siRNA treated and Oligofectamine™ not significant ( $P = 0.89$ ) but variation across the time points were significant ( $P = < 0.001$ ). Post hoc Bonferroni multicomparison tests identified significant differences between the means for RNAi and Oligofectamine™ for 15 vs 15, 30 vs 150, 15 vs 90 and 30 vs 90 min.

### **4.3. Annexin 2 and c-Src are phosphorylated upon POS phagocytosis in ARPE-19 cells**

It is well established that internalisation of outer segments strongly stimulates the activation of protein kinases in RPE cells<sup>187</sup>. Since annexin 2 is a substrate for both serine, threonine and tyrosine kinases, it was decided to investigate whether or not annexin 2 becomes phosphorylated during phagocytosis. ARPE-19 cells were challenged with isolated photoreceptor outer segments for 15, 30, 90 and 150 min, then lysed prior to immunoprecipitation with phosphotyrosine antibody conjugated beads. Lysates were collected at all time points for immunoprecipitation of tyrosine-phosphorylated proteins. The immunoprecipitates were then harvested using 2 x reducing sample buffer and resolved on 10% SDS PAGE followed by western blotting for annexin 2 or c-Src. Western blotting of whole cell lysates revealed that annexin 2 protein levels remained constant for all time points following POS feeding (Figure 4.4 C). However, when challenged with POS, annexin 2 tyrosine phosphorylation levels rapidly increased and peaked at 15 min (Figure 4.4 A). Figure 4.4 B and D show pixel density histograms for Figure 4.4 A and C respectively. Although there are a number of candidate tyrosine kinases that could be involved in the phosphorylation of annexin 2, c-Src was examined because of the well-characterised c-Src phosphorylation site at tyrosine 23 in the N-terminus of annexin 2. The western blots reveal that c-Src indeed became phosphorylated at both 15 and 30 min after POS stimulation, peaking at 30 min (Figure 4.4 E), whereas total c-Src levels remained constant throughout the experiment (Figure 4.4 G). Figure 4.4 F and H represent pixel density histograms for Figure 4.4 E and G respectively. The western blots show that c-Src phosphorylation peaks some 15 min after annexin 2 phosphorylation. This suggests that c-Src activation and signalling may be downstream of annexin 2, and that annexin 2 may have a role in regulating c-Src phosphorylation during POS internalisation. One Way ANOVA tests for Figures 4.4 B, D, F and H did not show significant levels of protein phosphorylation across time ( $P = 0.161, 0.903, 0.55$  and  $0.88$  respectively).

Confocal images showing the distribution of c-Src in response to POS challenge concur with the biochemical studies discussed above. ARPE-19 cells were plated onto Matek™ dishes and seeded with purified and labelled POS. In agreement with the phosphorylation data, c-Src co-localised with the POS during phagocytosis (Figure 4.5 A and C). On confocal sections, c-Src was often observed as a 'cloud' surrounding the POS during the early stages of internalisation. This can be observed in Figure 4.5 B and in higher magnification D.

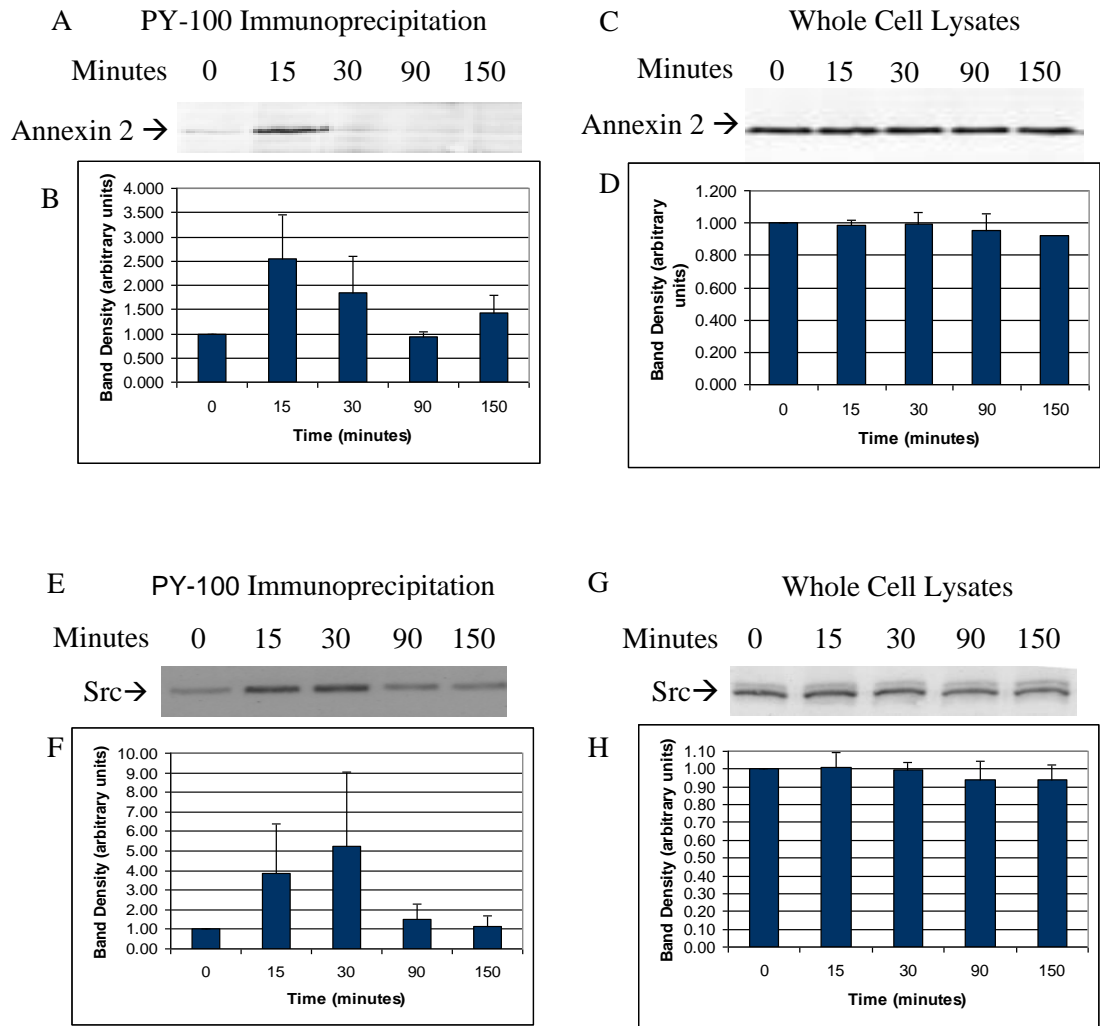


**Figure 4.4 Annexin 2 and c-Src are phosphorylated upon POS phagocytosis in ARPE-19 cells.**

Cells were challenged with isolated POS for 15, 30, 90 and 150 min. Cell extracts were incubated with phosphotyrosine conjugated beads overnight followed by western blotting for annexin 2 (A) and c-Src (E). Tyrosine phosphorylation of annexin 2 peaks at 15 min after POS challenge. c-Src phosphorylation is evident at 15 min before peaking at 30 min after POS challenge. Phosphorylation profiles of both annexin 2 and c-Src at the measured time points were created by measuring pixel densities from the blots (B) and (F) respectively. Western blots reveal equal expression of annexin 2 (C) and c-Src (G) in cell lysates. D and H are pixel density graphs of total annexin 2 and c-Src respectively. One Way ANOVA for (B):  $P = 0.161$ , not significant; (D):  $P = 0.903$ , not significant; (F):  $P = 0.55$ , not significant; (H):  $P = 0.88$ , not significant.

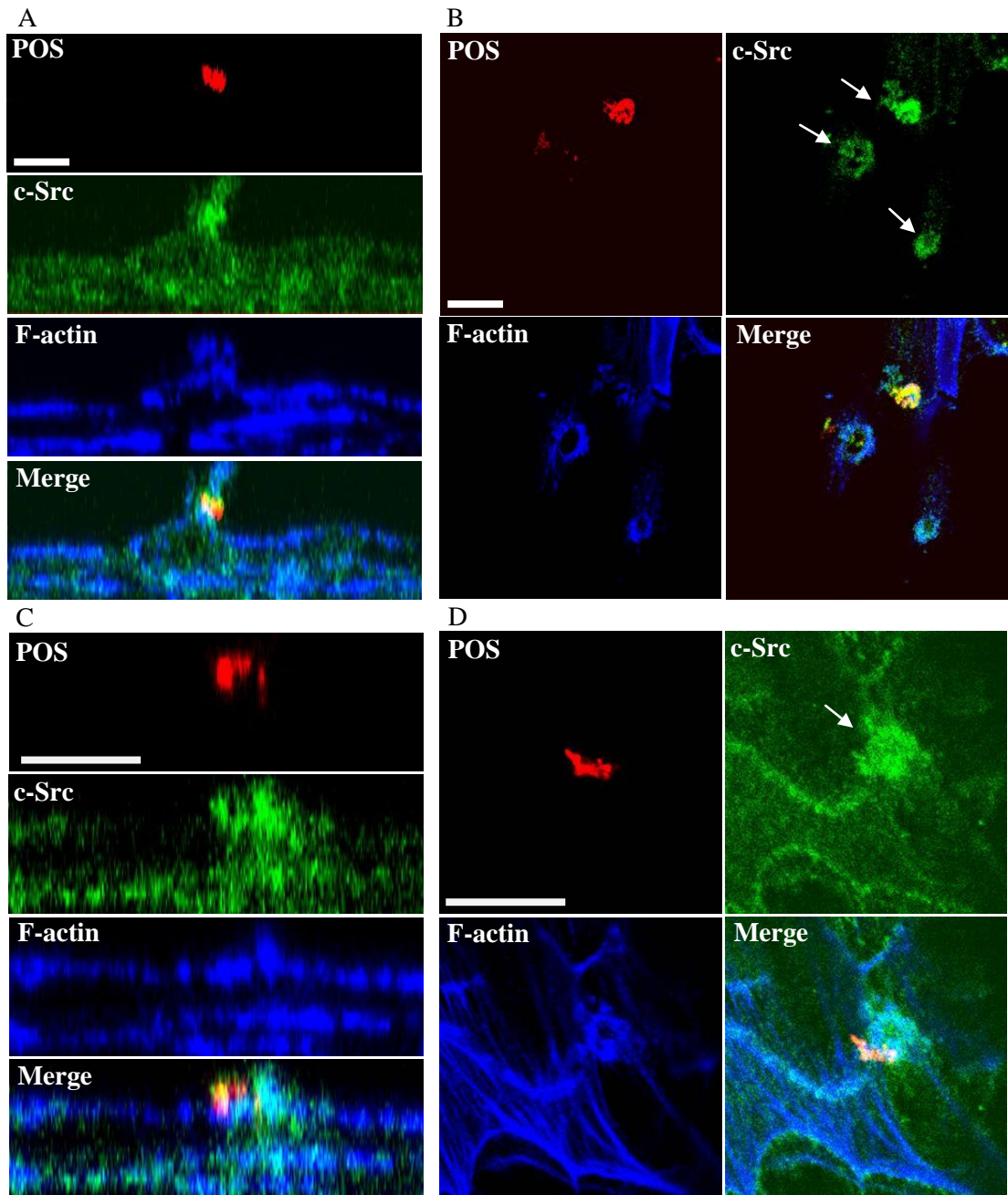


**Figure 4.5 c-Src is localised to the forming phagosome**

ARPE-19 cells were plated onto glass bottom Matek™ dishes and seeded with purified and labelled POS. Cells were then immunostained for c-Src (green) and F-actin (blue). Confocal image stacks through cells were collected to generate z-sections using a Leica TCS-SP2 confocal microscope and assembled using Zeiss LSM Image Browser software. A and C are z-stacked cross sections of a cell during the early stages of POS phagocytosis. c-Src is recruited to the POS during the early stages of engulfment and does not appear to associate with F-actin. B and D are x,y confocal sections showing that c-Src forms a ‘cloud’ which covers the engaged POS during the early stages of engulfment (white arrows). c-Src does not co-localise with the F-actin ring observed in these confocal slices. Note that the outer segment in (D) is irregular in shape and the area of the outer segment not covered by src is probably not yet fully engaged into the cell and so src has not yet localised to that region of the outer segment. POS were labelled with red succinimidyl ester dye, c-Src in green and F-actin in blue. Scale bar = 10 μm.

#### 4.4. Discussion

The *in vitro* studies presented in this chapter reveal that depletion of annexin 2 in the human RPE cell line, ARPE-19, leads to a significant quantitative delay in the phagocytosis of photoreceptor outer segments (POS). Two way analysis of variance (ANOVA) has concluded that the variation between annexin 2 siRNA and control cells treated with Oligofectamine™ only were significant ( $P = 0.02$ ). Two Way ANOVA also confirmed that Variations across the time points were also significant ( $P = <0.001$ ). Post hoc Bonferroni multicomparison tests identified significant differences between the means for annexin 2 RNAi and Oligofectamine™ treated ARPE-19 cells at the following time points: 15 vs 150; 30 vs 150; 90 vs 150 and 15 vs 90 min. Two Way ANOVA testing for the RPE-J cell line in POS phagocytosis did not show significant differences between annexin 2 siRNA and Oligofectamine™ treated samples ( $P = 0.888$ ) but the variations across the time points were significant ( $P = 0.001$ ). Post Hoc Bonferroni multicomparison tests also identified significant differences between the means for annexin 2 RNAi and Oligofectamine™ treated RPE-J cells at 15 vs 150, 30 vs 150, 15 vs 90 and 30 vs 90 minute time points. These significant effects of annexin 2 depletions RPE phagocytosis of POS is interesting given that intracellular calcium has been shown to rise during internalisation and that annexin 2 interacts with dynamic cellular membranes in pinocytosis and endocytosis, and has a direct role in actin remodelling<sup>130, 138, 188-190</sup>. Annexin 2 binds directly to PtdIns4,5P<sub>2</sub> and has been shown to localise to macropinosome membranes, and it also participates in the rapid reorganisation of the apical membrane actin cytoskeleton to form actin-rich pedestals following attachment of enteropathogenic *E.coli* to HeLa cells<sup>191</sup>. These studies are consistent with reports from our lab that annexin 2 has a role as a barbed-end capping protein that regulates actin filament turnover<sup>130</sup> and suggest that annexin 2 may be involved in the regulation of actin dynamics at sites of PtdIns4,5P<sub>2</sub> enrichment on newly forming phagosomes.

Actin polymerisation predominantly occurs at the barbed ends of actin filaments, and actin turnover is required for cell motility<sup>87, 89, 192</sup>. Annexin 2 has been shown to bind and sequester monomeric G-actin and together with its known membrane-binding properties, it thus has the potential to bind and deliver G-actin directly to the cell cortex for actin polymerisation. Annexin 2 is able to bind the barbed ends of actin filaments in the same way as capping proteins to stop filament growth. This process is required for active actin dynamics, a point exemplified by the observations that depletion of capping proteins can result in loss of cellular ruffles<sup>193</sup>. Similarly, the loss of annexin 2 by siRNA switches cells with dynamic, ruffling physiology to a flat and quiescent phenotype in which cells are dominated by stress fibres and cortical actin is

reduced<sup>130</sup>. Thus, the absence of annexin 2 influences processes that require the active remodelling of the actin cytoskeleton. Considering that the apical region of the RPE is rich in actin filaments, it is likely that annexin 2 is involved in the reorganisation of actin in the phagocytic function of RPE cells.

Whilst the phagocytosis assays with ARPE-19 cells showed a clear pattern of reduced phagocytic efficiency in annexin 2 knock-down cells, RPE-J cells showed a 'catch up' in internalisation after 90 min of POS feeding, beyond which annexin 2 siRNA treated cells actually showed a greater ability to phagocytose POS. There are several possible explanations for the 'catch up'. One is that  $\alpha\beta 5$ -independent phagocytosis may occur after specific recognition, binding and uptake of POS that typically occurs during the first 30 min of POS feeding. Alternatively, binding may occur minimally in annexin 2-depleted cells, but internalisation may occur via the activation and mobilisation of other actin regulatory proteins. This would suggest a 'two speed' mechanism for POS uptake, a fast one dependent on annexin 2, the other slower one being annexin 2-independent. It is however important to consider that both immortalised cell lines used in this study lack pigmentation, and that each cell line exhibits different protein expression and growth characteristics, which also differ to those of primary RPE cells. It is also noteworthy that due to incomplete knockdown of annexin 2 in ARPE-19 cells by siRNA treatment, the effects of reduced internalisation efficiency in the treated RPE cells are muted. Should 100% knock down of annexin 2 be achieved, the effects of reduced POS uptake efficiency would presumably be much greater. POS internalisation is also a saturable process and as neither graph reaches saturation, it may be insightful to increase both the incubation time with the isolated POS and the concentration of POS.

Annexin 2 is usually present as a monomer in the cell cytosol and as a heterotetrameric complex, formed of two annexin 2 molecules and two S100A10 monomers, on the membrane-cytoskeleton. During phagocytosis of POS, annexin 2 is shown here to localise to the phagocytic cup. Confocal imaging of RPE-J cells showed that annexin 2 and F-actin are enriched at the phagocytic cup upon POS binding at the apical surface (Figure 4.2 A). This enrichment is lost upon full internalisation of the POS (image not shown). These observations agree with the observations using ARPE-19 cells. In line with these observations, annexins 2 and 7 were identified as constituents of mature phagosomal membranes in macrophages, in a study by Rogers and Foster, (2007)<sup>194</sup>. Dissociation of annexin 2 away from the phagocytic cup once internalisation of the POS is complete suggests that it indeed has a role in POS internalisation in both RPE cell lines, and that during internalisation, annexin 2 is localised apically in the RPE at sites where actin filaments are actively reorganised.

Having observed the localisation of annexin 2 during phagocytosis and finding that knocking down annexin 2 in RPE results in reduced phagocytic efficiency of POS, the next stage was to elucidate how annexin 2 affects POS internalisation and where it fits with signalling molecules known to be involved in RPE phagocytosis. Since several tyrosine kinases are involved and because phosphorylation of proteins increases in the RPE during POS phagocytosis<sup>187</sup>, it was important to find out whether annexin 2 becomes phosphorylated. Biochemical studies revealed that tyrosine phosphorylation of annexin 2 temporally coincided with the formation of nascent phagosomes, with loss of tyrosine phosphorylation coincident with the loss of annexin 2 upon full POS internalisation. This raises the question of which kinases(s) phosphorylates annexin 2. Both FAK and MerTK are phosphorylated and activated upon  $\alpha v\beta 5$  mediated POS internalisation<sup>71</sup>.  $\alpha v\beta 5$  binding by POS activates FAK, which is in turn required for MerTK phosphorylation and engulfment of POS<sup>71</sup>. Annexin 2 is shown here to be involved in internalisation, and although both FAK and MerTK may theoretically phosphorylate annexin 2, the potential role of c-Src was studied. c-Src is a particularly intriguing candidate to examine since its role, if any, in the RPE, has not been studied and importantly, annexin 2 contains a phosphorylation site on tyrosine 23 in its N-terminus which is phosphorylated by c-Src. Moreover, c-Src was observed on the phagocytic cup during POS internalisation (Figure 4.5). Tyrosine phosphorylation of c-Src is generally taken to be indicative of c-Src activation and c-Src showed similar tyrosine phosphorylation kinetics to those of annexin 2. c-Src phosphorylation was evident at 15 min, peaked at 30 min and was virtually undetectable by 90 min. This broadly correlates with the phosphorylation pattern observed for annexin 2, which peaked slightly earlier at 15 min after stimulation with POS. The phosphorylation kinetics of c-Src and annexin 2 are generally similar to those of phagocytosis in RPE-J cells, which showed a rapid initial uptake of POS, peaking at 15 min and then slowing at 30 min. Knocking down annexin 2 in these cells decreased uptake by at least 50 % at 15 min of POS feeding and 35% at 30 min. The marked effects of reduced phagocytic efficiency in annexin 2 knock-down cells at 15 and 30 min, along with the phosphorylation kinetics of annexin 2 and c-Src, suggest that the early stages of POS phagocytosis are dependent on annexin 2 and that later events occur independently of annexin 2. The patterns of annexin 2 and c-Src phosphorylation observed however should be taken with prudence, since both do not show significant variances in phosphorylation across time ( $P = 0.16$  and  $0.55$  respectively for annexin 2 and c-Src phosphorylation).

To fully understand how c-Src may play a role in POS phagocytosis by RPE cells, it is worth considering structure-function relationships for this protein that underlie its mode of activation. c-Src is a 60 kDa non receptor protein tyrosine kinase consisting of SH3, SH2 and SH1

domains, followed by a 'unique' domain that is divergent among the src family members and a short C-terminal tail. The bi-lobed SH1 site, which is also the tyrosine kinase domain, contains the autophosphorylation site at tyrosine 416 and phosphorylation at this site is required for full catalytic activity. The C-terminus contains the autoinhibitory phosphorylation site (tyrosine 527). Under basal conditions, 90-95% of c-Src is phosphorylated at tyrosine 527, which associates intramolecularly with the SH2 domain. The SH3 domain binds to the small lobe of the kinase domain thus rendering the protein in a closed conformation and inactive. In this dormant conformation, tyrosine 416 is sequestered and is not available for phosphorylation by another kinase. The SH2 and SH3 domains of c-Src also function as binding sites for ligands that also contain SH2 and SH3 domains. Binding displaces the intramolecular association between SH2 and SH1 domains, allowing dephosphorylation of tyrosine 527 by phosphatases such as CD45. Displacement releases the protein into an open conformation exposing the tyrosine 416 site in the kinase domain for autophosphorylation by another Src molecule. Autophosphorylation then stabilises the enzyme in its active state<sup>195-197</sup>.

c-Src was observed in the phosphotyrosine immunoprecipitates at both 15 min and 30 min. The band at 15 min could represent intermolecular autophosphorylation at tyrosine 416 which promotes the kinase activity that may in turn be responsible for annexin 2 phosphorylation observed at that time. The band representing c-Src phosphorylation at 30 min could simply represent increased phosphorylation at tyrosine 416, i.e., more active protein, or it is possible that phosphorylation occurs at additional sites after the activation of the kinase domain. Clearly, resolution of these questions would require the use of a range of phospho-specific antibodies. c-Src was also observed on confocal images as a localised 'cloud', located around the POS during the initial stages of phagocytosis. In the confocal images, unlike annexin 2, c-Src did not appear to co-localise with actin. In the longer term, further imaging using phospho-specific antibodies to tyrosine 416 and 527 will provide a clearer picture of c-Src activity and localisation during internalisation.

To conclude, the experiments so far have identified annexin 2 as an essential component of the phagocytic machinery in RPE cells, and raise the possibility that its activity in this context may be regulated by c-Src.

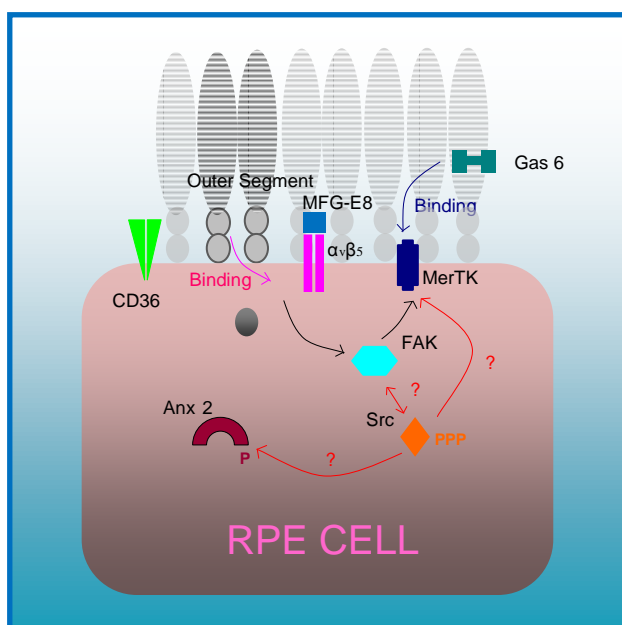


**Figure 4.6 RPE phagocytosis of photoreceptor outer segments.**

POS binding to  $\alpha v \beta 5$  activates FAK, which phosphorylates MerTK. Activation of MerTK triggers internalisation signals that result in the uptake of the bound POS. MFG-E8 exists in the interphotoreceptor matrix and is the ligand for  $\alpha v \beta 5$ . It is suggested to rhythmically activate  $\alpha v \beta 5$  to synchronise clearance of shed photoreceptor outer segments.

Although the data here suggests that annexin 2 is tyrosine phosphorylated during phagocytosis, insignificant variations of phosphorylation observed across time during phagocytosis and the absence of a phosphotyrosine annexin 2 antibody makes this difficult to prove unequivocally. In these experiments, the 'n' numbers were small and annexin 2 phosphorylation could only be studied by immunoprecipitation of phosphotyrosine proteins present in the RPE, followed by western blotting for annexin 2. The presence of annexin 2 in the immunoprecipitate could theoretically result from annexin 2 binding to another tyrosine phosphorylated protein. Similarly, c-Src phosphorylation studied in this way, raises the same questions although in this case, using commercially available phospho-src antibodies would determine if c-Src was directly phosphorylated. Increasing the 'n' numbers to study both annexin 2 and c-Src phosphorylation during POS phagocytosis by the RPE may also render the phosphorylation patterns observed for both annexin and c-Src during phagocytosis significant. To gain further insight into the role of c-Src in the phagocytosis of POS, and whether it phosphorylates annexin 2 during this process, phagocytosis assays could also be repeated using Src inhibitors.

## **Chapter 5**

**Does annexin 2 have a role in phagocytosis in the eye *in vivo*?**

## 5. Does annexin 2 have a role in phagocytosis in the eye *in vivo*?

The findings presented in chapter 4 are based on *in vitro* experiments that use cell lines and primary porcine cultures. As already mentioned, both ARPE-19 and RPE-J cells have distinct characteristics that differ to those of primary RPE cells and RPE cells *in vivo*. The *in vitro* models featured in chapter 4 have different advantages and disadvantages. Primary porcine cells used in the previous chapter resemble RPE *in vivo* more closely, but variability between preparations, limited availability and cost restricts their use to small scale experiments such as phagocytosis imaging which requires few cells. In contrast, cell lines are homogeneous and offer an unlimited number of cells, with high reproducibility and so are suitable for experiments that require large numbers of cells, such as phagocytosis assays. Despite these many advantages, *in vitro* models are unlikely to fully recapitulate the true *in vivo* biological interaction between the RPE and photoreceptor and the circadian nature of this interaction.

The availability of the annexin 2 knock out mouse raises the possibility of *in vivo* experiments that involve harvesting material directly from eyes for biochemical studies. Moreover, harvesting the eyes at various times in the light-dark cycle allows insight into the circadian aspects that play a key role in the regulation of shed POS phagocytosis in nature. The phagocytic uptake of shed POS by the RPE *in vivo* is also studied in this chapter by counting the number of phagosomes in the RPE from eyes taken from both knock-out and wild-type animals. Transmission electron microscope (TEM) studies on these eyes permits a more detailed analysis of the retinal ultrastructure and anatomy, since these may be abnormal in the annexin 2 knock out mice. Moreover, studies using TEM also provide a quantitative evaluation of phagocytosis *in vivo*.

Photoreceptors contain photosensitive molecules that form the phototransduction machinery. Phototransduction requires the proper function and structure of photoreceptor proteins, membranes and the recycling and formation of 11-*cis*-retinal. These molecules are exposed to high light intensities throughout the day and form photo-damaged adducts which accumulate at the tips of the POS. Through co-ordinated POS disk shedding, the photo-damaged molecules are displaced from the photoreceptors and ingested by the RPE for degradation. It is also through this process of regulated POS shedding, phagocytosis of shed POS and formation of new POS, that a constant length of POS and photoexcitability of the photoreceptors is maintained. Regulated POS shedding and POS phagocytosis are tightly co-ordinated between the RPE and photoreceptors, which is also absolutely vital for maintaining the structural integrity of the photoreceptors. Defects in this process can be observed in the Royal College of

Surgeons (RCS) rat, which has a mutation in the MerTK gene that leads to the expression of a truncated, non-functional MerTK protein<sup>73, 112</sup>. Biochemical studies have revealed that the truncated, non-functional form of MerTK cannot localise to the cell membrane to initiate phagocytosis of POS, and shed POS debris accumulates in the subretinal space. The failure of POS phagocytosis causes a progressive and rapid retinal degeneration<sup>72, 73, 112, 155, 157, 198</sup>. MerTK is also involved in phagocytosis and clearance of apoptotic cells in macrophages. Thus, macrophages isolated from mutant mice with a cytoplasmic truncation of MerTK were deficient in the clearance of apoptotic cells<sup>199, 200</sup>. Moreover, Gas6, a ligand for the Mer receptor, as well as having a well defined role in the phagocytosis of POS by the RPE, acts as an adhesion molecule that binds Gas6 receptor-expressing macrophages specifically to cells exposing phosphatidylserine (PS) on their surface<sup>199</sup>.

Other molecules that form the RPE phagocytosis machinery common to other cell types with phagocytic capabilities such as macrophages and dendritic cells, include the scavenger receptor CD36. This protein has long been implicated in the phagocytosis of POS by the RPE<sup>79, 80</sup> and more recently its function has been linked to the regulation of the rate of POS internalisation by the RPE<sup>81</sup>. In macrophages, CD36 has also been shown to play equivalent roles in the phagocytic clearance of bacteria and apoptotic bodies<sup>201-203</sup>. RPE cells also employ the apically expressed  $\alpha\beta5$  integrin to recognise and bind shed POS; a system related to the recognition and selective binding to apoptotic cells via  $\alpha\beta3$  on monocyte macrophages. Whilst both  $\alpha\beta5$  and  $\alpha\beta3$  receptors are able to bind to apoptotic cells and POS, RPE cells use  $\alpha\beta5$  integrin and macrophages use  $\alpha\beta3$  integrin to bind both POS and apoptotic cells<sup>204</sup>.

In the current model of POS phagocytosis, POS bind to  $\alpha\beta5$  which activates focal adhesion kinase (FAK), which in turn phosphorylates MerTK, which activates canonical signal transduction pathways, resulting in POS internalisation<sup>67, 71</sup>.  $\alpha\beta5$  is localised specifically to the apical microvilli of the RPE and contributes to retinal adhesion and thus maintains the tight RPE and photoreceptor interaction, essential for visual function<sup>68</sup>. Furthermore,  $\alpha\beta5$  synchronises diurnal POS phagocytosis by the RPE. The  $\beta5$  integrin knock out mouse, which specifically lacks  $\alpha\beta5$  receptors does not exhibit the rhythmic activation of FAK and MerTK which mediate phagocytosis in wild type mice, and the diurnal burst of phagocytosis, normally present approximately 1 hour after light onset was absent<sup>69</sup>. Recently, it has been reported that the engagement of  $\alpha\beta5$  integrin by its ligand, Milk fat globule-EGF8 (MFG-E8) is indispensable for the circadian synchronisation of phagocytosis<sup>70</sup>.

## 5.1. Phagocytosis of photoreceptor outer segments is delayed in the annexin 2 knock out mouse

Phagocytosis in the annexin 2 knock out mouse was compared to that in wild type mice. In mice aged 2 months, the retinal physiology and architecture appears normal, showing comparable numbers of photoreceptor nuclei, with all layers of the retina appearing intact and similar to the wild type retina (Figure 5.1). On closer examination by electron microscopy (EM), there were no obvious differences in POS and RPE ultrastructure (Figure 5.2). Immunofluorescence staining of 10  $\mu\text{m}$  cryosections confirmed that annexin 2 is absent from the RPE in the annexin 2 knock out retina, whereas it is normally located in the RPE of wild type eyes (Figure 5.3). The punctate staining observed on the photoreceptors is non-specific since photoreceptors do not express annexin 2. To study the localisation of annexin 2 during phagocytosis *in vivo*, annexin 2 knock out and wild type eyes harvested shortly after light onset were processed for cryo-immunoelectron microscopy. Consistent with earlier observations in ARPE-19, RPE-J and porcine primary RPE cultures (Chapter 4), newly formed phagosomes, which were defined by their apical localisation and membranous disks, showed association of annexin 2 gold labelling to the limiting membrane of the phagosome (Figure 5.4 A and B). In contrast, with the exception of a few non-specific gold particles observed on the phagosome, gold labelling was absent from most mature phagosomes which are localised to the basal compartment of the RPE (Figure 5.4 C). The gold labelling on the phagosomes is non-specific since the same labelling was also seen on phagosomes from annexin 2 knock out eyes (Figure 5.4 D).

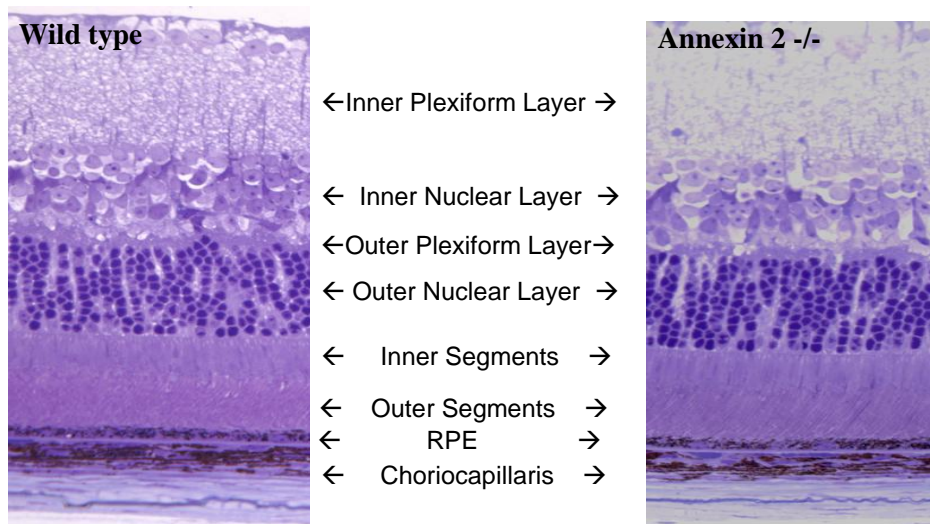


**Figure 5.1 Morphological organisation of annexin 2 knock out and wild type retinas**

Eyes were harvested, fixed and embedded in resin for Toluidine Blue staining. Images show transverse sections of wild type retina (left) and annexin 2 knock out retina (right). The annexin 2 knock out retina presents a normal morphological anatomy, comparable to wild type retina.

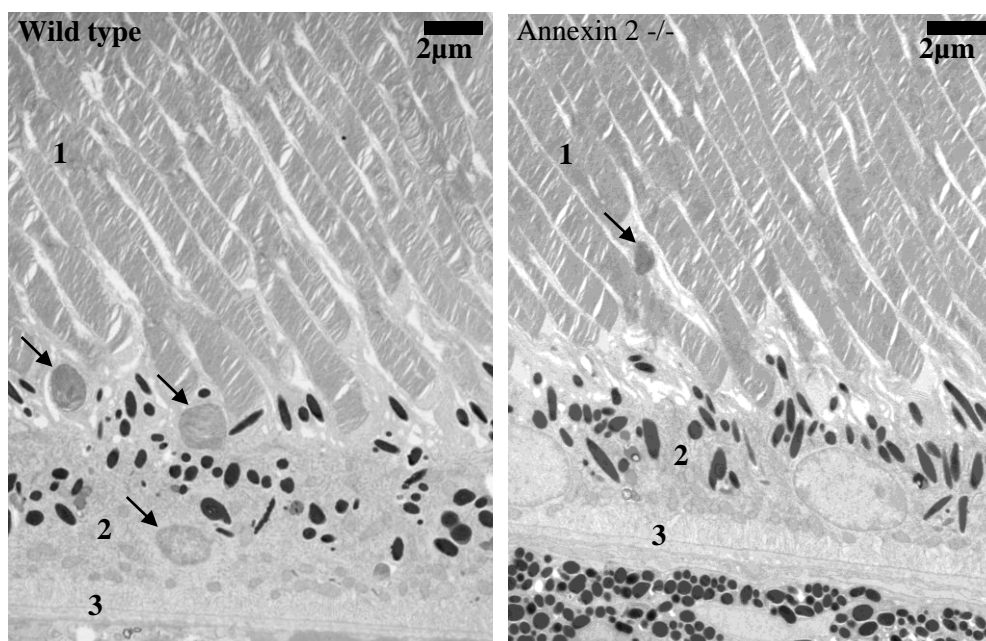


**Figure 5.2 Annexin 2 knock out mice have a normal retinal ultrastructure.**

Electron micrographs of transverse sections of wild type and annexin 2 mouse retinas, showing photoreceptor outer segments (1), RPE (2) and Bruch's membrane (3). Phagosomes were identified as approximately round structures exhibiting at least one of the following characteristics: a) the presence of membranous disks, b) a mean diameter of at least 75% of the diameter of the photoreceptor outer segments (POS) and c) for apical phagosomes, surface membranes enclosed and segregated from the apical membranes of the RPE. Phagosomes are indicated on the two micrographs with black arrows.

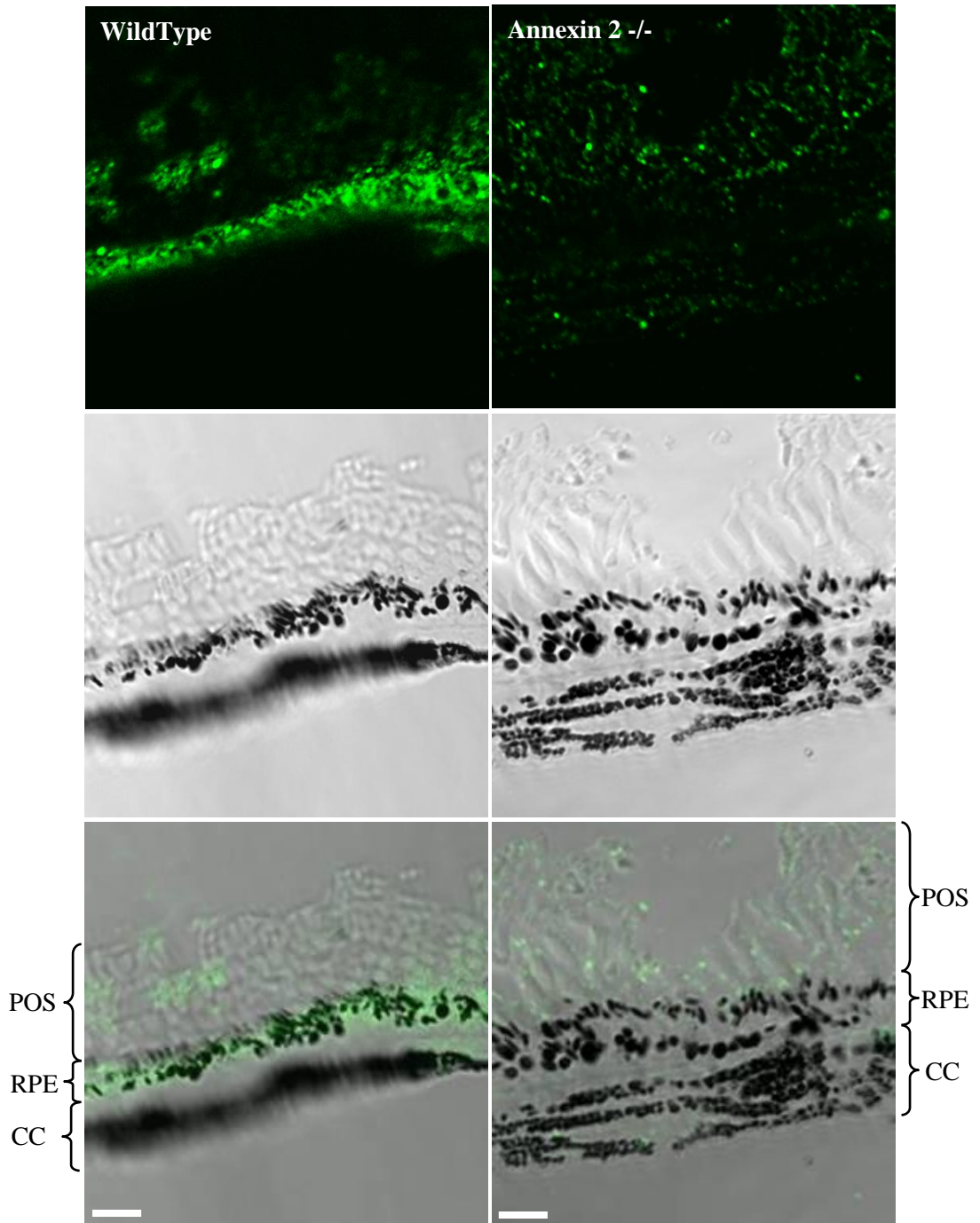


**Figure 5.3 Annexin 2 is present in wild type RPE**

Eyes from annexin 2 knock out and wild type retina were harvested, embedded with OCT, followed by cutting into 10  $\mu\text{m}$  sections for immunofluorescence imaging. Eyes were stained with a polyclonal rabbit annexin 2 antibody which shows that annexin 2 is present in wild type RPE but is absent in annexin 2 knock out RPE. The photoreceptor outer segments (POS), RPE and the choriocapillaris (CC) are indicated in these images. Scale bar = 50  $\mu\text{m}$ .

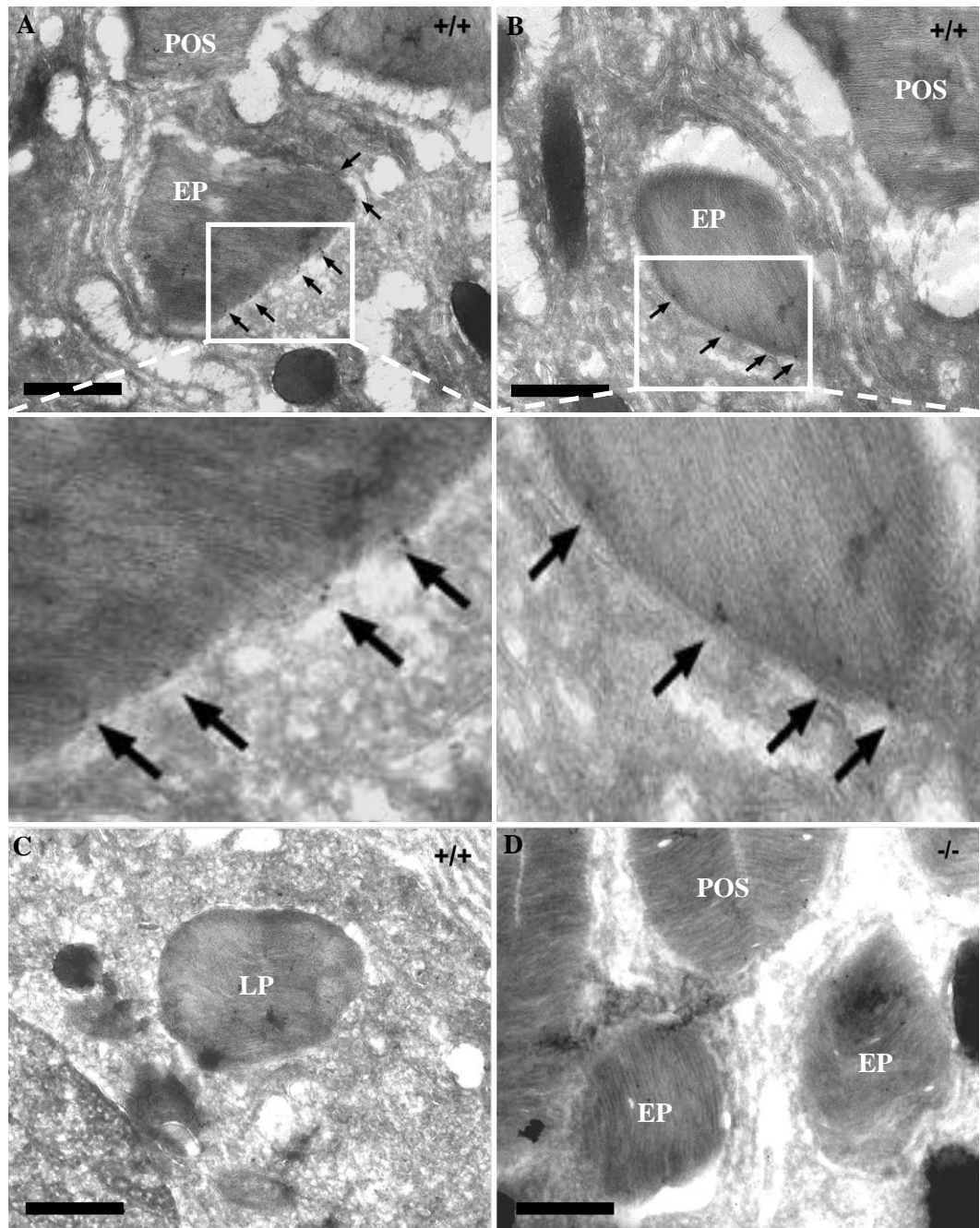


**Figure 5.4 Annexin 2 is localised to the early phagosomes in wild type RPE**

Eyes were enucleated 1 hour after light onset for both wild type and annexin 2 knock out mice and processed for cryo-immuno EM and stained for annexin 2. Early phagosomes were distinguished by their apical localisation and clearly defined membranous disks. Gold particles (indicated by arrows) were observed on both photoreceptor outer segments (POS) adjacent to the apical RPE and on apical early phagosomes (EP) in wild type mice (A) and (B). The boxed areas on (A) and (B) are shown in higher magnification beneath. In contrast, (C) shows that gold particles were absent from late phagosomes (LP). A small number of gold particles on the photoreceptor disks within the lumen of the phagosome are non-specific since they are present in both wild type and knock out mice (D). Scale bar = 0.5μm. The electron micrographs were taken by Dr Clare Futter, from Law *et al* (2009)<sup>1</sup>.

To investigate the role of annexin 2 in phagocytosis *in vivo*, the number of phagosomes in the RPE of annexin 2 knock out and wild type retinas was counted in electron micrographs of retina cross sections. In contrast to some other reports of a characteristic peak at approximately 1 hour after light onset<sup>69, 108</sup>, phagosomes quantified in wild type retinas in this work showed only a moderate increase in numbers 1 hour after light onset (Figure 5.5). In contrast to wild type RPE, annexin 2 knock out RPE did not even show this modest increase in the number of phagosomes shortly after light onset. Intriguingly, the total number of phagosomes in the knock out RPE was slightly higher than in wild type RPE at 2.5 hours after lights on, though the differences between knock out and wild type RPE fell short of statistical significance (Anova,  $P = 0.542$ ). Even when the numbers of phagosomes for all time points were aggregated to give an averaged total number of phagosomes per  $\mu\text{m}$  of RPE for knock out and wild type retinas, there was no significant difference (Figure 5.5). Phagosomes located in the cell body of the RPE were identified during quantification and this population was plotted as ‘percentage basal phagosomes’ calculated from the ratio of ‘basal’ phagosomes to the total number of phagosomes quantified for each of the time points. This analysis showed that the annexin 2 knock out mice had slightly fewer basal phagosomes at 1 hour after light onset in comparison to wild type RPE. From 105 minutes after light onset, the percentage basal phagosomes in the annexin 2 knock out RPE was higher than the wild types (Figure 5.6). However, statistical analysis revealed that the differences in percentage basal phagosomes between knock out and wild type mice were not significant (Anova,  $P = 0.125$ ). Intriguingly, positional mapping of phagosomes according to their distance from Bruch’s membrane revealed an accumulation of apical phagosomes and fewer basal phagosomes in the annexin 2 knock out retina in contrast to the wild type retina. In the normal retina, there was no evidence of phagosomes residing in the extreme apical region of the RPE, with most of the phagosomes internalised within the cell body at this time (Figure 5.7).

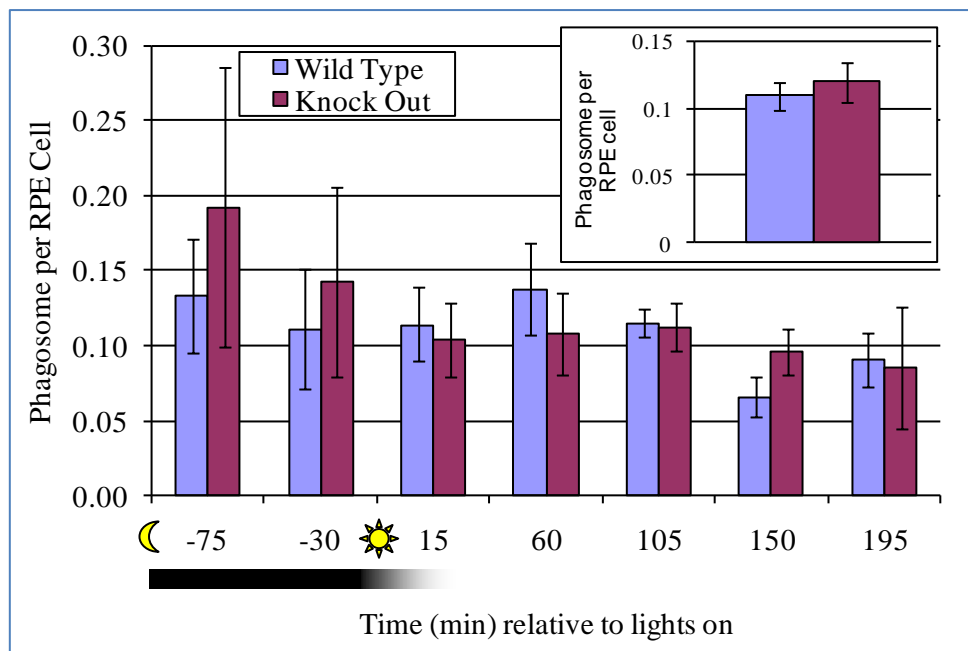
The quantitative evaluation from the electron micrographs reveals little difference between annexin 2 knock out and wild type RPE with regard to the synchronised circadian phagocytosis of POS. Two Way ANOVA testing on these data confirmed that differences observed in both analyses of phagosomes per RPE cell (Figure 5.5) and the percentage of phagosomes residing in the cell body ‘basal phagosomes’ (Figure 5.6) for both wild type and knock out RPE were insignificant ( $P = 0.60$  and  $P = 0.06$ , respectively for Figure 5.5 and Figure 5.6). Variation across the time points for both figures were also insignificant ( $P = 0.48$  and  $P = 0.05$  for figures 5.5 and 5.6 respectively). Similarly, both Figure 5.5 and Figure 5.6 showed no significant interaction between wild type and knock out animals with variation against the time points ( $P = 0.86$  and  $0.38$  respectively). The total phagosomes per RPE in the wild type and knock out

samples quantified in Figure 5.5 collected from all the time points shown in the graph inset was also revealed by T Test to be insignificant ( $P = 0.54$ ). Quantification of RPE phagocytosis *in vivo* based on counting the number of POS present in the RPE by EM has drawbacks, since it relies on single snap shots from each sample, of a dynamic and on-going process. The different size and appearance of early and late phagosomes contributes to the difficulty in the accurate identification of phagosomes. Moreover, specimens for EM analysis typically represent 70 nm thick cross-sections of the retina, which taken with issues of variability between individual animals means that sample sizes must therefore be large to assess minor differences between experimental groups. This is a challenge for EM-based quantification, which is time-consuming and laborious. Due to these limitations, an alternative method for analysing *in vivo* phagocytosis was developed.

Eyes from annexin 2 knock out and wild type animals were harvested before and after light onset, and fixed before separating and removing the anterior segment of the eye, along with the lens and vitreous. The neuroretina on the remaining posterior portion was carefully peeled away to expose the RPE before making incisions along the rim of the orbit to open the eye cup into a 'flower'. The 'flowers' were incubated with an antibody for the tight junction marker, ZO-1 to allow each individual RPE cell to be identified in the sample (Figure 5.8), and with the anti-rhodopsin 1D4 antibody, which specifically labels apical early phagosomes. In a recent observation, cryo-immuno EM gold labelling with 1D4 rhodopsin antibody was found to localise to apical, early phagosomes but not to late phagosomes (Figure 5.9 A-D). After antibody staining, the 'flowers' were flat-mounted onto glass slides for imaging (Figure 5.9 E-G). This method is simple, time efficient and allows sampling of a larger number of cells (in comparison to analysis by EM), and has all the advantages of an *in vivo* system in comparison to harvesting cells for primary cultures. Regions of interest were identified and the numbers of phagosomes and cells were counted in order to obtain an average for each retina. The numbers of 1D4 rhodopsin positive phagosomes per cell were plotted for the different time points for both wild type and annexin 2 knock out mice (Figure 5.10). These data show a transient increase in 1D4 rhodopsin positive phagosomes in control mice shortly after light onset, consistent with the characteristic burst of phagocytosis reported elsewhere<sup>69, 108</sup>. This increase was delayed in the annexin 2 knock out mice but was sustained for much longer. The differences observed here however showed no significant differences in variation across the time points for both wild type and knock outs ( $P = 0.91$  and  $0.24$  respectively). Integration of all the data to obtain total numbers of 1D4 rhodopsin positive phagosomes per cell across this experimental period, revealed that there were significantly more 1D4 rhodopsin positive

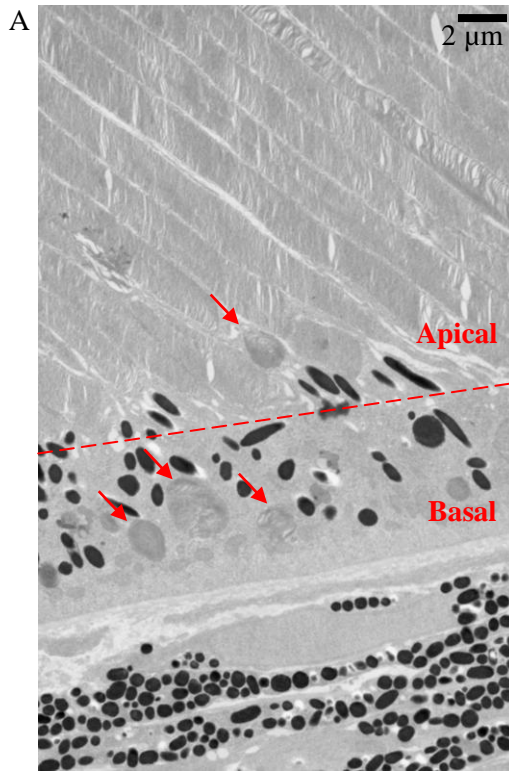
phagosomes in the annexin 2 knock out mice ( $P = 0.005$ ); shown with the graph inset in Figure 5.10.

These data suggests that whilst POS shedding probably occurs normally in the annexin 2 knock out mouse, phagocytosis is delayed resulting in the accumulation of apical phagosomes and fewer internalised basal phagosomes at the time of the maximal peak in RPE phagocytosis. Phagocytosis of these shed POS occurs some 1.5 hours later, indicated by the increased number of basal phagosomes or fewer apical phagosomes observed.



**Figure 5.5 Circadian analysis of POS shedding and phagocytosis by the RPE**

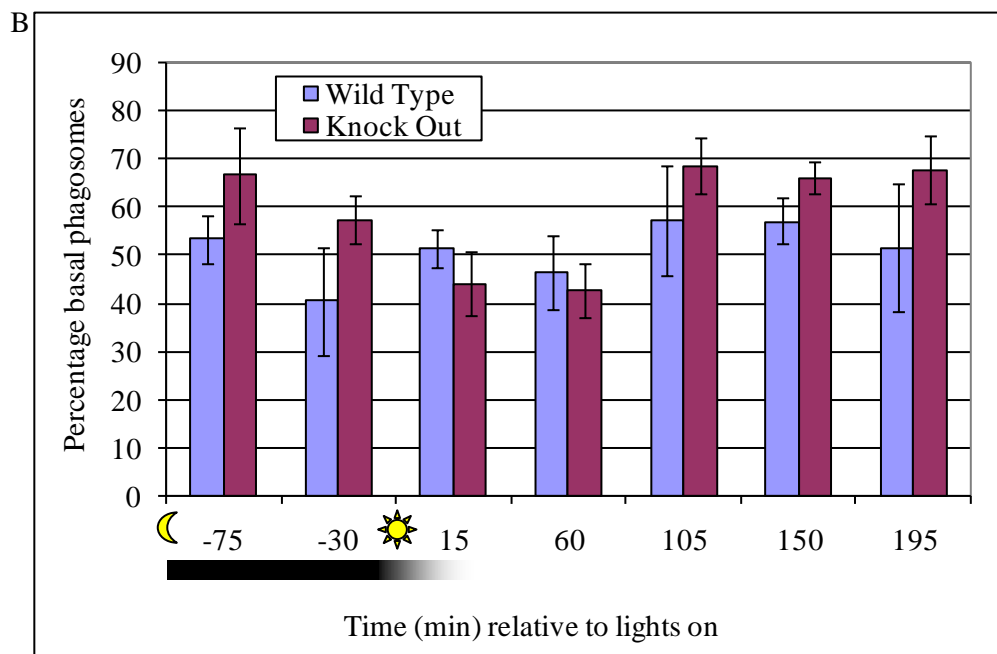
Eyes from wild type and annexin 2 knock out mice were harvested at various time points before and after light onset and processed for EM. Phagosome quantification in electron micrographs of retinal cross sections revealed that annexin 2 knock out retinas lacked the slight increase in POS uptake that follows about 1 hour after light onset as shown in wild type retina. The bars represent mean numbers of phagosomes for each time point.  $\pm$  SEM is shown. The graph inset represents the mean total number of electron dense phagosomes per  $\mu\text{m}$  of RPE for both wild type and annexin 2 knock out. Two Way ANOVA test for Wild Type and Knock Out,  $P = 0.60$ , not significant; variation across the time points,  $P = 0.48$ , not significant. ANOVA test also confirms that there is not a significant interaction between wild type and knock out animals with variation against the time points,  $P = 0.86$ . T Test for total number of phagosomes over time (graph inset),  $P = 0.54$ .

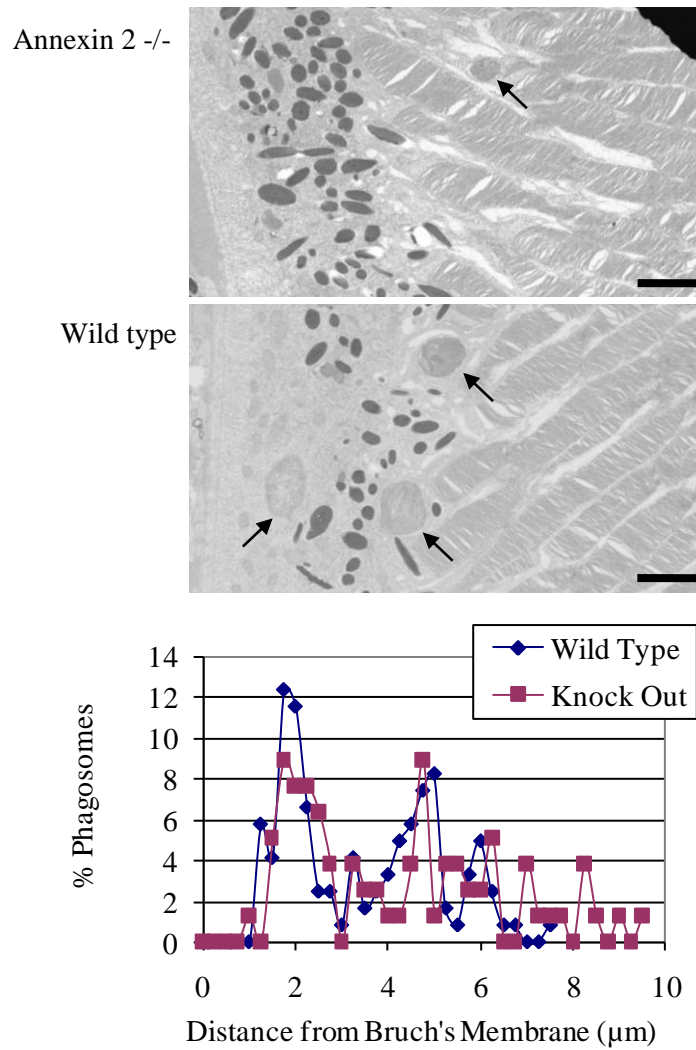


**Figure 5.6 Absence of annexin 2 delays internalisation of POS into the RPE**

Basal phagosomes were identified as electron-dense spherical structures with diameters of at least 75% of the mean diameters of the photoreceptor outer segments (POS), located within the cell body of the RPE. Basal phagosomes were counted along the length of RPE in electron micrographs taken for each sample. (A) illustrates how apical and basal phagosomes were classified. Arrows indicate phagosomes. (B) Quantification of samples harvested at the time points below revealed that the number of basal phagosomes in the annexin 2 knock out RPE exceeds that of wild type basal phagosomes from 105 min onwards. Each bar represents % basal phagosomes from at least three eyes.  $\pm$  SEM is shown (B).

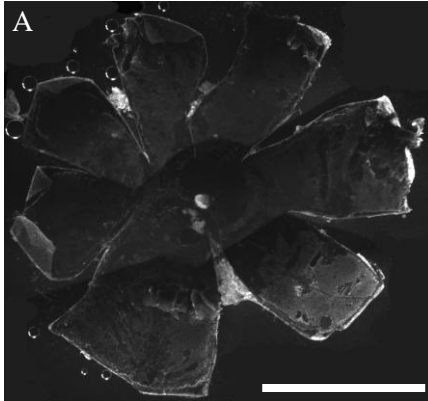
Two Way ANOVA test for Wild Type and Knock Out,  $P = 0.06$ , not significant; variation across the time points,  $P = 0.05$ , not significant. ANOVA test also confirms that there is not a significant interaction between wild type and knock out animals with variation against the time points,  $P = 0.38$





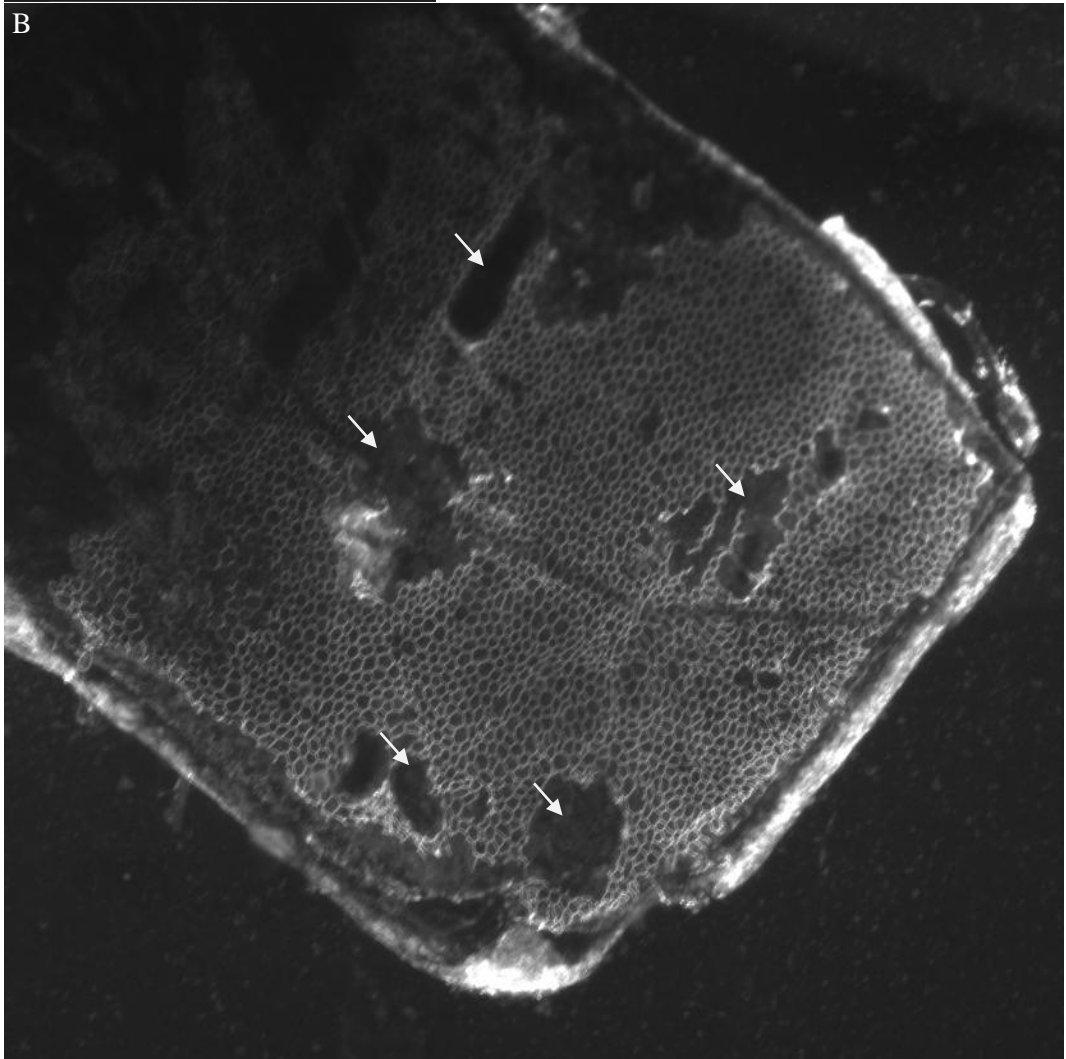
**Figure 5.7 Phagosomes are retarded in the apical processes in the annexin 2 knock out mouse**

The positions of phagosomes were mapped one hour after light onset, according to their distance from Bruch's membrane, using electron micrographs of wild type and annexin 2 knock out retina. The graph shows an accumulation of apical phagosomes in the annexin 2 knock out mice. (n = 121 for wild type, n = 78 for knock out). Black arrows indicate phagosomes. Scale bar = 2 µm.



**Figure 5.8 Visualisation of the RPE in retinal flatmounts**

The mouse eye was dissected and processed as described in the Materials and Methods, and the flatmount immunostained for the tight junction protein ZO-1 (A). The higher magnification image (B) shows that individual RPE cells can be readily resolved using this technique. The dark patches observed are where the RPE has come off during processing (indicated by the white arrows). Scale bar = 2mm.



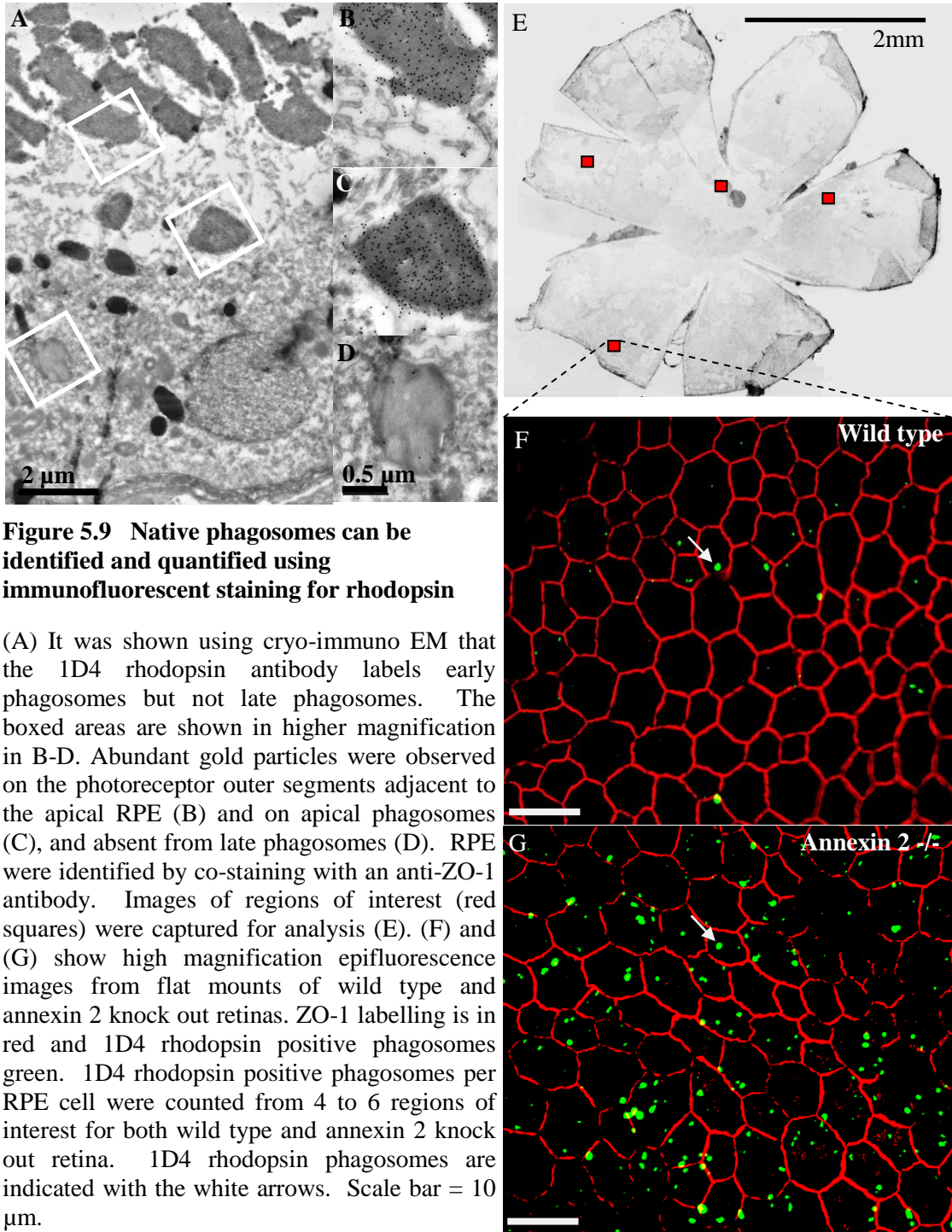


**Figure 5.9 Native phagosomes can be identified and quantified using immunofluorescent staining for rhodopsin**

(A) It was shown using cryo-immuno EM that the 1D4 rhodopsin antibody labels early phagosomes but not late phagosomes. The boxed areas are shown in higher magnification in B-D. Abundant gold particles were observed on the photoreceptor outer segments adjacent to the apical RPE (B) and on apical phagosomes (C), and absent from late phagosomes (D). RPE were identified by co-staining with an anti-ZO-1 antibody. Images of regions of interest (red squares) were captured for analysis (E). (F) and (G) show high magnification epifluorescence images from flat mounts of wild type and annexin 2 knock out retinas. ZO-1 labelling is in red and 1D4 rhodopsin positive phagosomes green. 1D4 rhodopsin positive phagosomes per RPE cell were counted from 4 to 6 regions of interest for both wild type and annexin 2 knock out retina. 1D4 rhodopsin phagosomes are indicated with the white arrows. Scale bar = 10  $\mu$ m.

The electron micrographs were taken by Dr Silène Wavre-Shapton from Law *et al* (2009)<sup>1</sup>.

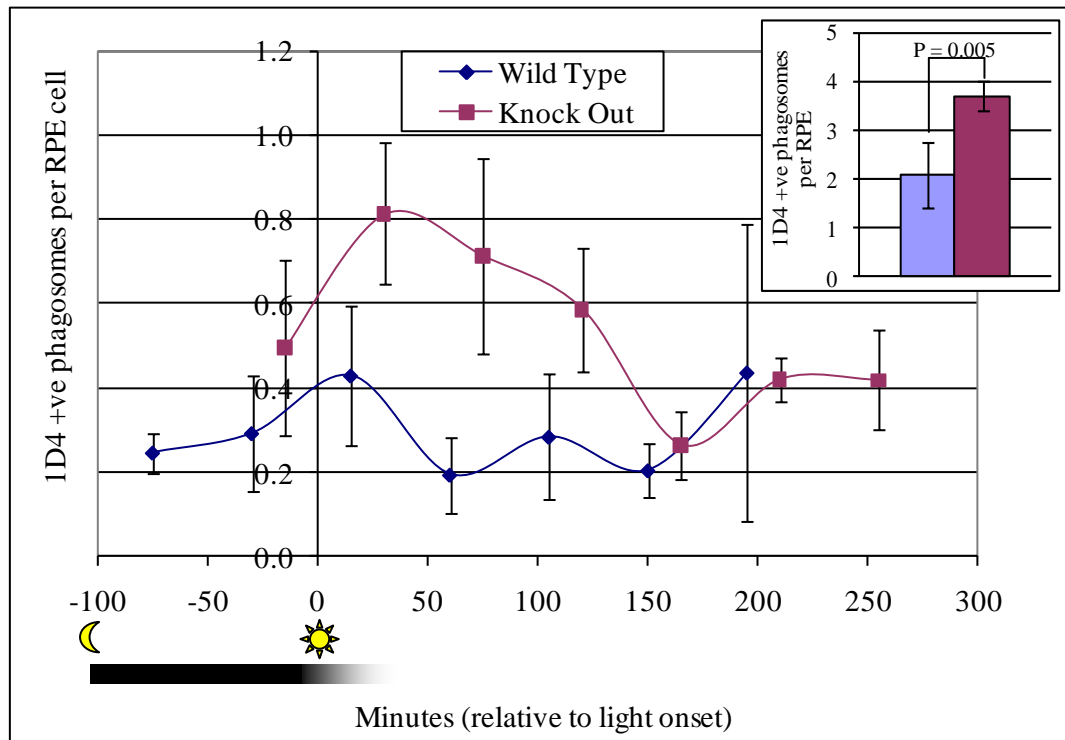


**Figure 5.10 Diurnal phagocytosis of photoreceptor outer segments (POS) is retarded in mice lacking annexin 2**

Eyes were harvested at various time points before and after light onset and were fixed and prepared for flat mounting as described in Figure 5.9. Average numbers of 1D4 rhodopsin positive phagosomes were counted from 4 to 6 regions of interest for both wild type and annexin 2 knock out mice at times before and after light onset as indicated ( $n = 3$  eyes per time point for wild type and  $n = 4$  for knock outs). Mean numbers of 1D4 rhodopsin positive phagosomes  $\pm$  SEM is shown. The graph inset shows the aggregate number of 1D4 rhodopsin positive phagosomes per RPE cell over the time course of the experiment, counted for wild type and annexin 2 knock out mice, revealing a significantly higher number in the latter (T test,  $P = 0.005$ ). Error bars show  $\pm$  SEM. One Way ANOVA for wild type and knock out samples showed no significant differences in variation across the time points ( $P = 0.91$  and  $0.24$  respectively).

## 5.2. FAK and c-Src activation are delayed in the annexin 2 knock out mouse

A previous study by Finnemann *et al.*, (2003), identified an essential signalling response to POS challenge that involved focal adhesion kinase (FAK) and MerTK signalling downstream of the  $\alpha\text{v}\beta 5$  integrin in RPE-J cells<sup>71</sup>. Work in the previous chapter suggested that tyrosine phosphorylation of annexin 2 and activation of c-Src may also have a role in signalling following POS challenge in ARPE-19 cells. It was therefore of interest to test whether retinal phagocytosis *in vivo* also involved signalling pathways that used annexin 2 and c-Src. Eyes were harvested from annexin 2 knock out mice and age-matched wild type mice at 45 minute intervals before and after light onset. Lysates prepared from these samples were incubated with PY-100 beads to immunoprecipitate tyrosine phosphorylated proteins, which were resolved by SDS PAGE and western blotted for annexin 2, c-Src and FAK (Figure 5.11). In wild type mice, tyrosine phosphorylation of annexin 2, c-Src and FAK was detected from just before light onset to a peak approximately 105 minutes after light onset, which then declined to baseline an hour and a half later. There was no or little change in the expression of annexin 2, c-Src and FAK at the protein level during this time period. The time course selected for the annexin 2 knock out mice was shifted one hour forward as preliminary data suggested a delay in signalling. Indeed, these results confirmed that in contrast to the wild type mice, where c-Src and FAK phosphorylation occurred just before light onset, tyrosine phosphorylation of c-Src and FAK in mice deficient in annexin 2 was markedly delayed, peaking some 2 hours later. One Way ANOVA confirmed that these patterns of phosphorylation in the wild type retinas were significant for FAK ( $P = < 0.001$ ). Post hoc Bonferroni multicomparison tests identified significant differences between -75 vs 105; -30 vs 105; -75 vs 150, -75 vs 60; -75 vs 195 and -75 vs 15 minutes. c-Src phosphorylation was also significant over time ( $P = 0.01$ ), with significant differences identified between -75 and 105 minutes after light onset by Bonferroni multicomparison tests. Similarly, FAK phosphorylation across the time points were significant ( $P = 0.02$ ), with Bonferroni multicomparison tests identifying significant differences between 75 vs 165. c-Src phosphorylation in the knock out samples however did not show significant variation across the time points ( $P = 0.06$ ). This delay in tyrosine phosphorylation of FAK and c-Src in annexin 2 knock out retinas matches almost exactly the delay in the disappearance of 1D4 rhodopsin positive phagosomes (Figure 5.10) described earlier, suggesting that internalisation and processing of phagosomes cannot occur until c-Src and FAK are activated.

Wild type

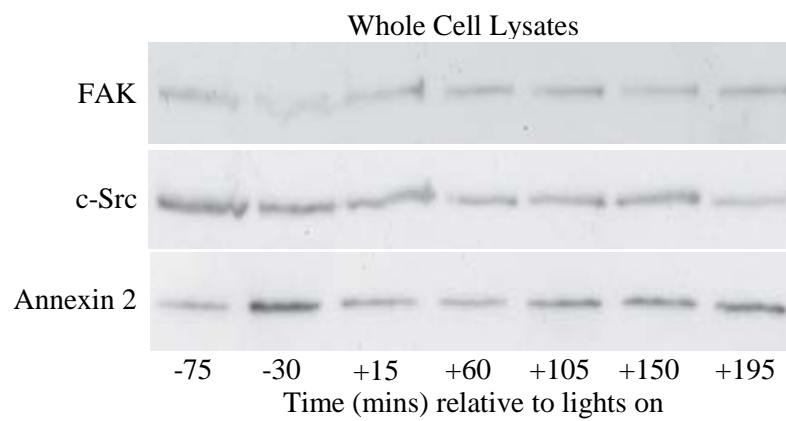
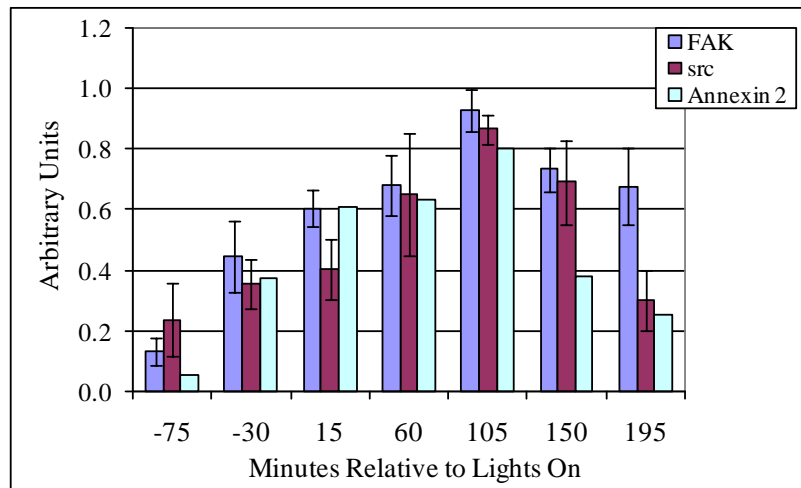
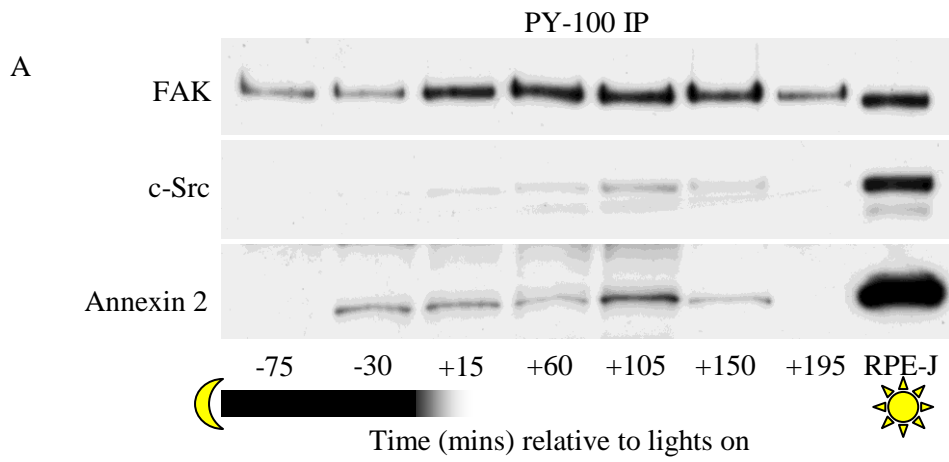


**Figure 5.11 Tyrosine kinase signalling is defective in annexin 2 deficient retina**

Figure continues over page.

## Annexin 2 Knock out

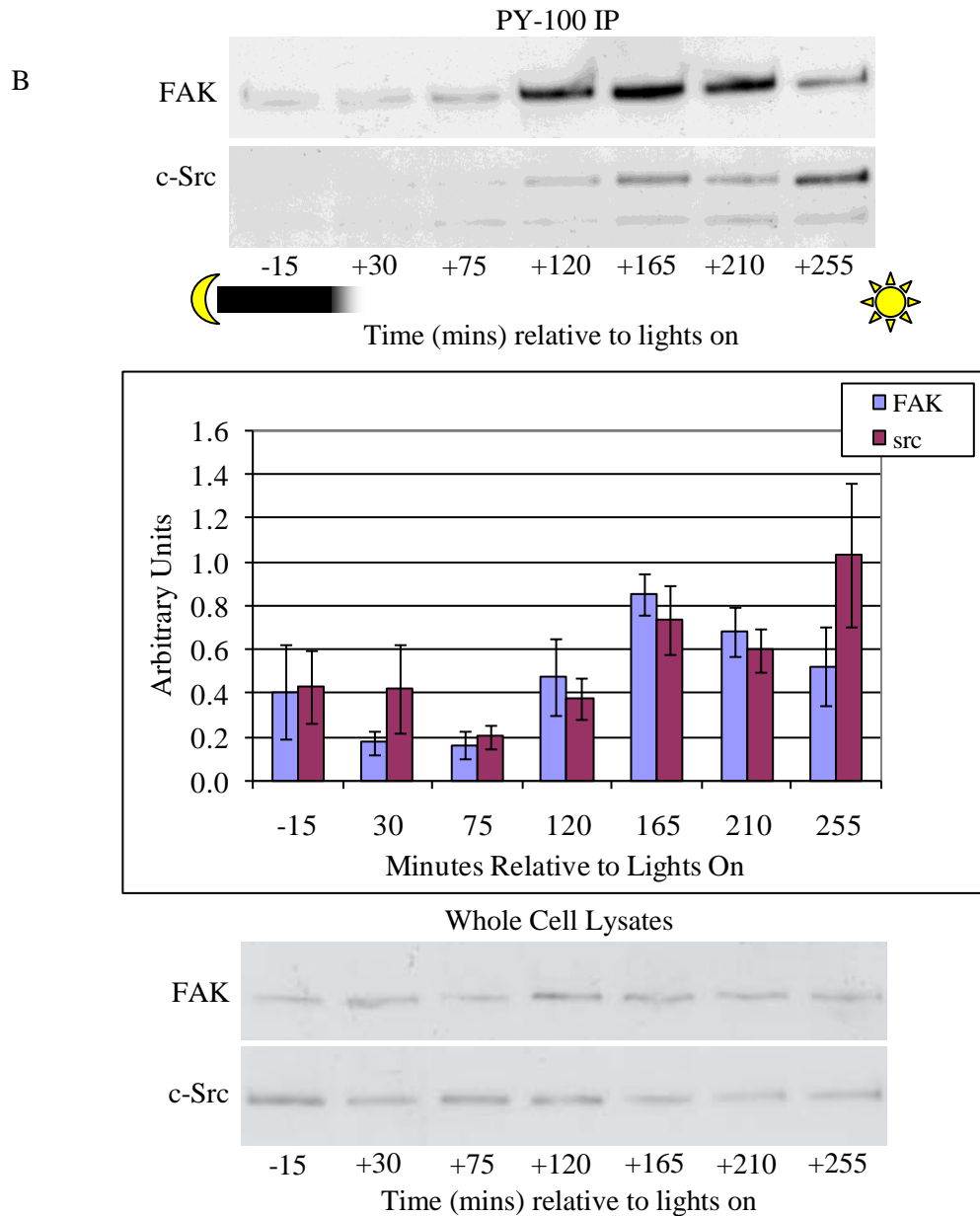


**Figure 5.11 Tyrosine kinase signalling is defective in annexin 2 deficient retinas**

Eyes from wild type and annexin 2 knock out mice were harvested at the time points indicated, before and after light onset. Lysates were prepared from the eye cups. Using the lysate from one eye, antiphosphotyrosine conjugated beads (PY-100 beads) were used for immunoprecipitations (IP). Tyrosine-phosphorylated proteins were then probed on western blots using antibodies to FAK, c-Src and annexin 2. Band intensities on the western blots were quantified  $\pm$  SEM, where  $n = 3$  for FAK and c-Src, with averaged data from two experiments for annexin 2 in wild type (A) and  $n = 4$  for FAK and c-Src in the annexin 2 knock outs (B). Western blots show total protein levels of FAK, c-Src and annexin 2 in whole cell lysates (WCL) from wild type eyes and total protein levels for FAK and c-Src in knock out eyes.

Figure continues over page.

### **Figure 5.11 Tyrosine kinase signalling is defective in annexin 2 deficient retinas**

One way ANOVA for Wild Type samples for FAK phosphorylation showed significant differences across the time points,  $P = < 0.001$ . Post hoc Bonferroni multicomparison tests identified significant differences between the following time points -75 vs 105; -30 vs 105; -75 vs 150; -75 vs 60; -75 vs 195 and -75 vs 15 min after light onset. Src phosphorylation was also significant,  $P = 0.01$ , with significant differences identified between -75 and 105 min by Bonferroni multicomparison tests.

One way ANOVA for Knock Out samples for FAK phosphorylation showed significant variation across the time points,  $P = 0.02$ . Bonferroni multicomparison tests identified significant differences between 75 vs 165 minutes after light onset. Src phosphorylation in Knock Out samples did not show significant differences across the time points,  $P = 0.06$ .

## **5.3. Discussion**

Work in this chapter shows that annexin 2 is involved in RPE phagocytosis of POS *in vivo*. The specific localisation of annexin 2 to the early phagosomes observed in cultured RPE cells in the previous chapter has been recapitulated *in vivo* (Figure 5.4). The data shown provide evidence that the activation of annexin 2 is under circadian regulation and that the absence of annexin 2 causes a delay in signalling to FAK and c-Src, the former already known to be an important activator of MerTK, which is indispensable for RPE phagocytosis of POS<sup>71</sup>. Although c-Src signalling in the annexin 2 knock out retinas across the time points confirmed by One Way ANOVA was insignificant, FAK phosphorylation was significantly variable over the time points in wild type retinas ( $P = 0.02$ ). FAK and c-Src phosphorylation over time were both significantly different ( $P = < 0.001$  and  $0.01$ , respectively). This is consistent with the delay in POS internalisation in annexin 2 deficient retinas, suggested by the EM quantifications, which shows the number of phagosomes per RPE cell (Figure 5.5) and percentage of phagosomes in the cell body 'basal phagosomes' (Figure 5.6) and also confirmed by the novel method of quantification of fluorescently labelled 1D4 rhodopsin positive phagosomes (Figure 5.9 and Figure 5.10). However, Two Way ANOVA tests performed on Figure 5.5 and Figure 5.6 were both insignificant ( $P = 0.86$  and  $P = 0.38$ ). Figure 5.10, which represents the number of fluorescently labelled 1D4 rhodopsin positive phagosomes per RPE cells also showed no significant variation across the time points for both wild type and knock out retinas ( $P = 0.91$  and  $0.24$  respectively) and so these quantification experiments remains inconclusive. However, a significant difference between wild type and knock out groups were observed in Figure 5.10 when all 1D4 rhodopsin positive phagosomes were collected together from all the time points, Moreover, when the positions of phagosomes on electron micrographs taken of retinas harvested at 1 hour after light onset were mapped according to their distance from Bruch's

membrane, phagosomes were found in both the apical RPE at the photoreceptor-RPE interface, and at the basal compartment of the RPE cell. Annexin 2 knock out retinas however had approximately 15% of the total phagosome population retarded in the apical processes above the photoreceptor-RPE interface, a feature not observed in the control retinas (Figure 5.7).

The results in this chapter suggest that annexin 2 recruitment to early and forming phagosomes is required for the synchronised circadian activation of c-Src and FAK (the latter required for phosphorylation of MerTK), critical for the coordinated circadian burst of phagocytosis that occurs approximately one hour after rod POS shedding at light onset. The kinetics of annexin 2 recruitment to early phagosomes during phagocytosis of POS, and its subsequent relocalisation during phagosome maturation, more or less mirror those of F-actin. The apical processes of the RPE are rich in actin filaments, with the majority of them (70%) orientated with their plus ends apically<sup>148, 205</sup>. The enrichment of actin in this region underlines the role of actin dynamics in driving phagosome formation during POS internalisation<sup>49</sup>. Actin polymerisation predominantly occurs at the barbed ends of actin filaments<sup>87, 89, 192</sup> and annexin 2 both binds and sequesters monomeric G-actin, and caps the barbed ends of actin filaments to stop filament growth. These processes are required for active actin dynamics, and depletion of capping proteins can result in loss of cellular ruffles. Similarly, our group has shown that depletion of annexin 2 by siRNA switches cells with dynamic, ruffling physiology to a flat and quiescent phenotype in which cells are dominated by stress fibres and cortical actin is reduced<sup>130</sup>.

In this context, other important and potentially relevant properties of annexin 2 are that it binds to cholesterol-rich membranes, calcium and phosphatidylinositol 4,5-bisphosphate (PtdIns4,5P<sub>2</sub>)<sup>115, 131, 132</sup>. PtdIns4,5P<sub>2</sub> is synthesised during early engulfment and accumulates at the phagocytic cup where it may control actin dynamics at the phagosome. In other cells, localised production of PtdIns4,5P<sub>2</sub> is required for phagocytosis, and reducing its availability inhibits FcγR-mediated phagocytosis<sup>206</sup>. Taken together, the properties of annexin 2 allow it to respond to second messengers and molecular signals to perhaps bridge the phagosome membrane with the actin cytoskeleton and mediate particle internalisation. In support of this idea, annexin 2 has been recently demonstrated to nucleate actin *in vitro* on beads coated with PtdIns4,5P<sub>2</sub><sup>140</sup>. In addition, annexin 2 has been shown to associate with early endosomes, where it mediates F-actin nucleation and polymerisation, required for early-late endosome transport. Annexin 2 was also found to interact with the actin nucleation factor Spire 1 which is also required in this process. These authors proposed that annexin 2 may have a role in stabilising Spire 1 on early endosomal membranes and may also mediate direct nucleation and polymerisation of F-actin in this process<sup>136</sup>. This would be consistent with the idea that the local

reorganisation of F-actin at the phagosome is mediated by the activation of actin-nucleating molecules<sup>207</sup>. At the interface between phagosome membranes and the actin cytoskeleton, annexin 2 may thus support the assembly of membrane lipids and mediate actin polymerisation required for phagocytosis.

Tyrosine phosphorylation of annexin 2, observed in the RPE after POS challenge in chapter 4 (Figure 4.4), is important in mediating the actin-regulating activities of annexin 2. Recent studies have shown that phosphomimetic mutants of annexin 2, produced by replacing the tyrosine 23 residue in the N-terminus of annexin 2 (phosphorylated by c-Src) with glutamic acid, can directly mobilise the F-actin cytoskeleton<sup>145, 208</sup>. In a separate study, another phosphomimicking mutant of annexin 2, in which tyrosine 23 was mutated to an aspartic acid, was reported to localise to endosomal membranes where it accelerated early to late endosome transport in HeLa cells<sup>137</sup>. In addition, the glutamic acid phosphomimetic mutant, a non-phosphorylatable annexin 2 mutant and wild type annexin 2, were all found to localise to the apical cell surface when microinjected into primary porcine RPE, and became enriched on forming phagosomes (Law *et al*, 2009. Submitted for publication). Annexin 2 is therefore likely to be recruited to the forming phagosome perhaps by  $\text{Ca}^{2+}$  or PtdIns4,5P<sub>2</sub> binding, where it is then tyrosine phosphorylated along with a number of other proteins activated by recognition and binding of POS<sup>3, 74, 187</sup>. This is also consistent with a recent finding that annexin 2 is required for the plasma membrane targeting and activation of c-Src<sup>144</sup>, which would account for the delay in c-Src activation in retinae deficient of annexin 2 (Figure 5.11).

Activation of c-Src is well known to lead to phosphorylation of annexin 2 which, as mentioned above, is required for stimulation of actin dynamics, necessary for phagocytosis<sup>144</sup>. The findings in Figure 5.11 introduce c-Src into the current RPE phagocytosis model, which might be expected given its known interactions with FAK<sup>209</sup> which already has an established role in phagocytosis in both RPE<sup>71</sup> and macrophages<sup>210</sup>. FAK signalling lies upstream of MerTK and downstream of  $\alpha\text{v}\beta\text{5}$  in the RPE phagocytosis machinery. The delay in FAK activation in annexin 2 deficient retinae suggests that annexin 2 signalling lies upstream of FAK and that the recruitment of annexin 2 to the forming phagosomes is therefore important for the synchronised circadian activation of FAK. The delay in c-Src and FAK signalling observed in the annexin 2 knock out mice coincides with the delay in phagosome internalisation into the RPE cell body. In these mice activation of c-Src and FAK does not occur until some 2 hours after light onset (Figure 5.11), which matches the delay in phagosome internalisation into the basal region of the RPE (Figure 5.6). Mapping of phagosomes relative to Bruch's membrane during peak phagocytosis (1 hour after light onset) revealed that the delay in activation of the kinases in the

annexin 2 knock out mice coincides with retardation of newly formed phagosomes in the apical region of the RPE (Figure 5.7). The number of apical phagosomes in the knock out mice returns to control levels after 3 hours (from light onset), as judged by counting 1D4 rhodopsin positive phagosomes in flat mounted annexin 2 knock out and control retinas (Figure 5.10). It is however unclear from these experiments, whether there may also be a defect in phagosome degradation, given that there are more basal phagosomes in comparison to the controls before light onset. Thus, the higher percentages of basal phagosomes observed before light onset could be due to a defect in phagosome degradation. 24 hour sampling would give more insight into the circadian process and allow one to capture the entire circadian process from shedding to degradation of both rod and cone POS. The significance of delayed signalling, internalisation and possibly a defect in phagosome degradation observed in these 3 month old mice over time is so far unknown, although normal retinal histology is retained in 18 month annexin 2 knock out mice (unpublished observations).

In the RPE, annexin 2 appears to function as a circadian regulator of POS phagocytosis. With the results obtained so far, it is possible to propose the following model: annexin 2 responds both to the localised rise in  $\text{PtdIns}4,5\text{P}_2$  which is rapidly synthesised upon POS engagement and accumulates at the phagocytic cup, and to the rise in intracellular calcium, by translocating from the cytosol to the nascent phagosome. c-Src is simultaneously targeted to the membrane by annexin 2, where it becomes activated and phosphorylates annexin 2 on its N-terminus at tyrosine 23. The rise in  $\text{InsP}_3$  and thus  $\text{Ca}^{2+}$  may also result in the activation of other kinases in the RPE, which may also phosphorylate both c-Src and annexin 2 at the apical membrane. Tyrosine phosphorylated annexin 2 is then able to mediate stimulation of actin dynamics required for particle internalisation. Simultaneously, activated c-Src is able to phosphorylate FAK and interact with integrins such as  $\alpha\beta5$  (which also activate FAK) to ultimately phosphorylate MerTK and subsequently stimulate internalisation. The absence of annexin 2 does not abolish tyrosine phosphorylation of c-Src, FAK or POS internalisation, but it is clearly essential for the prompt activation of these kinases. This suggests that other proteins and kinases downstream of annexin 2 may activate alternative signal transduction pathways as a molecular fail safe mechanism. Alternatively, other annexins may functionally substitute for annexin 2, though clearly less effectively. Together, the results in this chapter have identified annexin 2 and c-Src as two novel players in the RPE phagocytosis machinery, and shown that annexin 2 has a role in the circadian synchronised activation of FAK, which is indispensable for mediating the synchronised burst of phagocytosis that follows approximately 1 hour after light onset.

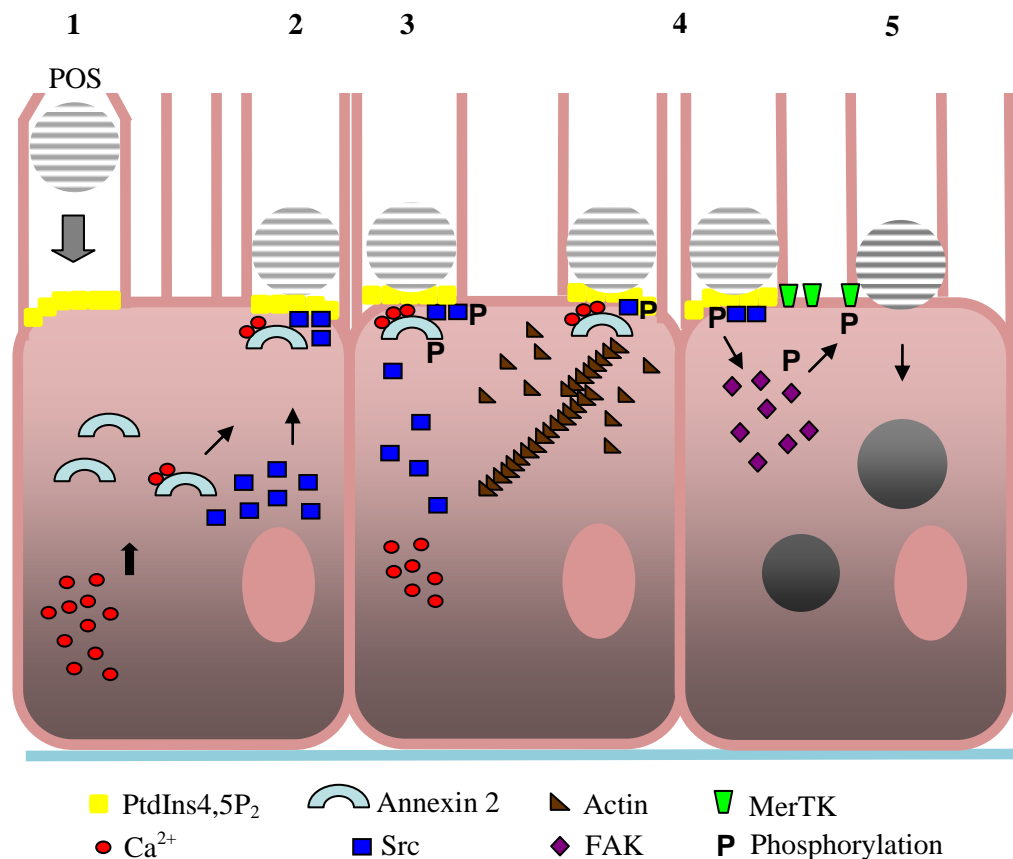


**Figure 5.12 Schematic diagram of the role of annexin 2 in RPE phagocytosis**

The localised rise in PtdIns4,5P<sub>2</sub> which is synthesised during early engulfment, increases calcium levels (1). Annexin 2 responds to calcium and moves to the PtdIns4,5P<sub>2</sub> rich phagosome membranes (2), simultaneously targeting c-Src to the plasma-membrane where it becomes activated (3) and phosphorylates annexin 2, which in turn mediates stimulation of actin dynamics required for particle internalisation (4). Concurrently, activated c-Src is able to phosphorylate FAK (4) and interact with the integrins such as  $\alpha\beta 5$  which also activates FAK to ultimately phosphorylate MerTK which is critical for internalisation (5).

# **Chapter 6**

## **Conclusions and Summary**

## 6. Conclusions and Summary

Work in this thesis examined cell differentiation in the two RPE cell lines, namely ARPE-19 and RPE-J, and in primary porcine RPE cells, in order to evaluate the best system for conducting phagocytosis experiments. The advantages and limitations of *in vitro* and *in vivo* systems were discussed, and were followed by a series of studies that used both systems to investigate the role of annexin 2 in RPE phagocytosis. Both ARPE-19 and RPE-J cells were cultured for a period of 8 weeks and the differences over time in culture for ARPE-19 cells were striking. It was evident from the characterisation studies that differentiation of RPE cell lines is time dependent and appears to rely on the interactions between junctional proteins at the cell membrane with F-actin. The actin stress fibres of ARPE-19 cells, which are typically more characteristic of fibroblasts, start to rearrange with time in culture into tight cortical actin bands around the cell circumference. Simultaneously, elongated, spindle-shaped cells evident at week 1 in culture differentiated into polygonal shaped cells, forming a cobble-stone pavement of cells, some bi-nucleate at week 8, all characteristic features of native RPE cells, as observed in the primary porcine RPE cultures. Intriguingly, when observed in culture at 4 months, ARPE-19 cells also developed pigmentation (Figure 3.4), which further supports the notion that they differentiate over time in culture, probably an effect of laying down their own extracellular matrices (ECM).

The changes observed with RPE-J cells over time in culture were less striking than those in ARPE-19 cells. Although both gene and protein expression of RPE65 were absent, RPE-J cells exhibited a polygonal morphology within a day or two of culture, similar to that of native RPE cells. As judged by confocal images and z-sections, these cells are not compact and form little functional contact with each other early in culture. The cortical actin arrangement at the cell circumference was not well defined at this stage but developed into organised structures at the cell periphery, linear to the cell junctions from 4 weeks in culture. Interestingly, discrete loci of F-actin also accumulated at the cell junctions from 4 weeks in culture. RPE-J cells were found to express key genes implicated in RPE phagocytosis throughout the 8 weeks in culture.

The mislocalised actin filaments and elongated morphology of ARPE-19 cells early in culture suggests that at this stage the cells are non-polarised and lack apical junctional complexes. Polarity is an important feature of epithelial cells and one of great importance to RPE cells that relates closely to their unique functions. The actin rearrangement, change in cell shape and development of polarity observed over time is a result of cell adaptation to changes in the environment. The fibroblastic-like ARPE-19 cells lay down their own extracellular matrix over time and essentially provide an environment that favours their differentiation into a more RPE-

like phenotype as seen in the cell characterisation studies in Chapter 3. This process of epithelial differentiation is in part reversed in primary porcine RPE cultures, where the cells appear to dedifferentiate, judged by their loss of pigmentation through time in culture (Figure 3.8 B), which would be an expected effect of removing the RPE from its native environment.

This process of epithelial differentiation or dedifferentiation, better known as Epithelial Mesenchymal Transition or EMT, where cells become more polarised or lose their polarity over time, is dependent on contacts between junctional complexes and their association with the actin cytoskeleton. Cell polarity requires establishing at least two plasma membrane domains: an apical domain, which in most epithelia faces the external medium or lumen, and the basolateral surface which adheres to adjacent cells and connective tissue. As evident from the F-actin staining and polygonal cell morphology that develop in ARPE-19 cells over the 8 weeks in culture, differentiation into polarised cells requires rearrangement of actin and junctional proteins. The phenomenon of epithelial polarisation involves the development of many types of intercellular junctions, two of which, namely the adherens junctions and the tight junctions, are proposed to associate with the actin cytoskeleton. Concomitant with F-actin rearrangement over time to the cell junctions, junctional staining of annexin 2 in ARPE-19 cells co-localised with that of F-actin from week 4. This is an intriguing observation as the actin regulating and membrane-binding activities of annexin 2 suggests a possible role for annexin 2 in EMT. This idea is already supported by several publications, which suggest that annexin 2 associates with various junctional proteins, including vascular endothelial cadherin (VE-cad), where it has a role in stabilising inter-endothelial adherens junctions<sup>181</sup>, and association to E-cadherin and to tight junctions in Madin-Darby canine kidney (MDCK) epithelial cells. In these cells, the tetrameric annexin-S100A10 complex was shown to be involved in E cadherin based adherens junctions formation<sup>182</sup> and tight junction assembly<sup>184</sup>. Perhaps even more significant, the interaction of tetrameric annexin 2 with AHNAK and Cdc42 has been shown to regulate cortical actin organisation and initiates the formation of an actin belt in the latter<sup>183, 185, 186</sup>.

Studies of *in vitro* and *in vivo* models allowed an evaluation of the advantages and disadvantages of both. For RPE phagocytosis studies, no culture model fully recapitulates the apical interactions of the RPE *in situ* as shown in the electron micrograph in Figure 3.12. but the use of *in vivo* models is limited by cost, unavailability of material and lack of reproducibility. *In vitro* models using unpassaged primary RPE cells, as discussed above, in which cells keep their polygonal morphology, pigment granules and apical processes and thus maintain many characteristics of RPE cells *in situ*, are useful for small scale experiments requiring few cells (i.e. studying phagocytosis by microscopy). In comparison, permanent cell lines are reasonably

homogeneous and so experiments are generally more reproducible. Material is unlimited and cultures are easy and cheap to maintain, making cell lines ideal for larger scale experiments such as analysis of protein phosphorylation in phagocytosis, and multiwell plate assays. The use of RPE tissue *in situ* in combination with both primary RPE and RPE cell lines allows unique insight into RPE phagocytic activity. The characterisation studies confirmed that both human and rat immortalised cell lines (ARPE-19 and RPE-J respectively) are suitable for studying the role of annexin in phagocytosis, providing that the cells are used at the correct time in culture. Work in Chapter 3 also established that for primary cell cultures, the pig eye is particularly suitable as RPE cells are relatively simple to isolate and maintain.

Phagocytosis experiments commenced with both ARPE-19 and RPE-J cells. ARPE-19 cells were grown and used within 2 weeks in culture as the characterisation studies showed that protein expression of MerTK was almost completely lost after two weeks (Figure 3.2). RPE-J cells did not grow well on glass after 1 week in culture and were fragile, and because expression of crucial phagocytosis molecules did not appear to be affected by time in culture, they were used after 1 week in culture. Using ARPE-19 at 2 weeks and RPE-J at 1 week in culture also restricted their ability to grow on top of each other, which may affect experimental outcomes. Both ARPE-19 and RPE-J cell lines and primary porcine RPE cells express annexin 2, which is recruited to the phagocytic cup during internalisation and remains with the early phagosome until internalisation is complete. Once fully engulfed, annexin 2 dissociates away from the phagosome (Figure 4.2). The kinetics of annexin 2 association with the phagosome corresponds to those of other actin regulators such as cofilin and gelsolin during phagocytosis<sup>92, 101</sup>. Gelsolin, which is also regulated by calcium, acts on actin filaments by either severing or capping them, and localises to the phagocytic cup during internalisation of particles in both polymorphonuclear (PMN) leukocytes and in macrophages<sup>101</sup>. Annexin 2 clearly has a role in the uptake of POS, probably through its actin nucleating and capping properties during internalisation<sup>130, 136, 140</sup>. Its role in RPE phagocytosis of POS was first studied by depleting it from both ARPE-19 and RPE-J cells by treatment with annexin 2 siRNA. In both cell types, phagocytosis of POS was reduced in annexin 2 siRNA treated cells in comparison to control cells (Figure 4.3). Moreover, the knock-down efficiency of annexin 2 in these cells was well below 100% as studied by immunofluorescence and western blotting (Figure 4.3). This suggests that the reduction in phagocytosis observed in the annexin 2 siRNA treated cells underestimates the true effect of annexin 2 depletion in phagocytosis.

The kinetic studies were followed by experiments to determine whether annexin 2 became phosphorylated during phagocytosis. This was of interest since internalisation of POS has been

shown to activate protein kinases in RPE cells<sup>187</sup> and annexin 2 is a substrate for both serine, threonine and tyrosine kinases. Indeed, annexin 2 was rapidly phosphorylated on tyrosine when challenged with POS, with phosphorylation peaking at 15 min. There are a number of candidate tyrosine kinases that could be involved in the phosphorylation of annexin 2, including c-Src, which is known to phosphorylate tyrosine 23 in the N-terminus of annexin 2. Western blots revealed that phosphorylation of c-Src after POS challenge showed similar kinetics to those of annexin 2. Although the experiments do not provide direct evidence that c-Src phosphorylates annexin 2, a recent publication from our lab showed that annexin 2 has a dual role, first in targeting c-Src to the plasma membranes, where it is activated, and then secondly, as a substrate and effector of c-Src<sup>144</sup>. In addition, a recent study has shown that tyrosine phosphorylation of annexin 2 promotes its association with endosomal membranes<sup>137</sup>. It is therefore likely that annexin 2 is recruited to the membrane following a localised rise in PtdIns4,5P<sub>2</sub> which is rapidly synthesised upon POS engagement, and accumulates at the phagocytic cup, to which annexin 2 is recruited in response to a rise in calcium. In agreement with this idea, c-Src is localised with the POS during phagocytosis (Figure 4.5 A and C). On confocal sections, c-Src was often observed as a ‘cloud’ surrounding the POS during the early stages of internalisation.

Annexin 2 and c-Src were also shown to be phosphorylated *in vivo*, along with FAK which already has a known role in phagocytosis in both RPE<sup>71</sup> and macrophages<sup>210</sup>. FAK signalling lies upstream of MerTK and downstream of  $\alpha\beta 5$  in the current RPE phagocytosis model. In the annexin 2 knock out mouse, the phosphorylation of both FAK and c-Src was delayed, which suggests that the role of annexin 2 lies upstream of FAK, and that the recruitment of annexin 2 to the forming phagosomes is therefore important for the synchronised circadian activation of FAK. The delay in c-Src and FAK signalling observed in the annexin 2 knock out mouse coincided with the delay in phagosome internalisation into the RPE cell body which was observed by counting basal phagosomes in the RPE in electron micrographs of eyes harvested at various times before and after light onset. An alternative method of phagosome counting was developed, in which the 1D4 rhodopsin antibody was used to visualise early phagosomes on flat mounted eyes, collected from before and after light onset. The numbers of 1D4 rhodopsin positive phagosomes per cell were calculated for both wild type and annexin 2 knock out mice, which showed a transient increase in 1D4 rhodopsin positive phagosomes in control mice shortly after light onset, consistent with the characteristic burst of phagocytosis reported elsewhere<sup>69, 108</sup>, but a more sustained increase in the number of apical phagosomes was observed in the knock out mice (Figure 5.10). These data support the observations made using electron microscopy that phagosome internalisation is delayed in the annexin 2 knock out mouse. Furthermore, positional mapping of phagosomes according to their distance from Bruch’s

membrane confirmed an accumulation of apical phagosomes and fewer basal phagosomes in the annexin 2 knock out retina in contrast to the wild type retina. In the normal retina, there was no evidence of phagosomes residing in the extreme apical region of the RPE, with most of the phagosomes internalised within the cell body at this time (Figure 5.7). Taken together, in addition to regulating actin dynamics during phagosome internalisation, annexin 2 also appear to function as a circadian regulator of POS phagocytosis by activating c-Src. The absence of annexin 2 does not abolish tyrosine phosphorylation of c-Src, FAK or POS internalisation, but it is clearly essential for the prompt activation of these kinases, which is in turn required for the synchronised circadian burst of phagocytosis that follows POS shedding.

The signalling mechanisms that regulate retinal phagocytosis may be compared to those that regulate phagocytosis in macrophages, which in the latter have been divided into two distinct types that are controlled by different Rho GTPases. Type 1 phagocytosis, which is mediated by the FcγR and is dependent on Rac1 and Cdc42, is characterised by dynamic protrusions, ruffling and formation of a continuous F-actin cup<sup>54, 60</sup>. Type 2 phagocytosis is mediated through CR3 receptors and requires Rho. Rho-dependent CR3 mediated phagocytosis leads to transient accumulation of F-actin and cytoskeletal molecules underneath the bound particle<sup>65</sup> and results in passive uptake of the complement-opsonised particle which characteristically ‘sinks’ into the cell with very few (if any) pseudopodia<sup>60</sup>. From the studies in this thesis, POS phagocytosis by the RPE is most likely to utilise the molecular mechanisms of Type 1 phagocytosis, which in the RPE is characterised by active actin and membrane dynamics and formation of a continuous F-actin cup.

## 6.1. Future perspectives

In summary, the results in this thesis suggest, providing one remains alert to their limitations, that both ARPE-19 and RPE-J cells are suitable for experiments on POS phagocytosis. Further studies of junctional proteins, proteins with known functions in EMT, and cell polarisation markers such as the Na/K-ATPase, will provide insight into the acquisition of polarity in these cells over time. The localisation of annexin 2 in cells also changed with time in culture and so studying these proteins alongside annexin 2 could reveal a role for annexin 2 in RPE differentiation. The signalling mechanisms that regulate actin dynamics during RPE phagocytosis of POS have also not yet been elucidated, so this is an area that requires investigation, particularly with regard to the roles of the different Rho GTPases: Rac1, Cdc42 and Rho A.

The data in this thesis have identified both annexin 2 and c-Src as two novel players in the RPE phagocytosis machinery. Since  $\text{Ca}^{2+}$  increases shortly after POS binding, investigating the effects of  $\text{Ca}^{2+}$  depletion in RPE phagocytosis would be interesting since membrane binding by annexin 2 is  $\text{Ca}^{2+}$  dependent. Furthermore, experiments studying the roles of annexin 2 in RPE phagocytosis when c-Src is inhibited will provide direct evidence that the two molecules interact with each other during POS internalisation. The data also revealed that annexin 2 has a role in the circadian synchronised activation of FAK, which is indispensable for mediating the synchronised burst of phagocytosis that follows after light onset. 24 hour sampling of retinas for EM or fluorescence analysis will give more insight into the circadian process and thus provide a more detailed analysis of the annexin 2 knock out mice in comparison wild type animals. Finally, future studies might make greater use of more sophisticated animal models, such as RPE-specific double knock outs (e.g. annexin 2 and c-Src), or transgenes with RPE-specific expression of annexin 2 mutants against the null background.

# Appendix

## 7. Appendix

Table 7.1 Two Way Analysis of Variance

		<b>Variation</b>	<b>DF</b>	<b>SS</b>	<b>MS</b>	<b>F</b>	<b>P</b>
Figure 4.3		Treatment (e)	7505556.570	7505556.570	5.428	0.023	
	ARPE-19	Time (t)	3.000	130643655.039	43547885.013	31.492	<0.001
		e x t	3.000	6875921.615	2291973.872	1.657	0.184
	RPE-J	Treatment (e)	1485751.685	1485751.685	0.106	0.745	
		Time (t)	3.000	610466780.449	203488926.816	14.578	<0.001
		e x t	3.000	84194445.964	28064815.321	2.011	0.117
Figure 5.5		<b>Variation</b>	<b>DF</b>	<b>SS</b>	<b>MS</b>	<b>F</b>	<b>P</b>
		Wild Type or Knock Out (e)	1	0.0016	0.0016	0.282	0.598
		Time (t)	6	0.0319	0.00532	0.937	0.476
		e x t	6	0.0144	0.0024	0.422	0.861
Figure 5.6		<b>Variation</b>	<b>DF</b>	<b>SS</b>	<b>MS</b>	<b>F</b>	<b>P</b>
		Wild Type or Knock Out (e)	929.555	929.555	3.6	0.063	
		Time (t)	3445.254	574.209	2.224	0.054	
		e x t	1695.119	282.52	1.094	0.377	

**Table 7.2 One Way Analysis of Variance**

Figure 4.4		<b>Variation</b>	<b>DF</b>	<b>SS</b>	<b>MS</b>	<b>F</b>	<b>P</b>
	annexin 2 phosphorylation	Time (t)	3	9.405	3.135	2.046	0.161
	c-Src phosphorylation	Time (t)	58.020	3.000	19.340	0.720	0.555
	annexin 2 WCL	Time (t)	3.000	0.012	0.004	0.188	0.903
	c-Src WCL	Time (t)	0.025	3.000	0.008	0.220	0.881
Figure 5.10		<b>Variation</b>	<b>DF</b>	<b>SS</b>	<b>MS</b>	<b>F</b>	<b>P</b>
	Wild Type	Time (t)	6	0.175	0.0291	0.328	0.911
	Knock Out	Time (t)	6	0.858	0.143	1.467	0.237
Figure 5.11		<b>Variation</b>	<b>DF</b>	<b>SS</b>	<b>MS</b>	<b>F</b>	<b>P</b>
	Wild Type FAK	Time (t)	6	2.296	0.383	8.108	<0.001
	Wild Type FAK	Time (t)	6	1.324	0.221	3.741	0.011
	Knock Out FAK	Time (t)	6	1.521	0.254	3.227	0.021
	Knock Out c-Src	Time (t)	6	1.826	0.304	2.427	0.061

## Reference List

- (1) Law AL, Ling Q, Hajjar KA et al. Annexin A2 regulates phagocytosis of photoreceptor outer segments in the mouse retina. *Mol Biol Cell* 2009;20(17):3896-3904.
- (2) de Jong PT. Age-related macular degeneration. *N Engl J Med* 2006;355(14):1474-1485.
- (3) Strauss O. The retinal pigment epithelium in visual function. *Physiol Rev* 2005;85(3):845-881.
- (4) Zinn KM, Benjamin-Henkind JV. Anatomy of the Human Retinal Pigment Epithelium. In: Marmor MF, editor. *The Retinal Pigment Epithelium*. Harvard University Press; 1979. 7-13.
- (5) Roth F, Bindewald A, Holz FG. Key pathophysiologic pathways in age-related macular disease. *Graefes Arch Clin Exp Ophthalmol* 2004;42(8):710-716.
- (6) Hogan MJ, Alvarado J. Studies on the human macula. IV. Aging changes in Bruch's membrane. *Arch Ophthalmol* 1967;77(3):410-420.
- (7) van der Schaft TL, de Bruijn WC, Mooy CM, Ketelaars DA, de Jong PT. Is basal laminar deposit unique for age-related macular degeneration? *Arch Ophthalmol* 1991;109(3):420-425.
- (8) van der Schaft TL, Mooy CM, de Bruijn WC, Oron FG, Mulder PG, de Jong PT. Histologic features of the early stages of age-related macular degeneration. A statistical analysis. *Ophthalmology* 1992;99(2):278-286.
- (9) Miller RF. The Physiology and Morphology of the Vertebrate Retina. In: Ogden TE, Hinton DR, Schachat AP, editors. *Retina*. St. Louis, Missouri: Mosby; 2001. 138-170.
- (10) Masland RH. The fundamental plan of the retina. *Nat Neurosci* 2001;4(9):877-886.
- (11) Smith RS, John SWM, Nishina PM. Posterior Segment and Orbit. In: Smith RS, editor. *Systematic Evaluation of the Mouse Eye. Anatomy, Pathology, and Biomethods*. CRC Press; 2002. 33-35.
- (12) Gordon WCaBNG. Retina. Organisation of the retina: cell types. In: Harding JJ, editor. *Biochemistry of the Eye*. London: Chapman and Hall; 1997. 144-152.
- (13) Bron AJ, Tripathi RC, Tripathi BJ. The Retina. *Wolff's Anatomy of the Eye and Orbit*. Eighth ed. Arnold; 2001. 454-488.
- (14) Kuwabara T. Species Differences. In: Zinn KM, Marmor MF, editors. *The Retinal Pigment Epithelium*. Harvard University Press; 1979. 63.

- (15) Zinn KM, Benjamin-Henkind JV. Anatomy of the Human Retinal Pigment Epithelium. In: Zinn KM, Marmor MF, editors. *The Retinal Pigment Epithelium*. Harvard University Press; 1979. 25-27.
- (16) Sarangarajan R, Apte SP. Melanization and phagocytosis: implications for age related macular degeneration. *Mol Vis* 2005;11:482-490.
- (17) Futter CE. The molecular regulation of organelle transport in mammalian retinal pigment epithelial cells. *Pigment Cell Res* 2006;19(2):104-111.
- (18) Jeffery G. The albino retina: an abnormality that provides insight into normal retinal development. *Trends Neurosci* 1997;20(4):165-169.
- (19) Wu J, Seregard S, Algvere PV. Photochemical damage of the retina. *Surv Ophthalmol* 2006;51(5):461-481.
- (20) Steinberg RH, Wood I. The Relationship of the Retinal Pigment Epithelium to Photoreceptor Outer Segments in Human Retina. In: Zinn KM, Marmor MF, editors. *The Retinal Pigment Epithelium*. Harvard University Press; 1979. 32-43.
- (21) Anderson DH, Fisher SK, Steinberg RH. Mammalian cones: disc shedding, phagocytosis, and renewal. *Invest Ophthalmol Vis Sci* 1978;17(2):117-133.
- (22) Bok D, Young RW. Phagocytic Properties of the Retinal Pigment Epithelium. In: Zinn KM, Marmor MF, editors. *The Retinal Pigment Epithelium*. Harvard University Press; 1979. 148-170.
- (23) Hartsock A, Nelson WJ. Adherens and tight junctions: structure, function and connections to the actin cytoskeleton. *Biochim Biophys Acta* 2008;1778(3):660-669.
- (24) Matter K, Balda MS. Signalling to and from tight junctions. *Nat Rev Mol Cell Biol* 2003;4(3):225-236.
- (25) Mege RM, Gavard J, Lambert M. Regulation of cell-cell junctions by the cytoskeleton. *Curr Opin Cell Biol* 2006;18(5):541-548.
- (26) Tepass U. Crumbs, a component of the apical membrane, is required for zonula adherens formation in primary epithelia of Drosophila. *Dev Biol* 1996;177(1):217-225.
- (27) Tepass U, Theres C, Knust E. crumbs encodes an EGF-like protein expressed on apical membranes of Drosophila epithelial cells and required for organization of epithelia. *Cell* 1990;61(5):787-799.
- (28) Grawe F, Wodarz A, Lee B, Knust E, Skaer H. The Drosophila genes crumbs and stardust are involved in the biogenesis of adherens junctions. *Development* 1996;122(3):951-959.
- (29) Wodarz A, Hinz U, Engelbert M, Knust E. Expression of crumbs confers apical character on plasma membrane domains of ectodermal epithelia of Drosophila. *Cell* 1995;82(1):67-76.
- (30) den Hollander AI, ten Brink JB, de Kok YJ et al. Mutations in a human homologue of Drosophila crumbs cause retinitis pigmentosa (RP12). *Nat Genet* 1999;23(2):217-221.

- (31) den Hollander AI, Heckenlively JR, van den Born LI et al. Leber congenital amaurosis and retinitis pigmentosa with Coats-like exudative vasculopathy are associated with mutations in the crumbs homologue 1 (CRB1) gene. *Am J Hum Genet* 2001;69(1):198-203.
- (32) Lotery AJ, Jacobson SG, Fishman GA et al. Mutations in the CRB1 gene cause Leber congenital amaurosis. *Arch Ophthalmol* 2001;119(3):415-420.
- (33) Lotery AJ, Malik A, Shami SA et al. CRB1 mutations may result in retinitis pigmentosa without para-arteriolar RPE preservation. *Ophthalmic Genet* 2001;22(3):163-169.
- (34) Hargrave PA. Rhodopsin structure, function, and topography the Friedenwald lecture. *Invest Ophthalmol Vis Sci* 2001;42(1):3-9.
- (35) Okada T, Ernst OP, Palczewski K, Hofmann KP. Activation of rhodopsin: new insights from structural and biochemical studies. *Trends Biochem Sci* 2001;26(5):318-324.
- (36) LaVail MM. Circadian nature of rod outer segment disc shedding in the rat. *Invest Ophthalmol Vis Sci* 1980;19(4):407-411.
- (37) LaVail MM. Rod outer segment disk shedding in rat retina: relationship to cyclic lighting. *Science* 1976;194(4269):1071-1074.
- (38) Garcia-Fernandez JM, Jimenez AJ, Foster RG. The persistence of cone photoreceptors within the dorsal retina of aged retinally degenerate mice (rd/rd): implications for circadian organization. *Neurosci Lett* 1995;187(1):33-36.
- (39) Jimenez AJ, Garcia-Fernandez JM, Gonzalez B, Foster RG. The spatio-temporal pattern of photoreceptor degeneration in the aged rd/rd mouse retina. *Cell Tissue Res* 1996;284(2):193-202.
- (40) Ebihara S, Tsuji K. Entrainment of the circadian activity rhythm to the light cycle: effective light intensity for a Zeitgeber in the retinal degenerate C3H mouse and the normal C57BL mouse. *Physiol Behav* 1980;24(3):523-527.
- (41) Brainard GC, Hanifin JP. Photons, clocks, and consciousness. *J Biol Rhythms* 2005;20(4):314-325.
- (42) Foster RG, Provencio I, Hudson D, Fiske S, De GW, Menaker M. Circadian photoreception in the retinally degenerate mouse (rd/rd). *J Comp Physiol [A]* 1991;169(1):39-50.
- (43) Provencio I, Jiang G, De Grip WJ, Hayes WP, Rollag MD. Melanopsin: An opsin in melanophores, brain, and eye. *Proc Natl Acad Sci U S A* 1998;95(1):340-345.
- (44) Hannibal J, Hindersson P, Ostergaard J et al. Melanopsin is expressed in PACAP-containing retinal ganglion cells of the human retinohypothalamic tract. *Invest Ophthalmol Vis Sci* 2004;45(11):4202-4209.
- (45) Provencio I, Rodriguez IR, Jiang G, Hayes WP, Moreira EF, Rollag MD. A novel human opsin in the inner retina. *J Neurosci* 2000;20(2):600-605.

- (46) Klerman EB, Shanahan TL, Brotman DJ et al. Photic resetting of the human circadian pacemaker in the absence of conscious vision. *J Biol Rhythms* 2002;17(6):548-555.
- (47) Lockley SW, Skene DJ, Arendt J, Tabandeh H, Bird AC, DeFrance R. Relationship between melatonin rhythms and visual loss in the blind. *J Clin Endocrinol Metab* 1997;82(11):3763-3770.
- (48) Griffin FM, Jr. Studies on the mechanism of phagocytosis. I. Requirements for circumferential attachment of particle-bound ligands to specific receptors on the macrophage plasma membrane. 1975.
- (49) May RC, Machesky LM. Phagocytosis and the actin cytoskeleton. *J Cell Sci* 2001;114(Pt 6):1061-1077.
- (50) Cougoule C, Hoshino S, Dart A, Lim J, Caron E. Dissociation of recruitment and activation of the small G-protein Rac during Fc $\gamma$  receptor-mediated phagocytosis. *J Biol Chem* 2006;281(13):8756-8764.
- (51) Groves E, Dart AE, Covarelli V, Caron E. Molecular mechanisms of phagocytic uptake in mammalian cells. *Cell Mol Life Sci* 2008;65(13):1957-1976.
- (52) Massol P, Montcourrier P, Guillemot JC, Chavrier P. Fc receptor-mediated phagocytosis requires CDC42 and Rac1. *EMBO J* 1998;17(21):6219-6229.
- (53) Hoppe AD, Swanson JA. Cdc42, Rac1, and Rac2 display distinct patterns of activation during phagocytosis. *Mol Biol Cell* 2004;15(8):3509-3519.
- (54) May RC, Caron E, Hall A, Machesky LM. Involvement of the Arp2/3 complex in phagocytosis mediated by Fc $\gamma$ R or CR3. *Nat Cell Biol* 2000;2(4):246-248.
- (55) Collins LR, Minden A, Karin M, Brown JH. Galph $\alpha$ 12 stimulates c-Jun NH $_2$ -terminal kinase through the small G proteins Ras and Rac. *J Biol Chem* 1996;271(29):17349-17353.
- (56) Coso OA, Chiariello M, Yu JC et al. The small GTP-binding proteins Rac1 and Cdc42 regulate the activity of the JNK/SAPK signaling pathway. *Cell* 1995;81(7):1137-1146.
- (57) Perona R, Montaner S, Saniger L, Sanchez-Perez I, Bravo R, Lacal JC. Activation of the nuclear factor-kappaB by Rho, CDC42, and Rac-1 proteins. *Genes Dev* 1997;11(4):463-475.
- (58) Abo A, Pick E, Hall A, Totty N, Teahan CG, Segal AW. Activation of the NADPH oxidase involves the small GTP-binding protein p21rac1. *Nature* 1991;353(6345):668-670.
- (59) Gabig TG, Crean CD, Mantel PL, Rosli R. Function of wild-type or mutant Rac2 and Rap1a GTPases in differentiated HL60 cell NADPH oxidase activation. *Blood* 1995;85(3):804-811.
- (60) Caron E, Hall A. Identification of two distinct mechanisms of phagocytosis controlled by different Rho GTPases. *Science* 1998;282(5394):1717-1721.
- (61) Law SKA, Reid KBM. Complement. *Complement*. Oxford: IRL Press; 2009. 1-7.

- (62) Cummings KL, Waggoner SN, Tacke R, Hahn YS. Role of complement in immune regulation and its exploitation by virus. *Viral Immunol* 2007;20(4):505-524.
- (63) Caron E, Self AJ, Hall A. The GTPase Rap1 controls functional activation of macrophage integrin  $\alpha$ M $\beta$ 2 by LPS and other inflammatory mediators. *Curr Biol* 2000;10(16):974-978.
- (64) Wiedemann A, Patel JC, Lim J, Tsun A, van KY, Caron E. Two distinct cytoplasmic regions of the  $\beta$ 2 integrin chain regulate RhoA function during phagocytosis. *J Cell Biol* 2006;172(7):1069-1079.
- (65) Allen LA, Aderem A. Molecular definition of distinct cytoskeletal structures involved in complement- and Fc receptor-mediated phagocytosis in macrophages. *J Exp Med* 1996;184(2):627-637.
- (66) Lambris JD, Ricklin D, Geisbrecht BV. Complement evasion by human pathogens. *Nat Rev Microbiol* 2008;6(2):132-142.
- (67) Finnemann SC, Bonilha VL, Marmorstein AD, Rodriguez-Boulan E. Phagocytosis of rod outer segments by retinal pigment epithelial cells requires  $\alpha$ v $\beta$ 5 integrin for binding but not for internalization. *Proc Natl Acad Sci U S A* 1997;94(24):12932-12937.
- (68) Nandrot EF, Anand M, Sircar M, Finnemann SC. Novel function for  $\alpha$ v $\beta$ 5 integrin in retinal adhesion and its diurnal peak. *Am J Physiol Cell Physiol* 2005.
- (69) Nandrot EF, Kim Y, Brodie SE, Huang X, Sheppard D, Finnemann SC. Loss of synchronized retinal phagocytosis and age-related blindness in mice lacking  $\alpha$ v $\beta$ 5 integrin. *J Exp Med* 2004;200(12):1539-1545.
- (70) Nandrot EF, Anand M, Almeida D, Atabai K, Sheppard D, Finnemann SC. Essential role for MFG-E8 as ligand for  $\alpha$ v $\beta$ 5 integrin in diurnal retinal phagocytosis. *Proc Natl Acad Sci U S A* 2007;104(29):12005-12010.
- (71) Finnemann SC. Focal adhesion kinase signaling promotes phagocytosis of integrin-bound photoreceptors. *EMBO J* 2003;22(16):4143-4154.
- (72) Chaitin MH, Hall MO. Defective ingestion of rod outer segments by cultured dystrophic rat pigment epithelial cells. *Invest Ophthalmol Vis Sci* 1983;24(7):812-820.
- (73) Feng W, Yasumura D, Matthes MT, LaVail MM, Vollrath D. Mertk triggers uptake of photoreceptor outer segments during phagocytosis by cultured retinal pigment epithelial cells. *J Biol Chem* 2002;277(19):17016-17022.
- (74) Heth CA, Marescalchi PA. Inositol triphosphate generation in cultured rat retinal pigment epithelium. *Invest Ophthalmol Vis Sci* 1994;35(2):409-416.
- (75) Hall MO, Abrams TA, Mittag TW. ROS ingestion by RPE cells is turned off by increased protein kinase C activity and by increased calcium. *Exp Eye Res* 1991;52(5):591-598.

- (76) Albert ML, Pearce SF, Francisco LM et al. Immature dendritic cells phagocytose apoptotic cells via  $\alpha$ v $\beta$ 5 and CD36, and cross-present antigens to cytotoxic T lymphocytes. *J Exp Med* 1998;188(7):1359-1368.
- (77) Fadok VA, Warner ML, Bratton DL, Henson PM. CD36 is required for phagocytosis of apoptotic cells by human macrophages that use either a phosphatidylserine receptor or the vitronectin receptor ( $\alpha$ v $\beta$ 3). *J Immunol* 1998;161(11):6250-6257.
- (78) Savill J, Hogg N, Ren Y, Haslett C. Thrombospondin cooperates with CD36 and the vitronectin receptor in macrophage recognition of neutrophils undergoing apoptosis. *J Clin Invest* 1992;90(4):1513-1522.
- (79) Ryeom SW, Sparrow JR, Silverstein RL. CD36 participates in the phagocytosis of rod outer segments by retinal pigment epithelium. *J Cell Sci* 1996;109 ( Pt 2):387-395.
- (80) Sparrow JR, Ryeom SW, Abumrad NA, Ibrahimi A, Silverstein RL. CD36 expression is altered in retinal pigment epithelial cells of the RCS rat. *Exp Eye Res* 1997;64(1):45-56.
- (81) Finnemann SC, Silverstein RL. Differential roles of CD36 and  $\alpha$ v $\beta$ 5 integrin in photoreceptor phagocytosis by the retinal pigment epithelium. *J Exp Med* 2001;194(9):1289-1298.
- (82) Chang Y, Finnemann SC. Tetraspanin CD81 is required for the  $\alpha$ v $\beta$ 5-integrin-dependent particle-binding step of RPE phagocytosis. *J Cell Sci* 2007;120(Pt 17):3053-3063.
- (83) Caron E. Regulation by phosphorylation. Yet another twist in the WASP story. *Dev Cell* 2003;4(6):772-773.
- (84) Higgs HN, Pollard TD. Activation by Cdc42 and PIP(2) of Wiskott-Aldrich syndrome protein (WASp) stimulates actin nucleation by Arp2/3 complex. *J Cell Biol* 2000;150(6):1311-1320.
- (85) Rohatgi R, Ho HY, Kirschner MW. Mechanism of N-WASP activation by CDC42 and phosphatidylinositol 4, 5-bisphosphate. *J Cell Biol* 2000;150(6):1299-1310.
- (86) Vicente-Manzanares M, Sanchez-Madrid F. Role of the cytoskeleton during leukocyte responses. *Nat Rev Immunol* 2004;4(2):110-122.
- (87) Carlier MF. Control of actin dynamics. *Curr Opin Cell Biol* 1998;10(1):45-51.
- (88) Chesarone MA, Goode BL. Actin nucleation and elongation factors: mechanisms and interplay. *Curr Opin Cell Biol* 2009;21(1):28-37.
- (89) Cooper JA, Schafer DA. Control of actin assembly and disassembly at filament ends. *Curr Opin Cell Biol* 2000;12(1):97-103.
- (90) Staiger CJ, Blanchoin L. Actin dynamics: old friends with new stories. *Curr Opin Plant Biol* 2006;9(6):554-562.
- (91) Carlier MF, Ressad F, Pantaloni D. Control of actin dynamics in cell motility. Role of ADF/cofilin. *J Biol Chem* 1999;274(48):33827-33830.

- (92) Aizawa H, Fukui Y, Yahara I. Live dynamics of Dictyostelium cofilin suggests a role in remodeling actin latticework into bundles. *J Cell Sci* 1997;110 ( Pt 19):2333-2344.
- (93) Nagaishi K, Adachi R, Kawanishi T et al. Participation of cofilin in opsonized zymosan-triggered activation of neutrophil-like HL-60 cells through rapid dephosphorylation and translocation to plasma membranes. *J Biochem* 1999;125(5):891-898.
- (94) Matsui S, Matsumoto S, Adachi R et al. LIM kinase 1 modulates opsonized zymosan-triggered activation of macrophage-like U937 cells. Possible involvement of phosphorylation of cofilin and reorganization of actin cytoskeleton. *J Biol Chem* 2002;277(1):544-549.
- (95) Edwards DC, Sanders LC, Bokoch GM, Gill GN. Activation of LIM-kinase by Pak1 couples Rac/Cdc42 GTPase signalling to actin cytoskeletal dynamics. *Nat Cell Biol* 1999;1(5):253-259.
- (96) Ohashi K, Nagata K, Maekawa M, Ishizaki T, Narumiya S, Mizuno K. Rho-associated kinase ROCK activates LIM-kinase 1 by phosphorylation at threonine 508 within the activation loop. *J Biol Chem* 2000;275(5):3577-3582.
- (97) Sumi T, Matsumoto K, Takai Y, Nakamura T. Cofilin phosphorylation and actin cytoskeletal dynamics regulated by rho- and Cdc42-activated LIM-kinase 2. *J Cell Biol* 1999;147(7):1519-1532.
- (98) Dharmawardhane S, Brownson D, Lennartz M, Bokoch GM. Localization of p21-activated kinase 1 (PAK1) to pseudopodia, membrane ruffles, and phagocytic cups in activated human neutrophils. *J Leukoc Biol* 1999;66(3):521-527.
- (99) Konzok A, Weber I, Simmeth E, Hacker U, Maniak M, Muller-Taubenberger A. DAip1, a Dictyostelium homologue of the yeast actin-interacting protein 1, is involved in endocytosis, cytokinesis, and motility. *J Cell Biol* 1999;146(2):453-464.
- (100) Sun HQ, Yamamoto M, Mejillano M, Yin HL. Gelsolin, a multifunctional actin regulatory protein. *J Biol Chem* 1999;274(47):33179-33182.
- (101) Yin HL, Albrecht JH, Fattoum A. Identification of gelsolin, a Ca<sup>2+</sup>-dependent regulatory protein of actin gel-sol transformation, and its intracellular distribution in a variety of cells and tissues. *J Cell Biol* 1981;91(3 Pt 1):901-906.
- (102) Serrander L, Skarman P, Rasmussen B et al. Selective inhibition of IgG-mediated phagocytosis in gelsolin-deficient murine neutrophils. *J Immunol* 2000;165(5):2451-2457.
- (103) Mansfield PJ, Shayman JA, Boxer LA. Regulation of polymorphonuclear leukocyte phagocytosis by myosin light chain kinase after activation of mitogen-activated protein kinase. *Blood* 2000;95(7):2407-2412.
- (104) Swanson JA, Johnson MT, Beningo K, Post P, Mooseker M, Araki N. A contractile activity that closes phagosomes in macrophages. *J Cell Sci* 1999;112 ( Pt 3):307-316.
- (105) Jung G, Wu X, Hammer JA, III. Dictyostelium mutants lacking multiple classic myosin I isoforms reveal combinations of shared and distinct functions. *J Cell Biol* 1996;133(2):305-323.

- (106) Schwarz EC, Neuhaus EM, Kistler C, Henkel AW, Soldati T. Dictyostelium myosin IK is involved in the maintenance of cortical tension and affects motility and phagocytosis. *J Cell Sci* 2000;113 ( Pt 4):621-633.
- (107) Titus MA. A class VII unconventional myosin is required for phagocytosis. *Curr Biol* 1999;9(22):1297-1303.
- (108) Gibbs D, Kitamoto J, Williams DS. Abnormal phagocytosis by retinal pigmented epithelium that lacks myosin VIIa, the Usher syndrome 1B protein. *Proc Natl Acad Sci U S A* 2003;100(11):6481-6486.
- (109) Strick DJ, Feng W, Vollrath D. Mertk drives myosin II redistribution during retinal pigment epithelial phagocytosis. *Invest Ophthalmol Vis Sci* 2009;50(5):2427-2435.
- (110) Liu X, Ondek B, Williams DS. Mutant myosin VIIa causes defective melanosome distribution in the RPE of shaker-1 mice. *Nat Genet* 1998;19(2):117-118.
- (111) Liu X, Udovichenko IP, Brown SD, Steel KP, Williams DS. Myosin VIIa participates in opsin transport through the photoreceptor cilium. *J Neurosci* 1999;19(15):6267-6274.
- (112) D'Cruz PM, Yasumura D, Weir J et al. Mutation of the receptor tyrosine kinase gene Mertk in the retinal dystrophic RCS rat. *Hum Mol Genet* 2000;9(4):645-651.
- (113) Herman KG, Steinberg RH. Phagosome movement and the diurnal pattern of phagocytosis in the tapetal retinal pigment epithelium of the opossum. *Invest Ophthalmol Vis Sci* 1982;23(3):277-290.
- (114) Moss SE, Morgan RO. The annexins. *Genome Biol* 2004;5(4):219.
- (115) Gerke V, Creutz CE, Moss SE. Annexins: linking Ca<sup>2+</sup> signalling to membrane dynamics. *Nat Rev Mol Cell Biol* 2005;6(6):449-461.
- (116) Gerke V, Moss SE. Annexins: from structure to function. *Physiol Rev* 2002;82(2):331-371.
- (117) Turnay J, Lecona E, Fernandez-Lizarbe S et al. Structure-function relationship in annexin A13, the founder member of the vertebrate family of annexins. *Biochem J* 2005;389(Pt 3):899-911.
- (118) Menell JS, Cesarman GM, Jacovina AT, McLaughlin MA, Lev EA, Hajjar KA. Annexin II and bleeding in acute promyelocytic leukemia. *N Engl J Med* 1999;340(13):994-1004.
- (119) Ling Q, Jacovina AT, Deora A et al. Annexin II regulates fibrin homeostasis and neoangiogenesis in vivo. *J Clin Invest* 2004;113(1):38-48.
- (120) Liu SH, Lin CY, Peng SY et al. Down-regulation of annexin A10 in hepatocellular carcinoma is associated with vascular invasion, early recurrence, and poor prognosis in synergy with p53 mutation. *Am J Pathol* 2002;160(5):1831-1837.
- (121) Goebeler V, Ruhe D, Gerke V, Rescher U. Atypical properties displayed by annexin A9, a novel member of the annexin family of Ca(2+) and lipid binding proteins. *FEBS Lett* 2003;546(2-3):359-364.

- (122) Iglesias JM, Morgan RO, Jenkins NA, Copeland NG, Gilbert DJ, Fernandez MP. Comparative genetics and evolution of annexin A13 as the founder gene of vertebrate annexins. *Mol Biol Evol* 2002;19(5):608-618.
- (123) Burger A, Berendes R, Liemann S et al. The crystal structure and ion channel activity of human annexin II, a peripheral membrane protein. *J Mol Biol* 1996;257(4):839-847.
- (124) Isacke CM, Trowbridge IS, Hunter T. Modulation of p36 phosphorylation in human cells: studies using anti-p36 monoclonal antibodies. *Mol Cell Biol* 1986;6(7):2745-2751.
- (125) Erikson E, Erikson RL. Identification of a cellular protein substrate phosphorylated by the avian sarcoma virus-transforming gene product. *Cell* 1980;21(3):829-836.
- (126) Rety S, Sopkova J, Renouard M et al. The crystal structure of a complex of p11 with the annexin II N-terminal peptide. *Nat Struct Biol* 1999;6(1):89-95.
- (127) Rescher U, Gerke V. S100A10/p11: family, friends and functions. *Pflugers Arch* 2008;455(4):575-582.
- (128) Filipenko NR, Waisman DM. The C terminus of annexin II mediates binding to F-actin. *J Biol Chem* 2001;276(7):5310-5315.
- (129) Jones PG, Moore GJ, Waisman DM. A nonapeptide to the putative F-actin binding site of annexin-II tetramer inhibits its calcium-dependent activation of actin filament bundling. *J Biol Chem* 1992;267(20):13993-13997.
- (130) Hayes MJ, Shao D, Bailly M, Moss SE. Regulation of actin dynamics by annexin 2. *EMBO J* 2006;25(9):1816-1826.
- (131) Hayes MJ, Merrifield CJ, Shao D et al. Annexin 2 binding to phosphatidylinositol 4,5-bisphosphate on endocytic vesicles is regulated by the stress response pathway. *J Biol Chem* 2004;279(14):14157-14164.
- (132) Rescher U, Ruhe D, Ludwig C, Zobiack N, Gerke V. Annexin 2 is a phosphatidylinositol (4,5)-bisphosphate binding protein recruited to actin assembly sites at cellular membranes. *J Cell Sci* 2004;117(Pt 16):3473-3480.
- (133) Emans N, Gorvel JP, Walter C et al. Annexin II is a major component of fusogenic endosomal vesicles. *J Cell Biol* 1993;120(6):1357-1369.
- (134) Harder T, Gerke V. The subcellular distribution of early endosomes is affected by the annexin II2p11(2) complex. *J Cell Biol* 1993;123(5):1119-1132.
- (135) Jost M, Zeuschner D, Seemann J, Weber K, Gerke V. Identification and characterization of a novel type of annexin-membrane interaction: Ca<sup>2+</sup> is not required for the association of annexin II with early endosomes. *J Cell Sci* 1997;110 (Pt 2):221-228.
- (136) Morel E, Parton RG, Gruenberg J. Annexin A2-dependent polymerization of actin mediates endosome biogenesis. *Dev Cell* 2009;16(3):445-457.

- (137) Morel E, Gruenberg J. Annexin A2 binding to endosomes and functions in endosomal transport are regulated by tyrosine 23 phosphorylation. *J Biol Chem* 2009;284(3):1604-1611.
- (138) Merrifield CJ, Rescher U, Almers W et al. Annexin 2 has an essential role in actin-based macropinocytic rocketing. *Curr Biol* 2001;11(14):1136-1141.
- (139) Diakonova M, Gerke V, Ernst J, Liautard JP, van d, V, Griffiths G. Localization of five annexins in J774 macrophages and on isolated phagosomes. *J Cell Sci* 1997;110 ( Pt 10):1199-1213.
- (140) Hayes MJ, Shao DM, Grieve A, Levine T, Bailly M, Moss SE. Annexin A2 at the interface between F-actin and membranes enriched in phosphatidylinositol 4,5,-bisphosphate. *Biochim Biophys Acta* 2008.
- (141) Mickleburgh I, Burtle B, Hollas H et al. Annexin A2 binds to the localization signal in the 3' untranslated region of c-myc mRNA. *FEBS J* 2005;272(2):413-421.
- (142) Hollas H, Aukrust I, Grimmer S, Strand E, Flatmark T, Vedeler A. Annexin A2 recognises a specific region in the 3'-UTR of its cognate messenger RNA. *Biochim Biophys Acta* 2006;1763(11):1325-1334.
- (143) Aukrust I, Hollas H, Strand E et al. The mRNA-binding site of annexin A2 resides in helices C-D of its domain IV. *J Mol Biol* 2007;368(5):1367-1378.
- (144) Hayes MJ, Moss SE. Annexin 2 has a dual role as regulator and effector of V-Src in cell transformation. *J Biol Chem* 2009.
- (145) de GM, Tijdens I, Smeets MB, Hensbergen PJ, Deelder AM, van de WB. Annexin A2 phosphorylation mediates cell scattering and branching morphogenesis via cofilin Activation. *Mol Cell Biol* 2008;28(3):1029-1040.
- (146) Lauvrak SU, Hollas H, Doskeland AP, Aukrust I, Flatmark T, Vedeler A. Ubiquitinated annexin A2 is enriched in the cytoskeleton fraction. *FEBS Lett* 2005;579(1):203-206.
- (147) Turowski P, Adamson P, Sathia J et al. Basement membrane-dependent modification of phenotype and gene expression in human retinal pigment epithelial ARPE-19 cells. *Invest Ophthalmol Vis Sci* 2004;45(8):2786-2794.
- (148) Bonilha VL, Bhattacharya SK, West KA et al. Proteomic characterization of isolated retinal pigment epithelium microvilli. *Mol Cell Proteomics* 2004;3(11):1119-1127.
- (149) West KA, Yan L, Shadrach K et al. Protein database, human retinal pigment epithelium. *Mol Cell Proteomics* 2003;2(1):37-49.
- (150) Molday RS, Hicks D, Molday L. Peripherin. A rim-specific membrane protein of rod outer segment discs. *Invest Ophthalmol Vis Sci* 1987;28(1):50-61.
- (151) Futter CE, Ramalho JS, Jaissle GB, Seeliger MW, Seabra MC. The role of Rab27a in the regulation of melanosome distribution within retinal pigment epithelial cells. *Mol Biol Cell* 2004;15(5):2264-2275.

- (152) Slot JW, Geuze HJ, Gigengack S, Lienhard GE, James DE. Immuno-localization of the insulin regulatable glucose transporter in brown adipose tissue of the rat. *J Cell Biol* 1991;113(1):123-135.
- (153) Deora AB, Kreitzer G, Jacovina AT, Hajjar KA. An annexin 2 phosphorylation switch mediates p11-dependent translocation of annexin 2 to the cell surface. *J Biol Chem* 2004;279(42):43411-43418.
- (154) Marmorstein AD. The polarity of the retinal pigment epithelium. *Traffic* 2001;2(12):867-872.
- (155) Vollrath D, Feng W, Duncan JL et al. Correction of the retinal dystrophy phenotype of the RCS rat by viral gene transfer of Mertk. *Proc Natl Acad Sci U S A* 2001;98(22):12584-12589.
- (156) Custer NV, Bok D. Pigment epithelium-photoreceptor interactions in the normal and dystrophic rat retina. *Exp Eye Res* 1975;21(2):153-166.
- (157) Edwards RB, Szamier RB. Defective phagocytosis of isolated rod outer segments by RCS rat retinal pigment epithelium in culture. *Science* 1977;197(4307):1001-1003.
- (158) Mayerson PL, Hall MO. Rat retinal pigment epithelial cells show specificity of phagocytosis in vitro. *J Cell Biol* 1986;103(1):299-308.
- (159) Bonilha VL, Finnemann SC, Rodriguez-Boulan E. Ezrin promotes morphogenesis of apical microvilli and basal infoldings in retinal pigment epithelium. *J Cell Biol* 1999;147(7):1533-1548.
- (160) Davis AA, Bernstein PS, Bok D, Turner J, Nachtigal M, Hunt RC. A human retinal pigment epithelial cell line that retains epithelial characteristics after prolonged culture. *Invest Ophthalmol Vis Sci* 1995;36(5):955-964.
- (161) Dunn KC, Otaki-Keen AE, Putkey FR, Hjelmeland LM. ARPE-19, a human retinal pigment epithelial cell line with differentiated properties. *Exp Eye Res* 1996;62(2):155-169.
- (162) Nabi IR, Mathews AP, Cohen-Gould L, Gundersen D, Rodriguez-Boulan E. Immortalization of polarized rat retinal pigment epithelium. *J Cell Sci* 1993;104 ( Pt 1):37-49.
- (163) Dunn KC, Marmorstein AD, Bonilha VL, Rodriguez-Boulan E, Giordano F, Hjelmeland LM. Use of the ARPE-19 cell line as a model of RPE polarity: basolateral secretion of FGF5. *Invest Ophthalmol Vis Sci* 1998;39(13):2744-2749.
- (164) Chowers I, Kim Y, Farkas RH et al. Changes in retinal pigment epithelial gene expression induced by rod outer segment uptake. *Invest Ophthalmol Vis Sci* 2004;45(7):2098-2106.
- (165) Kolko M, Wang J, Zhan C et al. Identification of intracellular phospholipases A2 in the human eye: involvement in phagocytosis of photoreceptor outer segments. *Invest Ophthalmol Vis Sci* 2007;48(3):1401-1409.

- (166) Sun K, Cai H, Tezel TH, Paik D, Gaillard ER, Del Priore LV. Bruch's membrane aging decreases phagocytosis of outer segments by retinal pigment epithelium. *Mol Vis* 2007;13:2310-2319.
- (167) Hall MO, Obin MS, Heeb MJ, Burgess BL, Abrams TA. Both protein S and Gas6 stimulate outer segment phagocytosis by cultured rat retinal pigment epithelial cells. *Exp Eye Res* 2005;81(5):581-591.
- (168) Rakoczy PE, Lai CM, Baines M, Di GS, Fitton JH, Constable IJ. Modulation of cathepsin D activity in retinal pigment epithelial cells. *Biochem J* 1997;324 ( Pt 3):935-940.
- (169) Hamel CP, Tsilou E, Pfeffer BA, Hooks JJ, Detrick B, Redmond TM. Molecular cloning and expression of RPE65, a novel retinal pigment epithelium-specific microsomal protein that is post-transcriptionally regulated in vitro. *J Biol Chem* 1993;268(21):15751-15757.
- (170) Burke JM, Skumatz CM, Irving PE, McKay BS. Phenotypic heterogeneity of retinal pigment epithelial cells in vitro and in situ. *Exp Eye Res* 1996;62(1):63-73.
- (171) Luo Y, Zhuo Y, Fukuhara M, Rizzolo LJ. Effects of culture conditions on heterogeneity and the apical junctional complex of the ARPE-19 cell line. *Invest Ophthalmol Vis Sci* 2006;47(8):3644-3655.
- (172) Proulx S, Landreville S, Guerin SL, Salesses C. Integrin alpha5 expression by the ARPE-19 cell line: comparison with primary RPE cultures and effect of growth medium on the alpha5 gene promoter strength. *Exp Eye Res* 2004;79(2):157-165.
- (173) Tian J, Ishibashi K, Honda S, Boylan SA, Hjelmeland LM, Handa JT. The expression of native and cultured human retinal pigment epithelial cells grown in different culture conditions. *Br J Ophthalmol* 2005;89(11):1510-1517.
- (174) West KA, Yan L, Miyagi M et al. Proteome survey of proliferating and differentiating rat RPE-J cells. *Exp Eye Res* 2001;73(4):479-491.
- (175) Thiery JP. Epithelial-mesenchymal transitions in development and pathologies. *Curr Opin Cell Biol* 2003;15(6):740-746.
- (176) Becker DL, Mobbs P. Connexin alpha1 and cell proliferation in the developing chick retina. *Exp Neurol* 1999;156(2):326-332.
- (177) Pearson RA, Luneborg NL, Becker DL, Mobbs P. Gap junctions modulate interkinetic nuclear movement in retinal progenitor cells. *J Neurosci* 2005;25(46):10803-10814.
- (178) Tibber MS, Becker D, Jeffery G. Levels of transient gap junctions between the retinal pigment epithelium and the neuroblastic retina are influenced by catecholamines and correlate with patterns of cell production. *J Comp Neurol* 2007;503(1):128-134.
- (179) Zhang J, Betson M, Erasmus J et al. Actin at cell-cell junctions is composed of two dynamic and functional populations. *J Cell Sci* 2005;118(Pt 23):5549-5562.
- (180) Frixen UH, Behrens J, Sachs M et al. E-cadherin-mediated cell-cell adhesion prevents invasiveness of human carcinoma cells. *J Cell Biol* 1991;113(1):173-185.

- (181) Heyraud S, Jaquinod M, Durmort C et al. Contribution of annexin 2 to the architecture of mature endothelial adherens junctions. *Mol Cell Biol* 2008;28(5):1657-1668.
- (182) Yamada A, Irie K, Hirota T, Ooshio T, Fukuhara A, Takai Y. Involvement of the annexin II-S100A10 complex in the formation of E-cadherin-based adherens junctions in Madin-Darby canine kidney cells. *J Biol Chem* 2005;280(7):6016-6027.
- (183) Benaud C, Gentil BJ, Assard N et al. AHNAK interaction with the annexin 2/S100A10 complex regulates cell membrane cytoarchitecture. *J Cell Biol* 2004;164(1):133-144.
- (184) Lee DB, Jamgotchian N, Allen SG, Kan FW, Hale IL. Annexin A2 heterotetramer: role in tight junction assembly. *Am J Physiol Renal Physiol* 2004;287(3):F481-F491.
- (185) Martin-Belmonte F, Gassama A, Datta A et al. PTEN-mediated apical segregation of phosphoinositides controls epithelial morphogenesis through Cdc42. *Cell* 2007;128(2):383-397.
- (186) Martin-Belmonte F, Mostov K. Phosphoinositides control epithelial development. *Cell Cycle* 2007;6(16):1957-1961.
- (187) Heth CA, Schmidt SY. Protein phosphorylation in retinal pigment epithelium of Long-Evans and Royal College of Surgeons rats. *Invest Ophthalmol Vis Sci* 1992;33(10):2839-2847.
- (188) Hayes MJ, Rescher U, Gerke V, Moss SE. Annexin-actin interactions. *Traffic* 2004;5(8):571-576.
- (189) Lorusso A, Covino C, Priori G, Bachi A, Meldolesi J, Chiergatti E. Annexin2 coating the surface of enlargeosomes is needed for their regulated exocytosis. *EMBO J* 2006;25(23):5443-5456.
- (190) Merrifield CJ, Moss SE, Ballestrem C et al. Endocytic vesicles move at the tips of actin tails in cultured mast cells. *Nat Cell Biol* 1999;1(1):72-74.
- (191) Zobiack N, Rescher U, Laarmann S, Michgehl S, Schmidt MA, Gerke V. Cell-surface attachment of pedestal-forming enteropathogenic E. coli induces a clustering of raft components and a recruitment of annexin 2. *J Cell Sci* 2002;115(Pt 1):91-98.
- (192) Borisy GG, Svitkina TM. Actin machinery: pushing the envelope. *Curr Opin Cell Biol* 2000;12(1):104-112.
- (193) Mejillano MR, Kojima S, Applewhite DA, Gertler FB, Svitkina TM, Borisy GG. Lamellipodial versus filopodial mode of the actin nanomachinery: pivotal role of the filament barbed end. *Cell* 2004;118(3):363-373.
- (194) Rogers LD, Foster LJ. The dynamic phagosomal proteome and the contribution of the endoplasmic reticulum. *Proc Natl Acad Sci U S A* 2007;104(47):18520-18525.
- (195) Boggon TJ, Eck MJ. Structure and regulation of Src family kinases. *Oncogene* 2004;23(48):7918-7927.

- (196) Roskoski R, Jr. Src protein-tyrosine kinase structure and regulation. *Biochem Biophys Res Commun* 2004;324(4):1155-1164.
- (197) Roskoski R, Jr. Src kinase regulation by phosphorylation and dephosphorylation. *Biochem Biophys Res Commun* 2005;331(1):1-14.
- (198) Duncan JL, LaVail MM, Yasumura D et al. An RCS-like retinal dystrophy phenotype in mer knockout mice. *Invest Ophthalmol Vis Sci* 2003;44(2):826-838.
- (199) Nandrot E, Dufour EM, Provost AC et al. Homozygous deletion in the coding sequence of the c-mer gene in RCS rats unravels general mechanisms of physiological cell adhesion and apoptosis. *Neurobiol Dis* 2000;7(6 Pt B):586-599.
- (200) Scott RS, McMahon EJ, Pop SM et al. Phagocytosis and clearance of apoptotic cells is mediated by MER. *Nature* 2001;411(6834):207-211.
- (201) Moodley Y, Rigby P, Bundell C et al. Macrophage recognition and phagocytosis of apoptotic fibroblasts is critically dependent on fibroblast-derived thrombospondin 1 and CD36. *Am J Pathol* 2003;162(3):771-779.
- (202) Ren Y, Silverstein RL, Allen J, Savill J. CD36 gene transfer confers capacity for phagocytosis of cells undergoing apoptosis. *J Exp Med* 1995;181(5):1857-1862.
- (203) Stuart LM, Deng J, Silver JM et al. Response to Staphylococcus aureus requires CD36-mediated phagocytosis triggered by the COOH-terminal cytoplasmic domain. *J Cell Biol* 2005;170(3):477-485.
- (204) Finnemann SC, Rodriguez-Boulan E. Macrophage and retinal pigment epithelium phagocytosis: apoptotic cells and photoreceptors compete for alphavbeta3 and alphavbeta5 integrins, and protein kinase C regulates alphavbeta5 binding and cytoskeletal linkage. *J Exp Med* 1999;190(6):861-874.
- (205) King-Smith C, Paz P, Lee CW, Lam W, Burnside B. Bidirectional pigment granule migration in isolated retinal pigment epithelial cells requires actin but not microtubules. *Cell Motil Cytoskeleton* 1997;38(3):229-249.
- (206) Botelho RJ, Teruel M, Dierckman R et al. Localized biphasic changes in phosphatidylinositol-4,5-bisphosphate at sites of phagocytosis. *J Cell Biol* 2000;151(7):1353-1368.
- (207) Greenberg S. Signal transduction of phagocytosis. *Trends Cell Biol* 1995;5(3):93-99.
- (208) Rescher U, Ludwig C, Konietzko V, Kharitononkov A, Gerke V. Tyrosine phosphorylation of annexin A2 regulates Rho-mediated actin rearrangement and cell adhesion. *J Cell Sci* 2008;121(Pt 13):2177-2185.
- (209) Mitra SK, Schlaepfer DD. Integrin-regulated FAK-Src signaling in normal and cancer cells. *Curr Opin Cell Biol* 2006;18(5):516-523.
- (210) Abram CL, Lowell CA. The diverse functions of Src family kinases in macrophages. *Front Biosci* 2008;13:4426-4450.